AGSO

STREAM SEDIMENT GEOCHEMISTRY OF THE EBAGOOLA 1:250 000 SHEET AREA, CAPE YORK PENINSULA, NORTH QUEENSLAND

by B I Cruikshank

RECORD 1994/8

AGSO

AUSTRALIAN GEOLOGICAL SURVEY ORGANISATION

AGSO

AUSTRALIAN GEOLOGICAL SURVEY ORGANISATION

Stream sediment geochemistry of the Ebagoola 1:250 000 sheet area, Cape York Peninsula, north Queensland

Record 1994/8

B I Cruikshank

DEPARTMENT OF PRIMARY INDUSTRIES AND ENERGY

Minister for Resources: Hon. David Beddall, MP
Secretary: Greg Taylor

AUSTRALIAN GEOLOGICAL SURVEY ORGANISATION

Executive Director: Harvey Jacka

ISSN: 1039-0073
ISBN: 0 642 20134 X

Contents

SUMMARY

A regional stream sediment sampling program in the Ebagoola 1:250 000 sheet area was carried out in association with geological and regolith mapping by the Australian Geological Survey Organisation (formerly Bureau of Mineral Resources) and the Geological Survey of Queensland, under the National Geoscience Mapping Accord. Samples were analysed for a suite of 40 elements, including Au by the bulk cyanide leach method, and image maps showing the spatial distribution of each element and a number of statistically derived parameters, including factor scores, element residuals and additive indices, have been prepared.

Variability in the data can be explained by 7 factors with the most important being due to accumulation of resistant minerals such as monazite and xenotime in the sediment lode (Factor 1), Fe minerals in the bedrock and/or scavenging by hydrated Fe-oxides in the secondary environment (Factor 2) and the weathering of K-rich minerals in granites (Factor 3). Residuals for Cu, Pb, U and Zn, estimated by removing lithochemical contributions, have been calculated and show areas which may be more prospective for these elements. Similarly, additive indices derived from standardised values for elements characteristic of known styles of mineralisation have been derived for gold, base metal, heavy mineral, porphyry copper, platinium and uranium mineralisation and show areas which may be prospective.

The greatest potential appears to be for gold, base metals and tin, and several areas potentially prospective in these commodities have been delineated.

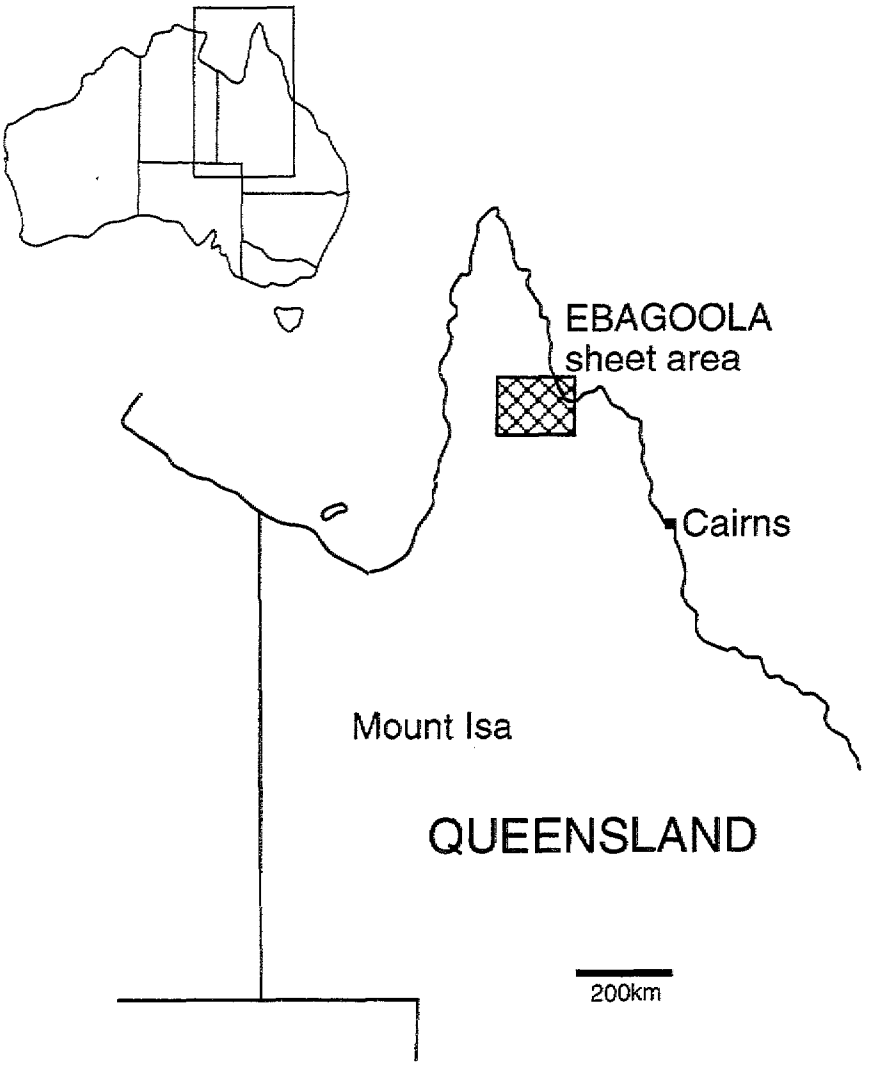

Figure 1 Location of EBAGOOLA 1:250 000 sheet area.

INTRODUCTION

This study forms part of the North Queensland, National Geoscience Mapping Accord (NGMA) project undertaken by the Australian Geological Survey Organisation and the Geological Survey of Queensland. The NGMA, endorsed by the Australian (now Australian and New Zealand) Minerals and Energy Council in August 1990, is a joint Commonwealth/State/Territory initiative to produce, using modern technology, a new generation of geoscientific maps, data sets, and other information on strategically important regions of Australia over the next 20 years.

The project area covers Cape York Peninsula and extends from Charters Towers in the south to Normanton in the west and Torres Strait in the north. The area has important mineral resources, for example the bauxite deposits at Weipa, but also contains areas of potential world heritage value. The project was undertaken to provide the sound geoscientific data necessary for resolution of potentially conflicting land-use demands.

This report describes the principal characteristics of the surficial (stream sediment) geochemistry of the EBAGOOLA 1:250 000 map sheet area (Figure 1), primarily part of the Coen Inlier. The Coen Inlier is a belt of Proterozoic metamorphic rocks intruded by plutons of the Siluro-Devonian to Permian Cape York Peninsula Batholith and partly overlain by Permian acid volcanics. It extends about 400km from Temple Bay in the north to 'Kimba' homestead in the centre of the HANN RIVER 1:250 000 sheet area in the south.

1.1 Study Area

In 1991 stream sediment sampling was carried out over most of the STRATHBURN, EBAGOOLA, STRATHMAY, and KALKAH, and parts of the PRINCESS CHARLOTTE BAY and MARINA PLAINS 1:100 000 map sheet areas, which together comprise the EBAGOOLA 1:250 000 sheet area. Land tenure in the area is mostly pastoral holdings, but includes several small mining leases and areas of national park in the east.

The area is remote with no sealed roads. The main access road, the Cape York Development Road, and secondary roads to Aurukun, Edward River and Port Stewart, are often impassable during the wet season due to many river and creek crossings, and are sometimes in poor condition during the rest of the year. Off-road vehicle and foot access is generally good in the pastoral leases because of tracks pushed into remote areas by the pastoralists, and because of cattle-paths along stream banks. There are no townships in the area, the closest being Coen about 10km north of the sheet area.

Cape York Peninsula has a monsoonal climate with heavy rains largely restricted to the period November-April. The highest and lowest annual rainfall figures recorded for Coen are 2000mm and 475mm respectively, with an average annual rainfall of about 1120mm (Bureau of Meteorology, 1971). Most streams are ephemeral and river and stream flow patterns closely follow rainfall.

The area can be divided into three broad physiographic regions or regolith- landform provinces (Pain & others, 1994)(Figure 2(a)). These are the uplands of the Peninsula Uplands Regolith-Landform Province, the eastern coastal plains of the Laura Regolith-Landform Province, and the western plains of the Merluna Regolith-Landform Province. Boundaries between many of the physiographic units coincide with geological boundaries. Much of the regolith material in the sheet area has been formed in situ, as shown in Figure 2(b) (after Blewett & others, 1992a).

The **Peninsula Uplands Regolith-Landform Province** occupies the central part of the sheet area and consists of ridges, hills and rises with intervening valleys and erosional plains. The province is

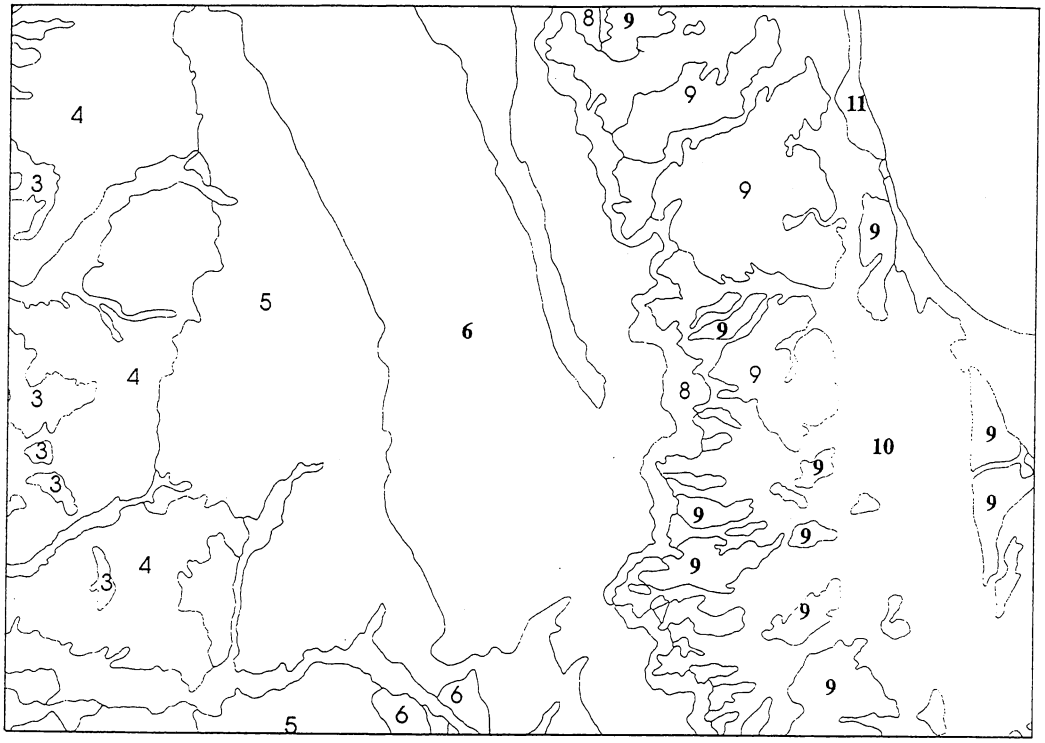

Regolith-Landform Associations
1 - Edward River, 2 - Holroyd, 3 - Weipa, 4 - Strathburn, 5 - Pollapa, 6 - Coleman, 7 - Wenlock, 8 - Great Escarpment, 9 - Leichhardt, 10 - Normanby, 11 - Princess Charlotte Bay.

Figure 2(a) Regolith-landform associations in the Ebagoola 1:250 000 sheet area (after Pain & others, 1994).

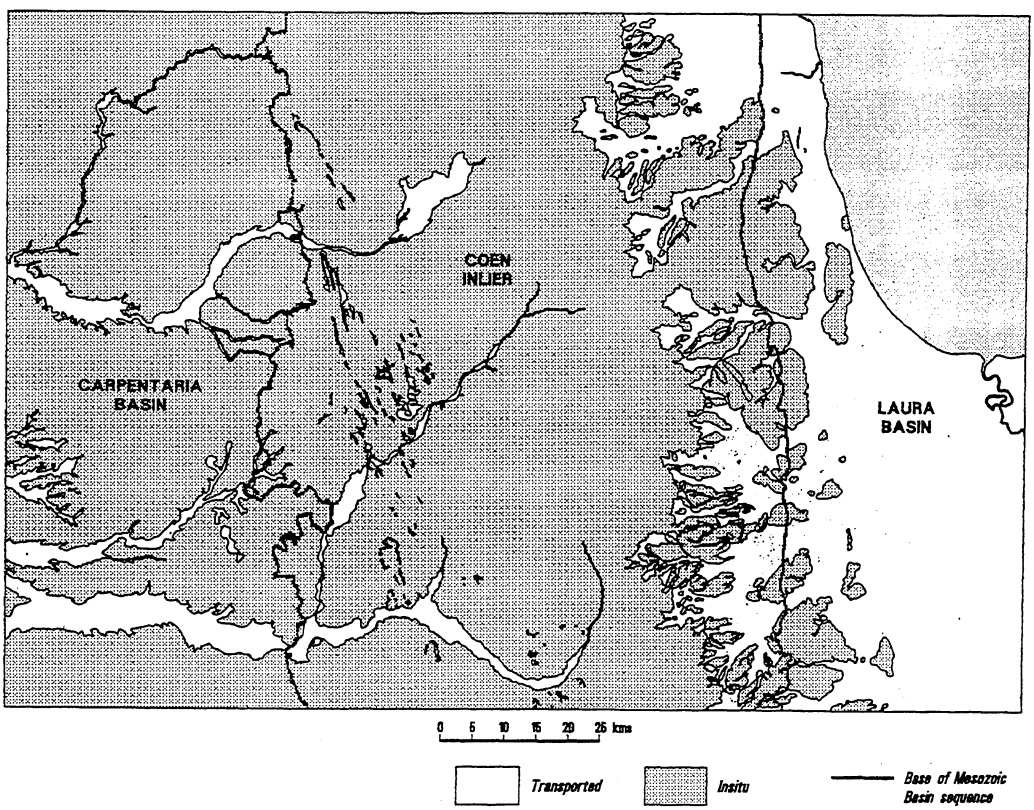

Figure 2(b) Areas of insitu and transported regolith in the Ebagoola 1:250 000 sheet area (after Blewett & others, 1992).

developed on metamorphic and granitic rocks of the Coen Inlier and corresponds to the McIlwraith Uplands and Coleman Plateau of Whitaker & Gibson (1977). The province is sub-divided (Pain & others, 1994) into:-

- The **Pollappa Regolith-Landform Association** which is found over the metamorphic rocks of the province. Quartzite ridges form topographic highs with more subdued areas overlying weathered gneisses and schists. Soils tend to be poorly developed with colluvial deposits at the footslopes of ridges. Vegetation is Eucalyptus (E.) tetrodonta open forest and access is generally good except in the more rugged areas.

- The **Coleman Regolith-Landform Association** corresponds roughly to the Coleman Plateau of Whitaker & Gibson (1977) and has formed over granitic rocks in the province. It is characterised by erosional plains and rises with moderately to highly weathered saprolite or residual sands. The area is covered by E. tetrodonta open forest and access is generally good.

- The **Wenlock Regolith-Landform Association** corresponds to the McIlwraith Uplands of Whitaker & Gibson (1977) and consists of hills formed over granite. Vegetation is thick evergreen and semi- deciduous rainforest, E. tetrodonta open forest, or a mosaic of both. Access is extremely difficult due to the ruggedness and thick vegetation.

- The **Great Escarpment Regolith-Landform Association** is a continuous, east-facing escarpment forming the boundary between the Peninsula Uplands Regolith-Landform Province and the Laura Regolith-Landform Province. This association occurs mostly over granite. Access is difficult.

The **Merluna Regolith-Landform Province** covers the western third of the sheet area and consists of erosional plains, with some mesas and cuestas, formed over weathered sedimentary rocks. The province is sub-divided into:

- The **Edward River Regolith-Landform Association** which is mainly channel deposits along the major rivers in the province.

- The **Weipa Regolith-Landform Association** contains low mesas and cuestas above the erosional plain. These are formed over weathered sedimentary rocks. Bauxitic cover is common in the west of the sheet area, with residual sands and highly weathered saprolite elsewhere. The scarps surrounding the mesas and cuestas made access difficult in places.

- The **Strathburn Regolith-Landform Association** is an erosional plain on moderately weathered saprolite overlain by residual sand. Soils, where formed, are sandy, yellow earth. Access was generally good.

The **Laura Regolith-Landform Province** occupies the eastern third of the sheet area, and consists largely of transported alluvium from weathered granitic and metamorphic rocks to the west. The province is sub-divided into:

- The **Leichhardt Regolith-Landform Association,** consisting of small hills and rises.

- The **Normanby Regolith-Landform Association,** which is the major association in the province, consists of low-lying active and inactive alluvial plains.

- The **Princess Charlotte Bay Regolith-Landform Association** of sandy beach deposits, mudflats and tidal lagoons of the coastal plains.

Owing to the lack of relief away from the escarpment, stream channel development in the province is poor and little sampling was carried out in this area although access was generally good.

There are five major river systems in the sheet area: the east draining Stewart and Morehead Rivers, and the west draining Holroyd, Edward and Coleman Rivers. The Stewart River has an average run-off of approximately 420 megalitres/km^2, marginally more than the the west draining rivers with an average run-off of 350 megalitres/km^2 (Connell Wagner, 1989).

GEOLOGY and MINERALISATION

2.1 Geology

The following is a brief account of the principal features of the surficial geology and mineralisation of the EBAGOOLA 1:250 000 sheet area. For a more comprehensive description geology, mineralisation and regolith refer to:

- EBAGOOLA 1:250 000 Basement Geological Map (Blewett & others, 1992a)
- EBAGOOLA 1:250 000 Preliminary Geological Map Commentary (Ewers & Bain, 1992)
- EBAGOOLA 1:250 000 General Geology Map (in prep)
- EBAGOOLA 1:250 000 Regolith-Landforms Map (Pain & Wilford, 1992)

and the following AGSO/BMR and GSQ maps, bulletins and records:

- Culpeper, 1993
- Pain & others, 1994
- Blewett & von Gnielinski, 1991
- Blewett & others, 1992b
- Culpeper & others, 1992a and 1992b
- Mackenzie & Knutson, 1992
- Wellman, 1992a and 1992b
- Smart & others, 1980
- Whitaker & Gibson, 1977
- Willmott & others, 1973
- de Keyser & Lucas, 1968
- Trail & others, 1968

The Coen Inlier is a north-south trending belt of igneous and metamorphic rocks stretching some 400 km from Hann River in the south to Temple Bay in the north. The oldest rocks cropping out in the area are Proterozoic metamorphic rocks which have been intruded by Siluro-Devonian granites of the Cape York Peninsula Batholith. These are overlain by unconformably Mesozoic sediments of the Laura Basin in the east and the Carpentaria Basin in the west. The later are also overlain,

unconformably, by Late Cretaceous or younger sediments of the Karumba Basin. Simplified geology of the EBAGOOLA sheet area is shown in Figure 3.

2.1.1 Metamorphic Rocks

The exposed Proterozoic metamorphics have been divided into 4 roughly north- south trending groups, from west to east the Edward River Metamorphic Group, the Holroyd Group, the Coen Metamorphic Group and the Newberry Metamorphic Group (see Figure 3). A full description of the stratigraphy of the metamorphic rocks is contained in Blewett & others (1992b and 1992c).

The **Edward River Metamorphic Group** is poorly exposed with less than 5% of its 1000 km^2 area, as inferred by geophysical studies, cropping out.

The **Holroyd Metamorphic Group** crops out over an area of some 3500 km^2 and has been divided into the Lukin and Kalkah Structural Domains, separated by the Lindalong Shear Zone. The Lukin Structural Domain comprises 9 units of slate/phyllite and quartzite, plus a unit of metadolerite/metabasalt (greenstone). The Kalkah Structural Domain to the east is more sheared and of higher metamorphic grade, and is believed to be underlain by granites of the Cape York Batholith (Blewett & others, 1992b and 1992c). Units of the stratigraphy of the Lukin Structural Domain are recognised in the Kalkah Structural Domain but the sequence is not complete.

The **Coen Metamorphic Group** crop out over 700 km^2 of the north-central map sheet area. The rocks are gneiss/schist/quartzite and higher-grade than the Holroyd Metamorphic Group, but are deeply weathered and less well exposed. The group is entirely enclosed within the Granites of the Cape York Batholith. The Hamilton Gold and Mineral Field occurs within the group.

The **Newberry Metamorphic Group** is poorly exposed along the eastern margin of the inlier. The group comprises units of gneiss and quartzite.

2.1.2 Siluro-Devonian Granites

The metamorphics have been intruded by granitic rocks of the Siluro-Devonian **Cape York Peninsula Batholith**, which, in the study area, has been classified into two supersuites, the S-type **Kintore Supersuite** and the I-type **Flyspeck Supersuite** (Mackenzie & Knutson, 1992; Mackenzie & others, 1992).

The Kintore Supersuite is further divided into the **Ebagoola Suite** and the generally more porphyritic **Lankelly Suite.** The Ebagoola Suite accounts for about 60% of the surface exposure of the batholith in the sheet area, and the more areally extensive of the 9 units of the suite are the Kintore, Barwon, Burns and Ebagoola Granites. The Lankelly Suite accounts for about 10% of the granite exposure in the sheet area, mostly as the Lankelly Granite. All are *muscovite-biotite* granites, from weakly to strongly porphyritic, and with varying combinations of *allanite, apatite, garnet, ilmenite, monazite, and zircon* as accessory minerals.

The Flyspeck Supersuite contains 8 units of *hornblende-biotite* granite and granodiorite. These rocks are richer in Fe_2O_3, FeO, MgO and CaO than the rocks of the Kintore Supersuite, but lower in K_2O. All granites are considered to be very iron-poor (Mackenzie & Knutson, 1992).

The metamorphics and the Siluro-Devonian granites form much of the Peninsula Uplands Regolith-Landform Province (see Figure 2(a)).

2.1.3 Sedimentary Rocks

The basal unit of the Laura Basin in the east is the **Dalrymple Sandstone** but this does not crop out in the sheet area. It is unconformably overlain by the **Gilbert River Formation,** a clayey quartzose sandstone with minor mudstone and conglomerate. This is overlain by the **Rolling Downs Group** and by Tertiary and Quarternary alluvial and colluvial sediments of the eastern plains.

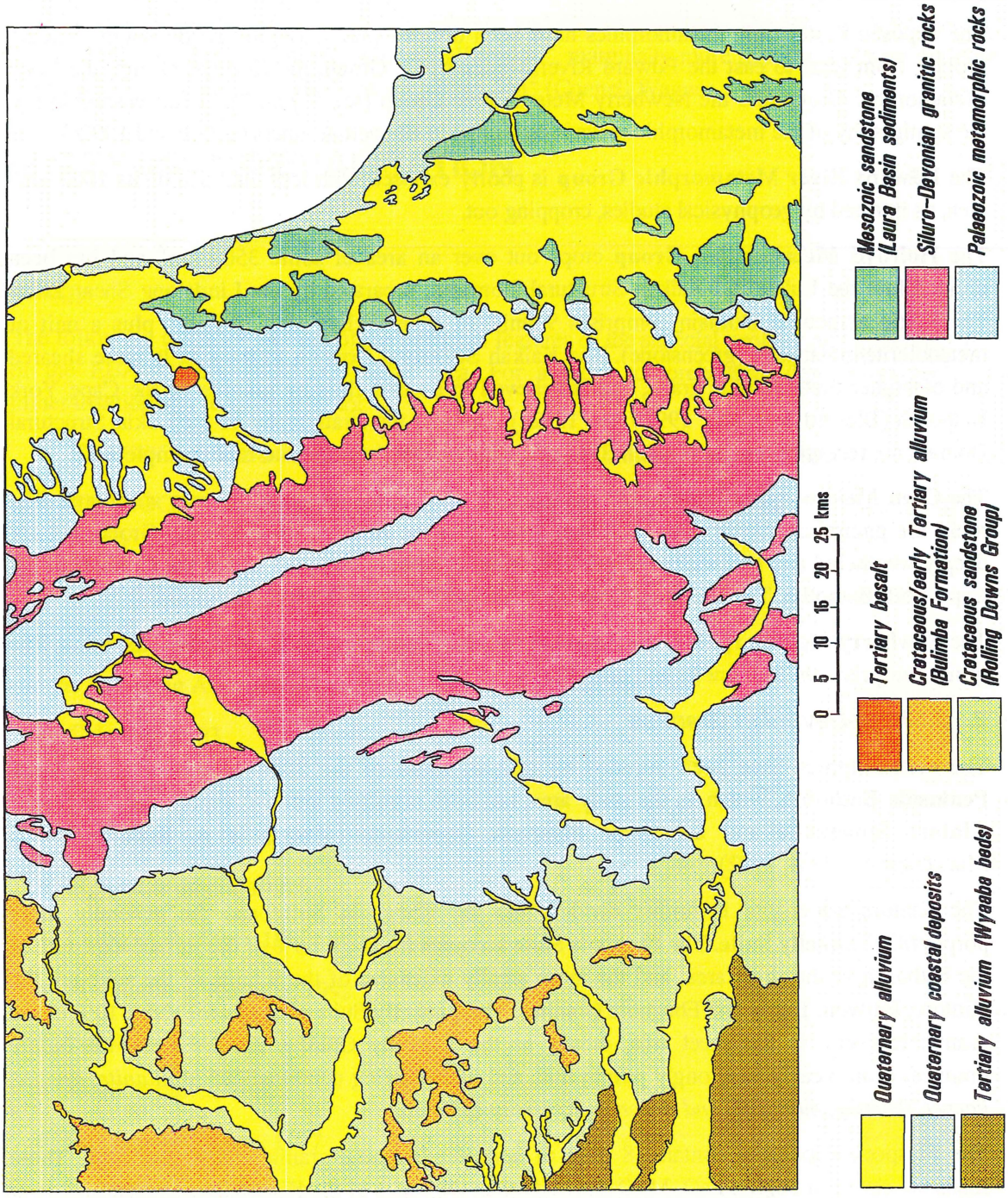

Figure3 Simplified surficial geology of the EBAGOOLA 1:250 000 sheet area (after Pain & others, 1994). More detailed descriptions can be found in Blewett & others (1992a and 1992b), Ewers & Bain (1992), and Mackenzie & Knutson (1992).

The basal unit of the Carpentaria Basin is the **Gilbert River Formation** which is overlain conformably by the **Rolling Downs Group,** comprising mudstone, siltstone and quartzose sandstone, and by the clayey, quartzose sandstones of the **Bulimba Formation.**

Some of the sheet area is Cainozoic alluvium and colluvium comprising clays, silts and sands. However, most has formed by in situ weathering of the underlying igneous, metamorphic and sedimentary rock units (see Figure 3(b)).

2.2 Mineralisation

The known mineralisation in the area is described by Culpeper (1993), Culpeper & others (1992a and 1992b), Whitaker & Gibson (1977) and Willmott & others (1973). Gold is the only commodity to have been mined in significant amounts in the area, approximately 2320kg being recovered between the early 1890's and 1951. Mineral occurrences are shown in Figure 4.

Gold

Gold mining began at **The Springs** in the early 1890s in reefs in sheared Flyspeck Granodiorite and Lankelly Adamellite in the Coen Shear Zone. This may be considered as part of the Coen Gold and Mineral Field. Total recorded production is 31kg and operations ceased in 1901 after the Hamilton Gold and Mineral Field was discovered.

The **Hamilton Gold and Mineral Field** covers workings at Ebagoola discovered in 1900 (Ball, 1901; Cameron, 1906), and workings at Yarraden (not Yarraden homestead) between the Lukin River and Spion Kop commenced the following year. At Ebagoola, gold occurs in quartz leaders in granite or schist at or near the contact between Kintore Granite and Coen Metamorphics. At Yarraden mineralised reefs occur within the Flyspeck Granodiorite. Most activity occurred between 1900 and the start of the First World War when production virtually ceased. Between 1900 and 1951 total recorded production was 2292kg comprising 1372kg from reef mining, 683kg from alluvial mining and 238kg from treatment of tailings.

2.3 Recent Exploration

A review of exploration in the peninsula from 1969 to 1990 is contained in Culpeper & others (1992b).

Systematic exploration in the sheet area over the past 25 years has been for gold, base metals and heavy minerals, including rare-earth minerals, with tin, tungsten and uranium as minor targets. Authorities to Prospect (ATPs) have centred largely on the Coen Inlier (gold and base metals) or the coastal plains (heavy minerals). No major discoveries have been reported and the only current mining activity involves several one or two man operations looking for surface gold, usually as small alluvial lodes or quartz vein systems.

Between 1968 and 1988 about 40 ATPs acknowledged **Gold** as an exploration target, sometimes in association with heavy minerals. These concentrated on the Coen Inlier with targets including quartz fissure lodes and stockworks, epithermal quartz veins and eluvial and alluvial deposits. Overall results have not been encouraging.

Exploration for **base metals** tailed off in the mid 1980s and only recently appears to have been revived by interest from BHP, CRAE and MIM who, in 1991, held most of the ground over the

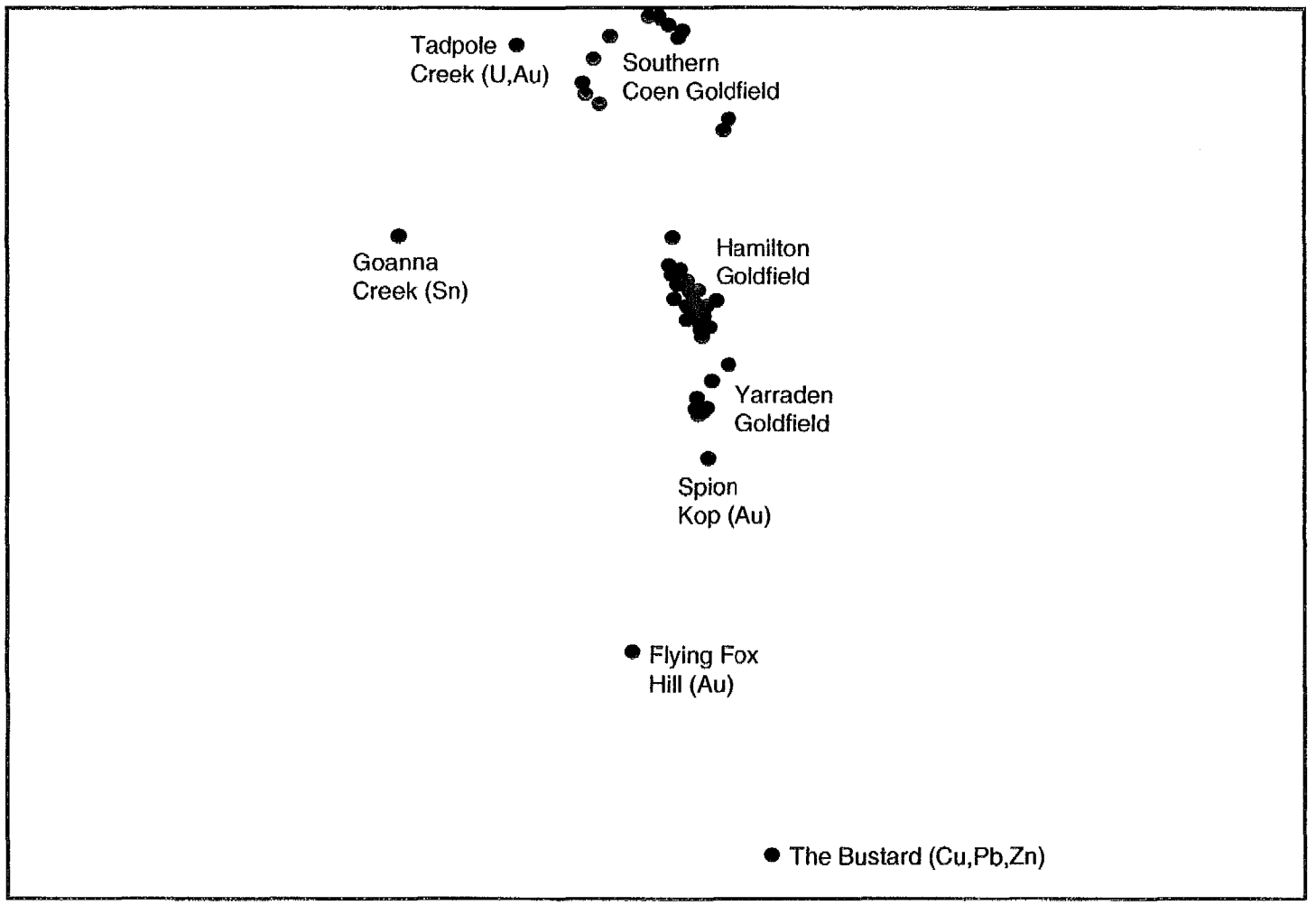

Figure 4 Mineral occurrences and mines in the EBAGOOLA 1:250 000 sheet area (sourced from the MINOCC/MINLOC digital databases - after Blewett & others, 1992a).

Coen Inlier in the sheet area. As with gold, results reported have not been encouraging with anomalies traced to low grade mineralisation, small pockets of base metal accumulations in weathered ultramafics or to rock units carrying high lithological concentrations of target elements.

In the late 1970s some interest was shown in **uranium** with graphitic and chloritic schists in the Holroyd Metamorphics near contacts with granites attracting most attention. Several interesting anomalies proved to be too low grade to of be economic interest. Exploration for **tin** and **tungsten** have proved no more rewarding.

The search for **heavy minerals** picked up in the late 1980s after a lapse of about 15 years, with a greater emphasis on rare-earth minerals. Exploration concentrated on the coastal areas and in the bed lodes of the larger drainage systems. Nothing of serious interest appears to have been found.

SAMPLING, CHEMICAL ANALYSIS and DATA PROCESSING METHODS

3.1 Sampling

Recent and current regional surveys have been carried out at sample densities ranging from one sample per km^2 in South Africa (Labuschagne & others, 1993), through one sample per 13 km^2 in Canada (Darnley, 1991) to one sample per 30 km^2 in Fennoscandia (Steenfelt, 1990). A mid point density of one sample per 10-15 km^2 was chosen because of its ability to provide maximum information within the constraints of the available resources and the designated life of the project.

The aim was to cover as much of the sheet area as possible, including areas overlying sedimentary rocks, but in the extremities of the eastern and western plains drainage was often too poorly defined to warrant sampling. Major drainage basins were outlined on 1:100 000 topographic (Series R631, Edition 1-AAS) maps and sample sites positioned to give basins of the required average size while ensuring good coverage of important rock units, specifically the granitic and metamorphic rocks of the Coen Inlier. The inlier lies largely within the EBAGOOLA and KALKAH 1:100 000 sheet areas. Access to nominated sample sites was by 4-wheel drive vehicle with occasional walks into sample sites in more rugged terrain. Each sampling team was equipped with a Magellan Nav 1000 Pro Global Positioning System (GPS) which was used for navigation and site location. During the sampling program twenty-four hour GPS coverage was available in 2-D (3 satellite) mode.

At each sample site two size fraction samples were collected. The first was 50-70g of -180u (-#80mesh) fine sediment stored in a plastic vial and is considered to be the 'standard' sieved stream sediment. The second was 5-6kg of -1mm coarse sediment, doubled bagged in large plastic sample bags, and was collected specifically for Bulk Cyanide Leach (BCL) determination of Au (+-Pd and Pt), and for possible future heavy mineral analysis. BCL was selected over other sampling techniques as it is capable of collecting the ultra fine particles of *Gold* from epithermal deposits common in north Queensland, and also coarser particles from other types of mineralisation (Elliott and Towsey, 1989). Non-trap sites in the active stream channel were preferred as natural sediment traps were rarely present within reasonable working distance of the nominated sampling sites in the mostly second order streams sampled. Where possible sieving was carried out at the sample site using aluminium bodied sieves fitted with nylon bolting cloth to minimise contamination. Wet samples were placed in plastic trays on return to base camp, dried in the sun and sieved. The fine sediment was pulverised further using motor driven mortar grinders

fitted with agate vessels. Samples were shipped to Canberra in AGSO vehicles for sorting, analysis and storage. Sample residues have been stored in Canberra for future study.

Duplicate samples (labelled as splits A and B) were collected at a number of sites to test the reproducibility of the sampling. These were analysed separately but for most of the statistical tests and mapping exercises the average value of the two splits was used.

A total of 744 sites in the EBAGOOLA sheet area were sampled, including 28 in duplicate. The outlines of drainage basins are shown in Figure 5 and the area covered is approximately 12,500km^2, including all of the Coen Inlier. Table 1 lists the 1:100 000 map sheet areas in which samples were collected, and the range of sample numbers allocated to each sheet.

Table 1. Map sheet areas sampled (all maps in Series R631, Edition 1-AAS, Australian Geodetic Datum 1966)

Sheet Name (Number)	Number of samples	Sample Numbers
Strathburn (7469)	139	7301-7481
Ebagoola (7569)	221	7001-7238
Princess Charlotte Bay (7669)	2	7601-7624
Strathmay (7468)	129	8301-8500
Kalkah (7568)	197	8001-8203
Marina Plains (7668)	56	8601-8691

Samples are prefixed by 9102

3.2 Chemical Analysis

The fine sediment was analysed for 35 elements in AGSO's Geochemical Laboratory using X-ray Fluorescence Spectrometry (XRFS) and Atomic Absorption Spectrophotometry (AAS). An aliquot of the fine sediment was split off and sent to Analabs in Perth for analysis of 9 elements by Inductively-Coupled Plasma/Mass Spectrometry (ICP-MS).

Since the BCL separation for Au determination would effectively consume the entire coarse sample (i.e. render it unsuitable for further analysis) it was decided to split off a 2kg aliquot of each coarse sample for BCL analysis and to archive the remaining sediment for future study. The 2kg splits were sent to Australian Laboratory Services (ASL) in Brisbane for analysis. Pt and Pd were included for screening purposes although the BCL method is generally considered unsuitable for Pt due to incomplete extraction (thought to be approx. 20%).

3.2.1 AGSO Analyses

Thirty-one elements (As, Ba, Bi, Ce, Cr, Cu, Fe, Ga, Ge, Hf, La, Mn, Mo, Nb, Nd, Ni, Pb, Rb, Sc, Se, Sn, Sr, Ta, Th, Ti, U, V, W, Y, Zn and Zr) were analysed for by XRFS, and 4 (Ag, Be, Co and Li) by AAS.

For XRFS analysis, sample powder was mixed with a binder and pressed into a 40mm diameter pellet. After air-drying, the pellet was analysed using Philips PW1404 and PW1450 X-ray spectrometers with 72 and 60 position sample changers respectively. Raw count-rates were corrected for inter-element and mass- absorption effects and converted into element concentrations using the methodology of Norrish & Chappell (1977). Analysis was in 3 separate runs determined

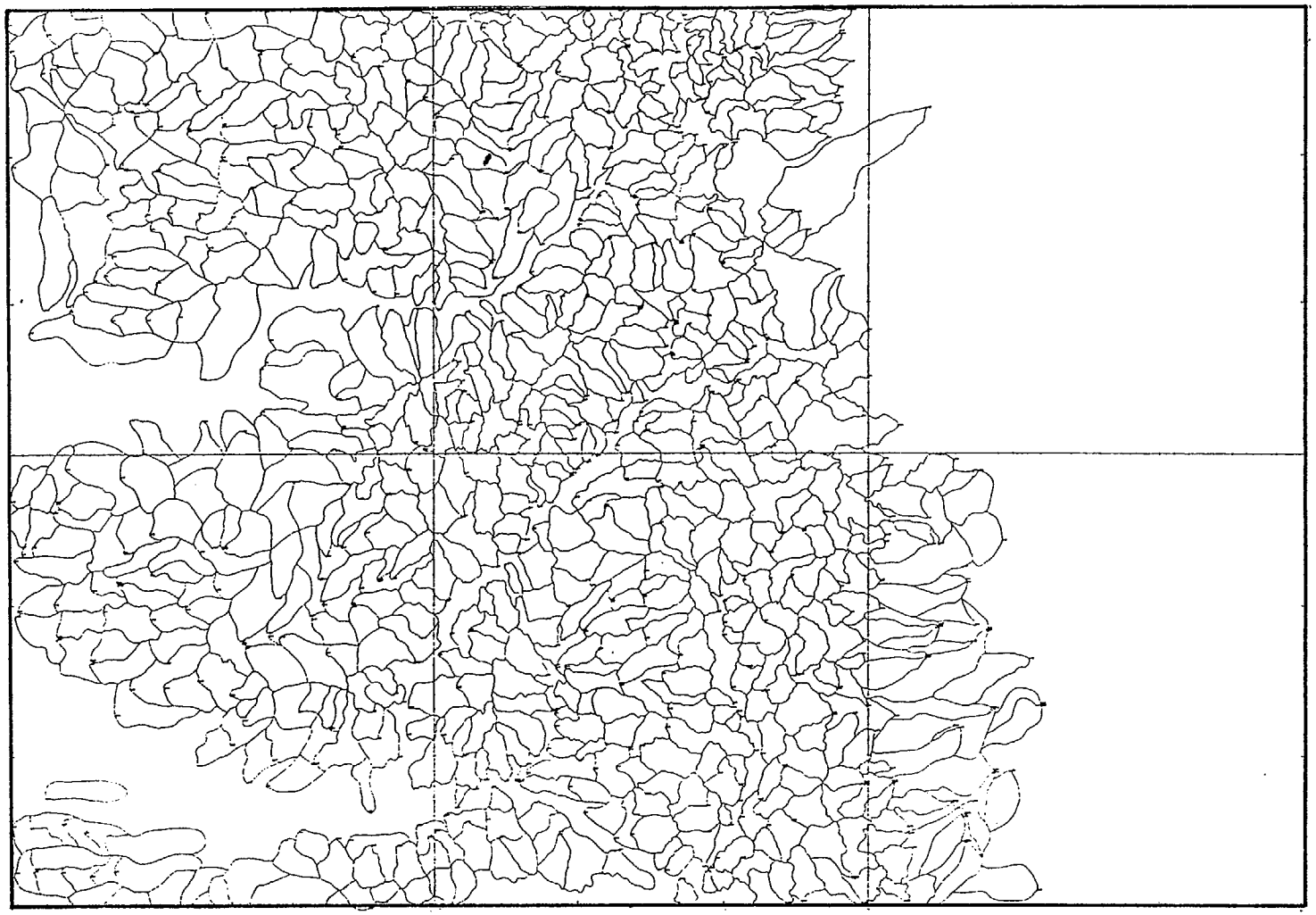

Figure 5 Outlines of the drainage basins sampled during the survey. Area covered is approximately 12,500 km^2.

by the X-ray tube used, the inter-element corrections necessary and the excitation conditions used. The elements analysed in each of the runs are listed in Table 2.

For AAS analysis, sample powder was digested in $HF/HClO_4$ taken to dryness. The residue was dissolved in HCl and made up to volume in a volumetric flask. The digest was analysed using a Varian AA-975 spectrophotometer with sample changer. The N_2O/C_2H_2 flame was used for Be and the method of standard additions for Li. Detection limits, in ppm, were Ag (1), Be (1), Co (2) and Li (1).

Table 2. Analytical runs for XRFS listing tube target, and tube voltage and current. Values in parenthesis are detection limits in ppm.

	1	2	3
Tube target	Mo	Au	Au
Voltage (kV)	90	90*/60	60
Current (mA)	30	30*/40	40
	Th (2)	Sn (2)*	Fe (1000)
	Rb (1)	Nb (2)*	Ti (5)
	Pb (2)	Zr (1)*	Mn (2)
	Y (1)	Mo (2)*	V (2)
	Sr (1)	Ni (1)	Cr (1)
	U (0.5)	Cu (1)	Ba (4)
	Se (1)	Zn (1)	La (2)
	Ga (1)	Hf (2)	Ce (5)
	As (0.5)	Ta (2)	Nd (2)
	Bi (2)		Sc (1)
	W (3)		
	Ge (0.5)		

Two samples from those collected in the 1990 program (and subsequently labelled CY-1 and CY-2) had been used as temporary XRFS secondary standards and were analysed with each batch of the EBAGOOLA samples. Estimated from these replicate analyses, the analytical precision (1s) for most elements was better than ± 8% for concentrations about 10ppm, better than ± 4% between 20 and 100ppm, and less than ± 2% at concentrations greater than 100ppm. Precision for XRFS Runs 1 and 2 was consistently better by a factor of about 2 than that for Run 3, which involved measurements at long wavelengths (1.74A) and used an Fe corrected mass absorption coefficient.

Full descriptions of the methodology used are given in Cruikshank & Pyke (1993).

3.2.2 ICP-MS Analyses

Several of the 35 elements listed above, for example Ag, Bi, Mo and W, gave few, if any, detectable values by XRFS and AAS. Analabs offer an ICP-MS method (Code GI222) involving a $HClO_4/HCl/HF$ total digestion and detection limits an order of magnitude or more better then XRFS and AAS. Aliquots of the fine sediment samples were split off and sent for analysis by this scheme. Several elements not in the original list were added. The elements analysed, with detection limits (ppm) in parenthesis, were Ag (0.1), Be (0.1), Bi (0.1), Cd (0.1), Mo (0.1), P (20), Sb (0.05), Tl (0.5) and W (0.1).

The sensitivity and ability to analyse for most naturally occurring elements makes the ICP-MS technique highly suitable for environmental geochemical studies.

3.2.3 Bulk Cyanide Leach Analyses

BCL has become a de facto standard for the detection of Au mineralisation. Its advantages include the ability to detect the ultra fine Au common to epithermal deposits, and the large sample weight (1-10kg) used gives very low detection limits at the ppt level (Elliot and Towsey, 1989). Unfortunately methodology for both sampling and analysis varies greatly starting with the coarseness of the material collected, through the use of static or dynamic leaching, and ending with the analytical method used to determine Au in the cyanide solution. It is intended that all coarse samples collected during the life of the North Queensland Project will be of the same size fraction, that is -1mm, and that the same laboratory also will be used if possible.

After examining technical details of commercially available methodology Australian Laboratory Services (ALS) in Brisbane were chosen and the 2kg aliquots were analysed by their method PM216. Although the extraction of Pt is reputed to be as low as 20% by BCL, both Pt and Pd were included in the analyses for screening purposes. The only detected concentrations of Pt and Pd reported were at the limit of detection of 10ppt.

Additional aliquots of several samples which gave very high Au values (20 ppb) were resubmitted for analysis by ALS and gave new results in the 100-300 ppt range. These new data were used in subsequent processing and the reason for the discrepancy is still being sought.

The analytical data, along with location data, were collated into a flat ASCII data file in MS-DOS format for data processing. Copies of the data file (CY91SGD) are available from AGSO Sales Centre (see below).

3.3 Data Analysis

The sheer amount of data resulting from a regional geochemical survey can be reduced to more manageable proportions by the application of univariate and multivariate statistical methods to describe the behaviour of the elements and their inter-element relationships. Similarly, the spatial distribution of the elements can be shown by either using a digitised representation of each sample's drainage basin coloured (or greyscaled, patterned, etc) according to the concentration of the element in the sample (Bonham-Carter & others, 1987; Cruikshank, 1990), or as images prepared from data systematically gridded from the essentially random data (sample) points of the survey (Eggo & others, in prep.). The former honours the spatial integrity of the data but is time consuming to implement, while the later is quick and, with care, sufficiently spatially honest to adequately show regional geochemical distribution patterns.

Basic univariate and multivariate statistics for the dataset were estimated using proprietary software on an IBM-compatible micro-computer.

More detailed univariate and multivariate analyses of the data, including multiple and stepwise regression and principal component factor analysis, were made using STATVIEW II (Abacus Concepts, Berkeley, California) and DATA DESK PROFESSIONAL (Odesta Corporation, Northbrook, Illinois) running on an Apple Macintosh II computer. DATA DESK PROFESSIONAL also allowed a more visual/intuitive approach to data analysis. These programs also produced tables and graphs (histograms, scattergrams, etc) which were cut and pasted directly into the Microsoft WORD 4.0 (Microsoft Corporation, Redmond, Washington) text files of this record. Line maps and diagrams were drawn using CANVAS 3.0 (Deneba Software, Miami, Florida) also running on the Macintosh.

Locations on the Australian Map Grid (AMG) were converted to Latitude/ Longitude using a propriety program so that plots could be related exactly to the boundaries of the map sheet area. XYZ data for each element (X=Longitude, Y=Latitude, Z=Element value) were gridded using

GRID from SURFER V4 (Golden Software, Golden, Colorado) on an IBM-compatible computer. Four equal area panels bounded by longitudes 142.50, 143.25 and 144.00°E, and latitudes 14.00, 14.50 and 15.00°E (each 301 columns by 201 rows, or 60,501 grid points) were gridded since GRID could produce only 65536 grid points per grid file. The grid files for the 4 panels were seamlessly combined to give a working grid file with the following parameters:

Longitude	minimum	142.50°E
	maximum	144.00°E
Latitude	minimum	14.00°S
	maximum	15.00°S
Grid spacing		0.0025°
No. of columns		601
No. of rows		401
Interpolation method		Kriging
Search radius		0.050°
Nearest neighbours		10

A location approximating to the geometric centre (centroid) of each sample basin was used in preference to the sample site as this more accurately represents the spatial relationship between drainage basins, and reduces the possibility of averaging effects on data points which may be close together although actually representing widely spaced drainage basins. This later effect is a significant problem when gridding data from low density sampling programs (Eggo & others, in prep.). For large drainage basins several location points may have been assigned to each basin.

Grid files were converted to 8-bit (0-255) 'image' files by 'slicing' (classification) into 9 ranges based on preset proportions of the number of non-zero values (Table 3). All grid points more than the distance equivalent to 0.050° (about 5.5km) from any sample point have been assigned a value of zero and a colour of white. The conversion programs also added a border and location marks, usually decimals of degrees of latitude and longitude.

Image files were translated into Macintosh format and loaded into IMAGE (National Institute of Health, USA) using pseudo colour or greyscale palettes with the pseudo colours/greys also listed in Table 3.

Table 3. Percentage ranges for 'sliced' images and corresponding pseudo colours and greyscales

	Percentage of values	Range	Approx. pseudo colour	Greyscale
1	100.0-99.9	0.1	Black	Black
2	99.9-99.0	0.9	Red	Darkest grey
3	99.0-98.0	1.0	Orange	
4	98.0-95.0	3.0	Yellow	
5	95.0-90.0	5.0	Yellow-green	8 steps
6	90.0-80.0	10.0	Green	of grey
7	80.0-60.0	20.0	Green-blue	
8	60.0-30.0	30.0	Light blue	
9	30.0- 0.0	30.0	Dark blue	Lightest grey

Colour and greyscale versions of the same image (As) are shown in Figure 6. The colour images are more visually appealing and permit rapid identification of areas belonging to each of the ranges. However, low volume colour reproduction is relatively expensive and in this record greyscale images have been used for reasons of economy. Colour images for most elements (raw data) and many statistically derived parameters are included in a separate atlas (Cruikshank & Butrovski, 1993).

Additional image processing, including production of RGB composite images, was carried out using PHOTOSHOP V2.0 (Adobe Systems Inc.). The pseudo colour or greyscale images were stored as PICT files and imported into CANVAS for annotation and addition of the concentration key. Colour and greyscale images were reproduced on a Tektronix ColorQuick Ink-jet Printer (Model 4697), a Tektronix 4693DX Color (wax transfer) Printer or a Canon Postscript colour photocopier/printer.

Copies of the analytical data file (CY91SGD) and the 'EBAGOOLA Stream Sediment Geochemical Atlas' (Cruikshank & Butrovski, 1993) are available from:

- AGSO Sales Centre GPO Box 378 CANBERRA ACT 2601
  Phone: 06-2499519 Fax: 06-2576466

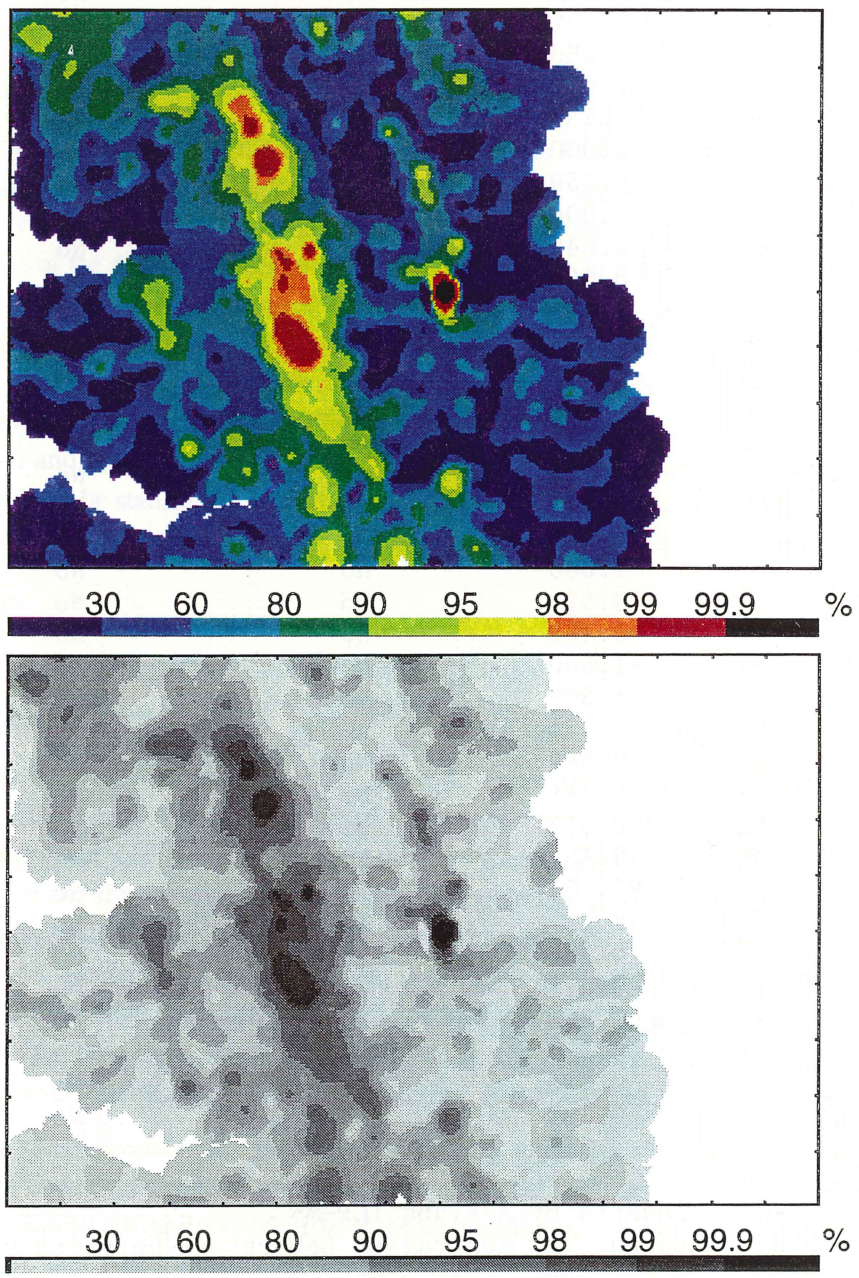

Figure 6 Colour and greyscale image maps of As. Greyscale images are used in this record - colour images are available in the EBAGOOLA atlas (see text).

Table 4. Paired t-test results on 27 duplicate samples.

	t statistic	different at 2% confidence level	different at 10% confidence level
Ag*	0.113	No	No
As	0.046	No	No
Au#	0.034	No	No
Ba	0.656	No	No
Be*	1.076	No	No
Bi	all ND values		
Bi*	0.889	No	No
Cd*	0.092	No	No
Ce	0.563	No	No
Cr	0.524	No	No
Cu	-1.734	No	Yes
Fe	0.000	No	No
Ga	-0.550	No	No
Ge	1.000	No	No
Hf	0.646	No	No
La	0.357	No	No
Mn	-1.061	No	No
Mo	0.000	No	No
Mo*	-0.872	No	No
Nb	0.534	No	No
Nd	0.527	No	No
Ni	-0.910	No	No
P*	-0.852	No	No
Pb	1.495	No	No
Pd#	1.000	No	No
Pt#	-0.570	No	No
Rb	0.409	No	No
Sb*	-1.560	No	No
Sc	-1.309	No	No
Se	all ND values		
Sn	0.589	No	No
Sr	-0.145	No	No
Ta	0.817	No	No
Th	0.094	No	No
Ti	-0.133	No	No
Tl*	-0.229	No	No
U	0.369	No	No
V	-0.516	No	No
W	0.278	No	No
W*	0.587	No	No
Y	0.526	No	No
Zn	-0.102	No	No
Zr	0.557	No	No

* - elements by Analabs ICP-MS
\# - elements by Australian Laboratory Services bulk cyanide leach

$t_{1\%}$ = 2.479 (2% confidence level)
$t_{5\%}$ = 1.706 (10% confidence level) with 26 degrees of freedom.

STATISTICAL ANALYSIS

Element values below the detection limit of the analytical method used (Not Detected or ND values) appear in the datafile as the negative of the detection limit value. For the following statistical calculations a value of half the detection limit has been substituted. For example, Sn by XRFS has a theoretical detection limit of 2ppm under the analytical conditions used, and ND values appear as -2 in the datafile and are treated as 1 (ppm) in the calculations.

An element symbol suffixed with an asterisk (*) indicates that analysis was by ICP-MS. Similarly, a cross-hatch (#) indicates BCL/GFAAS. No suffix indicates analysis in AGSO's laboratory.

4.1 Duplicate Samples

Duplicate samples were collected at a number of sample sites to test the overall reproducibility of the sampling and analytical procedures. Data for 27 pairs of duplicate samples were compared using the 'paired t-test' (Koch & Link, 1970) which computes a confidence interval for the population mean of the differences between paired observations, in this case the duplicate samples. A confidence interval is used because experimental error (sampling plus analytical) would normally preclude obtaining the same results for the duplicate samples. If the confidence interval includes zero, or the calculated t-statistic is inside the range +-T, then the conclusion is that the duplicate samples are not statistically different. No significant difference was found at the 2% confidence level and only Cu differed at the 10% confidence level (Table 4). The sampling, and analysis, was held to be statistically reproducible at the confidence levels tested. An average value for each element in each 'duplicate' sample has been used for all following data analysis and imagery.

4.2 Summary Univariate Statistics

Summary univariate statistics are shown in Table 5. These include the minimum, maximum, median, arithmetic mean, standard deviation, skewness (raw data), coefficient of variation, geometric mean, geometric deviation, skewness (log- transformed data), and arithmetic mean, standard deviation and skewness of a trimmed sample population in which the top and bottom 15% of values for the total dataset were deleted. The trimmed data and geometric statistics are considered (Ellis & Steele, 1982; Eggo & others, in prep.) to be more robust, that is less subject to the effects of outliers, than the raw data statistics and therefore better define the background character of the data. Five elements (Bi, Mo, Pd#, Pt#, and Se) comprised a majority (80%) of ND values and no statistical parameters other than minimum, maximum and median were recorded.

The number of sample populations and their distribution types for each element were assessed from histograms, and raw data and log-transformed data probability plots (Sinclair, 1974 and 1991) generated by DATA DESK and STATVIEW II. Most populations had one or more outliers which did not fit the assessed distributions, but which were of insufficient numbers to constitute a separate population. Where two or more populations were identified, the element concentration corresponding to the break in slope of the probability plots has been recorded. The assessments, which are subjective, are also included in Table 5 and these plots are shown in Appendix A.

Table 5 Summary univariate statistics for EBAGGOLA dataset (N=744). Not Detected values set to half Detection Limit in calculations but are shown as negatives of Detection Limit in table. All values in ppm except Au#, Pd#, Pt# which are in ppb.

				Raw data				Log-transformed		
	Min.	Max.	Median	Mean	Stand. Devn	Skew.	Coeff. of var.	Mean	Geom. Devn	Skew.
Ag*	-0.10	5.71	0.31	0.40	0.47	6.34	118	0.28	2.349	-0.30
As	-0.5	77.5	2.0	2.82	3.78	11.3	134.0	1.93	2.357	-0.04
Au#	-0.01	11.2	0.05	0.158	0.585	12.5	369.3	0.392	5.307	0.14
Ba	23	1694	422.5	501.6	344.9	0.57	68.8	369.4	2.366	-0.56
Be*	-0.10	5.56	1.29	1.42	0.78	1.29	54.9	1.22	1.774	-0.48
Bi	-2	6	-2							
Bi*	-0.10	1.59	0.22	0.27	0.21	2.27	78	0.21	2.084	-0.18
Cd*	-0.10	1.76	0.15	0.16	0.11	7.58	69	0.14	1.680	-0.24
Ce	10	1946	78.5	153.0	225.3	4.04	147.3	92.3	2.454	0.84
Cr	-1	332	21	27.25	28.06	3.37	103.0	15.9	3.276	-0.70
Cu	-1	37	2	4.12	5.65	2.84	137.1	1.97	3.413	0.29
Fe	2000	75000	10000	12975	10005	1.72	77.1	9897	2.118	-0.05
Ga	-1	19	7	6.98	3.26	0.47	46.7	6.08	1.785	-1.23
Ge	-0.5	3	1.5	1.56	0.30	0.24	19.2	1.53	1.224	-1.31
Hf	-2	251	10	14.27	15.11	6.77	105.9	10.8	2.008	0.40
La	4	1028	39.5	77.70	116.1	4.13	149.4	46.3	2.495	0.76
Mn	9	3064	253	354.2	373.4	2.98	105.4	225.2	2.795	-0.56
Mo	-2	5	-2							
Mo*	-0.10	3.18	0.49	0.56	0.40	1.37	71	0.41	2.454	-0.86
Nb	3	127	13	15.57	10.75	3.39	69.0	13.29	1.706	0.55
Nd	4	840	32	64.21	95.96	4.03	149.4	37.79	2.532	0.74
Ni	-1	73	3	5.30	7.33	3.66	138.3	2.71	3.232	0.13
P*	-20	2710	181	292.2	361.2	3.05	123.6	164.5	3.141	-0.42
Pb	3	75	21	26.53	16.76	0.72	63.2	21.38	1.978	-0.18
Pd#	-0.01	0.01	-0.01							
Pt#	-0.01	0.01	-0.01							
Rb	-1	287	71	92.98	75.47	0.59	81.2	52.32	3.834	-1.09
Sb*	-0.05	4.32	0.43	0.52	0.42	2.56	81	0.39	2.391	-0.92
Sc	-1	25	4	5.08	3.68	1.27	72.4	3.75	2.361	-0.70
Se	-1	1	-1							
Sn	-2	348	-2	4.95	18.43	14.14	372.3	2.10	2.728	1.48
Sr	3	216	53	62.61	44.04	0.53	70.3	43.69	2.659	-0.83
Ta	-2	49	-2							
Th	-2	505	17	41.09	65.49	3.64	159.4	21.53	2.812	0.73
Ti	314	46779	3359	4178	4004	4.37	95.8	3072	2.231	-0.29
Tl*	-0.5	2.29	0.67	0.76	0.51	0.62	67	0.59	2.094	-0.03
U	-0.5	80.5	3.5	6.65	9.39	3.70	141.2	3.97	2.565	0.52
V	-2	262	29	38.38	35.01	1.97	91.2	24.81	2.837	-0.69
W	-3	50	4	4.94	4.53	4.12	91.7	3.77	2.044	0.23
W*	-0.10	48.2	1.58	1.85	2.13	14.31	115.1	1.33	2.513	-1.37
Y	4	1014	31	61.01	93.77	5.07	153.7	38.36	2.302	1.05
Zn	2	201	15	18.08	14.53	4.16	80.4	14.20	2.021	-0.11
Zr	54	13994	423.5	654.3	806.0	7.59	123.2	466.2	2.144	0.55

__Trimmed raw data__ Mean	Stand. Devn	Skew.	No. of pops., distn. types and concentration at break in slope	
0.32	0.12	0.29	2 -logn + norm(?) - 1.2 ppm	Ag*
2.10	0.94	0.73	1 -logn	As
0.066	0.059	0.78	2 -logn (x2) - 580 ppt	Au#
463.8	233.4	0.31	2+ -logn (x2??) -?	Ba
1.33	0.39	0.23	2(?) -logn (x2?)	Be*
				Bi
0.23	0.09	0.50	1 -logn	Bi*
0.15	0.03	0.35	1 -logn	Cd*
92.60	47.00	1.25	2 -logn (x2) - 100 ppm	Ce
22.19	12.92	0.37	1 -logn (?)	Cr
2.60	2.09	0.72	1 -logn	Cu
10977	4858	0.54	1 -logn	Fe
6.80	1.78	0.04	1 -norm (? or complex)	Ga
1.55	0.15	2.71	1 -?	Ge
11.09	4.12	0.71	1 -logn	Hf
46.82	23.64	1.23	2 -logn (x2) - 50 ppm	La
273.2	128.3	0.54		Mn
				Mo
0.51	0.22	0.23	1 -?	Mo*
13.34	3.87	0.67	2(?) -logn (x2??) -30 ppm	Nb
38.49	20.12	1.26	2 -logn (x2) -45 ppm	Nd
3.38	2.29	0.87	1 - logn (? or complex)	Ni
203.9	110.7	0.65	1 -logn	P*
24.10	10.89	0.47	2+(?) -complex	Pb
				Pd#
				Pt#
83.78	51.26	0.39	2+(?) -complex -?	Rb
0.46	0.18	0.38	1(?) -logn	Sb*
4.54	2.02	0.51	1 -logn (?)	Sc
				Se
1.97	1.28	1.05	1(?) -logn	Sn
58.51	29.62	0.32	2+(?) -complex -?	Sr
				Ta
22.60	14.45	1.36	2 -logn (x2) -20 ppm	Th
3498	1351	0.25	1 -logn	Ti
0.68	0.37	0.17	1 -norm	Tl*
4.14	2.26	1.24	2 (?) -logn (x2) -3.5 ppm	U
31.36	15.79	0.46	2+(?) - complex	V
4.08	1.70	-0.14	1 -logn	W
1.63	0.59	0.26	1(?) -?	W*
37.31	17.15	1.28	2 -logn (x2) -35 ppm	Y
15.64	6.00	0.44	2 -logn, ? -75 ppm	Zn
481.4	207.8	0.87	1 -logn	Zr

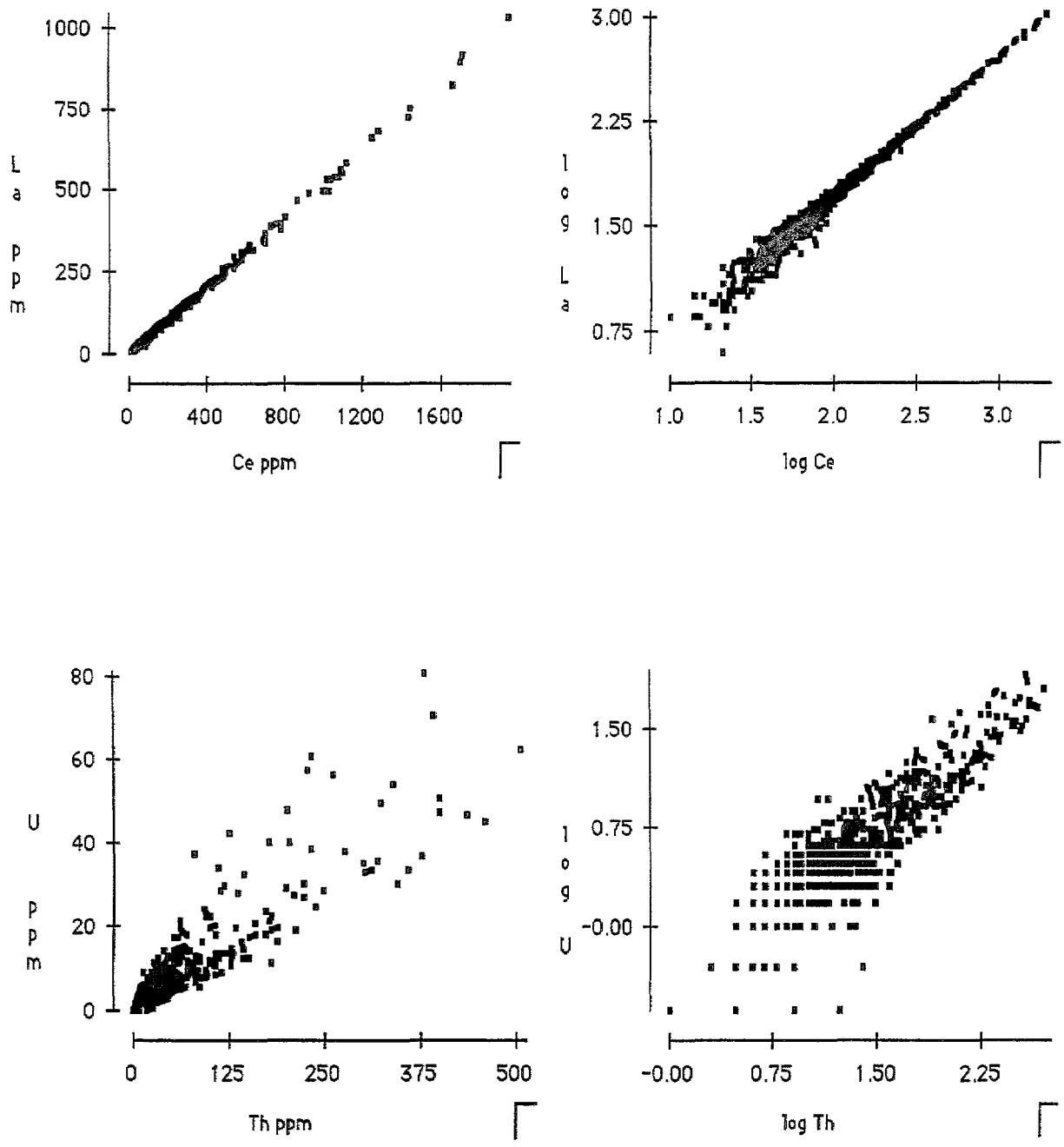

Figure 7 Examples of scatterplots used to verify relationships between elements, and absence of outliers. At top are normal and log-transformed plots of La against Ce, and at bottom U against Th.

4.3 Summary Multivariate Statistics

4.3.1 Correlations

The statistical correlation between pairs of elements often highlights significant geochemical associations but must be treated with some caution. A high correlation 'does not prove cause and effect' (Eggo & others, in prep.) but, if an underlying geochemical rationale can be elucidated, may quantify the relationship. The size of the EBAGOOLA dataset (N=744) reduces the possibility of chance correlations sometimes found in small datasets. The Pearson product-moment correlation method assumes normally distributed sample populations and as many elements (see Table 5) appear to follow the log-normal distribution, matrices of coefficients calculated from both raw data and log- transformed data are shown in Tables 6 and 7, respectively. Spearman Rank Correlation is a non-parametric method which makes no assumptions about the distributions the data follow. A matrix of correlation coefficients from this method is shown in Table 8. All data were included in the calculations but coefficients for Bi, Mo, Pd#, Pt# and Se may be considered as suspect but informative. Figure 7 shows the tightness of some of these element-pair correlations, for example between raw and log-transformed values for Ce and La, and Th and U. These diagrams not only confirm the correlation between element pairs but also reveal any outliers which may compromise the Pearson coefficient (Eggo & others, in prep.).

For a population of 744 samples any Pearson coefficient greater than 0.09 or less than -0.09 is statistically significant. However, to separate highly correlated associations from the less correlated and potentially chance associations, only coefficients of 0.5 and higher or -0.50 or less (for which variation in element X cause 25% or more of the variation in element Y) have been considered and several highly correlated groupings are discernible from all three methods. These are:-

1) Ce, La, Nd, P*, Th, U and Y

2) Ba, Be*, Ga, Pb, Rb, Sr and Tl*

3) Cr, Cu, Fe, Mn, Ni, Sc, V and Zn

4) Hf and Zr

5) Nb and Ti

6) Pd# and Pt#

Group 1 appears to represent concentration of resistant heavy minerals such as monazite in the sediment. Group 2, given the stronger association between Ba, Pb, Rb and Sr, probably represents an abundance of weathered potassium minerals (Ba - Puchelt, 1972; Pb - Wedepohl, 1974; Rb - Heier & Billings, 1970; Sr - Faure, 1978), most likely from granites. Group 3 suggests a 'mafic' or basic rock/mineral association.

Supplementary associations and exclusions (negative correlations) vary with method. Raw data correlations suggest an association between elements of Group 1 and Nb, W and Ti but this is replaced by an association between the group and Ba, Pb, Rb and Sr of Group 2 in the log-transformed and ranked data correlations. These procedures also highlight negative correlations between key elements of Group 3 and Groups 1 and 2. Also evident in these is an association between Hf and Zr of Group 4 and Nb, Sn and Ti.

Of concern is the absence of strong correlation between replicate element analyses such as Bi and Bi*, Mo and Mo*, and W and W*, and between Cd* and Zn. The lack of correlation in the three

Table 6. Pearson product-moment correlation coefficients for EBAGOOLA sheet area raw data (N=744).

	Ag‡	As	Au‡	Ba	Be‡	Bi	Bi‡	Cd‡	Ce	Cr	Cu	Fe	Ga	Ge	Hf	La	Mn	Mo	Mo‡	Nb	Nd	Ni
Ag‡		0.07	0.02	0.05	0.28	0.21	0.33	0.10	0.15	0.00	0.05	0.06	0.15	0.14	0.28	0.14	0.12	0.00	0.09	0.28	0.15	0.04
As			0.10	-0.05	0.16	0.20	0.28	0.09	-0.07	0.15	0.37	0.38	0.19	0.07	0.00	-0.07	0.16	0.12	0.25	0.08	-0.07	0.26
Au‡				0.00	0.01	-0.03	0.01	0.00	-0.02	-0.01	0.04	0.02	0.03	-0.02	-0.05	-0.02	0.02	-0.02	-0.02	-0.04	-0.02	0.01
Ba					0.49	0.01	0.13	0.17	0.19	-0.43	-0.30	-0.32	0.54	-0.01	-0.17	0.18	0.04	-0.24	-0.08	-0.26	0.19	-0.27
Be‡						0.09	0.52	0.19	0.13	-0.09	0.08	0.12	0.70	0.37	-0.15	0.13	0.31	-0.06	0.07	-0.06	0.14	0.10
Bi							0.21	-0.02	0.15	-0.01	-0.03	0.01	0.02	0.03	0.51	0.15	0.08	0.04	0.00	0.33	0.15	-0.04
Bi‡								0.25	0.13	-0.13	0.06	0.04	0.29	0.36	-0.01	0.12	0.25	-0.03	0.15	0.07	0.13	-0.02
Cd‡									0.10	-0.09	-0.02	-0.02	0.12	0.04	0.00	0.10	0.07	0.01	0.08	0.01	0.10	-0.04
Ce										0.05	-0.08	0.04	0.27	-0.06	0.32	1.00	0.21	-0.17	-0.03	0.54	1.00	-0.05
Cr											0.51	0.63	0.09	0.03	0.15	0.05	0.27	0.13	0.12	0.33	0.05	0.67
Cu												0.81	0.19	0.19	-0.07	-0.07	0.53	0.21	0.21	0.11	-0.08	0.86
Fe													0.33	0.11	0.08	0.05	0.56	0.23	0.24	0.27	0.05	0.82
Ga														0.27	-0.09	0.27	0.35	-0.10	0.12	0.09	0.27	0.23
Ge															-0.09	-0.06	0.13	0.05	0.07	0.01	-0.06	0.14
Hf																0.32	0.09	0.06	-0.04	0.64	0.32	0.00
La																	0.21	-0.17	-0.03	0.54	1.00	-0.05
Mn																		0.03	0.14	0.17	0.21	0.60
Mo																			0.10	0.05	-0.17	0.17
Mo‡																				0.05	-0.03	0.19
Nb																					0.53	0.12
Nd																						-0.05
Ni																						
P‡																						
Pb																						
Pd‡																						
Pt‡																						
Rb																						
Sb‡																						
Sc																						
Se																						
Sn																						
Sr																						
Ta																						
Th																						
Ti																						
Tl‡																						
U																						
V																						
W																						
W‡																						
Y																						
Zn																						
Zr																						

P*	Pb	Pd#	Pt#	Rb	Sb*	Sc	Se	Sn	Sr	Ta	Th	Ti	Tl*	U	V	W	W*	Y	Zn	Zr	
0.23	0.18	0.12	0.14	0.15	0.14	0.08	0.09	0.04	0.10	0.39	0.16	0.00	0.13	0.31	0.00	0.25	0.10	0.28	0.17	0.30	Ag*
-0.07	-0.11	-0.01	-0.03	-0.06	0.20	0.32	0.01	0.07	-0.04	0.09	-0.09	0.04	-0.07	-0.06	0.26	0.21	0.69	-0.06	0.31	0.01	As
0.00	0.01	0.08	0.07	0.02	0.02	0.02	0.00	-0.03	0.00	-0.01	-0.01	-0.03	0.00	-0.01	-0.01	-0.01	-0.01	0.00	0.02	-0.06	Au#
0.39	0.84	0.06	0.15	0.88	0.06	-0.35	0.00	-0.18	0.91	-0.05	0.22	-0.29	0.78	0.19	-0.47	0.08	0.05	0.18	-0.05	-0.21	Ba
0.33	0.62	0.04	0.10	0.66	0.17	0.06	-0.02	-0.09	0.59	0.04	0.14	-0.13	0.57	0.23	-0.07	0.18	0.16	0.22	0.32	-0.16	Be*
0.12	0.08	0.00	0.00	0.05	0.05	0.05	-0.01	0.14	0.03	0.41	0.15	0.14	0.06	0.22	0.02	0.21	0.24	0.15	-0.01	0.53	Bi
0.22	0.43	-0.02	0.03	0.37	0.27	0.06	0.12	-0.04	0.17	0.04	0.17	-0.01	0.36	0.39	-0.07	0.50	0.36	0.47	0.14	0.00	Bi*
0.13	0.15	0.05	0.07	0.16	0.15	-0.02	0.03	0.00	0.17	-0.04	0.11	-0.01	0.13	0.13	-0.08	0.10	0.06	0.12	0.05	-0.02	Cd*
0.87	0.30	0.04	0.02	0.20	-0.12	0.05	0.11	-0.03	0.24	0.02	0.99	0.51	0.16	0.87	-0.01	0.55	0.02	0.69	0.16	0.28	Ce
-0.05	-0.42	0.03	-0.02	-0.45	-0.03	0.61	-0.02	0.11	-0.33	0.07	0.02	0.43	-0.44	-0.03	0.66	-0.01	0.03	-0.12	0.34	0.14	Cr
-0.12	-0.31	0.04	0.02	-0.31	0.19	0.79	-0.01	0.04	-0.26	0.05	-0.11	0.20	-0.34	-0.12	0.75	0.01	0.15	-0.14	0.52	-0.06	Cu
0.00	-0.32	0.07	0.00	-0.34	0.09	0.84	-0.01	0.13	-0.16	0.07	0.01	0.37	-0.36	-0.02	0.89	0.05	0.13	-0.08	0.62	0.07	Fe
0.42	0.56	0.09	0.12	0.59	0.11	0.33	-0.01	-0.07	0.64	0.00	0.28	0.09	0.50	0.24	0.15	0.14	0.18	0.15	0.46	-0.14	Ga
-0.01	0.18	-0.05	0.00	0.18	0.15	0.17	-0.01	0.02	0.02	-0.02	-0.06	-0.03	0.13	0.03	0.07	0.06	0.12	0.05	0.22	-0.09	Ge
0.18	-0.10	0.03	0.02	-0.18	-0.08	0.19	0.02	0.36	-0.09	0.52	0.32	0.36	-0.15	0.38	0.19	0.25	0.04	0.22	-0.05	0.98	Hf
0.86	0.29	0.04	0.02	0.19	-0.12	0.05	0.10	-0.03	0.23	0.02	0.98	0.52	0.15	0.86	0.00	0.54	0.02	0.67	0.17	0.27	La
0.22	0.10	0.10	0.04	0.05	0.07	0.53	0.02	-0.01	0.13	0.00	0.20	0.25	0.05	0.25	0.46	0.23	0.06	0.21	0.42	0.08	Mn
-0.19	-0.24	-0.09	-0.09	-0.22	0.10	0.17	-0.02	0.21	-0.23	0.08	-0.18	0.01	-0.21	-0.15	0.22	-0.03	0.05	-0.12	0.08	0.07	Mo
-0.01	-0.09	-0.07	-0.09	-0.10	0.40	0.24	0.03	0.02	-0.07	0.00	-0.04	0.04	0.10	-0.02	0.21	0.05	0.48	-0.01	0.14	-0.04	Mo*
0.35	-0.17	0.05	0.04	-0.23	-0.04	0.31	0.05	0.22	-0.20	0.43	0.52	0.79	-0.21	0.48	0.28	0.31	0.06	0.26	0.32	0.63	Nb
0.87	0.30	0.04	0.02	0.20	-0.12	0.05	0.11	-0.03	0.24	0.02	0.99	0.51	0.16	0.87	-0.01	0.56	0.02	0.69	0.16	0.28	Nd
-0.07	-0.27	0.06	0.01	-0.29	0.10	0.78	-0.02	0.06	-0.17	0.04	-0.08	0.22	-0.31	-0.11	0.79	-0.03	0.07	-0.14	0.54	0.00	Ni
	0.47	0.01	-0.01	0.40	-0.07	-0.01	0.09	-0.04	0.43	0.00	0.90	0.24	0.34	0.83	-0.09	0.56	0.06	0.72	0.16	0.17	P*
		0.03	0.13	0.96	0.07	-0.34	0.05	-0.15	0.81	-0.04	0.34	-0.24	0.87	0.41	-0.46	0.27	0.06	0.42	-0.07	-0.13	Pb
			0.63	0.03	-0.10	0.03	0.04	-0.06	0.11	0.05	0.03	0.04	-0.01	0.00	0.04	-0.05	-0.09	-0.03	0.13	0.02	Pd#
				0.14	-0.02	-0.03	-0.02	-0.07	0.16	0.06	0.02	0.04	0.08	0.01	-0.06	-0.06	-0.10	-0.04	0.11	-0.01	Pt#
					0.10	-0.36	0.02	-0.18	0.83	-0.04	0.24	-0.30	0.89	0.28	-0.51	0.16	0.08	0.29	-0.03	-0.21	Rb
						0.10	0.04	-0.03	0.02	0.03	-0.12	-0.08	0.15	-0.08	0.02	0.04	0.29	-0.04	0.06	-0.08	Sb*
							-0.01	0.15	-0.22	0.08	0.02	0.38	-0.36	0.02	0.84	0.09	0.16	-0.06	0.46	0.18	Sc
								0.00	-0.01	-0.02	0.13	0.01	0.03	0.21	-0.02	0.28	0.04	0.28	0.01	0.04	Se
									-0.14	0.13	-0.04	0.09	-0.15	-0.01	0.22	0.07	0.06	-0.01	-0.03	0.40	Sn
										-0.03	0.26	-0.21	0.73	0.24	-0.30	0.11	0.04	0.22	0.05	-0.13	Sr
											0.02	0.08	-0.05	0.09	0.06	0.05	0.06	-0.01	0.07	0.55	Ta
												0.47	0.20	0.90	-0.05	0.59	0.02	0.73	0.14	0.28	Th
													-0.27	0.35	0.38	0.19	0.01	0.14	0.34	0.30	Ti
														0.25	-0.48	0.15	0.14	0.27	-0.11	-0.17	Tl*
															-0.07	0.77	0.06	0.91	0.08	0.37	U
																0.00	0.07	-0.12	0.43	0.20	V
																	0.28	0.86	0.03	0.28	W
																		0.06	0.13	0.05	W*
																			-0.01	0.24	Y
																				-0.07	Zn
																					Zr

Table 7. Pearson product-moment correlation coefficients for EBAGOOLA sheet area on log-transformed data (N=744).

	Ag‡	As	Au‡	Ba	Be‡	Bi	Bi‡	Cd‡	Ce	Cr	Cu	Fe	Ga	Ge	Hf	La	Mn	Mo	Mo‡	Nb	Nd	Ni
Ag‡		0.24	0.18	0.18	0.34	0.06	0.38	0.19	0.21	0.04	0.15	0.23	0.28	0.17	0.04	0.21	0.30	-0.01	0.12	0.22	0.22	0.15
As			0.23	0.03	0.32	0.03	0.33	0.11	-0.04	0.36	0.56	0.61	0.29	0.13	-0.05	-0.04	0.42	0.16	0.27	0.21	-0.03	0.48
Au‡				0.14	0.25	-0.02	0.27	0.00	-0.03	-0.05	0.11	0.09	0.15	0.15	-0.12	-0.03	0.22	-0.04	0.03	-0.13	-0.03	0.11
Ba					0.67	0.01	0.16	0.19	0.50	-0.56	-0.32	-0.19	0.65	0.00	-0.34	0.50	0.42	-0.26	-0.04	-0.33	0.50	-0.25
Be‡						0.09	0.52	0.19	0.37	-0.22	0.08	0.20	0.74	0.31	-0.30	0.38	0.60	-0.06	0.07	-0.11	0.39	0.11
Bi							0.15	-0.01	0.17	-0.01	-0.02	0.03	0.02	0.05	0.26	0.16	0.11	0.05	-0.02	0.17	0.17	-0.02
Bi‡								0.20	0.15	-0.08	0.12	0.15	0.33	0.40	-0.08	0.17	0.33	0.03	0.20	0.07	0.16	0.02
Cd‡									0.17	-0.12	-0.07	0.00	0.16	0.01	0.02	0.17	0.13	0.03	0.07	0.04	0.17	-0.10
Ce										-0.19	-0.12	0.04	0.42	-0.05	0.22	0.99	0.42	-0.27	0.01	0.38	0.99	-0.14
Cr											0.78	0.72	-0.09	0.00	0.34	-0.18	0.15	0.20	0.20	0.53	-0.18	0.79
Cu												0.84	0.16	0.14	0.08	-0.11	0.40	0.23	0.24	0.40	-0.11	0.89
Fe													0.34	0.11	0.24	0.05	0.57	0.20	0.27	0.47	0.05	0.83
Ga														0.20	-0.16	0.42	0.52	-0.10	0.11	0.00	0.42	0.22
Ge															-0.12	-0.05	0.11	0.04	0.09	0.02	-0.05	0.11
Hf																0.19	0.00	0.02	0.03	0.59	0.21	0.12
La																	0.43	-0.27	0.01	0.37	0.99	-0.13
Mn																		-0.03	0.15	0.16	0.44	0.42
Mo																			0.08	0.06	-0.26	0.19
Mo‡																				0.12	0.00	0.20
Nb																					0.38	0.35
Nd																						-0.13
Ni																						
P‡																						
Pb																						
Pd‡																						
Pt‡																						
Rb																						
Sb‡																						
Sc																						
Se																						
Sn																						
Sr																						
Ta																						
Th																						
Ti																						
Tl‡																						
U																						
V																						
W																						
W‡																						
Y																						
Zn																						
Zr																						

P‡	Pb	Pd‡	Pt‡	Rb	Sb‡	Sc	Se	Sn	Sr	Ta	Th	Ti	Tl‡	U	V	W	W‡	Y	Zn	Zr	
0.32	0.22	0.12	0.12	0.25	0.25	0.18	0.06	0.06	0.24	0.15	0.18	0.11	0.14	0.26	0.10	0.24	0.27	0.29	0.32	0.05	Ag‡
0.05	-0.09	0.02	-0.03	0.10	0.26	0.44	0.02	0.25	0.10	0.13	-0.12	0.25	-0.11	-0.03	0.42	0.16	0.32	0.00	0.57	-0.07	As
0.06	0.15	0.15	0.14	0.17	0.20	0.05	0.03	-0.04	0.14	-0.01	-0.02	-0.15	0.12	0.03	-0.03	0.03	0.09	0.03	0.11	-0.12	Au‡
0.67	0.88	0.12	0.19	0.91	0.08	-0.30	0.01	-0.43	0.93	-0.08	0.51	-0.43	0.76	0.36	-0.51	0.08	0.05	0.28	0.21	-0.40	Ba
0.55	0.67	0.08	0.14	0.73	0.16	0.08	0.00	-0.15	0.73	0.06	0.33	-0.23	0.52	0.34	-0.17	0.20	0.21	0.32	0.52	-0.34	Be‡
0.08	0.09	-0.01	-0.02	0.04	0.04	0.04	-0.01	0.16	0.03	0.10	0.16	0.04	0.07	0.23	0.03	0.19	0.05	0.21	0.00	0.26	Bi
0.18	0.33	-0.02	0.02	0.33	0.30	0.13	0.09	0.06	0.19	0.03	0.15	-0.07	0.24	0.33	-0.02	0.36	0.36	0.40	0.26	-0.07	Bi‡
0.22	0.19	0.05	0.07	0.20	0.09	-0.04	0.04	-0.02	0.17	-0.02	0.18	-0.02	0.17	0.18	-0.07	0.11	0.05	0.17	0.11	-0.01	Cd‡
0.81	0.55	0.06	0.10	0.52	-0.14	-0.03	0.08	-0.11	0.50	0.00	0.97	0.22	0.37	0.85	-0.15	0.50	0.08	0.80	0.32	0.21	Ce
-0.28	-0.61	0.00	-0.08	-0.50	-0.03	0.72	-0.05	0.39	-0.44	0.16	-0.27	0.71	-0.61	-0.17	0.85	0.03	0.10	-0.19	0.37	0.35	Cr
-0.16	-0.41	0.06	0.00	-0.24	0.09	0.75	-0.01	0.31	-0.21	0.16	-0.24	0.58	-0.47	-0.15	0.79	0.08	0.21	-0.16	0.61	0.08	Cu
0.02	-0.27	0.10	0.02	-0.13	0.07	0.83	-0.01	0.37	-0.02	0.14	-0.08	0.62	-0.36	0.00	0.84	0.15	0.22	-0.01	0.72	0.22	Fe
0.54	0.67	0.12	0.15	0.61	0.10	0.24	0.00	-0.07	0.72	0.03	0.38	-0.04	0.49	0.34	0.00	0.16	0.19	0.25	0.52	-0.22	Ga
-0.02	0.12	-0.07	-0.01	0.09	0.15	0.14	-0.01	0.08	0.00	-0.02	-0.05	-0.07	0.08	0.07	0.02	0.08	0.22	0.10	0.17	-0.11	Ge
-0.05	-0.22	0.01	-0.01	-0.36	-0.09	0.36	0.03	0.47	-0.25	0.14	0.21	0.53	-0.26	0.39	0.45	0.25	-0.02	0.32	-0.04	0.97	Hf
0.81	0.55	0.06	0.10	0.53	-0.13	-0.02	0.08	-0.14	0.50	0.00	0.97	0.22	0.37	0.85	-0.15	0.49	0.08	0.79	0.32	0.18	La
0.47	0.34	0.18	0.14	0.49	0.09	0.39	0.04	-0.03	0.52	0.01	0.33	0.17	0.22	0.34	0.25	0.25	0.17	0.33	0.67	-0.02	Mn
-0.22	-0.26	-0.09	-0.10	-0.19	0.11	0.16	-0.02	0.21	-0.23	0.13	-0.30	0.10	-0.21	-0.23	0.21	-0.02	0.08	-0.19	0.08	0.02	Mo
0.03	-0.06	-0.09	-0.10	-0.05	0.49	0.28	0.03	0.13	-0.02	0.04	-0.04	0.11	0.11	0.05	0.23	0.06	0.68	0.07	0.17	0.03	Mo‡
0.10	-0.25	0.04	0.02	-0.25	-0.07	0.48	0.06	0.45	-0.26	0.25	0.35	0.85	-0.29	0.43	0.54	0.39	0.14	0.37	0.38	0.60	Nb
0.82	0.55	0.07	0.10	0.53	-0.14	-0.02	0.08	-0.11	0.51	0.01	0.96	0.22	0.36	0.85	-0.14	0.50	0.08	0.80	0.33	0.21	Nd
-0.14	-0.35	0.09	0.01	-0.21	0.10	0.76	-0.02	0.29	-0.13	0.15	-0.26	0.54	-0.41	-0.20	0.78	-0.02	0.17	-0.24	0.58	0.10	Ni
	0.66	0.06	0.08	0.65	-0.06	-0.10	0.06	-0.17	0.70	-0.01	0.78	-0.06	0.52	0.65	-0.25	0.36	0.13	0.63	0.34	-0.06	P‡
		0.06	0.18	0.85	0.09	-0.31	0.04	-0.34	0.84	-0.05	0.59	-0.43	0.81	0.52	-0.56	0.19	0.08	0.43	0.09	-0.27	Pb
			0.63	0.10	-0.13	0.04	0.04	-0.09	0.16	0.01	0.04	0.06	0.02	0.03	0.06	-0.06	-0.12	0.01	0.16	-0.01	Pd‡
				0.21	-0.06	-0.03	-0.02	-0.15	0.20	0.03	0.11	0.03	0.11	0.08	-0.03	-0.07	-0.13	0.00	0.13	-0.05	Pt‡
					0.09	-0.28	0.03	-0.47	0.85	-0.04	0.54	-0.37	0.73	0.42	-0.49	0.13	0.08	0.34	0.33	-0.42	Rb
						0.08	0.04	0.07	0.03	0.06	-0.14	-0.09	0.22	-0.07	0.02	0.05	0.52	-0.06	0.03	-0.10	Sb‡
							-0.02	0.42	-0.16	0.14	-0.12	0.60	-0.38	0.03	0.82	0.17	0.21	0.01	0.51	0.35	Sc
								0.02	0.00	-0.03	0.08	0.02	0.04	0.11	-0.02	0.13	0.05	0.13	0.00	0.04	Se
									-0.31	0.23	-0.17	0.39	-0.34	0.00	0.50	0.19	0.15	0.04	0.06	0.52	Sn
										-0.04	0.49	-0.33	0.70	0.36	-0.36	0.10	0.07	0.31	0.32	-0.31	Sr
											-0.01	0.17	-0.08	0.05	0.14	0.05	0.08	0.02	0.13	0.14	Ta
												0.15	0.44	0.88	-0.25	0.47	0.04	0.80	0.22	0.20	Th
													-0.49	0.19	0.74	0.24	0.07	0.13	0.43	0.52	Ti
														0.38	-0.59	0.09	0.15	0.31	-0.03	-0.30	Tl‡
															-0.11	0.56	0.13	0.90	0.20	0.40	U
																0.09	0.11	-0.11	0.43	0.46	V
																	0.22	0.64	0.14	0.29	W
																		0.16	0.22	-0.02	W‡
																			0.14	0.36	Y
																				-0.08	Zn
																					Zr

Table 8. Spearman rank correlation coefficients for EBAGOOLA sheet area data (N=744).

	Ag‡	As	Au‡	Ba	Be‡	Bi	Bi‡	Cd‡	Ce	Cr	Cu	Fe	Ga	Ge	Hf	La	Mn	Mo	Mo‡	Nb	Nd	Ni
Ag‡		0.24	0.16	0.14	0.33	0.07	0.41	0.24	0.20	0.06	0.16	0.23	0.29	0.21	0.03	0.21	0.28	-0.01	0.15	0.21	0.21	0.15
As			0.22	-0.07	0.30	0.00	0.33	0.08	-0.04	0.40	0.57	0.63	0.23	0.14	-0.08	-0.04	0.40	0.16	0.25	0.23	-0.03	0.51
Au‡				0.11	0.25	-0.01	0.30	0.01	-0.02	-0.01	0.10	0.09	0.15	0.18	-0.12	-0.01	0.21	-0.02	0.05	-0.11	-0.02	0.11
Ba					0.61	0.02	0.14	0.23	0.56	-0.60	-0.43	-0.29	0.61	0.01	-0.34	0.56	0.26	-0.25	-0.08	-0.40	0.55	-0.35
Be‡						0.08	0.51	0.22	0.41	-0.17	0.04	0.14	0.73	0.36	-0.32	0.41	0.51	-0.05	0.06	-0.15	0.41	0.07
Bi							0.13	0.01	0.15	0.00	-0.02	0.04	0.03	0.04	0.17	0.15	0.11	0.06	-0.02	0.11	0.15	-0.02
Bi‡								0.22	0.17	-0.06	0.12	0.15	0.30	0.43	-0.15	0.19	0.31	0.03	0.19	0.05	0.17	0.04
Cd‡									0.18	-0.12	-0.04	0.03	0.20	0.02	0.01	0.18	0.16	0.01	0.05	0.03	0.18	-0.08
Ce										-0.19	-0.15	-0.01	0.45	-0.03	0.09	0.99	0.39	-0.30	-0.02	0.25	0.99	-0.15
Cr											0.84	0.79	-0.22	0.04	0.32	-0.20	0.27	0.20	0.21	0.55	-0.18	0.86
Cu												0.86	0.11	0.15	0.10	-0.15	0.39	0.22	0.25	0.45	-0.14	0.91
Fe													0.29	0.12	0.23	-0.01	0.58	0.18	0.27	0.49	0.01	0.85
Ga														0.25	-0.12	0.44	0.49	-0.11	0.12	0.00	0.45	0.17
Ge															-0.16	-0.03	0.15	0.06	0.09	0.01	-0.03	0.12
Hf																0.06	0.05	-0.04	0.02	0.55	0.09	0.12
La																	0.38	-0.31	-0.01	0.24	0.98	-0.16
Mn																		-0.03	0.14	0.17	0.39	0.43
Mo																			0.10	0.05	-0.30	0.18
Mo‡																				0.14	-0.01	0.21
Nb																					0.25	0.39
Nd																						-0.14
Ni																						
P‡																						
Pb																						
Pd‡																						
Pt‡																						
Rb																						
Sb‡																						
Sc																						
Se																						
Sn																						
Sr																						
Ta																						
Th																						
Ti																						
Tl‡																						
U																						
V																						
W																						
W‡																						
Y																						
Zn																						
Zr																						

P‡	Pb	Pd‡	Pt‡	Rb	Sb‡	Sc	Se	Sn	Sr	Ta	Th	Ti	Tl‡	U	V	W	W‡	Y	Zn	Zr	
0.25	0.22	0.10	0.11	0.21	0.29	0.20	0.04	0.09	0.18	0.12	0.17	0.14	0.15	0.27	0.11	0.24	0.29	0.29	0.32	0.04	Ag‡
-0.03	-0.13	0.05	-0.01	-0.06	0.26	0.49	0.02	0.30	-0.02	0.11	-0.15	0.29	-0.15	-0.04	0.48	0.17	0.28	0.02	0.58	-0.10	As
0.02	0.16	0.15	0.14	0.17	0.18	0.07	0.04	-0.02	0.11	-0.02	-0.02	-0.12	0.13	0.04	0.00	0.02	0.12	0.01	0.11	-0.12	Au‡
0.69	0.90	0.09	0.17	0.93	0.07	-0.34	0.01	-0.40	0.93	-0.09	0.59	-0.47	0.79	0.38	-0.56	0.04	0.01	0.29	0.09	-0.39	Ba
0.53	0.66	0.06	0.13	0.70	0.20	0.09	-0.01	-0.09	0.67	0.05	0.35	-0.21	0.54	0.35	-0.14	0.21	0.20	0.33	0.45	-0.34	Be‡
0.08	0.10	-0.02	-0.02	0.06	0.07	0.06	-0.01	0.12	0.04	0.03	0.14	0.03	0.08	0.21	0.05	0.19	0.01	0.20	0.00	0.17	Bi
0.14	0.33	-0.01	0.04	0.32	0.35	0.14	0.08	0.11	0.14	0.01	0.15	-0.04	0.24	0.31	-0.01	0.34	0.36	0.35	0.25	-0.12	Bi‡
0.22	0.22	0.08	0.12	0.24	0.11	0.01	0.05	-0.01	0.22	0.00	0.18	-0.03	0.17	0.20	-0.06	0.11	0.06	0.17	0.13	-0.01	Cd‡
0.83	0.60	0.07	0.13	0.55	-0.11	-0.05	0.07	-0.14	0.55	-0.02	0.94	0.15	0.43	0.80	-0.20	0.43	0.05	0.75	0.31	0.09	Ce
-0.28	-0.59	0.01	-0.07	-0.62	-0.01	0.80	-0.03	0.45	-0.51	0.17	-0.32	0.71	-0.62	-0.16	0.91	0.10	0.14	-0.12	0.45	0.33	Cr
-0.23	-0.44	0.06	-0.01	-0.42	0.10	0.81	-0.01	0.37	-0.36	0.18	-0.30	0.61	-0.50	-0.16	0.85	0.11	0.21	-0.12	0.63	0.10	Cu
-0.06	-0.30	0.09	0.01	-0.31	0.09	0.87	0.00	0.43	-0.16	0.15	-0.16	0.62	-0.39	-0.02	0.88	0.18	0.21	0.01	0.73	0.22	Fe
0.58	0.64	0.10	0.13	0.61	0.12	0.29	-0.01	0.01	0.69	0.03	0.40	-0.03	0.52	0.36	0.05	0.16	0.19	0.28	0.48	-0.17	Ga
-0.01	0.15	-0.04	0.00	0.16	0.17	0.14	-0.01	0.10	0.03	-0.02	-0.04	-0.04	0.10	0.07	0.05	0.10	0.23	0.10	0.19	-0.15	Ge
-0.09	-0.25	0.01	-0.03	-0.36	-0.11	0.34	0.03	0.40	-0.24	0.08	0.09	0.49	-0.28	0.33	0.40	0.19	-0.09	0.28	-0.03	0.97	Hf
0.83	0.60	0.06	0.13	0.55	-0.11	-0.05	0.07	-0.16	0.54	-0.02	0.95	0.14	0.43	0.80	-0.21	0.43	0.06	0.75	0.31	0.06	La
0.39	0.28	0.17	0.12	0.28	0.12	0.48	0.05	0.10	0.36	0.01	0.28	0.21	0.17	0.32	0.34	0.25	0.15	0.31	0.63	0.05	Mn
-0.25	-0.26	-0.09	-0.10	-0.22	0.13	0.16	-0.03	0.18	-0.24	0.10	-0.33	0.09	-0.21	-0.26	0.21	-0.02	0.09	-0.21	0.08	-0.04	Mo
-0.01	-0.07	-0.08	-0.10	-0.10	0.49	0.28	0.03	0.18	-0.07	0.06	-0.08	0.12	0.11	0.02	0.25	0.06	0.67	0.06	0.18	0.02	Mo‡
0.03	-0.32	0.02	-0.01	-0.37	-0.03	0.49	0.07	0.47	-0.35	0.18	0.20	0.88	-0.36	0.36	0.55	0.40	0.15	0.35	0.40	0.56	Nb
0.83	0.58	0.07	0.13	0.54	-0.13	-0.04	0.07	-0.13	0.55	-0.02	0.93	0.16	0.41	0.80	-0.19	0.43	0.05	0.76	0.32	0.10	Nd
-0.20	-0.38	0.09	0.01	-0.37	0.11	0.81	-0.02	0.33	-0.27	0.16	-0.30	0.57	-0.44	-0.19	0.84	0.02	0.17	-0.18	0.61	0.10	Ni
	0.70	0.04	0.08	0.66	-0.08	-0.12	0.05	-0.17	0.71	-0.02	0.80	-0.07	0.57	0.64	-0.28	0.34	0.10	0.61	0.26	-0.09	P‡
		0.05	0.18	0.95	0.10	-0.32	0.04	-0.33	0.86	-0.08	0.65	-0.44	0.84	0.53	-0.55	0.15	0.06	0.42	0.04	-0.28	Pb
			0.63	0.06	-0.10	0.04	0.04	-0.08	0.13	0.00	0.05	0.05	0.01	0.04	0.05	-0.04	-0.13	0.03	0.15	-0.02	Pd‡
				0.18	-0.03	-0.03	-0.03	-0.14	0.17	0.03	0.14	-0.01	0.10	0.11	-0.05	-0.05	-0.14	0.04	0.12	-0.06	Pt‡
					0.11	-0.36	0.03	-0.41	0.87	-0.08	0.61	-0.49	0.85	0.47	-0.60	0.09	0.05	0.35	0.11	-0.40	Rb
						0.11	0.05	0.08	0.02	0.07	-0.12	-0.06	0.22	-0.04	0.04	0.04	0.50	-0.04	0.07	-0.12	Sb‡
							-0.01	0.50	-0.23	0.15	-0.18	0.61	-0.40	0.01	0.88	0.20	0.23	0.03	0.57	0.34	Sc
								0.02	-0.01	-0.03	0.06	0.03	0.04	0.07	-0.02	0.08	0.06	0.08	0.01	0.03	Se
									-0.30	0.19	-0.22	0.44	-0.32	0.00	0.56	0.23	0.17	0.07	0.15	0.43	Sn
										-0.06	0.55	-0.40	0.75	0.39	-0.44	0.06	0.01	0.32	0.18	-0.28	Sr
											-0.03	0.17	-0.09	0.02	0.17	0.03	0.07	0.04	0.13	0.08	Ta
												0.06	0.50	0.84	-0.34	0.39	0.01	0.75	0.18	0.08	Th
													-0.51	0.17	0.70	0.27	0.11	0.18	0.47	0.48	Ti
														0.40	-0.60	0.06	0.15	0.30	-0.07	-0.30	Tl‡
															-0.14	0.49	0.10	0.87	0.20	0.34	U
																0.13	0.16	-0.09	0.48	0.41	V
																	0.22	0.55	0.18	0.24	W
																		0.14	0.21	-0.07	W‡
																			0.20	0.31	Y
																				-0.06	Zn
																					Zr

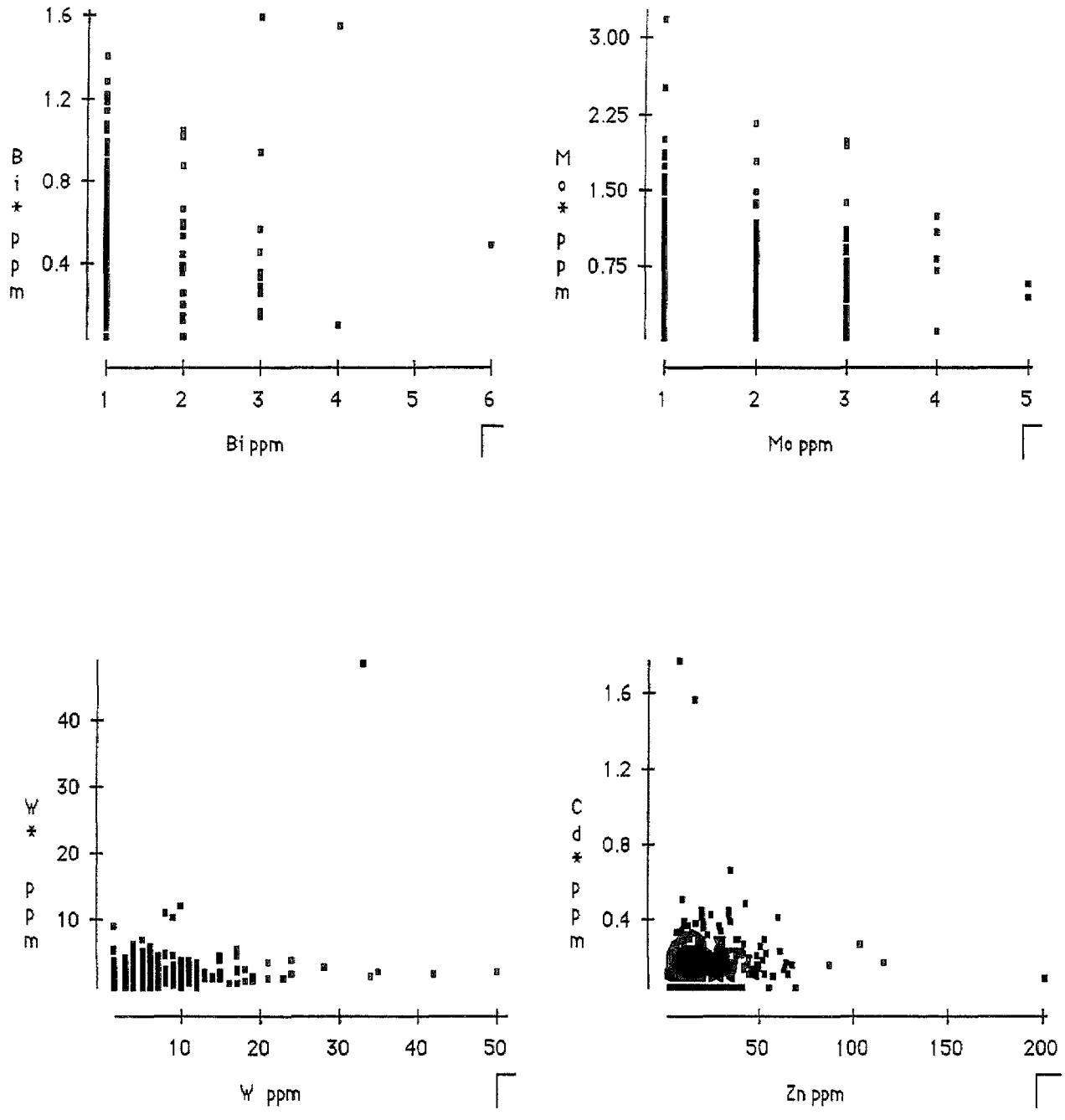

Figure 8 Scatterplots showing the relationships between duplicate analyses (AGSO/XRFS and Analabs/ICP-MS) for Bi, Mo and W, and between Cd (Analabs/ICP-MS) and Zn (AGSO/XRFS).

replicate analyses is not due solely to the relatively high detection limits of the XRFS method since there is little apparent correspondence between the higher values as shown in scattergrams (see Figure 8). Similarly Cd and Zn usually occur in a more or less fixed ratio of about 1:200 unless external processes have intervened (Hawkes & Webb, 1962). These anomalies are still under investigation.

4.3.2 Factor Analysis

In order to quantify the obvious interdependence of many of the variables the data were subjected to Principal Component Factor Analysis. Factor analysis determines whether multi-variate data occupy the same number of dimensions as the number of variables, or are contained in a smaller number of dimensions implying a lesser number of independent variables (Koch & Link, 1971; Dillon & Goldstein, 1984). The procedure operates from a matrix of Pearson product- moment correlation coefficients and therefore is bound by the same assumptions and limitations of that technique, principally the assumption that data are normally distributed, and the limitation of the adverse effects of outliers. For these reasons log-transformed data were used and scattergrams of apparently highly correlated element pairs (see Table 7) were viewed to reduce the incidence of outlier effects. The procedure was carried out, using STATVIEW II, on log-transformed data for the 38 elements for which full parameters are listed in Table 5. The analysis produced 7 factors each with Eigenvalues greater than 1 and which between them 'explained' at least 75% of the variability in the data (STATVIEW II manual, Feldman & others, 1990).

The factor loadings indicate the correlation between the variables and the factors. In this exercise the pattern matrix contains 266 values from 38 variables and 7 factors and many loadings, although statistically significant, are below an arbitrary level of 'practical significance'. This is the minimum amount of a variable's variance which reasonably is to be accounted for by the factor, a general level being +-0.30 (Dillon & Goldstein, 1984). Alternatively, only the loading with the largest absolute value for each variable is considered. In this exercise a composite approach has been used with the largest absolute value for each element labelled as a major contributors to a factor, while other practically significant loadings will be labelled as minor contributors. Table 9(a) lists the more significant factor loadings and the proportion of variation in the dataset due to each factor, and Table 9(b) the primary intercorrelations between factors. The communalities represent the proportion of the variance of the variable that can be predicted by the factors extracted, that is high communalities (0.6) are desirable since low communalities are generally given by elements which have significant numbers of 'not detected' values, or which are not strongly correlated with any other element (Eggo & others, in prep.).

Factor 1 comprises a strong association between Ce, La, Nd, Th, U, Y, P*, W and Nb, with minor contributions from Zr, Pb, Ti, Hf and Rb, and accounts for 27.7% of the total variability in the dataset. The communalities of these elements, except W (0.558), are very high (0.7) indicating that most of the variance due to these elements is accounted for by the factors extracted. Association between the Rare Earth Elements (REE) Ce, La and Nd, and Th, is extremely strong, both statistically ($r>0.9$, see Tables 6, 7 and 8) and spatially (see next section), and between these and Nb, P*, U, W and Y very strong.

The primary association probably reflects the presence of resistant accessory heavy minerals such as *Monazite* and *Xenotime*, and possibly *Apatite*, in the sediment (Price & Ferguson, 1980). These are likely to have been derived from the weathering of granitic rocks. High concentrations of these heavy minerals could be of economic interest.

Hf, Nb, Ti and Zr suggest other resistant heavy minerals such as *Zircon* and *Samarskite*, and Ti-bearing minerals such as *Ilmenite* or *Sphene*. Pb and Rb are from Factor 3 which shows high intercorrelation with Factor 1 (see Table 9(b), and below).

Table 9(a). Rotated factor loadings, eigenvalues and communalities for EBAGOOLA sheet area log-transformed data (N=744). Principal loadings in boldface.

	Communalities	F1	F2	F3	F4	F5	F6	F7
Ag*	0.461					0.308		**0.491**
As	0.572		**0.592**					
Au#	0.345					**0.510**		
Ba	0.928			**0.878**				
Be*	0.826			**0.735**		0.399		
Bi*	0.739					**0.741**		
Cd*	0.338							**0.536**
Ce	0.965	**0.915**		0.332				
Cr	0.836		**0.814**	-0.358				
Cu	0.881		**0.914**					
Fe	0.924		**0.943**					
Ga	0.751			**0.778**				
Ge	0.515					**0.703**		
Hf	0.893	0.328					**0.826**	
La	0.959	**0.912**		0.332				
Mn	0.700		0.527	**0.552**				
Mo*	0.809				**0.872**			
Nb	0.800	**0.534**	0.504	-0.333			0.310	
Nd	0.963	**0.912**		0.338				
Ni	0.865		**0.908**					
P*	0.796	**0.663**		0.568				
Pb	0.910	0.345	-0.353	**0.797**				
Rb	0.891	0.302		**0.800**			-0.324	
Sb*	0.662				**0.747**			
Sc	0.800		**0.826**					
Sn	0.599		0.309				**0.613**	
Sr	0.916			**0.916**				
Ta	0.544							**0.675**
Th	0.955	**0.910**		0.318				
Ti	0.833	0.342	**0.693**	-0.370				
Tl*	0.791		-0.453	**0.693**				
U	0.904	**0.887**						
V	0.905		**0.850**				0.321	
W	0.558	**0.643**				0.310		
W*	0.778				**0.838**			
Y	0.876	**0.878**						
Zn	0.815		**0.750**	0.333				
Zr	0.930	0.352		-0.311			**0.822**	
Eigenvalues		10.53	8.19	4.77	2.42	1.40	1.20	1.03
Proportion of original variance (%)		27.7	21.5	12.6	6.4	3.7	3.2	2.7
Cumulative (%)		27.7	49.2	61.8	68.2	71.9	75.1	77.8

Table 9(b). Primary intercorrelations for Factors in Table 9(a).

	F1	F2	F3	F4	F5	F6	F7
F1							
F2	-0.119						
F3	0.503	-0.225					
F4	0.014	0.131	0.108				
F5	0.105	0.076	0.295	0.329			
F6	0.041	0.251	-0.434	-0.019	-0.166		
F7	0.223	0.095	0.231	0.187	0.204	0.059	

Factor 2 comprises Fe, Cu, Ni, V, Sc, Cr, Zn, Ti and As, with minor contributions from Mn, Nb and Sn, and also negative contributions from Tl* and Pb. This factor accounts for 21.5% of the variance in the dataset. The communalities of As (0.572) and Sn (0.599) are low and indicate that a significant proportion of the variance of these elements is not accounted for by the factors extracted, and suggests that their importance in the factor is suspect.

The primary association centres on Fe and is probably partly due to the weathering of ferro-magnesium or Fe-sulphide minerals, and partly due to secondary Fe and Mn oxide scavenging. The latter would be facilitated by high Fe concentrations from the former.

Factor 3 comprises Sr, Ba, Rb, Pb, Ga, Be*, Tl* and Mn with lesser contributions from P*, Zn, Nd, Ce, La and Th, and negative contributions from Ti, Cr, Nb and Zr. This factor accounts for 12.6% of the variance of the dataset.

This factor also appears to be derived from the weathering of granitic rocks, primarily from the weathering of potassium minerals such as *K-feldspar*, *Biotite* and *Muscovite*. Ba, Pb, Rb, Sr and Tl* all concentrate in K-minerals, substituting for K^+ (see Section 4.3.1), and Ga has an association with Al (Burton & Culkin, 1972). Be also concentrates in *Biotite*, *Muscovite* and *Plagioclase* (Hormann, 1969).

This factor intercorrelates highly with Factor 1, no doubt due to their suspected granitic origins, and is negatively intercorrelated with Factor 2 since the later is more 'mafic' in character.

Factor 4 comprises Mo*, W* and Sb*. Although this factor accounts for 6.4% of the variance of the dataset, its basis is not apparent.

Factor 5 comprises Bi*, Ge and Au# with lesser contributions from Be*, W and Ag*. This factor accounts for 3.7% of the total variance of the dataset but the communalities of Ge (0.515), Au# (0.345), W (0.558) and Ag* (0.461) are very low and indicate that much of the variance of these elements is not accounted for by the factors. Despite this the association between Bi*, Au#, W and Ag* may have some geochemical significance.

Factor 6 comprises Hf, Zr and Sn with lesser contributions from V and Nb, and a negative contributions from Rb. The communality of Sn (0.599) is marginal. This factor is obviously due to *Zircon*, possibly containing U (factor loading 0.214 — see above) and *Cassiterite*, both resistant heavy minerals weathered from granitic rocks. {The negative contribution from Rb and Ba from Factor 3 suggests granitic rocks containing lower concentrations of K-mineral.}

Factor 7 comprises Ta, Cd and Ag*. This factor accounts for only 2.7% of the total variability in the data and the communalities of the variables are all very low. The association is difficult to explain.

INTERPRETATION

Interpretation of the surficial geochemistry of the EBAGOOLA sheet area will be in terms of the factor groupings discussed in the previous section (see Table 9).

5.1 Factor 1

Factor 1 comprises Ce, La, Nd, Th, U, Y, P*, W and Nb with minor contributions from Zr, Pb, Ti, Hf and Rb, and is considered to be due primarily to the concentration in the sediment of resistant accessory minerals from weathered granitic and metamorphic rocks, plus elements released during weathering of K-minerals mainly from granitic rocks. The relative abundances of the principal

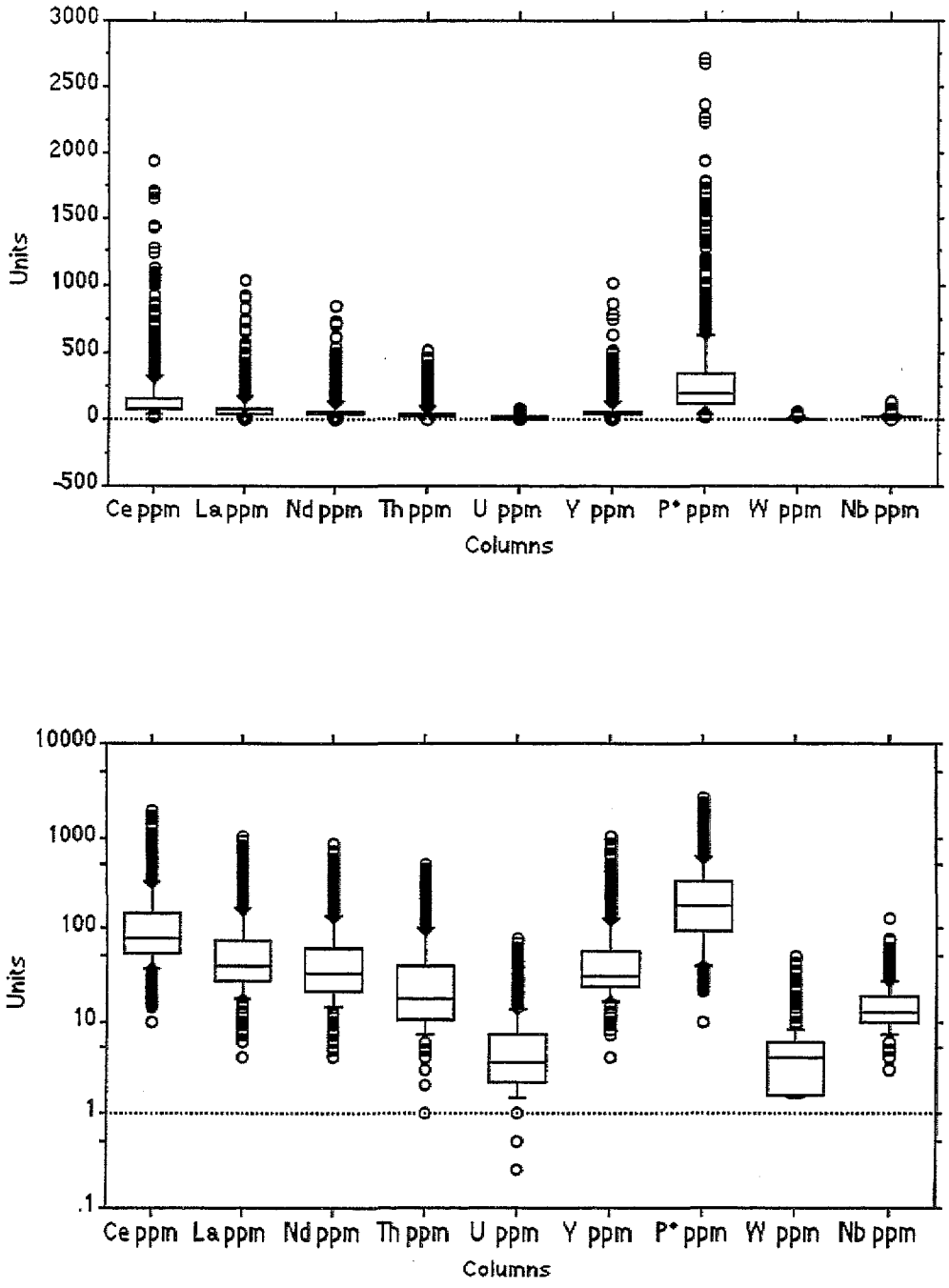

Figure 9 Box plots showing relative abundances of Factor 1 elements (Ce, La, Nd, Th, U, Y, P*, W and Nb). The top and bottom of the box are the 1*s* limits and the line in the box is the mean.

elements in the factor are shown in the box plots in Figure 9. Figure 10 shows image maps of the distribution of Ce, Th, Y, U, Nb and scores for Factor 1 (F1) in the EBAGOOLA sheet area and Figure 11 the outlines of the areas containing the top 20% of grid values of the factor scores and principal elements.

High scores for the factor concentrate over two areas (**1A** and **1B** in Figure 10) in the north, and a larger area (**1C**) in the south of the sheet area. Three smaller areas (**1D**, **1E** and **1F**) are also of interest.

Area **1A** (see Figure 10) is west of the Stewart River in the headwaters of the Holroyd River and of Thornbury Creek. Regolith is weathered saprolite in rises and low hills of the Coleman Regolith-Landform Association and formed from in situ weathering of rocks of the Coen Metamorphics, and to a lesser extent from Ebagoola and Burns Granites. The area shows highs for Ce, La, Nd, Th, U and P^*, and to a lesser extent in Y and Ti.

Area **1B** is to the east of **1A** and covers the coastal escarpment. Above the escarpment the area centres on Little Stewart and Penny Creeks, and below it on Knife Creek. The area above the escarpment overlays Newberry Metamorphics with some Lankelly and Kintore Granite in the west. The hills and rises have been formed by in situ weathering of the bedrock. Below the escarpment the regolith a mixture of in situ, highly-weathered saprolite from metamorphics, and flood plains of transported sediments derived from from granites and metamorphics, presumably from above the escarpment. The transported sediments may be responsible for extension, or enhancement, of the anomaly below the escarpment. The area shows highs in Ce, La, Nd, Th, U, P^*, Nb, Ti and Hf, with lesser Y and Zr. The Hf and Zr seem to be concentrated below the escarpment. The presence of transported regolith in drainage basins below the escarpment may have the effect of enlarging the apparent anomaly as these sediments are reincorporated in the stream bed lode.

Area **1C** covers an arc west of the Musgrave homestead from Bamboo homestead in the north to Saltwater Creek in the south. Many of the streams are left bank tributaries of the Coleman River. Underlying rocks are from the Kintore and Ebagoola Granites. Above the escarpment landforms include rises of weathered saprolite and residual sand formed by in situ weathering of the bedrock. Below the escarpment is a mixture of in situ and transported regolith with low hills and rises of weathered saprolite and residual sand formed on granite, and transported sediments derived from granite overlying granite and metamorphics. The element patterns differ markedly from areas **1A** and **1B** in that Y, U, P and W are more pronounced than are Ce, La, Nd and Th. Pb and Rb also show highs.

Area **1D** is to the west of **1C** in the headwaters of Two Rail and Swamp Creeks. Weathering is in situ and the rises and residual sands overlay another outcrop of Ebagoola Granite and/or Barwon Granite. The area shows highs in Ce, La, Nd, Th, U, Y and P^*.

Area **1E** consists of rises in an erosional plain of weathered saprolite from the Bulimba Formation, in an area bounded by Emu and Moonlight Creeks and the Big Spring. Regolith is in situ. The F1 score appears to be due mainly to the presence of Hf, Nb and Zr.

Area **1F** is over the Warner Granite and possibly units of the Holroyd Metamorphics, in south of the sheet area. The area comprises rises and low hills. The area shows highs in U, Y and W.

As one would expect from the very high statistical correlation shown between Ce and the other light REE's, La and Nd ($r = 0.98$-1.00; see Tables 6, 7 and 8), their spatial correlation is also extremely close, there being very little difference between the 3 image maps. This is also shown in Figure 11 in which the outlines for Ce, La and Nd (plus Th, U, Y and P) are almost indistinguishable.

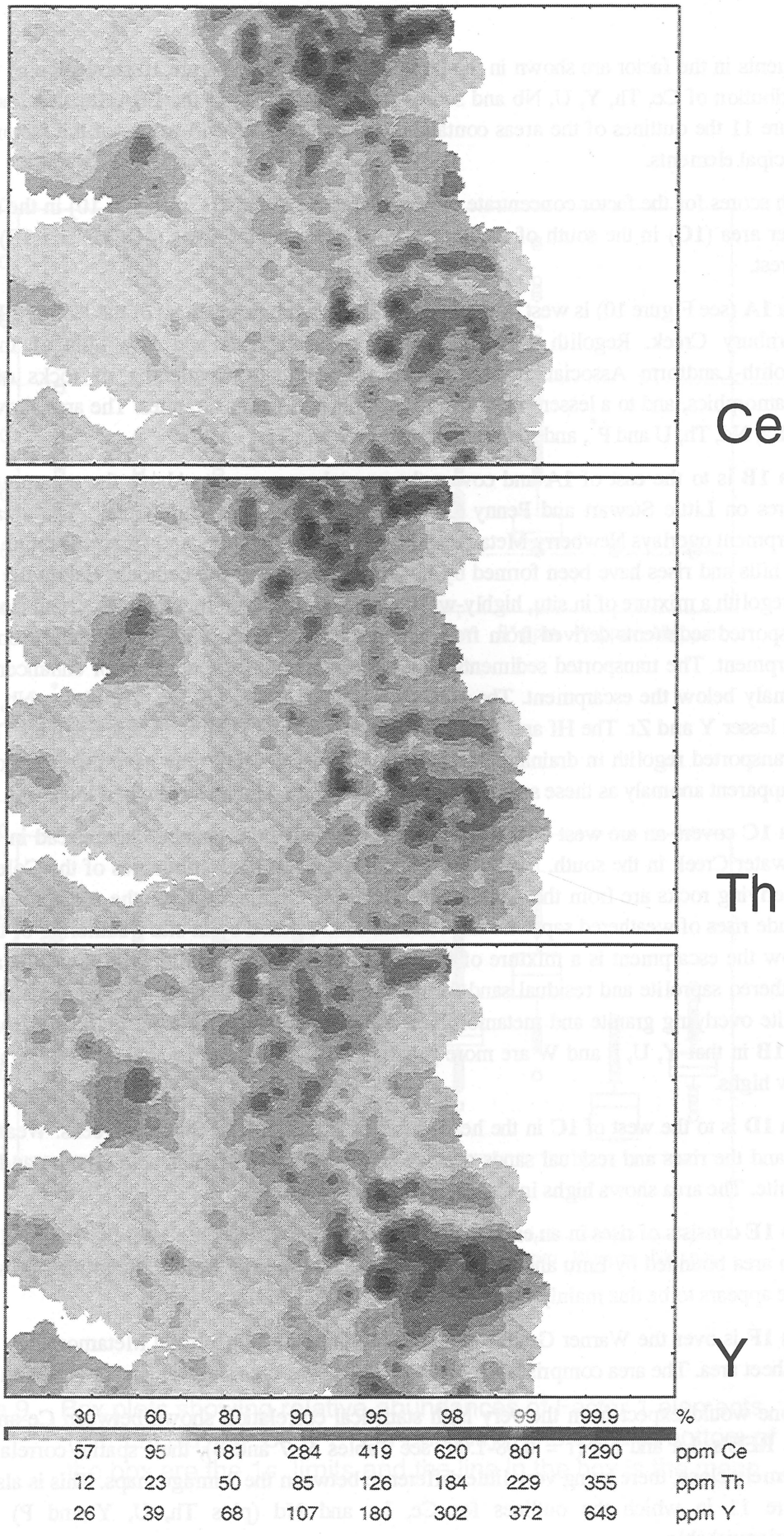

Figure 10 Image maps for selected Factor 1 elements (Ce, Th, Y, U and Nb) and for Factor 1 scores (F1).

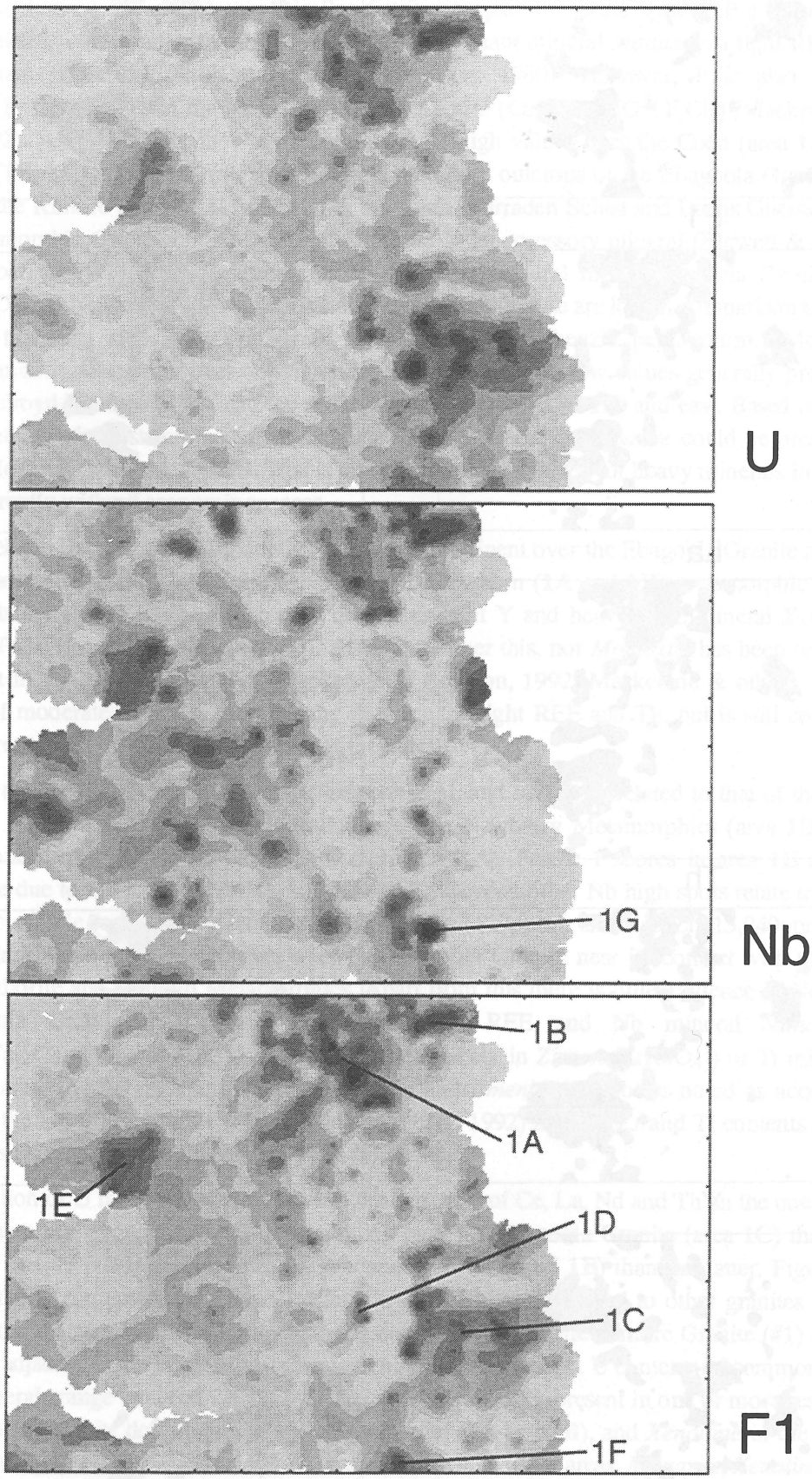

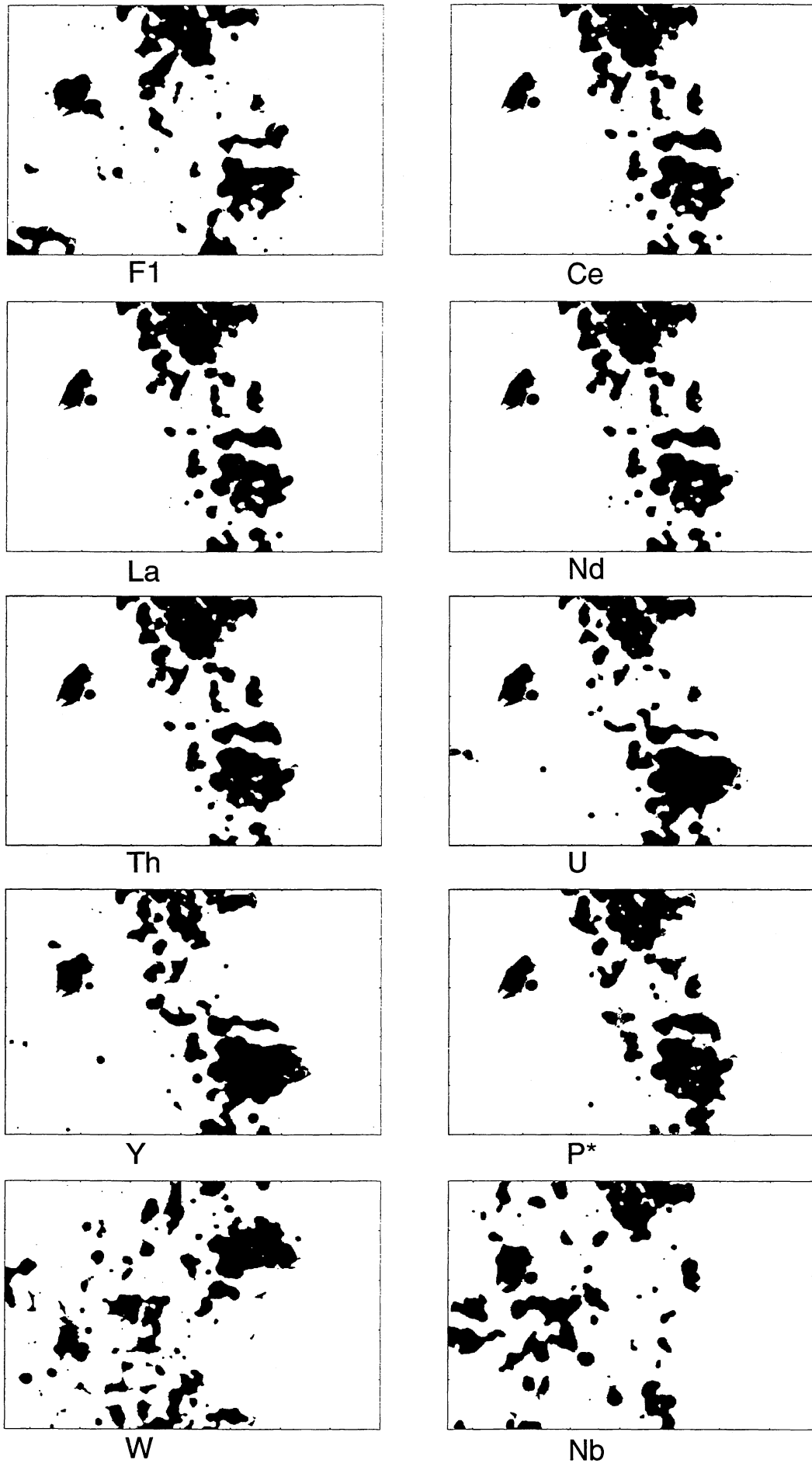

Figure 11 Areas covered by upper 20% of grid values for Factor 1 scores (F1) and major Factor 1 elements (Ce, La, Nd, Th, U, Y, P*, W and Nb).

As already observed, Th and P* show similar distribution patterns to the light REE's (Figures 10 and 11) which is consistent with their presence in the resistant mineral *Monazite*, a light REE and Th phosphate ([Ce,La,Nd,Th]PO_4) (Price & Ferguson, 1980). However, P is also widely distributed in the granites in the accessory mineral *Apatite* ($Ca_5[PO_4]_3[OH,F,Cl]$) (Mackenzie & others, 1992). All 5 elements show a predominance of high values over the Coen (area **1A**) and Newberry (**1B**) Metamorphic Groups in the north, and both outcrops of the Ebagoola Granite and an area of the Kintore Granite (**1C** and **1D**) in the south. Yarraden Schist and Lochs Gneiss of the Coen Metamorphic Group contain abundant *Monazite* as an accessory mineral (Blewett & others, 1992b). *Monazite* has not been reported as an accessory mineral in the Ebagoola Granite and values for Ce, La, Nd and Th for whole rock analyses of that granite are low in comparison to other granites in the sheet area (see #9 in Figure 12; Knutson & Mackenzie, pers. comm.). Moderate stream sediment values occur over other granites in the inlier, with low values generally prevalent over the Holroyd Metamorphics, and the sediments to the west (area **1E**) and east. Based on REE and Th contents of the stream sediment samples as much as 0.7% *Monazite* could be present in some samples from areas **1A** and **1B**. This is one of the areas explored for heavy minerals in recent times, apparently without economic success.

Although related statistically and spatially, Y is more prominent over the Ebagoola Granite and the adjacent Kintore Granite (**1C** and **1D**), than over the northern (**1A** and **1B**) metamorphic rocks. This is probably due to a greater presence of the resistant Y and heavy REE mineral *Xenotime* ([Y,HREE]PO_4) (Price & Ferguson, 1980), although neither this, nor *Monazite*, has been reported as abundant in the Ebagoola Granite (Mackenzie & Knutson, 1992; Mackenzie & others, 1992). Coverage of moderate values is more patchy than for the light REE and Th, but is still confined largely to areas overlying the granitic rocks of the inlier.

The spatial distribution of Nb is somewhat less coherent, and largely unrelated to that of the light REE's, Th, P and Y, but shows concentration over the Newberry Metamorphics (area **1B**), and scattered concentrations over the Coen Metamorphics (**1A**). Factor 1 scores in area **1E** appear mainly to be due to the presence of Nb, and Hf and Zr. Several other Nb high spots relate to other factors. One sample (area **1G**) is particularly high in Nb (127ppm), and also Zr (13,940ppm), Hf (251ppm) and Ta (49ppm), and occurs over the Ebagoola Granite near its contact with the Tea Tree Granodiorite and Holroyd Metamorphics. Apart from this there is little evidence of Nb over the Ebagoola Granite. Nb possibly occurs in the REE and Nb mineral *Samarskite* ($[REE,Nb,Ta]_2O_6$) (Price & Ferguson, 1980), or more likely in *Zircon* ($Zr[SiO_4]$) or Ti minerals such as *Ilmenite* ($FeTiO_3$) (Heinrich, 1978). *Zircon* and *Ilmenite* have been noted as accessory minerals in the Ebagoola Granite (Mackenzie and others, 1992) and the Zr and Ti contents of the sample (G) suggest about 3% *Zircon* and 0.8% *Ilmenite*.

The distribution of U falls somewhere between the extremes of Ce, La, Nd and Th on the one hand, and Y on the other, showing greater concentration over the Ebagoola Granite (area **1C**) than the former, and greater concentration over the metamorphics (**1A** and **1B**) than the latter. Figure 12 shows that the U content of the Ebagoola Granite (#9) is high compared to other granites in the sheet area, and that the Warner Granite (#4) and some samples of the Kintore Granite (#1) (these samples are adjacent to the Ebagoola Granite) are higher than average. U contents of common rock forming minerals range between 2 and 8ppm but most is probably present in one or more resistant minerals with *Monazite* dominating in the northern area (**1A** and **1B**), and *Xenotime* in the south (C), and possibly in other resistant minerals, such as *Zircon*, in other areas. *Monazite*, *Xenotime* and *Zircon* can contain up to 20,000 ppm, 35,000ppm and 10,000ppm U respectively (Price & Ferguson, 1980). The more readily mobile forms of U which can be adsorbed onto clays and hydrated Fe and Mn oxides, rather than U contained in resistant minerals, are of greater economic interest as these are more likely to have originated in the weathering of U mineralisation. The most

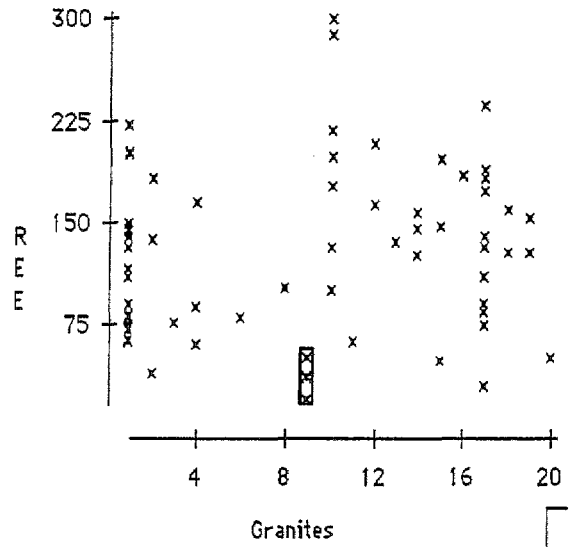

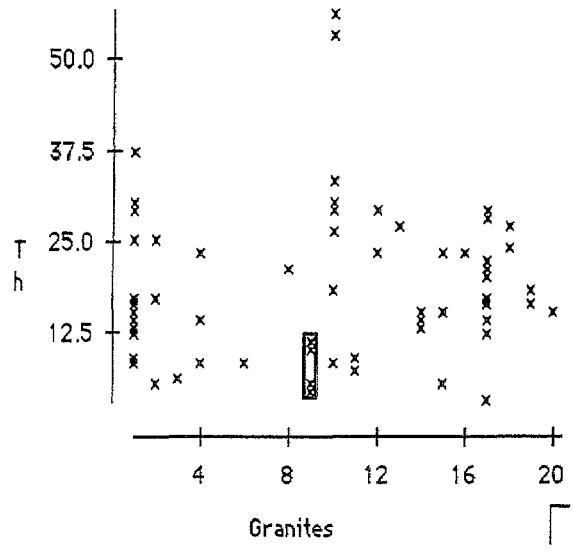

REE = Ce + La + Nd

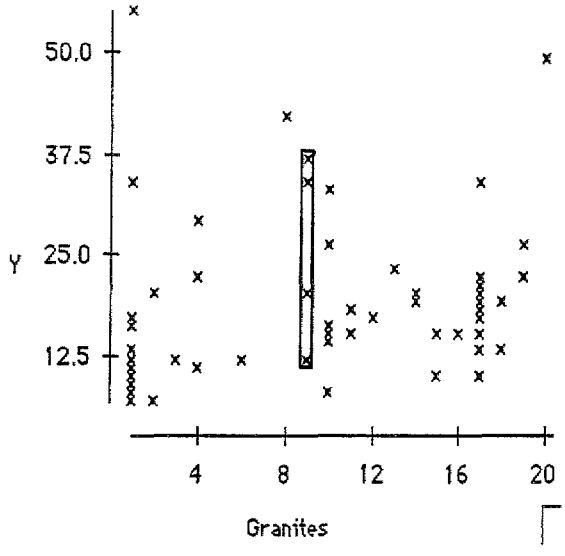

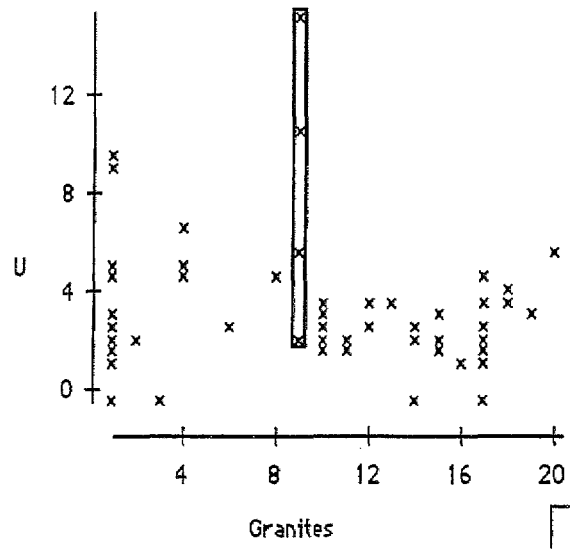

Number of samples in parenthesis

1 - Kintore Granite (19)
2 - Barwon Granite (3)
3 - Leconsfield Granite (1)
4 - Warner Granite (3)
5 - Lindalong Granite (0)
6 - Burns Granite (1)
7 - Heneage Granite (0)
8 - Tadpole Granite (1)
9 - Ebagoola Granite (4)
10 - Lankelly Granite (8)
11 - Kendle River Granite (2)
12 - Flyspeck Granodiorite (2)
13 - Glen Garland Granodiorite (1)
14 - Peringa Tonalite (3)
15 - Artemis Granodiorite (3)
16 - Tea Tree Granodiorite (1)
17 - Two Rail Monzogranite (13)
18 - Carleton Monzogranite (2)
19 - Kirkwood Monzogranite (2)
20 - Lindsay Flat Microgranite (1)

Figure 12 Concentrations of REE (Ce+La+Nd), Th, Y and U occurring in samples of granites from the EBAGOOLA sheet area. Values for samples of the Ebagoola Granite (#9) are enclosed in boxes (after Mackenzie & Knutson 1992 and pers. comm.).

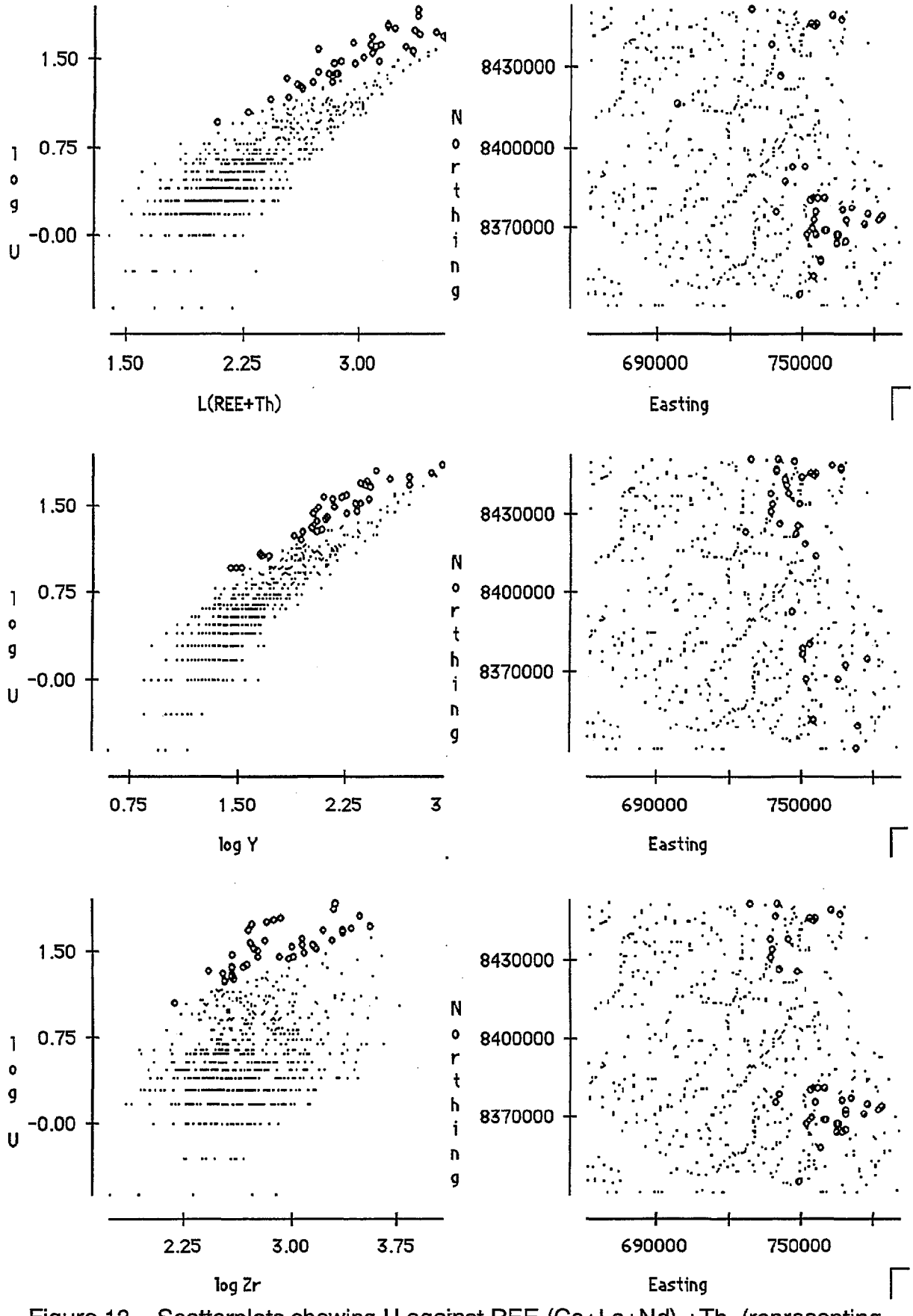

Figure 13 Scatterplots showing U against REE (Ce+La+Nd) +Th (representing Monazite), against Y (representing Xenotime), and against Zr (representing Zircon). Data are log-transformed and values with high U/other ratios are shown as circles. Scatterplots on right show approximate locations (in AMG's) of samples with high ratios.

satisfactory method to estimate mobile U is to leach the sample and to determine U in the leachate. In the absence of these data Price & Ferguson (1980) used ratios of U to elements which are essential components of the resistant minerals, and which could be determined by Instrumental Neutron Activation Analysis (INAA). These were Hf for *Zircon*, Ce and Th for *Monazite* and Dy for *Xenotime*. Samples which plotted above certain ratios were deemed to be of interest, especially if so for all element/mineral ratios. Plots of log(U) against log(Ce+La+Nd+Th), log(Y) and log(Zr) are shown in Figure 13, (Ce+La+Nd+Th) being used for *Monazite* instead of Ce and Th separately, Y for *Xenotime* instead of Dy, and Zr for *Zircon* instead of Hf. The top 5% of samples, 37 in number, for each ratio were listed and the 12 samples listed below were present in all 3 lists, hopefully indicating a lesser likelihood of all U being contained in one or more of the resistant minerals. The drainage basins are shown in Figure 14.

Sample	U ppm
7009	54
7037	46.5
7040	49.5
7041	62
7044	38
7063	45
7110	35
8081	56
8087	80.5
8111	47.5
8119	70.5
8618	60.5

Sample 7009 drains Lochs Gneiss and Yarraden Schist of the Coen Metamorphic Group (western part of area **1A**) and is near low level U mineralisation found in the Tadpole Creek Prospect (ATP 1880) by CRA Exploration in the late 1970s (Culpeper & others, 1992a and 1992b). Samples 7037, 7040, 7041 and 7044 occur over the Newberry Metamorphics in area **1B**, an area high in light REE and Th, and probably *Monazite*. Samples 8081, 8087, 8111 and 8618 are in area **1C** and form an arc about 10km north to north-west of Musgrave homestead, over Kintore and Ebagoola Granite. This area is high in Y, and presumably *Xenotime*.

Price & Ferguson (1980) also used estimates of residual U contents derived from correction of total U values for U in common rock forming minerals, the resistant minerals discussed above, and in organics, etc, as suggested by Koch & others (1979), and from correction of total U values for values predicted by linear regressions of U against the values of associated elements and against principal component factor scores. Eggo & others (in prep.) used log- transformed data regressed against factor scores, after deletion of highly anomalous residuals in order to produce a regression equation representing the background population (Lindqvist & others, 1987). A further complication is that dispersion trains from U mineralisation are usually very limited in areas with tropical climates (Foy & Gingrich, 1977; Cruikshank & others, 1993) and in a regional survey may be overwhelmed by the signal from the more persistent U in resistant heavy minerals.

In this study a number of approaches were evaluated using the simple, multiple and stepwise regression procedures in STATVIEW II on raw and log-transformed element values and Factor 1 scores. However, log-transformed element values were preferred as these are generally closer to normality than the raw data values and were used in the estimation of the factor scores.

Log-transformed U values were regressed against Factor 1 scores and all samples (30 in number)

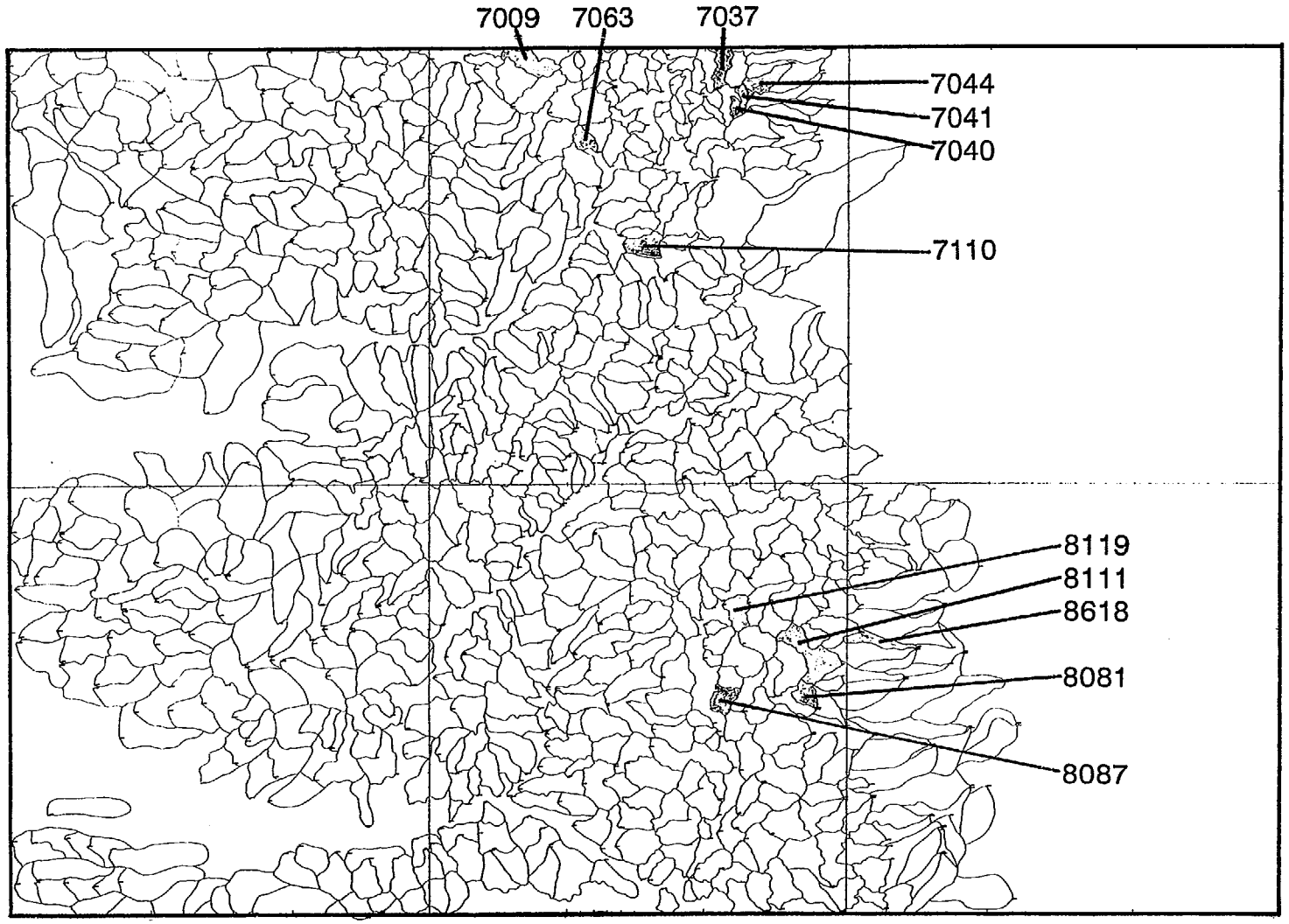

Figure 14 Drainage basins for which the ratios of U against Ce+La+Nd+Th, U against Y, and U against Zr are each in the top 5% of values. These basins may have higher potential for U mineralisation.

with residual U values greater than mean plus 2 standard deviations (equal to 13.82ppm residual U) were eliminated from a recalculation of the regression equation. The final regression equation used was:

$$\log(U_p) = 0.206*F1 + 0.577$$

where U_p is the predicted U value. The residual is U_p, converted to ppm, subtracted from the total U value. An image map of the residuals is shown in Figure 15(a).

Multiple and stepwise regression procedures gave essentially the same results as shown by image maps and only the stepwise procedure was used further as this eliminates variables which are highly correlated with variables already in the equation and produces a more compact regression equation. Stepwise regression of log(U) on log-transformed values for the 8 principal and 5 minor contributors to Factor 1 gave the following regression equation:

$$\log(U_p) = 0.186*\log(Nb) - 0.154*\log(Nd) + 0.194*\log(Pb)$$
$$0.039*\log(P) + 0.055*\log(Rb) + 0.443*\log(Th)$$
$$+ 0.536*\log(Y) + 0.204*\log(Zr) - 1.617$$

with Ce, Hf, La, Ti and W eliminated from the equation. An image map of the residuals, calculated as above, is shown in Figure 15(b). As found by Price & Ferguson (1980) the two methods, while generally similar, do emphasise different areas. Figure 15(a) defines the Tadpole Creek area (sample 7009), the Newberry Metamorphics (samples 7037, 7040, 7041 and 7044) and the area near Musgrave (samples 8081, 8087, 8111, 8119 and 8618), all defined as anomalous by the ratio method, but does not really high-light samples 7063 and 7110. The image also high-lights a number of other samples in these and adjacent areas. Figure 15(b), in contrast, high-lights the Yarraden Schist and Lochs Gneiss of the Coen Metamorphics in the Tadpole Creek area and to the south-east. This area contains samples 7063 and 7110 delineated by the ratios method. Low grade U mineralisation was found in the Tadpole Creek area (Culpeper & others, 1992a) by CRAE. The image also defines the high near Musgrave but over a more restricted area, and the Warner Granite (area F) on the southern edge of the sheet area.

Both approaches only suggest areas in which U may have been derived from sources other than resistant secondary minerals, that is areas where U mineralisation is more likely to be found rather than areas where it is definitely present.

5.2 Factor 2

Factor 2 comprises Fe, Cu, Ni, V, Sc, Cr, Zn, Ti and As, with minor contributions from Mn, Nb and Sn, and negative contributions from Tl* and Pb. The relative abundances of the principal elements are shown in box plots in Figure 16, and Figure 17 shows images of the distribution of Fe, Cu, Cr, Zn, As and scores for Factor 2 (F2) in the EBAGOOLA sheet area. Outlines of the distributions of the top 20% of grid values for each principal element are shown in Figure 18.

The factor relates to Fe geochemistry and its common element associations, including the entry of elements such as Cr, Cu, Ni, Sc, V, etc into Fe-rich, mafic minerals such as *Pyroxenes, Amphiboles* and *Biotite* in basalts, diorites and their metamorphic products (e.g. 'greenstones'), and the co-precipitation with, or adsorption onto, hydrated Fe-oxides in the secondary environment by these and other metal ions such as Zn (Wedepohl, 1972). The apparently bimodal distribution of Factor 2 scores (Figure 19) confirms that several processes, namely lithochemical/mineralogical variations and secondary scavenging, contribute to this factor. Scattergrams (Figure 20) of Fe against several of the elements in the factor also confirm the relationship.

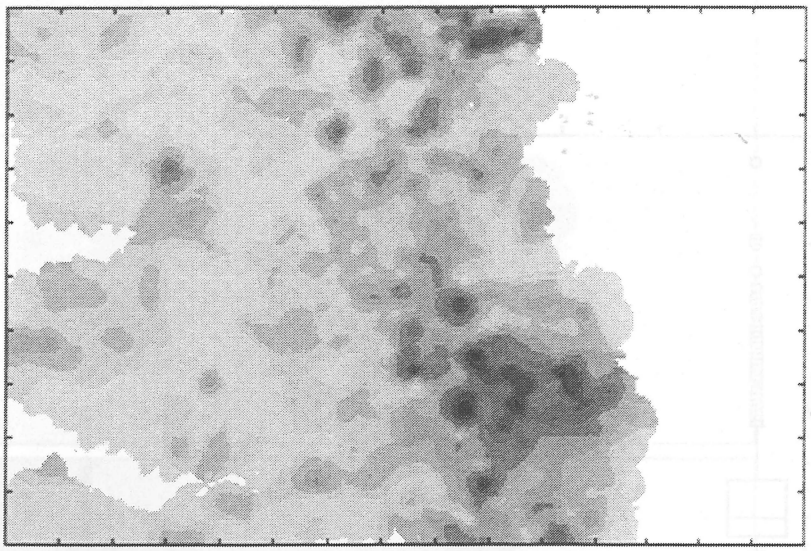

(a) Simple regression of log(U) on Factor 1

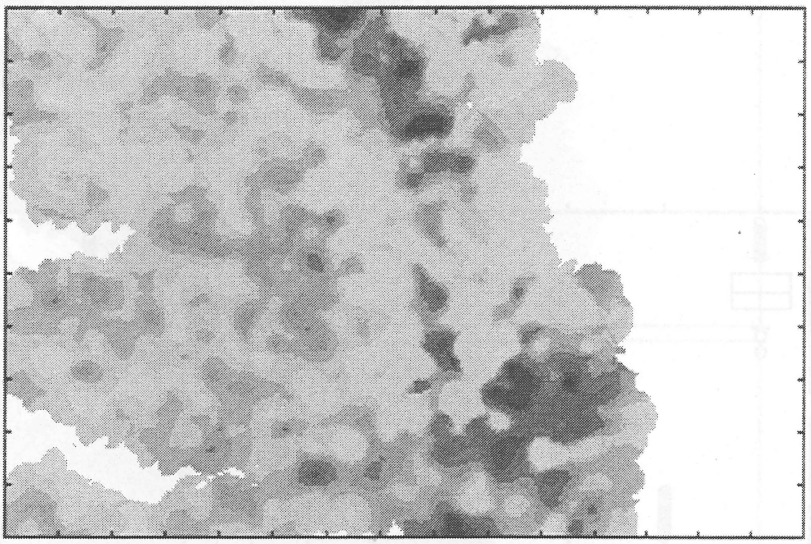

(b) Stepwise multiple regression of log(U) on log-transformed values of Ce, Hf, La, Nb, P, Pb, Rb, Th, Ti, W, Y and Zr

	30	60	80	90	95	98	99	99.9	%
(a)	-0.8	0.5	2.8	6.1	11.2	18.8	24.2	36.1	ppm
(b)	-0.3	0.2	0.6	1.2	2.3	3.6	5.0	9.5	

Figure 15 Images of U residuals estimated from predicted values (U_p) from (a) simple regression of log(U) against Factor 1 scores, and (b) stepwise multiple regression of log(U) against log-transformed values of major and minor Factor 1 elements.

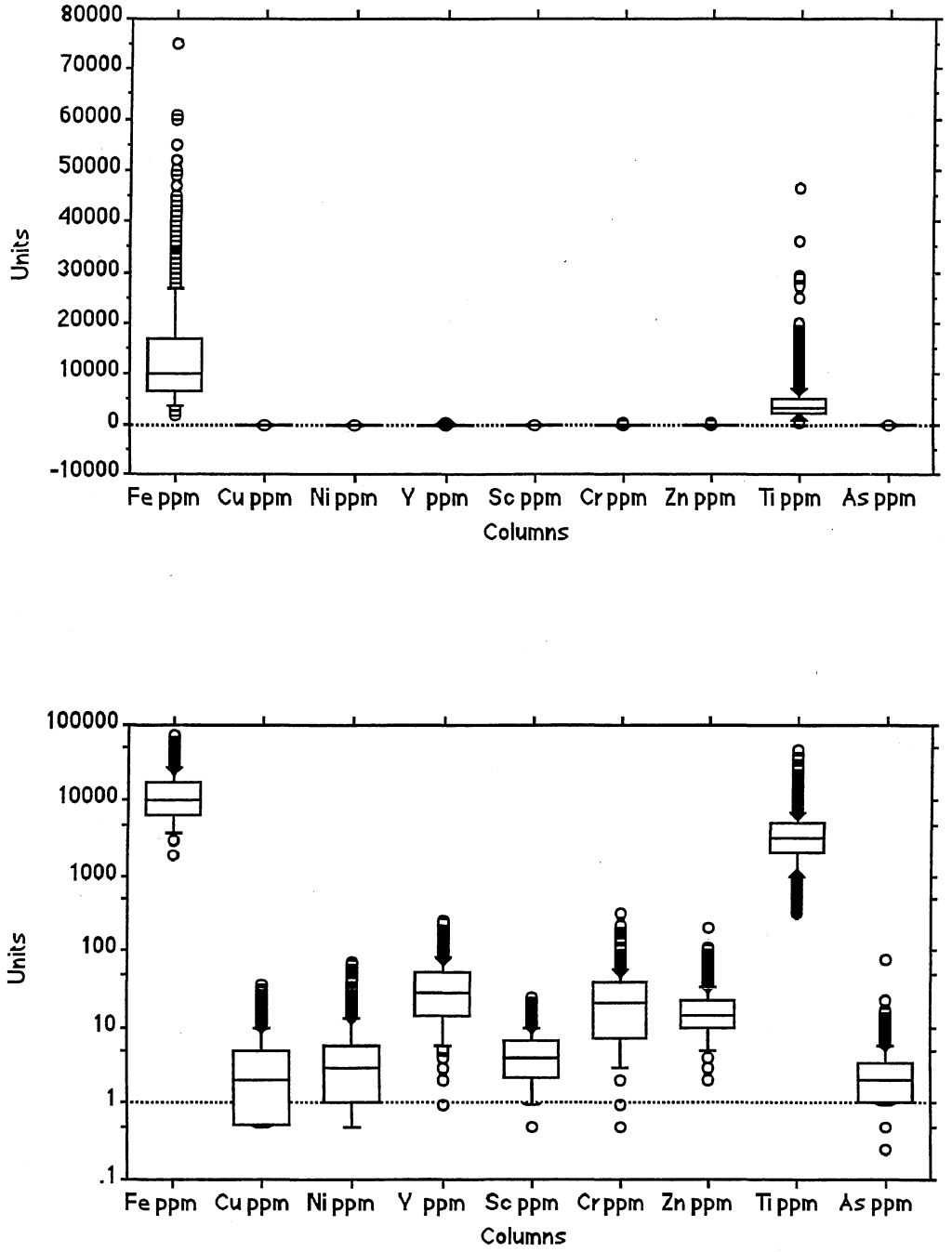

Figure 16 Box plots showing relative abundances of Factor 2 elements (Fe, Cu, Ni, V, Sc, Cr, Zn, Ti and As).

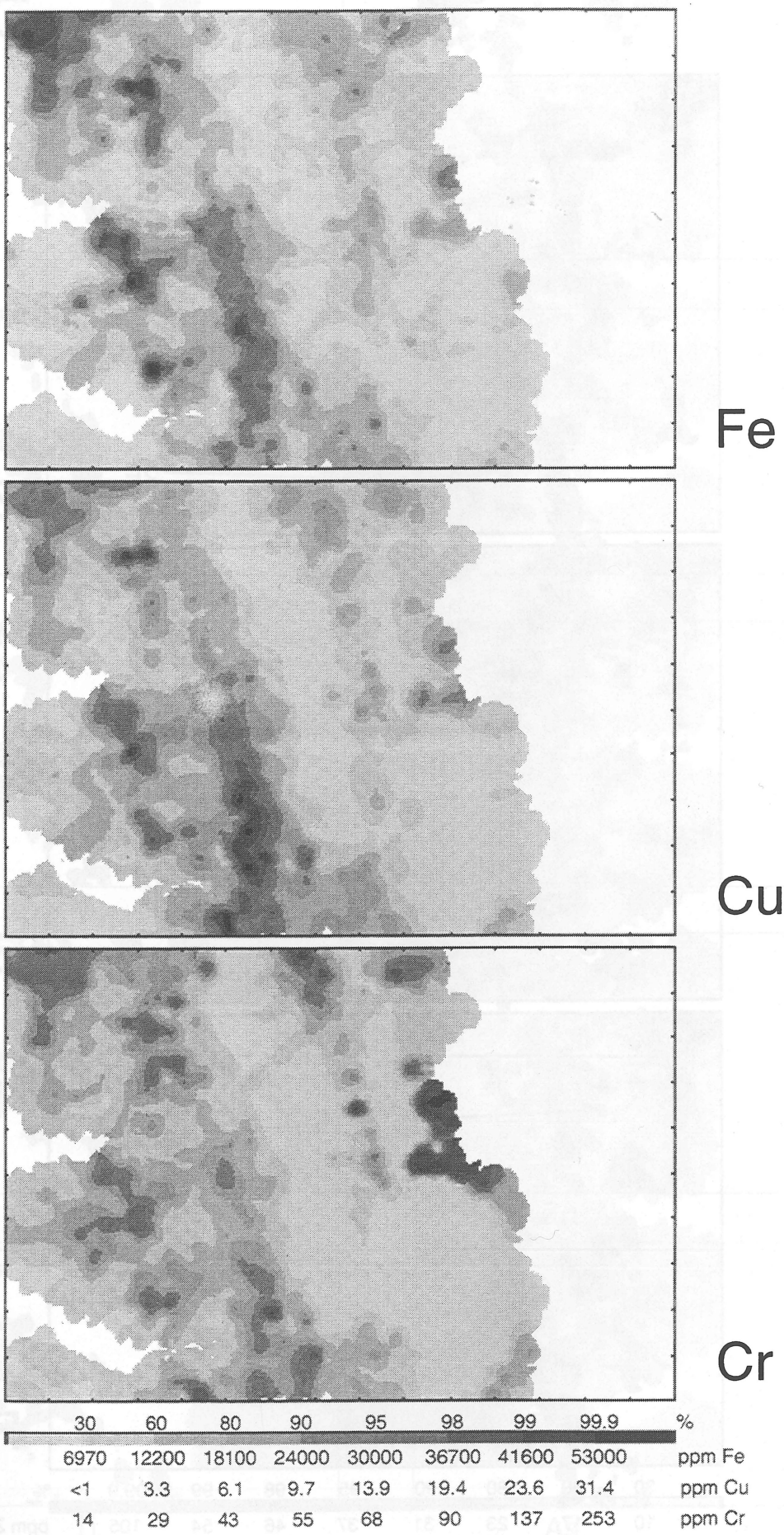

Figure 17 Image maps for selected Factor 2 elements (Fe, Cu, Cr, Zn and As) and for Factor 2 scores (F2).

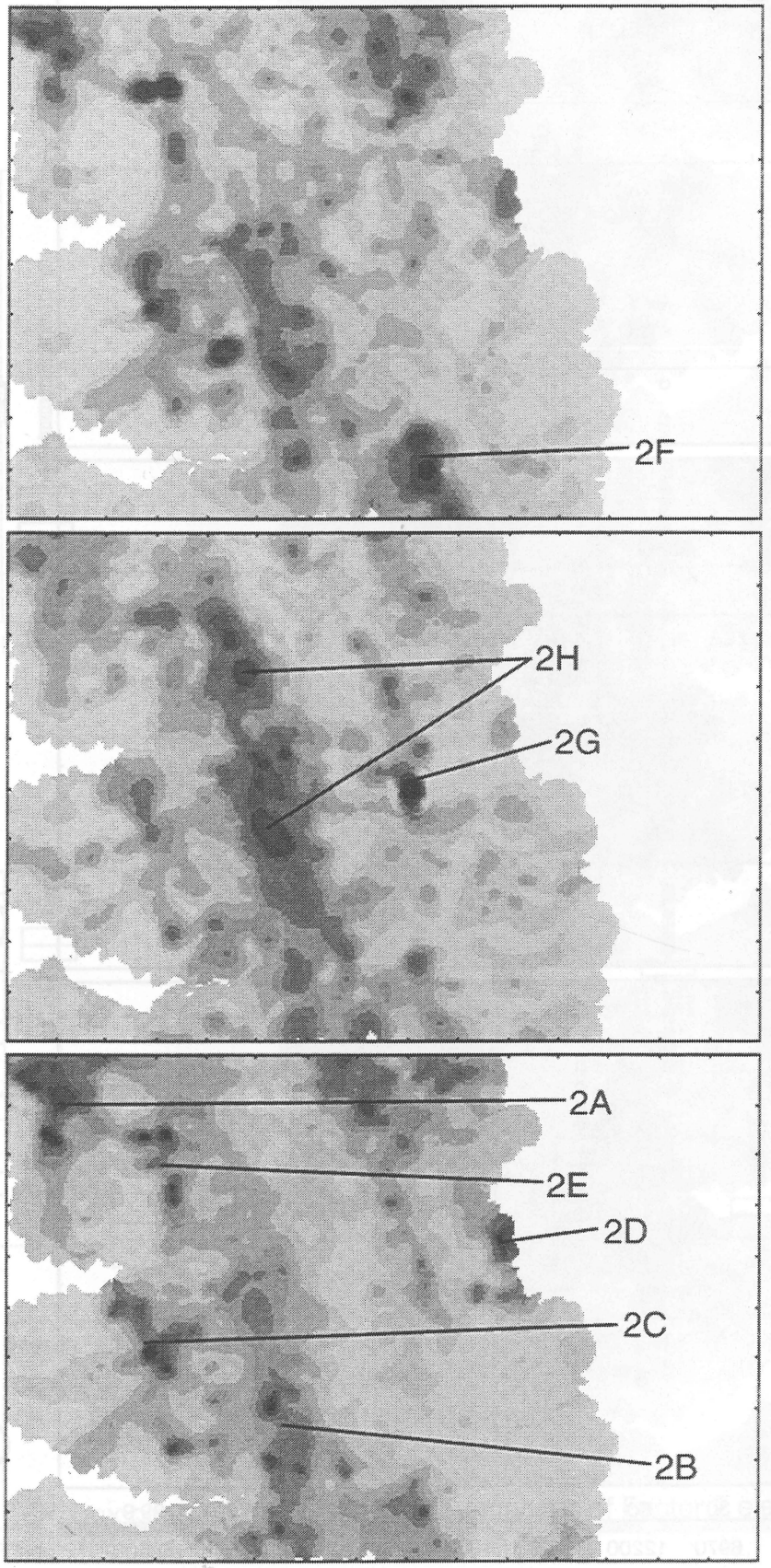

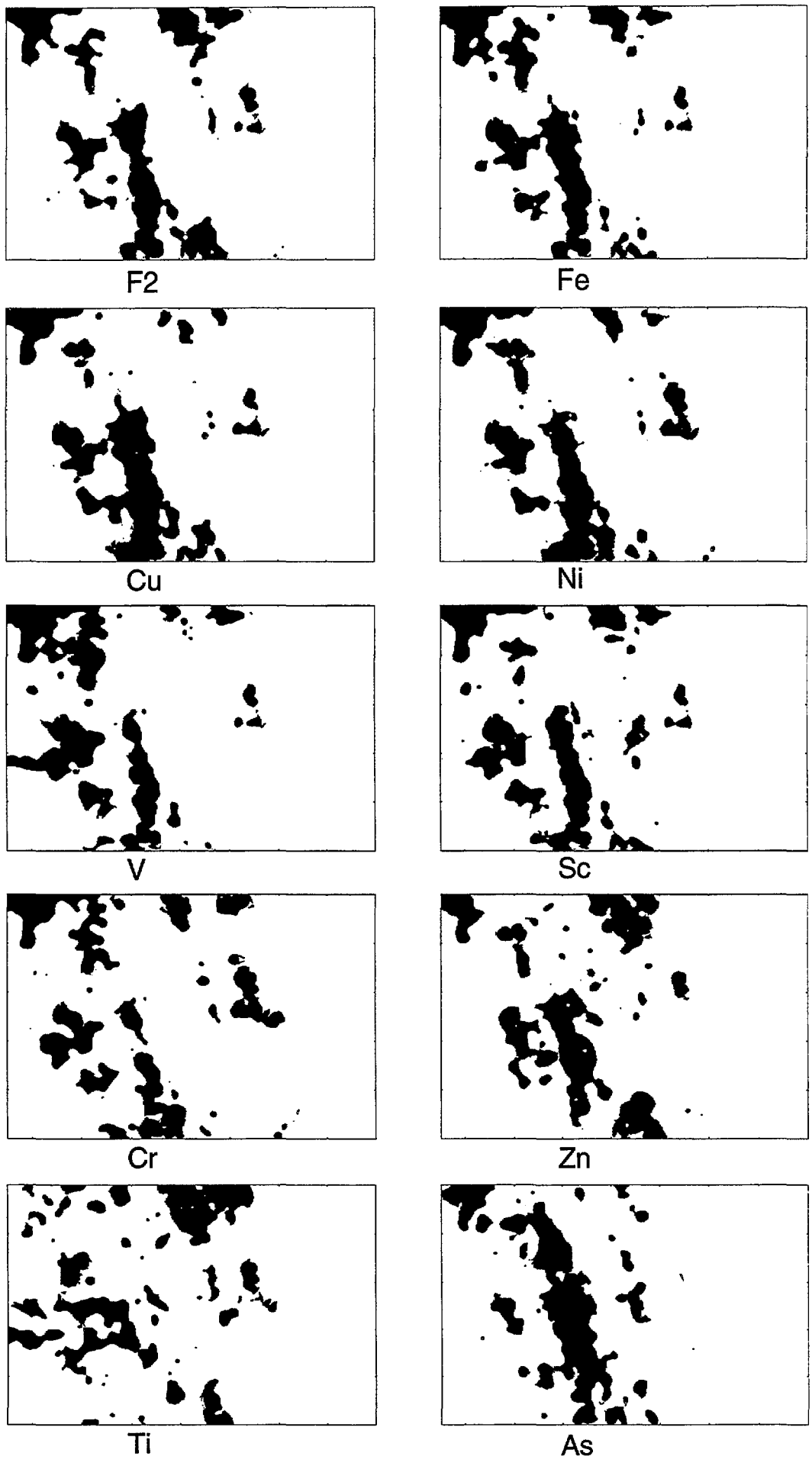

Figure 18 Areas covered by upper 20% of grid values for Factor 2 scores (F2) and major Factor 2 elements (Fe, Cu, Ni, V, Sc, Cr, Zn, Ti and As).

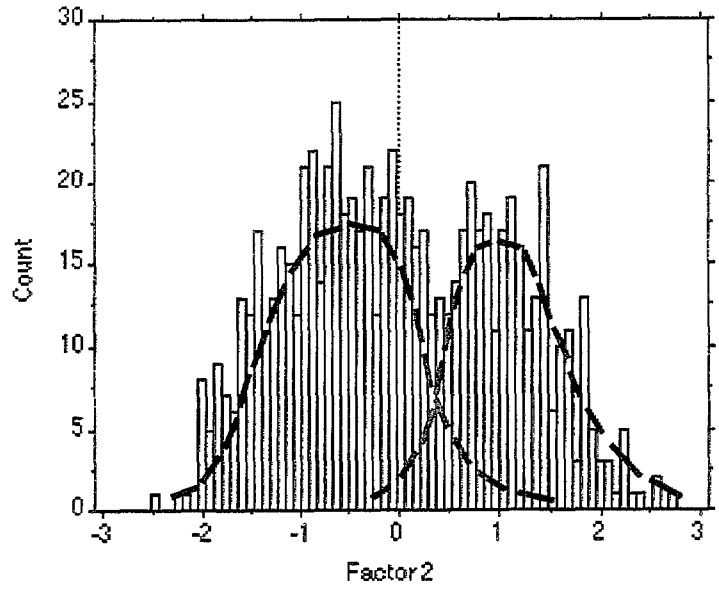

Figure 19 Histogram showing bi-modal distribution of Factor 2 scores suggesting that several processes are responsible for the relationship between the elements.

The image maps for F2 and Fe differ primarily in the slightly greater emphasis placed by F2 on the areas of Coen (area **1A** in Figure 10) and Newberry (**1B**) Metamorphics and an area near Mount Walsh. In general both F2 and Fe show moderate to high scores or values over areas underlain by metamorphic rocks.

Area **2A** (see Figure 17) is north-west of Bally Junction on Pretender Creek. The regolith is from in situ weathering of Rolling Downs Group and Bulimba Formation sedimentary rocks, and comprises weathered saprolite to residual sands in an erosional (black soil) plain. Steam sediments usually consisted of ferruginous pisoliths or nodules. Element highs include Fe, V, Ni, Cr, Mn, Zn and Sc. Unfortunately little is known of the geochemistry of the bedrock sedimentary rocks of the sheet area.

Area **2B** runs northward from the Coleman River near Dinah's Yard, to the Lukin River near the Gorge. Underlying rocks are Holroyd Metamorphics of the Astrea Formation, Carew Greenstone, Dinah Formation and Craysfoot Quartzite in the south, and Gorge Quartzite, and Strathburn and Strathmay Formations in the north. Regolith is in situ and comprises weathered saprolite and soil in rises and low hills. There are patchy areas of ferruginous nodules. Element highs include Cu, Sc, Mn, Fe, Ni and Zn.

Area **2C** is west to south-west of Strathburn homestead and includes Windberry Creek. The area is an erosional plain over weathered saprolite and residual sands from Rolling Downs Group and Bulimba Formation sedimentary rocks. Regolith is in situ, although the area is largely flat and swampy. Element highs are Fe, V, Mn, Sc, Ni, Cu, Zn and Cr.

Area **2D** runs along the escarpment from Mount Newberry in the north past Mount Walsh in the south. Regolith is largely in situ from Kitja Quartzite of the Newberry Metamorphics, and from Lindsay Flat Microgranite and Kintore Granite. Landforms include the escarpment, and low hills and flood plains below the escarpment. Transported sediments in the flood plains are from granitic, metamorphic and sedimentary rocks. Element highs in Cr, Ni, Ti and Nb are most prominent.

Area **2E** covers Shovel Camp and Montamine Creeks over sedimentary rocks of the Rolling Downs Group. Regolith has been formed in situ and comprises weathered saprolite in rises and erosional plains. Element highs in Fe, V, Mn, Cu, Ni and Zn are noted.

The image maps of F2, Fe, Cu, Ni, V, Sc and Cr show very similar spatial distributions. While adhering to these patterns in general, the spatial distributions of Zn, Ti and As are slightly more diverse with Ti high over the northern metamorphics (areas **1A** and **1B** in Figure 10). Also, Ni and Cr appear to be largely responsible for the factor high near Mounts Newberry and Walsh (**2D**).

The highest concentrations of Fe occur over sedimentary rocks of the Rolling Downs Group and Bulimba Formation (areas **2A**, **2C** and **2E**) and metamorphic rocks of the Holroyd Metamorphics (**2B**). In the Holroyd Group the Strathburn Formation, Gorge Quartzite and Newirie Formation contain schist units which have *Hematite* as a major component, and the Carew Greenstone is primarily metabasalt-metadolerite. The metamorphic rock tend to be richer in Fe overall than the granites (analyses of Holroyd Group rocks range up to 10.2% total Fe_2O_3 compared with averages of 3.2% for I-type and 1.9% for S-type granites; Blewett, R.S., & Knutson, J., pers. comm.) as the moderate (greens) and high values (yellow to red and black) Fe values in the image map define the metamorphic groups in sharp contrast to the low (blue) values over most granite terrains. In area **2A** stream sediments consist mainly of lateritic(?) ferruginous nodules and this is reflected in the image map. The reason for this is not known and this type of sediment was not widespread elsewhere in the sheet area. In most areas of high Fe the regolith is from in situ weathering.

Copper shows a coherent band of highs over the Holroyd Metamorphics (area **2B**), presumably over the Fe-rich schists, and metadolerite and metabasalt. In the late 1960s and early 1970s Cu and Ni anomalies associated with weathered ultrabasics (metabasalt?) were reported in the area (ATP 520: Culpeper & others, 1992b). A sub-economic gossan was also reported. The raw Cu values, with a maximum of 37ppm, would not seem to indicate the presence of significant mineralisation. However, as the 13-15km^2 average drainage basin allows linear stream runs of up to 4-5km and as the dispersion train of Cu in stream sediment in monsoonal areas can be restricted to 1-2km (Rossiter, 1975; Cruikshank & others, 1993) it is not inconceivable that Cu from mineralisation may not be detected, or at least not be as prominent as one would expect. Figure 21 shows Cu residuals calculated from regression of log(Cu) against Factor 2 with 32 samples with initial Cu residuals exceeding 7.68ppm excluded, as for U above. The regression equation is:

$$\log(Cu_p) = 0.410*F2 + 0.275$$

where Cu_p is the predicted Cu value. The Cu residuals image emphasises the Holroyd metamorphics (area **2B**) at the expense of areas **2C** and **2E** to the west and north-west respectively.

Zinc shows similar distribution to the other Factor 2 elements but also shows a large area (area **2F** in Figure 21) of high values over the eastern-most outcrop of the Kalkah Structural Domain, from Glen Garland homestead to the bottom edge of the sheet area at Sugarloaf Creek, in units of the Strathburn Formation and Gorge Quartzite. Figure 21 shows Zn residuals calculated from regression of log(Zn) against Factors 2 and 3 (19 samples exceeding 21.45ppm excluded), the equation being:

$$\log(Zn_p) = 0.209*F2 + 0.026*F3 + 1.141$$

where Zn_p is the predicted Zn value. Factors 2 and 3 were used in the regression because Zn has significant factor loadings against each (see Table 9). Most areas of moderate to high values, in particular Zn associated with the Fe-rich sediment in areas **2A**, **2B**, **2C** and **2E** are reduced in significance relative to area **2F** near Glen Garland. This area contains 'the Bustard' Cu-Pb- Zn Lease in which Zn appears to have a stronger signature (up to 320ppm) than either Cu (83 ppm) or Pb (62 ppm)(Culpeper & others, 1992b).

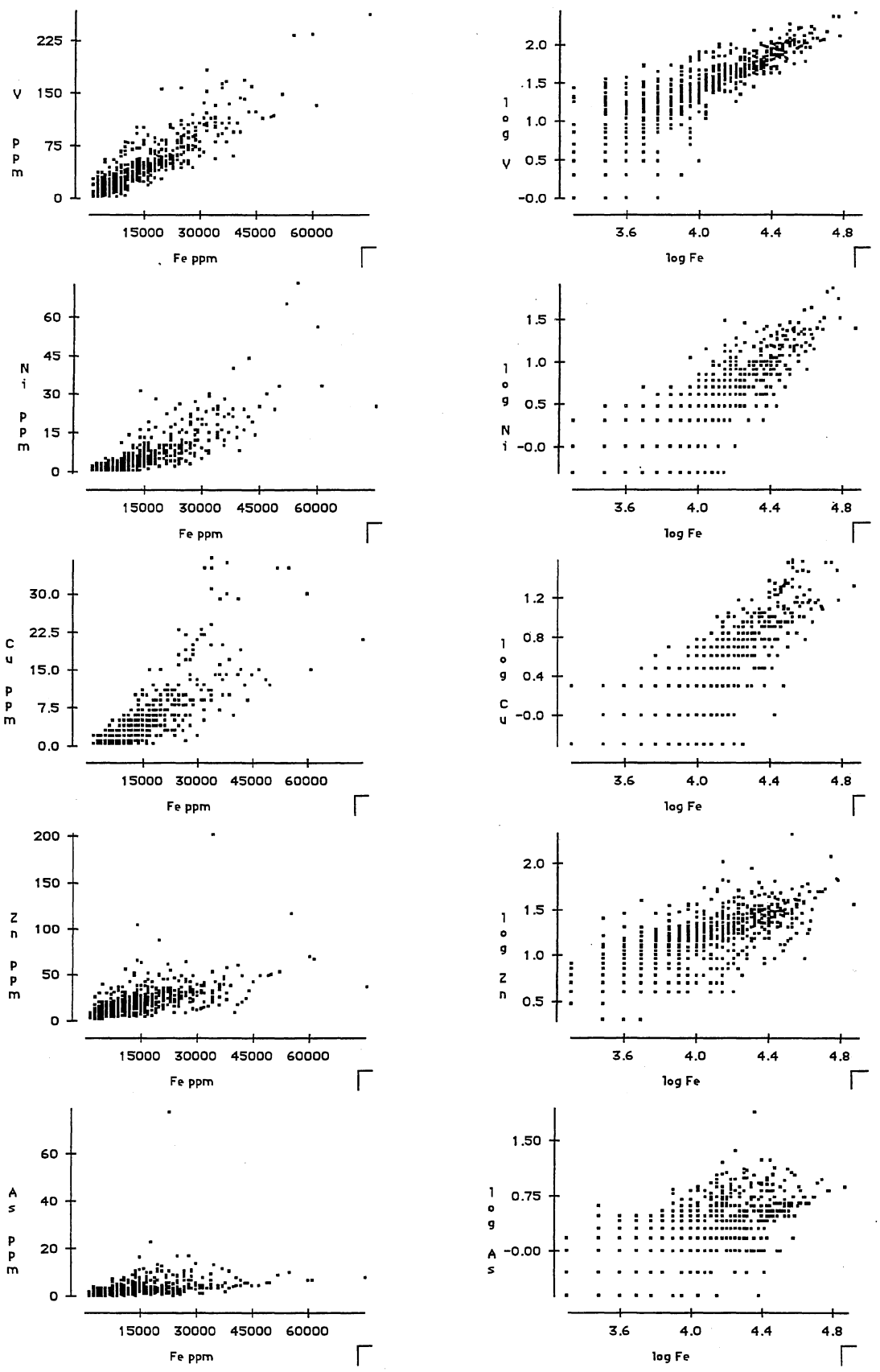

Figure 20 Scatterplots of V, Ni, Cu, Zn and As (normal and log-transformed) against Fe.

Titanium is concentrated over the Newberry (area **1B**) and Coen (**1A**) Metamorphics and is no doubt the main cause of the moderate Factor 2 scores in these areas. However, the most significant similarity between Ti and other Factor 2 elements is the large areas of low (blue) values over the granite outcrops indicating areas of low values for both Ti and F2 elements. Ti also has a minor factor loading with Factor 1 suggesting that at least part of the variation in Ti is due to the presence of resistant heavy minerals such as *Ilmenite* ($FeTiO_3$) or *Rutile* (TiO_2). The later is an accessory mineral in units of the metamorphics (Blewett & others, 1992b).

The association of Cr and Ni in area **2D** near Mount Walsh suggests the presence of mafic or ultra-mafic rocks. The area covers the margin between the Kintore Granite and the Kitja Quartzite of the Newberry Metamorphic Group. Dolerite dykes occur in the area but are low (ppm) in Cr and Ni. An outcrop of basaltic nephelinite, the Silver Plains Nephelinite, occurs 10-15 km north to north-east of the area and contains high concentrations of Cr (213 ppm) and Ni (176 ppm) (Mackenzie & Knutson, 1992), but no similar outcrop has been observed in area K (D. Mackenzie, pers. comm.).

Arsenic shows an extreme high (area **2G**) at Spion Kop, an old *Gold* mining area in Flyspeck Granodiorite. This is no doubt due to the presence of *Arsenopyrite* in the mineralisation (Culpeper & others, 1992b). There is also a low level anomaly (7 to 22.5 ppm As) in an elongated, almost north-south belt (area **2H**) which follows a chain of hills (the Curlew Range?) from Curlew Creek in the south along a line slightly west of north to the Yarraden-Aurukun road in the north. The hills are formed by resistant units of the Holroyd Metamorphics, such as the Gorge Quartzite. The Holroyd Metamorphics and the granites containing Spion Kop and the Hamilton Gold Field to the north (see Factor 5) are generally delineated by moderate As values (5 ppm) in contrast to the remainder of the granite terrain and the Coen and Newberry Metamorphics, which are generally 2 ppm or less.

5.3 Factor 3

Factor 3 comprises Sr, Ba, Rb, Pb, Ga, Be*, Tl* and Mn with lesser contributions from P*, Zn, Nd, Ce, La and Th, and negative contributions from Ti, Cr, Nb and Zr. The factor is considered to be associated with the weathering of K-rich minerals in granites since all but Mn of the main factor elements are know to concentrate in the common K/Al minerals such as *K- Feldspar*, *Biotite* and *Muscovite* (Sr - Faure, 1978; Ba - Puchelt, 1972; Rb - Heier & Billings, 1970; Pb - Wedepohl, 1974; Ga - Burton & Culkin, 1972; Be - Hormann, 1969; Tl - de Albuquerque & Shaw, 1972). The inclusion of P*, Nd, Ce, La and Th as minor components of the factor is reflected in the high intercorrelation between Factors 1 and 3 listed in Table 9(b). This may indicate that the factors have the same or closely related sources such as the weathering of rocks of similar mineralogy.

The relative abundances of the principal elements are shown in box plots in Figure 22, and image maps for Sr, Rb, Pb, Tl*, Mn and scores for Factor 3 (F3) are shown in Figure 23. The 20% outlines for F3, Sr, Ba, Rb, Pb, Ga, Be*, Tl* and Mn are shown in Figure 24 (P*, Nd, Ce, La, Th and Nb in Figure 11: Zn, Ti and Cr in Figure 18).

Sr, Ba, Rb, Pb, and, to a lesser extent Tl and Be, tend to be concentrated over the granites, as would be expected if K-rich minerals are the primary source of the elements in the secondary environment. In granites, K_2O, Rb and Pb are more abundant in rocks of the Kintore Supersuite, and Sr in the Flyspeck Supersuite. Ba is more or less evenly distributed between the two (values from Mackenzie & Knutson, 1992). Ga is more scattered, probably reflecting its association with Al_2O_3 rather than K_2O.

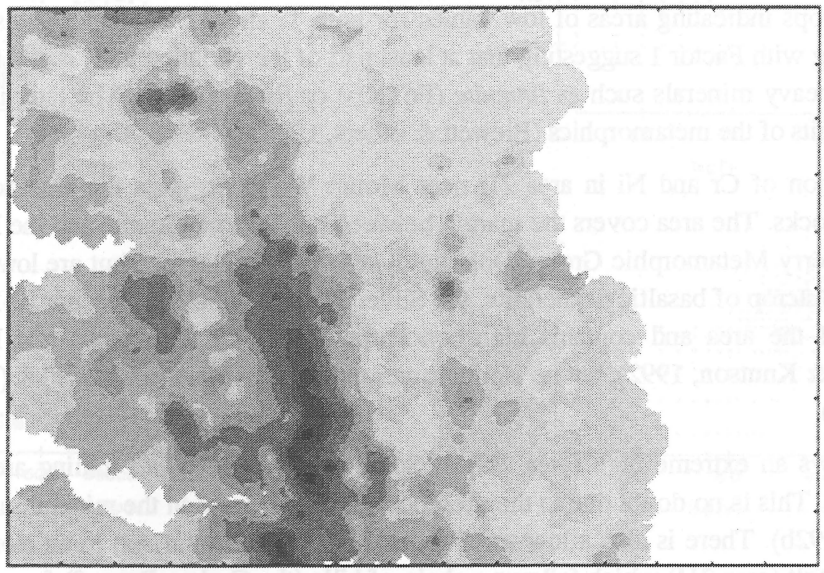

(a) Residual Cu from regression of log(Cu) against F2

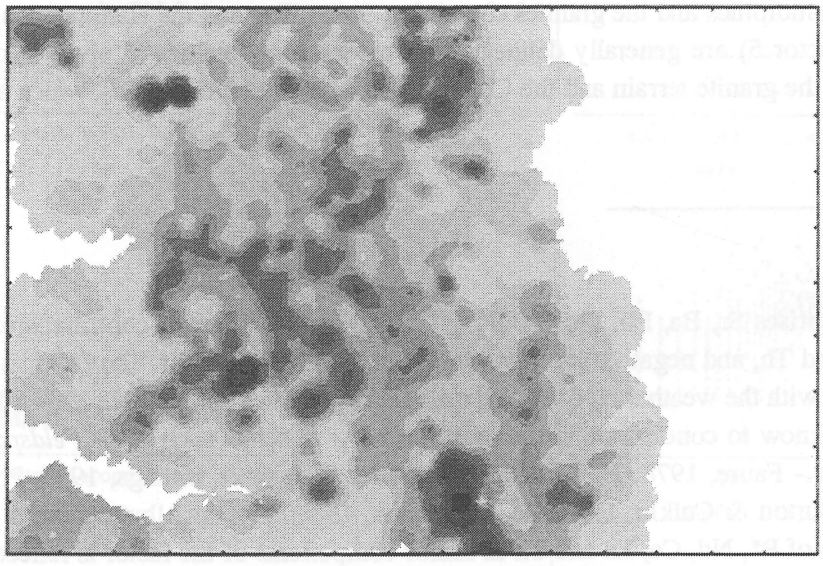

(b) Residual Zn from regression of log(Zn) against F2 and F3

	30	60	80	90	95	98	99	99.9	%
Residual Cu	-0.2	0.5	1.9	3.7	6.5	11.3	14.5	22.2	ppm
Residual Zn	-2.2	1.5	4.8	8.4	12.5	19.3	29.6	78.4	ppm

Figure 21 Images of (a) Cu and (b) Zn residuals from predicted values from regression of (a) log(Cu) against F2 scores, and (b) log(Zn) against F2 and F3 scores.

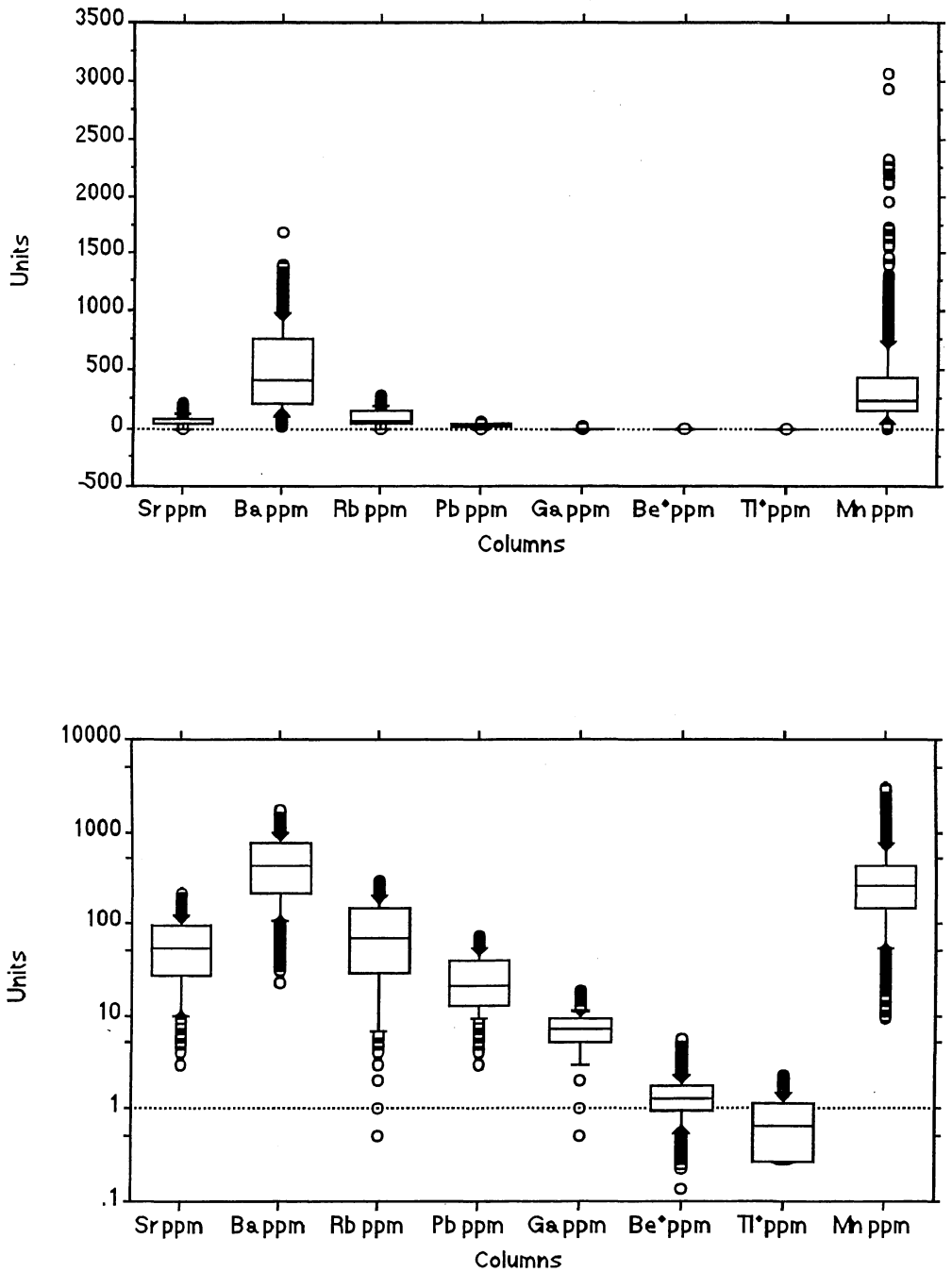

Figure 22 Box plots showing relative abundances of Factor 3 elements (Sr, Ba, Rb, Pb, Ga, Be*, Tl* and Mn)

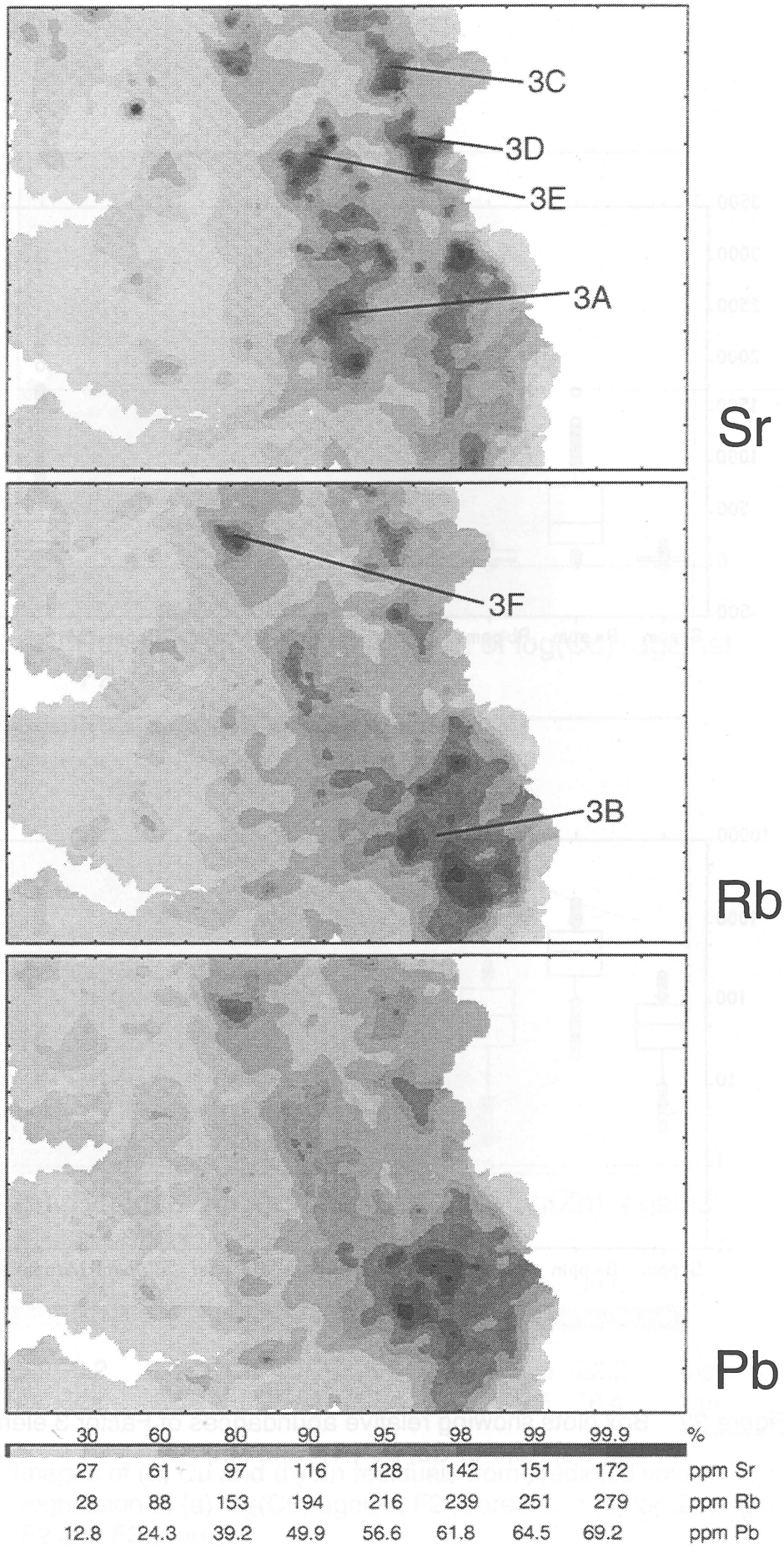

Figure 23 Image maps for for selected Factor 3 elements (Sr, Rb, Pb, Tl* and Mn) and for Factor 3 scores (F3).

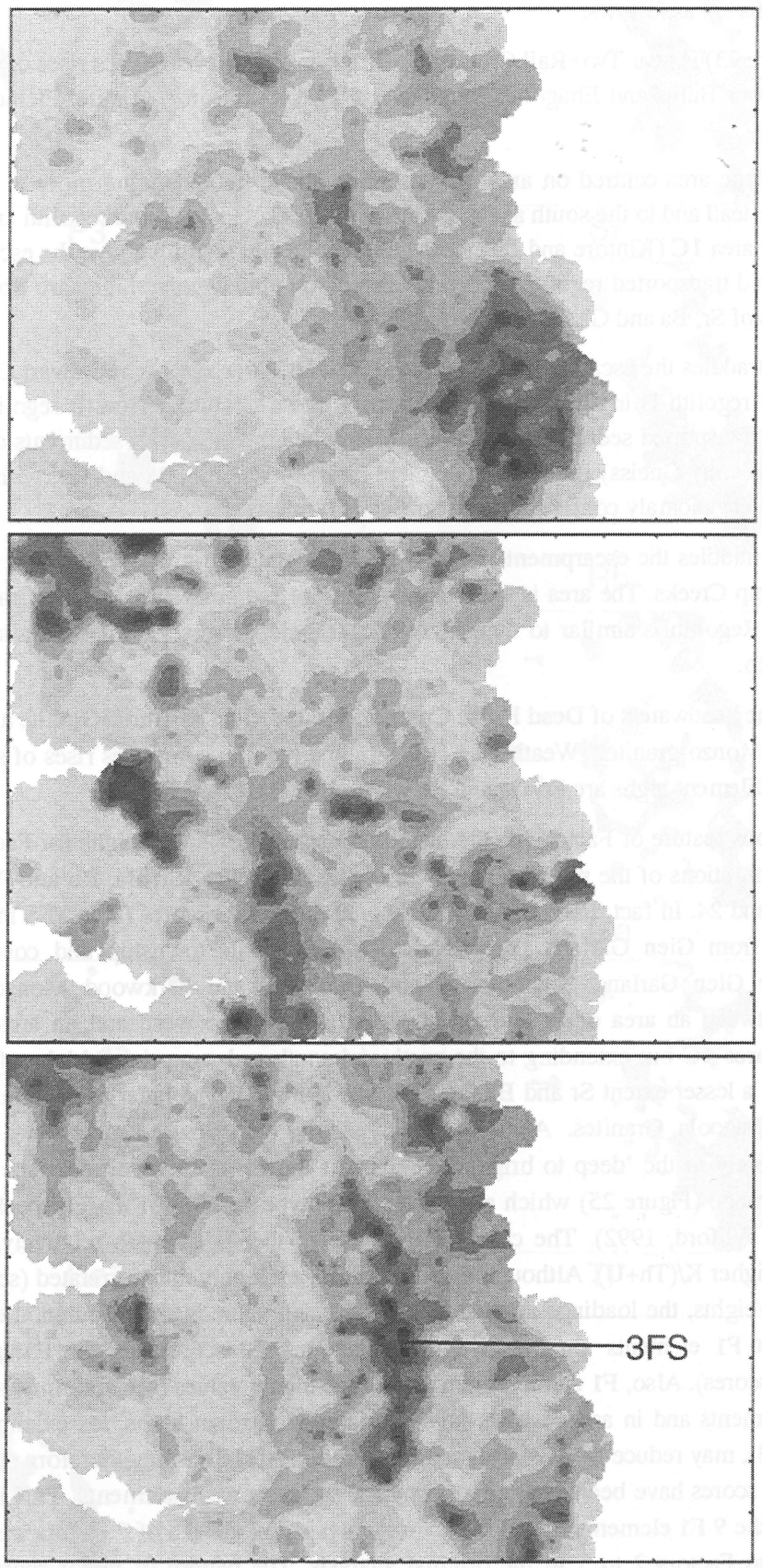

30	60	80	90	95	98	99	99.9	%
0.34	0.75	1.16	1.40	1.60	1.77	1.88	2.11	ppm Tl*
175	312	484	701	940	1340	1670	2440	ppm Mn
-0.75	0.18	1.00	1.52	1.94	2.39	2.64	3.18	Factor Scores

F3 element highs are as follows:

Area **3A** (Figure 23) is near Two Rail Creek. Regolith is in situ and comprises rises of saprolite and residual sand over Burns and Ebagoola Granites and Two Rail Monzo-granite. Element highs are Sr and Ba only.

Area **3B** is a large area centred on area **1C** described above but extending more to the north of Bamboo Homestead and to the south as far as O'Briens Creek. Geology and regolith are essentially the same as for area **1C** (Kintore and Ebagoola Granites: in situ regolith above the escarpment and mixed in situ and transported regolith in flood plains below) but element highs are Rb, Pb, Be and Tl with patches of Sr, Ba and Ga.

Area **3C** also straddles the escarpment between the Stewart River and Little Stewart Creek. Above the escarpment regolith is in situ and derived from Kintore Granite. Below it regolith is mostly flood plains of transported sediments derived from granite admixing with sediments derived from metamorphics (Penny Gneiss) in the east. Element highs include Sr, Ba and Ga, with very minor Rb and Pb. The Ga anomaly continues to the north and north-west.

Area **3D** also straddles the escarpment between areas **2D** and **3C**, in the headwaters of Balclutha and Kirbys Camp Creeks. The area is underlain by Kintore and possibly Lankelly Granites and by Penny Gneiss. Regolith is similar to that in area **3C**. Element highs are for Sr, Ba and Ga, with minor Pb and Rb.

Area **3E** is in the headwaters of Dead Horse Creek and is underlain by Burns Granite and Two Rail and Kirkwood Monzo-granites. Weathering is in situ and regolith comprises rises of saprolite and residual sands. Element highs are Sr, Ga and Be with minor Ba.

The most obvious feature of Factor 3 is the lack of consistency between highs for Factor 3 scores and high concentrations of the major elements in the factor, namely Sr, Ba, Rb and Pb, as shown by Figures 23 and 24. In fact, the most prominent area of high F3 scores (area **3FS** in Figure 23), running north from Glen Garland homestead to old Ebagoola township and covering I-type granites of the Glen Garland Granodiorite, and Two Rail and Kirkwood Monzogranites, is sandwiched between an area of Sr and Ba highs (area **3A**)to the west, and an area to the east encompassing area **1C** but extending to the north and south and comprising highs of Rb, Pb, Be and Tl*, and to a lesser extent Sr and Ba (area **3B** in Figure 23). The latter is underlain by S-type Kintore and Ebagoola Granites. Area **3B** mostly shows very low factor scores. Area **3FS** corresponds closely to the 'deep to bright red' areas of the EBAGOOLA composite gamma ray spectrometric image (Figure 25) which also cover the I- type granites of the Flyspeck Supersuite (Mackenzie & Wilford, 1992). The colour is because of the supersuite's relatively lower total K+Th+U and higher K/(Th+U). Although Factors 1 and 3 are highly intercorrelated (see above, the Factor Score Weights, the loadings applied to each element value in the calculation of the factor score, for most F1 elements are negative for calculating F3 scores (as are F3 elements for calculating F1 scores). Also, F1 elements generally have higher values (see maximums in Table 5) than the F3 elements and in areas which have overlapping element highs, for example areas **1C** (F1) and **3B** (F3), may reduce the F3 factor score markedly. Area **3FS** may therefore represent area in which factor scores have been least effected by the presence of F1 elements. This is confirmed by eliminating the 9 F1 elements from the Factor Analysis. Six instead of 7 factors were extracted corresponding to Factors 2 to 7 in the original analysis. The pattern of factor scores for F2 is relatively unchanged, but for F3 there is a significant difference with the suppression of the prominent area **3FS** and greater emphasis in the north on areas **3C** and, surprisingly, **1B** (Figure

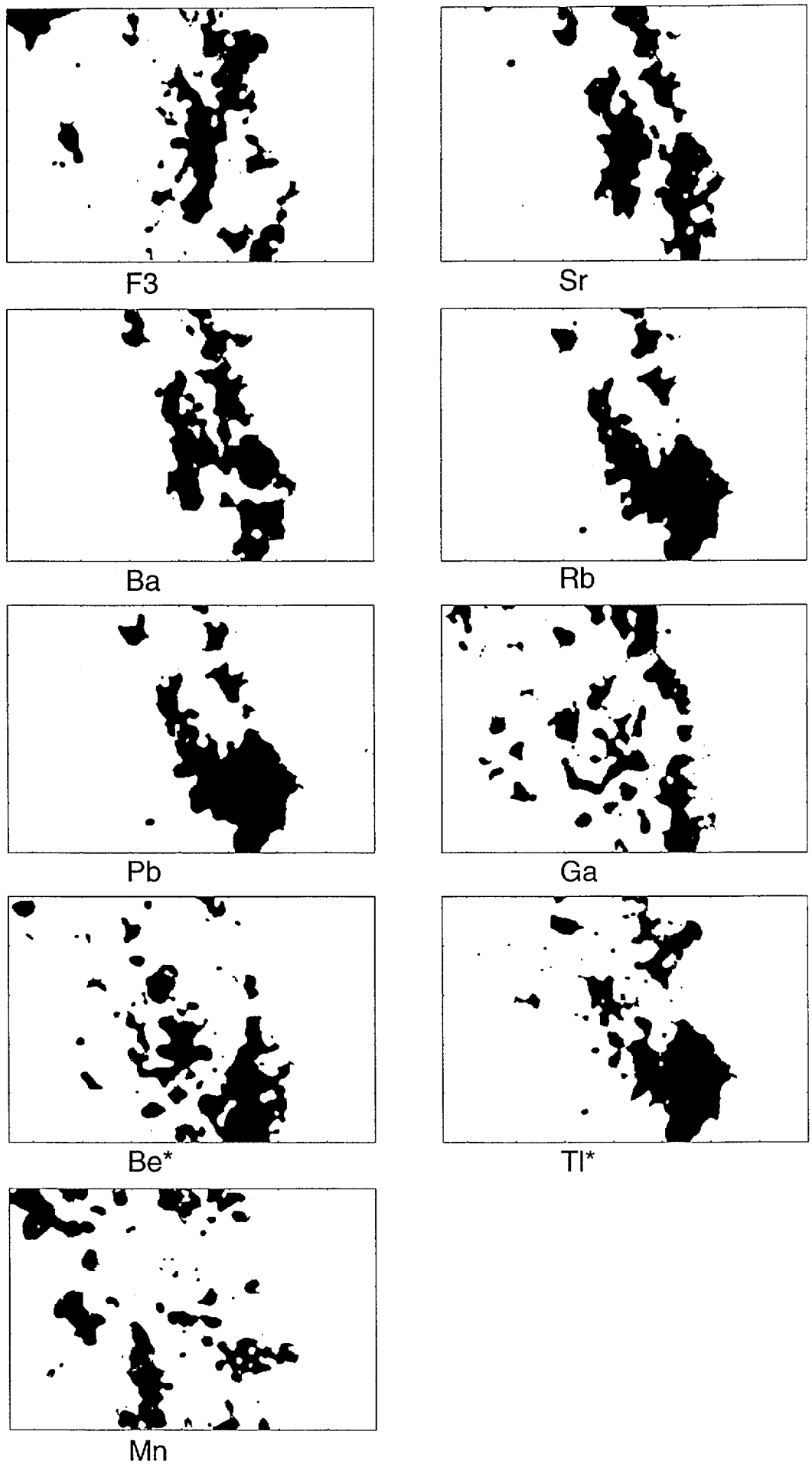

Figure 24 Areas covered by upper 20% of grid values for Factor 3 scores (F3) and major Factor 3 elements (Sr, Ba, Rb, Pb, Ga, Be*, Tl* and Mn).

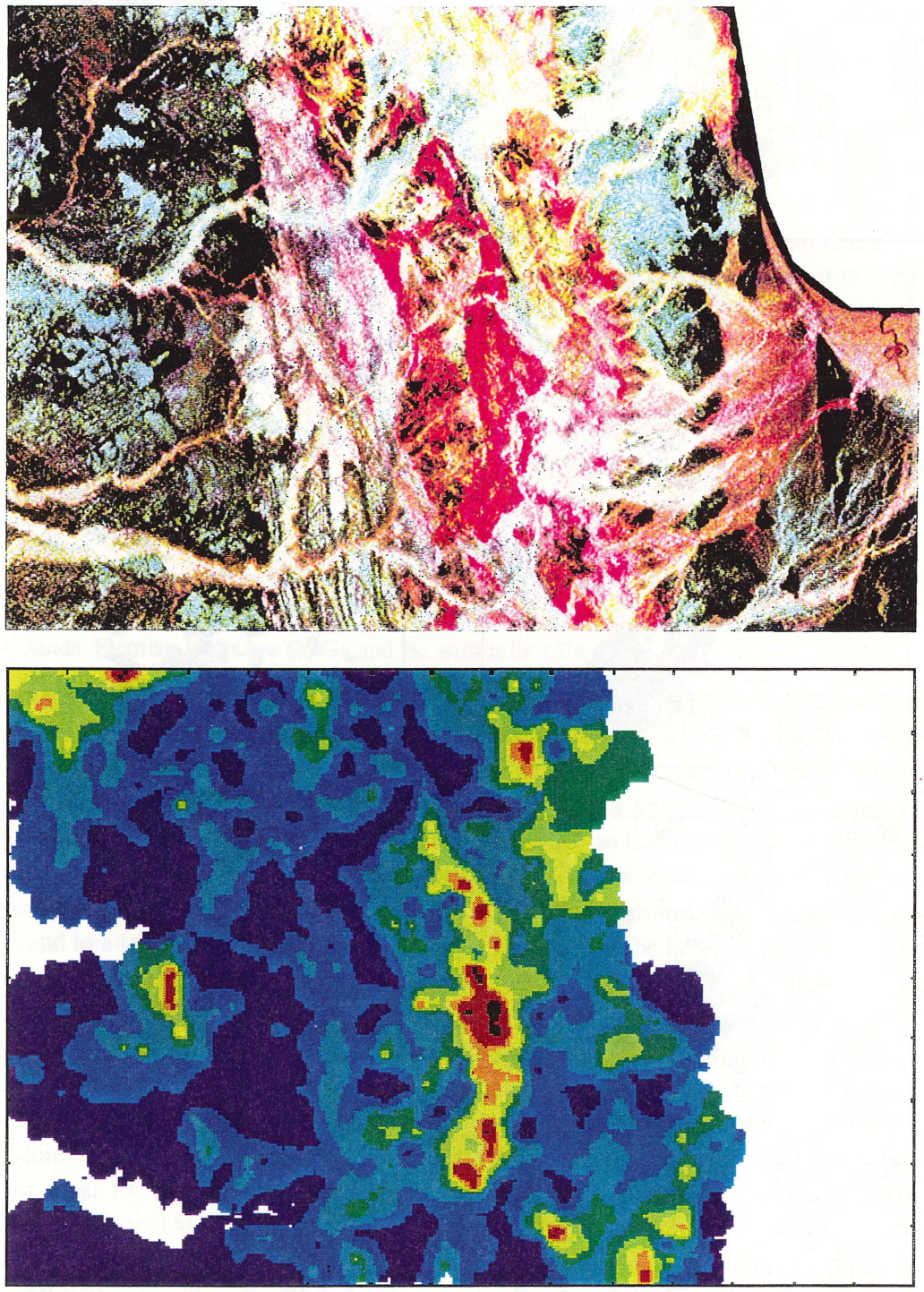

Figure 25 The composite gamma-ray spectrometric image (top - Red (K), Blue (Th) and Green (U) - after Wilford, 1992) and the image map of Factor 3 scores (botom - F3). The red patches in the composite image are due to generally lower total K+Th+U and higher K/(Th+U).

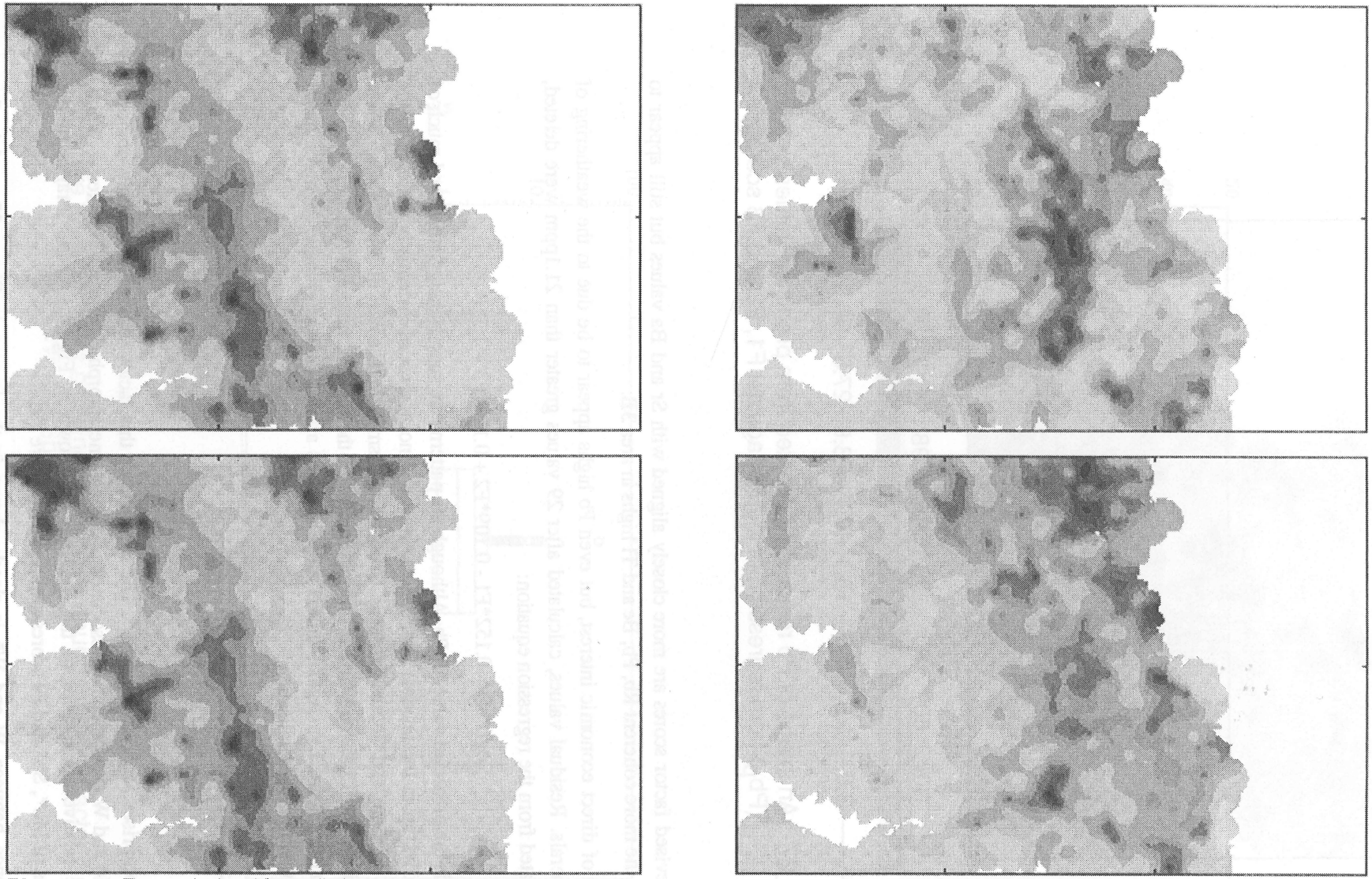

F2 scores Top - calculated from all elements
Bottom - F1 elements deleted

F3 scores Top - calculated from all elements
Bottom - F1 elements deleted

Figure 26 Image maps for F2 and F3 scores calculated as in original factor analysis (top) and deleting major F1 elements (Ce, La, Nd, Th, U, Y, P*, W and Nb)(bottom).

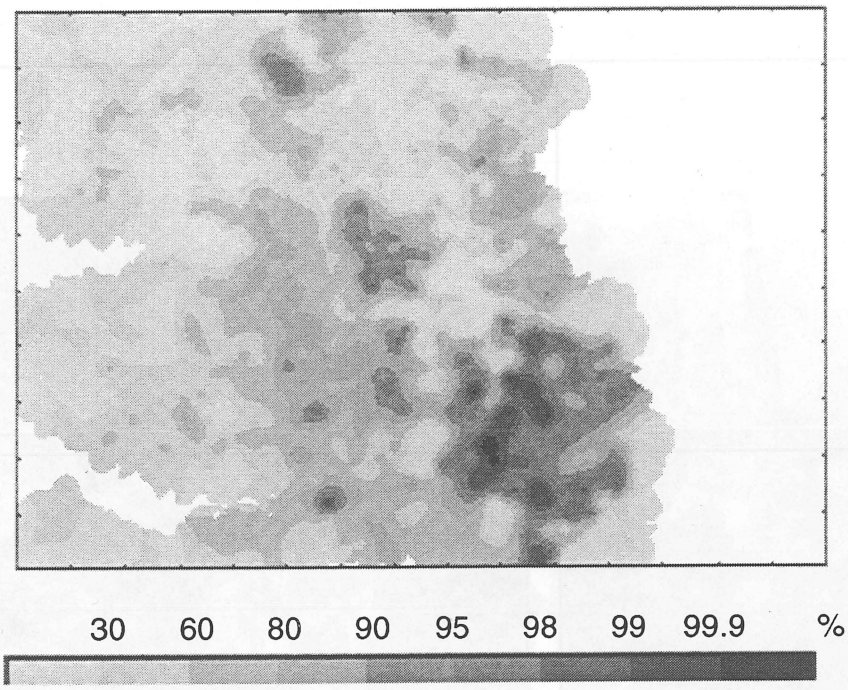

Figure 27 An image of Pb residuals estimated from predicted values (Pb_p) from regression of log(Pb) against F1, F2 and F3 scores.

26). The revised factor scores are more closely aligned with Sr and Ba values but still appear to down-play the more coherent Rb, Pb, Be and Tl highs in area **3B**.

Only Pb is of direct economic interest, but even Pb highs appear to be due to the weathering of K-rich minerals. Residual values, calculated after 29 values greater than 21.1ppm were deleted, were estimated from the regression equation:

$$\log(Pb_p) = 0.152*F1 - 0.109*F2 + 0.197*F3 + 1.318$$

where Pb_p is the predicted value for Pb. Although the patterns are superficially similar and much of area **3B** shows up in the residual image, areas west and north-west of Artemis homestead in the headwaters of Emu and South Five Mile Creeks and a small high south of the Coleman River between Dinah and Lindalong Creeks are highlighted in the residual image (Figure 27) over the raw Pb image (Figure 23). Again, this is only indicates areas which may have higher mineral potential rather than mineralisation.

5.4 Factor 4

Factor 4 comprises Mo*, W* and Sb*. The rationale of this factor is not immediately obvious, although Mo and W are sometimes associated in contact- metamorphic deposits (Hawkes & Webb, 1962). The relative abundances of the elements are shown in Figure 28, and images of the distributions of Mo*, Sb* and F4 scores are shown in Figure 29.

The difference between W and W* is clearly shown in the images in Figure 30, and in the scatterplot of W*/W in Figure 8, and may lie in the analytical methods used. The XRFS method used in AGSO's laboratory uses a press powder pellet and is a total determination of W in all its'

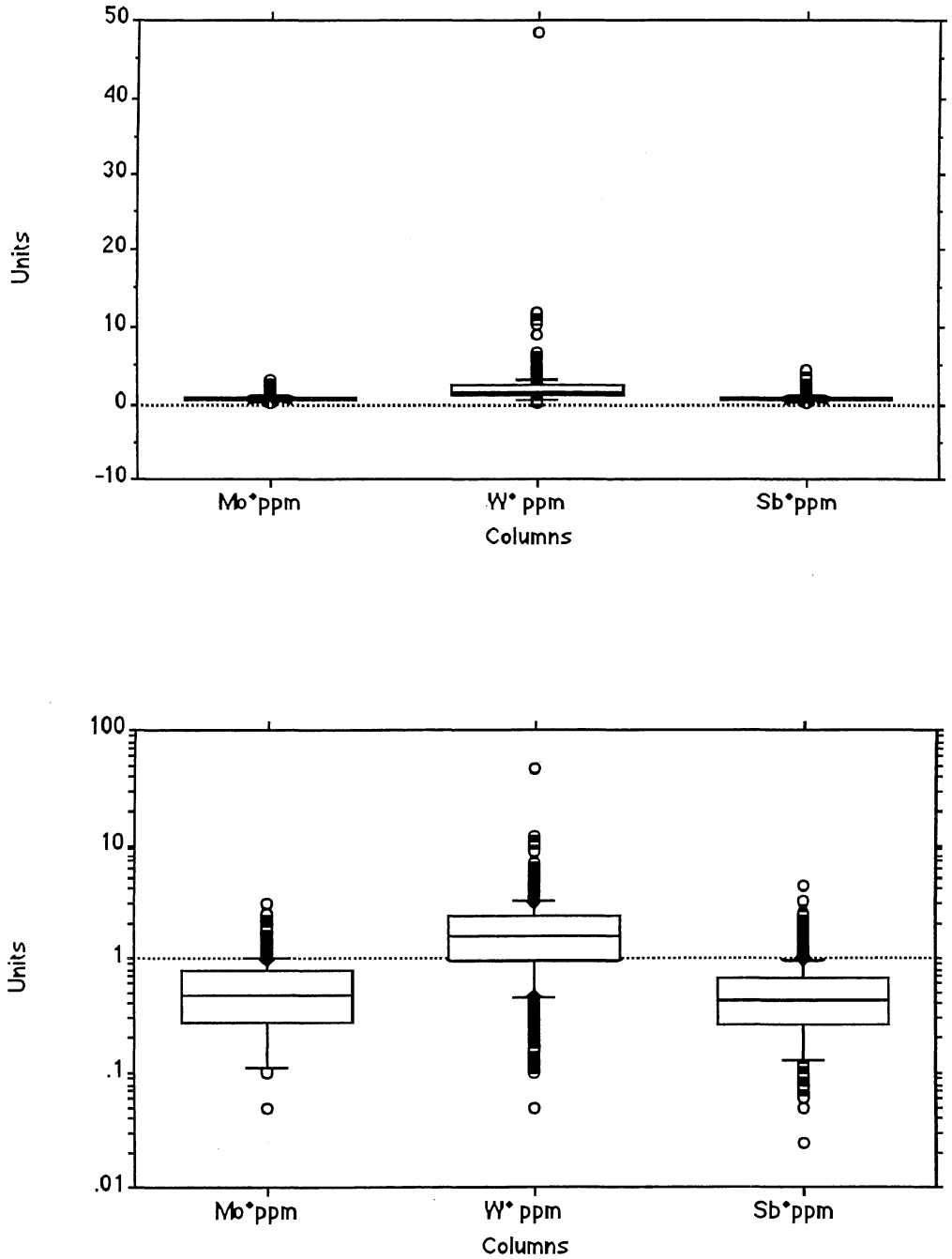

Figure 28 Box plots showing the relative abundances of Factor 3 elements (Mo*, W* and Sb*).

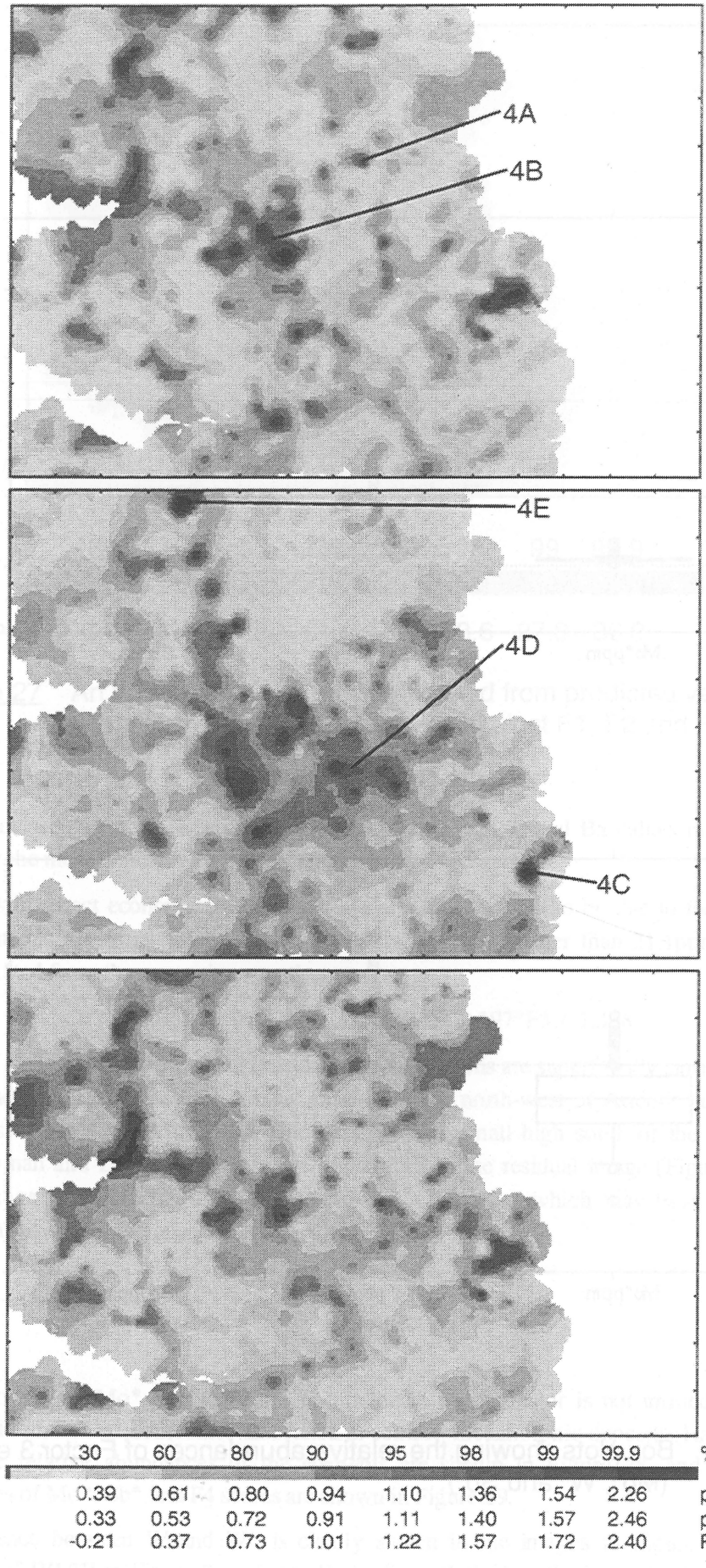

Figure 29 Image maps for selected Factor 4 elements (Mo* and Sb*) and for Factor 4 scores (F4).

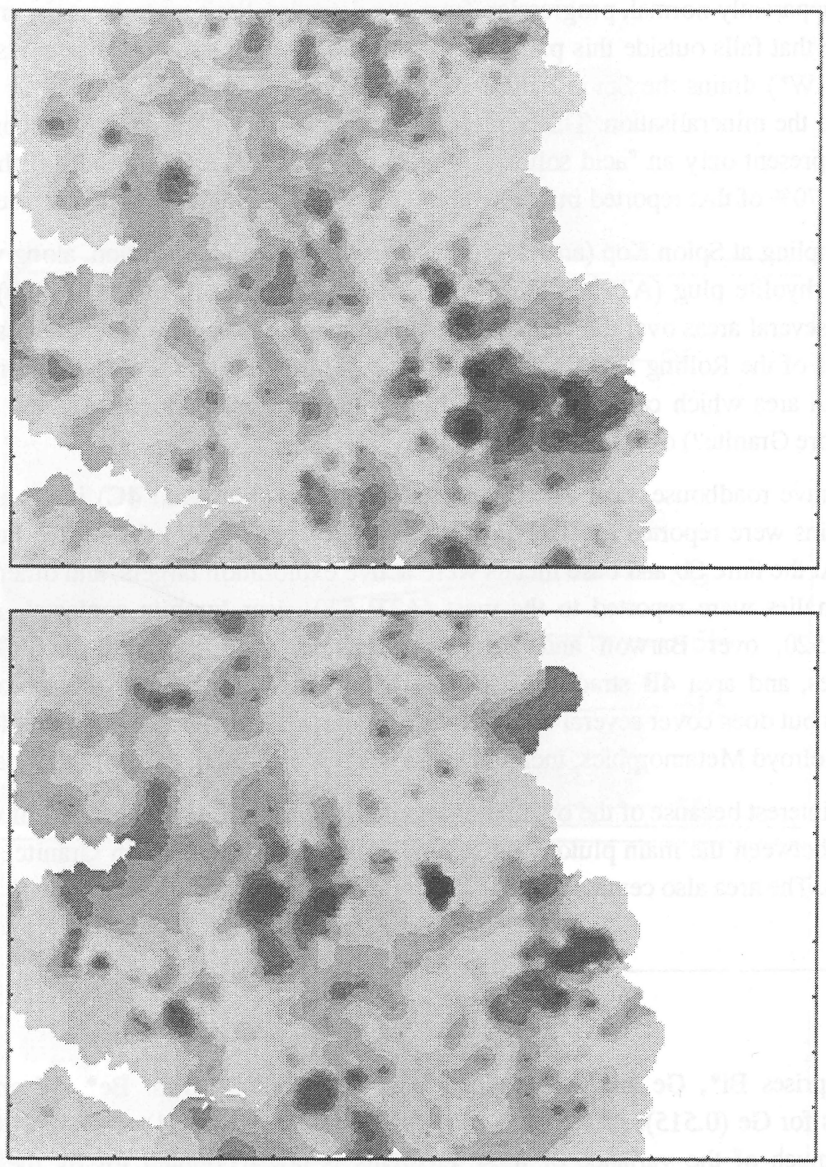

Figure 30 Image maps of W and W* showing the differences in spatial distribution.

mineralogical forms. The digestion method for the ICP-MS determination of W* is a mixed acid digestion using perchloric, hydrofluoric and hydrochloric acids and although it is usually taken as a 'total' digestion, since the hydrofluoric acid decomposes most silicate minerals, it is possible that one or more W-bearing minerals are not taken completely into solution during digestion of the sample. The laboratory notes 'that these are "acid soluble" values'. This is suggested also by the W*/W plot in Figure 8 in which all but 5 W* values are less than 7 ppm although W values show an even, and apparently normal, progression from the detection limit up to a maximum of 50 ppm. The one value that falls outside this pattern and shows high values for both methods (33 ppm W and 48.2 ppm W*) drains the Spion Kop Gold mine at area **4A** and the W may be contained in sulphides from the mineralisation. This sample also contains 77.5 ppm As. In this context the W* values may represent only an "acid soluble" sub-set of the W values, especially if the W* values are reduced to 70% of that reported in line with the 33/48.2 ppm values reported above.

Rock chip sampling at Spion Kop (area **4A**) showed minor Mo mineralisation, along with *Gold*, in fractures in a rhyolite plug (ATP's 2255M and 2256M: Culpeper & others, 1992b). Others Mo highs include several areas over the Holroyd Metamorphics (mainly area **4B**) and areas to the west over sediments of the Rolling Downs Group, Bulimba Formation and associated ferricrete. In the east there is an area which consists of a flood plain transported sediments derived mainly from granites (Kintore Granite?) over metamorphics.

East of Musgrave roadhouse, near Artemis Creek, is an Sb high (area **4C**) in an area in which Sb-bearing veins were reported (ATP 719: Culpeper & others, 1992b) during the late 1960s and early 1970s. At the time Sb and base metals were active exploration targets, and other Sb (plus Au and Ag) anomalies were reported to the west (ATP 520) near 'granite contacts'. Area **4D** lies within ATP 520, over Barwon and Ebagoola Granites and Two Rail and Glen Garland Monzo-granites, and area **4B** straddles its western border, although it is mostly over Holroyd Metamorphics but does cover several small granite outcrops. Several smaller anomalies also occur over or near Holroyd Metamorphics, including area **4E** at the northern edge of the sheet area.

Area **4B** is of interest because of the overlap of anomalies from all 3 elements, part of which occurs over contacts between the main pluton and several small bodies of Barwon Granite, and Holroyd Metamorphics. The area also centres on the Lindalong and Lukin River Shear Zones.

5.5 Factor 5

Factor 5 comprises Bi*, Ge and Au#, with minor contributions from Be*, W and Ag*. The communalities for Ge (0.515), Au# (0.345), W (0.558) and Ag* (0.461) are low to marginal and indicate that much of the variance of these elements is not accounted for by the factors. The association of Ag*, Bi* and W with Au# may be geochemically significant as a *Gold* indicator, although the low communality of the latter suggests it has little correlation with the other elements. Figure 31 shows images of Bi*, Au# and F5, and shows major differences between the patterns for Bi* and F5, and for Au#.

Bi* highs occur in an area almost coinciding to area **1C** over Ebagoola and Kintore Granites near Musgrave roadhouse, at Spion Kop (area **4A**) and in the north of the sheet area over Holroyd Metamorphics near Snake Creek. The latter occurrence is associated with Ti and Nb. Bi is a chalcophile element and is usually concentrated in sulphides, such as *Arsenopyrite* at Spion Kop. Its concentration over the granites is a mystery and the concentrations found do not suggest high level Bi mineralisation.

Gold is the most economically important and interesting element in the EBAGOOLA sheet area

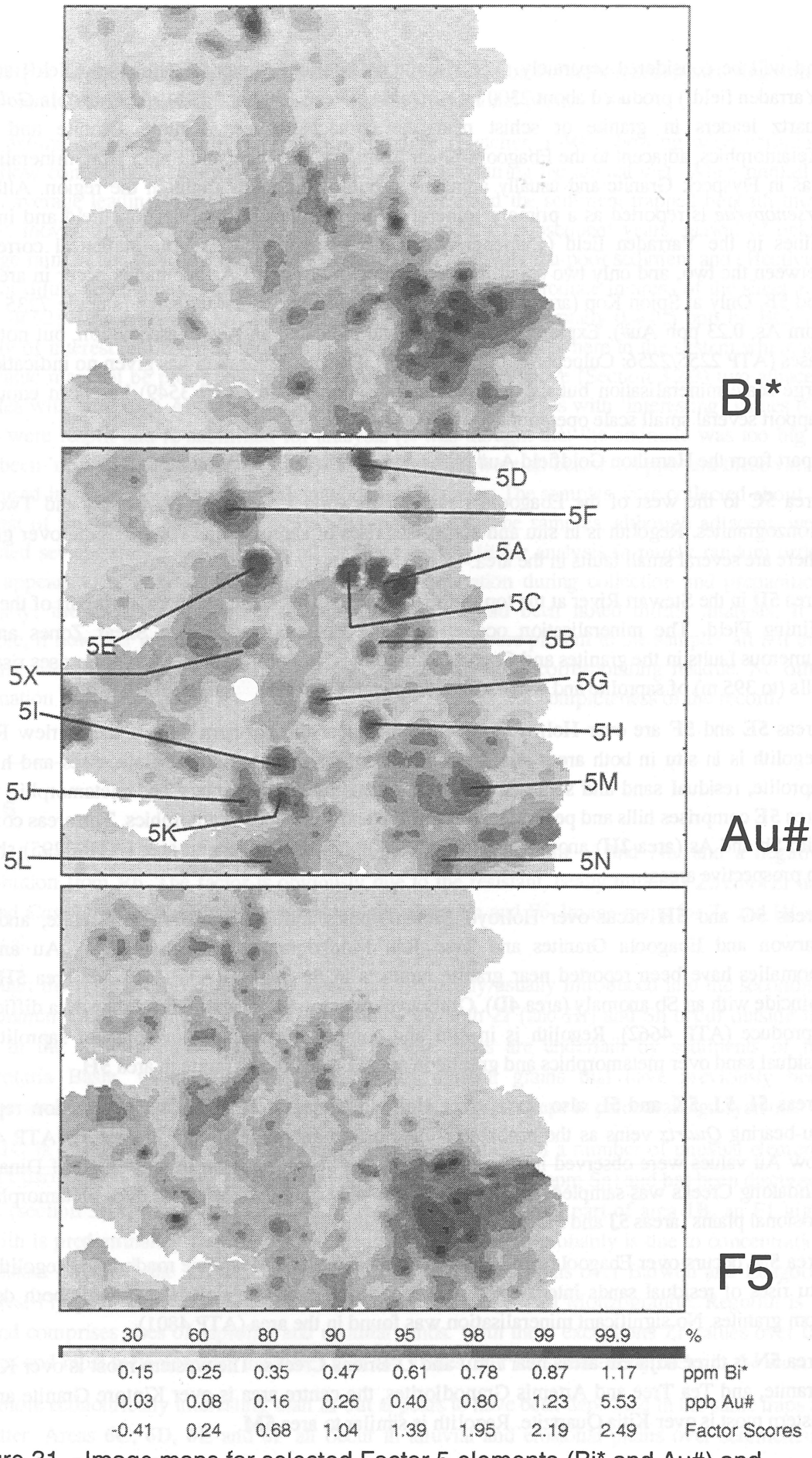

Figure 31 Image maps for selected Factor 5 elements (Bi* and Au#) and for Factor 5 scores (F5).

and will be considered separately. The Hamilton Goldfield (areas **5A** [Ebagoola field] and **5B** [Yarraden field]) produced about 2300 kg of *Gold* between 1900 and 1951. At Ebagoola *Gold* is in quartz leaders in granite or schist near the contact between Kintore Granite and Coen Metamorphics, adjacent to the Ebagoola Shear Zone. At Yarraden, and Spion Kop, mineralisation was in Flyspeck Granite and usually adjacent to one of the many faults in the region. Although *Arsenopyrite* is reported as a primary mineral in many mines in the Ebagoola field and in most mines in the Yarraden field (Culpeper & others, 1992b), there is little statistical correlation between the two, and only two small, moderate level (5-10 ppm) As anomalies occur in areas **5A** and **5B**. Only at Spion Kop (area **4A**) is As really in evidence, but Au# is not (sample 7235 - 77.5 ppm As, 0.23 ppb Au#). Exploration sampling had indicated an As/Au association, but not in all cases (ATP 2255/2256: Culpeper & others, 1992b). Recent exploration has given no indications of large scale mineralisation but the patchy mineralisation found (ATP 3549) has been enough to support several small scale operations.

Apart from the Hamilton Goldfield Au# highs occurred in the following areas:

Area **5C** to the west of the Ebagoola field in Kirkwood Creek, over Kirkwood and Two Rail Monzogranites. Regolith is in situ and comprises rises of saprolite and residual sand over granite. There are several small faults in the area.

Area **5D** in the Stewart River at the top of the sheet area. This is the southern most part of the Coen Mining Field. The mineralisation occurs near the Ebagoola and Coen Shear Zones and the numerous faults in the granites and Coen Metamorphics. Regolith is in situ and comprises rises and hills (to 395 m) of saprolite and some soil over metamorphics and granite.

Areas **5E** and **5F** are over Holroyd Metamorphics near the northern part of the Curlew Range. Regolith is in situ in both areas and in area **5F** consists of an erosional plain, rises and hills of saprolite, residual sand and some colluvial sediments over sedimentary and metamorphic rocks. Area **5E** comprises hills and pediments of saprolite and soil over metamorphics. The areas coincide with Sb and As (area **2H**) anomalies. Recent exploration in the general area (ATP 3295) showed no prospective areas.

Areas **5G** and **5H** occur over Holroyd Metamorphics intruded by Barwon Granite, and over Barwon and Ebagoola Granites and Two Rail Monzogranite, respectively. Sb, Au and Ag anomalies have been reported near granite contacts in the region (ATP 520) and area **5H** does coincide with an Sb anomaly (area **4D**). Other explorers found Au anomalies in the area difficult to reproduce (ATP 4662). Regolith is in situ and comprises rises and low hills of saprolite and residual sand over metamorphics and granite in area **5G**, and over granite in area **5H**.

Areas **5I**, **5J**, **5K** and **5L** also occur over Holroyd Metamorphics. Recent exploration reported Au-bearing *Quartz* veins as the probable source of Au anomalies found in area **5I** (ATP 4820). Low Au values were observed in area **5K** and an Au-bearing gossan in the region of Dinah and Lindalong Creeks was sampled. Regolith is in situ and consists of saprolite over metamorphics in erosional plains (areas **5J** and **5L**) or rises and low hills (areas **5I** and **5K**).

Area **5M** occurs over Ebagoola and Kintore Granites, west of Musgrave roadhouse. Regolith is in situ rises of residual sands interspersed with flood plains of transported sediments both derived from granites. No significant mineralisation was found in the area (ATP 4801).

Area **5N** is three adjacent areas near Emu and O'Briens Creeks. The western most is over Kintore Granite, and Tea Tree and Artemis Granodiorites, the centre area is over Kintore Granite and the eastern most is over Kitja Quartzite. Regolith is similar to area **5M**.

Area **5O** is on the western edge of the sheet area over Bulimba Formation sediments. Regolith is undifferentiated alluvial sediments plus saprolite in an erosional plain.

Gold anomalies are frequently difficult to reproduce (Fletcher, 1990), showing wide variations with flow conditions. Sediments are reworked each year during the annual wet. When rainfall is above average leading to high flow rates, even pebbles, and the sediment trapped beneath them, can be moved and Au brought into the active bed lode. In subsequent years, period of below average rainfall and low flow may mobilise only light, relatively Au-poor sediment and effectively bury or dilute an anomaly. Anomalies were found difficult to reproduce in areas of the sheet area (ATP 4662). However, and for this reason, any high Au value (usually 0.4-0.5 ppb by BCL) is usually of interest and taken to indicate the presence of *Gold* somewhere in the system whereas a low value may not be proof positive of its absence. As stated above (Section 3.2.3) two adjacent samples with very high Au values (20 ppb) and two nearby samples with 'interesting' values (0.5 ppb) were resplit and re-submitted for analysis (it was thought that the anomaly was too big to have been 'missed' by previous workers). The new values were all below 0.4 ppb and these values were used in subsequent statistical calculations and imaging. The samples were collected about 10 km east of Strathburn homestead in the area marked **5X**. The samples, although adjacent, were collected several weeks apart and, as all samples were split for analysis in purely random order, there appears to be little chance of systematic contamination during collection and preparation. Similarly, the analyst indicated that nothing untoward had been noted during analysis. It is possible, if however unlikely, that whatever gains of *Gold* were present in the samples all fell into the first aliquot taken for each sample, or were retained in the corresponding residue. No other explanation is possible at this time and the details are included for completeness of the record.

5.6 Factor 6

Factor 6 comprises Hf, Zr and Sn with minor contributions from V and Nb, and a negative contribution from Rb. The factor is obviously due to the resistant, heavy minerals *Zircon* (Zr and Hf) and *Cassiterite* (Sn). Figure 32 shows images of Zr, Sn and F6. Image maps for Zr and Hf are identical.

Although the resistant *Zircon* and *Cassiterite* are frequently/usually introduced into the secondary environment from weathered granites, most highs for both Zr (and Hf) and Sn occur outside the inlier in the western part of the sheet area. These areas are underlain by sediments of the Carpentaria Basin, which suggests reworking of mineral grains that have previously been incorporated into the sedimentary rocks, possibly from sediment traps in paleodrainage systems.

Area **1G** is a single sample which contains high concentrations of a number of unusual elements (e.g. 13,940 ppm Zr, 251 ppm Hf, 127 ppm Nb, 49 ppm Ta and 17 ppm Sn) and has been discussed above (section 5.1). Area **6A**, a Zr high, corresponds to the eastern part of area **1B**, an F1 high. Regolith is predominantly transported sediments and the Zr high probably is due to concentration of resistant *Zircon* in the stream bed lode. Area **6B** contains 3 highs over Barwon and Ebagoola Granites, Flyspeck and Glen Garland Granodiorites, and Two Rail Monzogranite. Regolith is in situ and comprises rises of saprolite and residual sands. With these exceptions Zr values over the granites and most metamorphics are lower than the values over the sedimentary rocks to the west.

Sn is more economically interesting than Zr but appears to have been deposited in the same traps as the latter. Areas **6C**, **6D**, **6E** and **6F** all occur in alluvial and erosional plains over sedimentary rocks of the Rolling Downs Group and/or the Bulimba Formation, although areas **6C** and **6F**

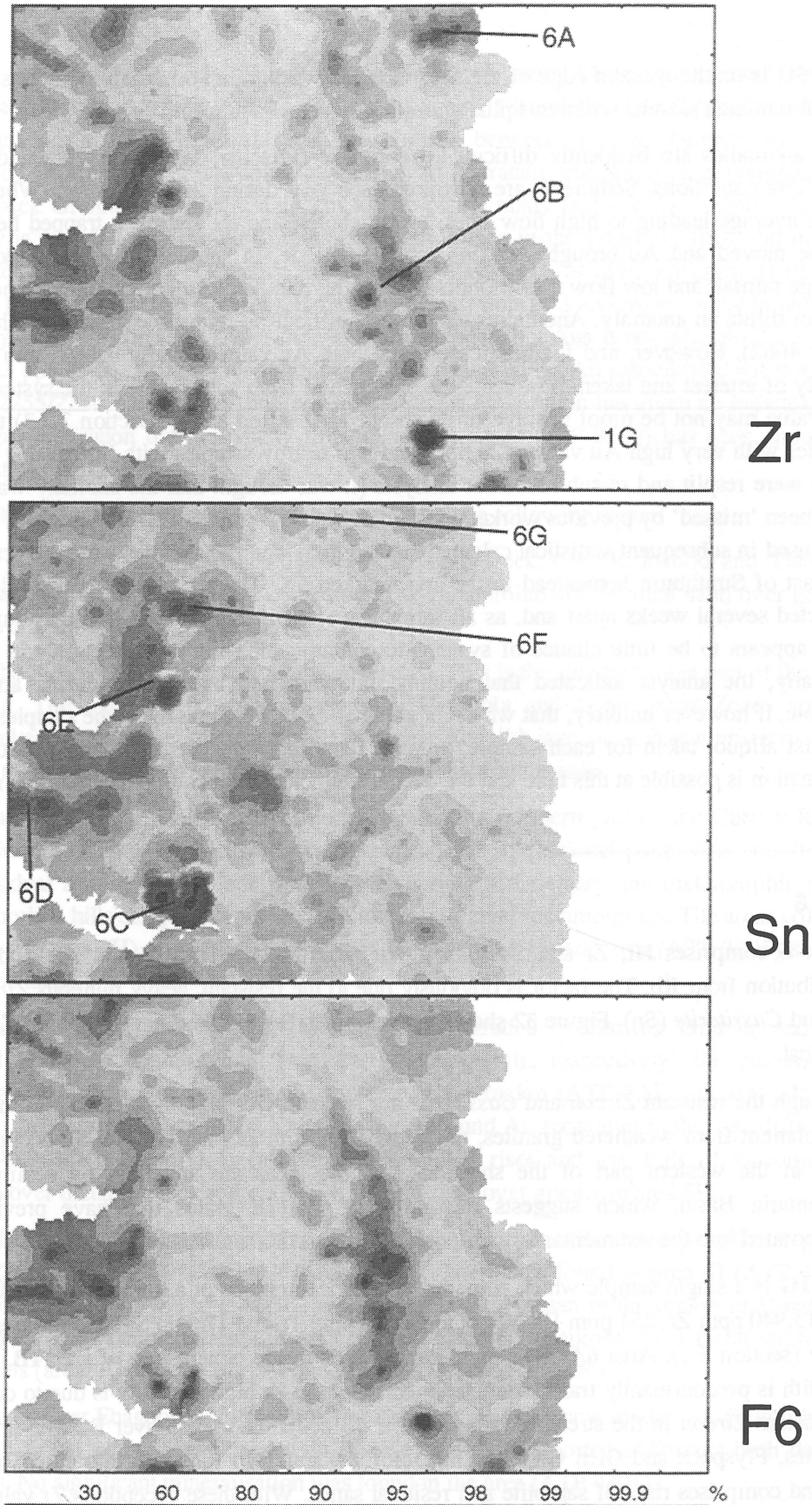

Figure 32 Image maps for selected Factor 6 elements (Zr and Sn) and for Factor 6 scores (F6).

overlap Holroyd Metamorphics in the east. Area **6F** is about 2 km north-west of the Goanna Creek Tin Prospect in which 'quartz floaters with large cassiterite crystals (to about 15 mm across)' were found in a creek bed although no definite mineralisation source was found and no late Palaeozoic granites (the usual source of Sn mineralisation in north Queensland) have been mapped in the area (Culpeper & others, 1992b). Anomalous Sn values were restricted to isolated and very short drainage trains'. In both these areas (and in area **6E** and near area **6D**) inverted paleodrainage, which once flowed from the east or from the direction of the metamorphics and granites, has been observed (Pain & Wilford, 1992) and the weathering of heavy mineral traps contained in these systems is a possible in situ source of these resistant, heavy minerals in existing drainage systems. This does not define the original source of Sn mineralisation.

A sample of the Tadpole Granite, from the north end of the Ebagoola Shear Zone in the sheet area, contained 14 ppm Sn (Mackenzie & Knutson, 1992) and shows moderate values in area **6G** in Figure 32. The only other Sn 'highs' over the granites are at Spion Kop and at area **1G**, the single sample with high Zr, Hf, Nb and Ta.

5.7 Factor 7

Factor 7 comprises Ta, Cd* and Ag*, and accounts for only 2.7% of the total variance. All have low communalities and the lack of any apparent geochemical relationship suggests a meaningless, garbage bin association. Figure 33 shows images for Cd* and Ag*.

Geochemically Cd and Zn show an almost universal association with a Zn:Cd ratio of about 500:1 (i.e. between 250:1 and 1000:1), and Cd follows Zn in the secondary environment except during oxidation of sulphides where Cd tends to remain after the Zn sulphides have been oxidised and Zn leached away (Hawkes & Webb, 1962). As stated above (section 4.3.1) Cd and Zn values do not appear to follow this association (see Figure 34) and the Zn:Cd ratio varies from 4.5 (8 ppm Zn and 1.76 ppm Cd*) to 2010 (201 ppm Zn and 0.10 ppm Cd*), with an average value of 143.5 for the ratio. Cd shows a high value (area **7A**) in Dinner Creek, a tributary of Station Creek, which shows little else of geochemical interest (e.g. 16 ppm Zn). The second high (area **7B**) is in Flying Fox Creek and is part of a large area of Cd highs. As would be expected from Cd* inclusion in the final factor, this area is superficially similar to highs for several other elements but does not correspond closely to any, including Ag* and Zn. It is unlikely that this is an area in which Zn sulphides have been oxidised and Zn removed wholesale.

Ag* shows a high in area **1G** (section 5.1), in the single, unusual sample and in the sample downstream. This is part of a high which roughly corresponds to the Zn anomaly containing the Bustard lease (area **2F**) near Glen Garland homestead. Other high are west of the Musgrave roadhouse in the western part of area **1C**, and near Eight Mine and Bamboo Creeks west of Lapunya Mount (area **7C**). There is little coincidence between Ag* and Au# (except at area **5K**), or between Ag* and As.

5.8 Elements Excluded From Factor Analysis

Five elements (Bi, Mo, Pd#, Pt# and Se) were excluded from the factor analysis because of their high numbers of 'Not Detected' values (712, 605, 607, 604 and 742 respectively from a total of 744) and the low communalities that could be expected. However, only Se might be regarded as unusable. The data are also characterised by the small range of detected values, for example data

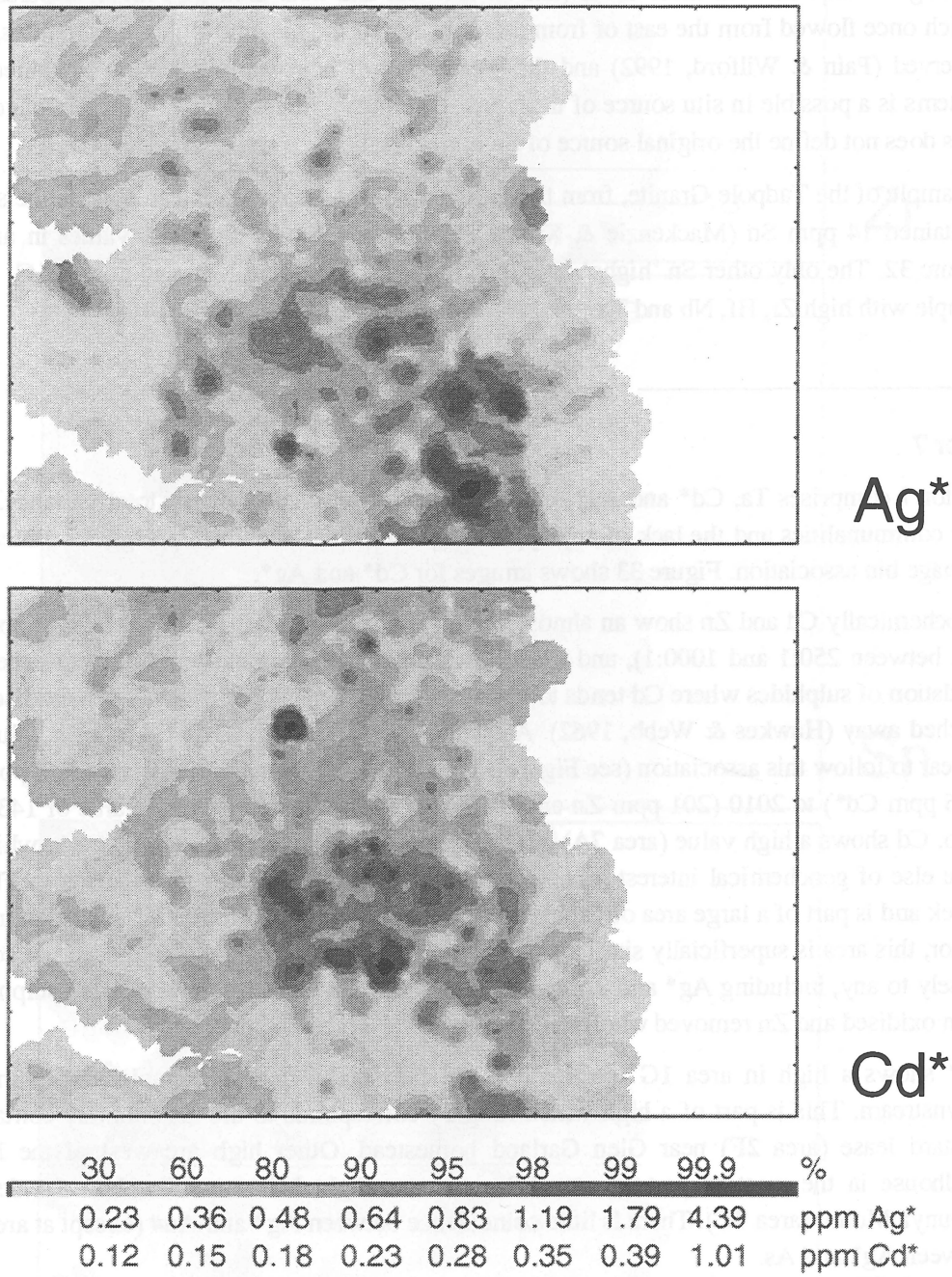

Figure 33 Image maps for Factor 7 elements (Ag* and Cd*).

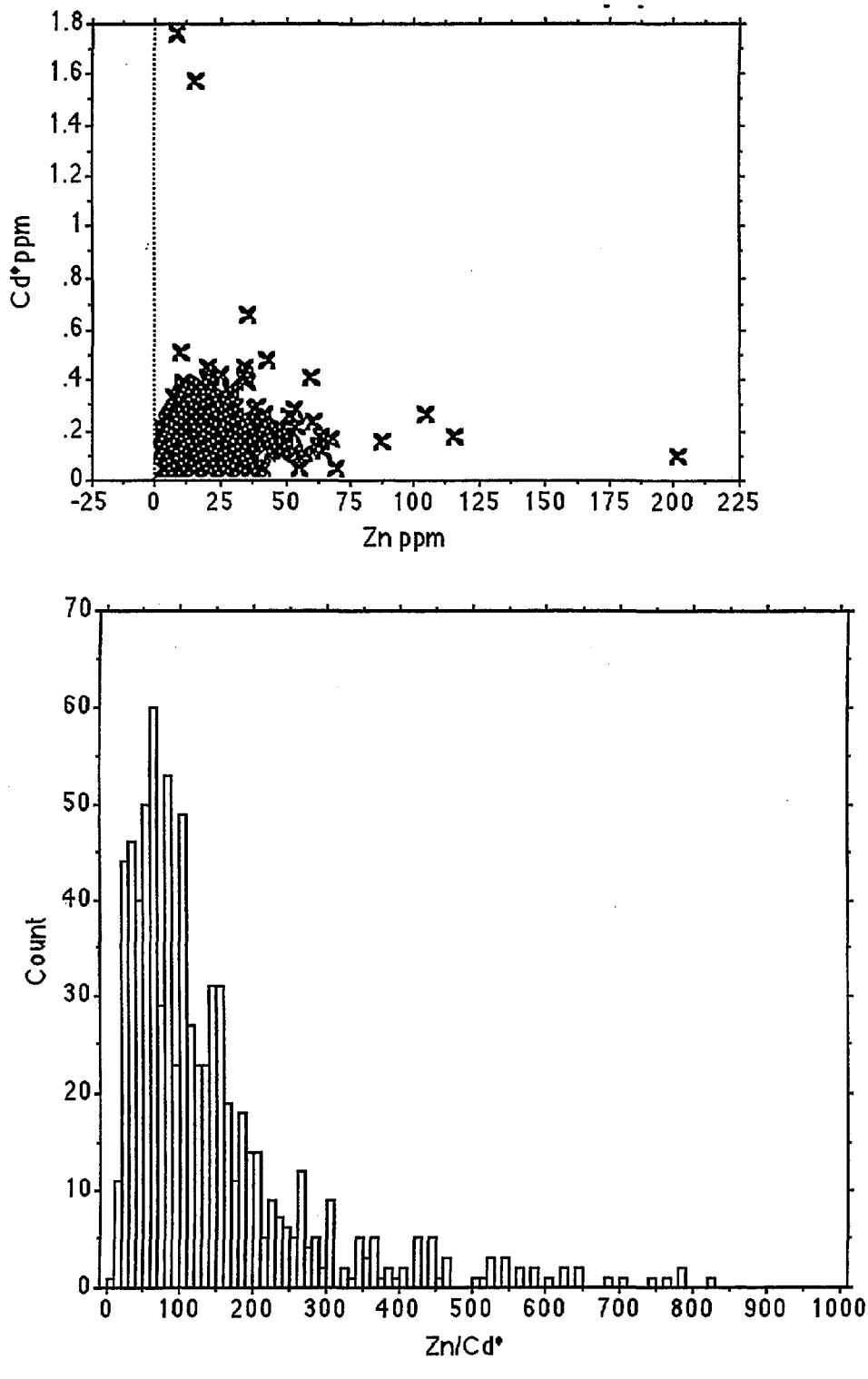

Figure 34 Scatterplot of Cd* against Zn (top) and bar chart showing frequency distribution of the Zn/Cd* ratio.

for both Pd# and Pt# comprise only the 'Not Detected' values (ppt in both cases, or 5ppt as used in statistical calculations) and the minimum detected value of 10ppt, which itself must be regarded with suspicion.

Figure 35 shows modified images for Bi, Mo, Pd# and Pt#. PGE potential is considered to be extremely low.

5.9 Mineral Potential

To assist in the assessment of the economic potential of an area it is necessary to emphasise concentrations of economically important elements, or their pathfinders elements, which possibly have been derived directly or indirectly from mineralisation. It is therefore necessary to remove effects due to lithochemical and secondary processes from the data, as in the estimation of 'residuals' by regression methods, or to high-light coincident concentrations of elements characteristic of known mineralisation types, as in the method of 'additive indices'.

5.9.1 Residuals

Residuals have been estimated for U (Figure 15), and for Cu, Zn (Figure 21) and Pb (Figure 27), by regression against factor scores for factors into which the elements have significant contributions. Thus the U concentration as measured has been corrected for U trapped in resistant minerals such as *Monazite, Xenotime* and *Zircon*, as represented by Factor 1, and areas more likely to contain U from possible mineralisation defined. Similarly, total Cu, Zn and Pb concentrations have been corrected for lithological and secondary effects represented by Factors 1, 2 and 3 as appropriate and areas of high residuals defined. Figure 36 shows outlines of areas for the top 20%, 10% and 5% of grid values for the residuals for each of the elements superimposed in an RGB diagram with Cu as RED, Pb as GREEN and Zn as BLUE. Where Pb and Zn coincide the image is coloured as CYAN (light blue), and where all three coincide as WHITE. The most promising Cu-Pb-Zn target would appear to be east of Strathaven homestead over the Holroyd Group metamorphics. An area of possible Pb-Zn mineralisation occurs further to the east, also over Holroyd Metamorphics.

5.9.2 Additive Indexes

An alternative and more powerful method of defining potential targets is that of additive indices (Chaffee, 1983; Eggo & others, in prep.) in which values for economic and pathfinder elements characteristic of particular types of mineralisation are summed with the highest totals defining the most likely potential target areas. To compensate for the large variations in the ranges of element values that the components of a particular characteristic group may contain, a standardised value (SV) is estimated as follows:

$$SV_i = (X_i - X)/SD$$

where X_i is the value of an element in sample i, and X and SD are the mean and standard deviation respectively for that element estimated from the total population. The standardised value is therefore in 'SD' or standard deviation units with a mean of zero, and high values, for example greater than 2, may be considered to be 'highly' anomalous in traditional terms as these are greater than 'mean plus two standard deviations'. Index values for each sample were calculated as follows:

$$Index_i = \sum_{e=1}^{e=n} SV_{e,i}$$

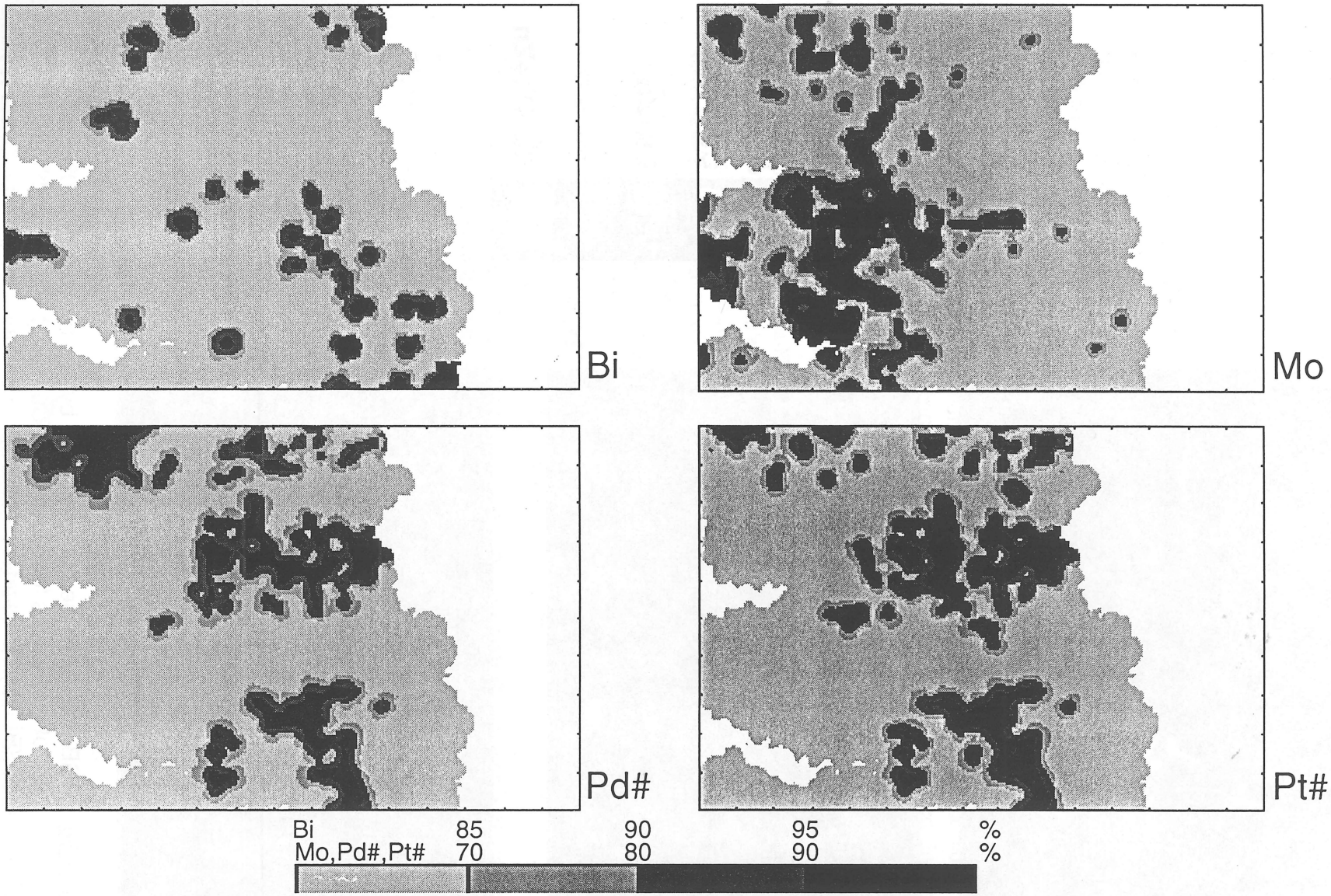

Figure 35 Reduced level image maps for Bi, Mo, Pd# and Pt#. Data for these elements contained large numbers of ND values so only percentage slice points are shown on density bar.

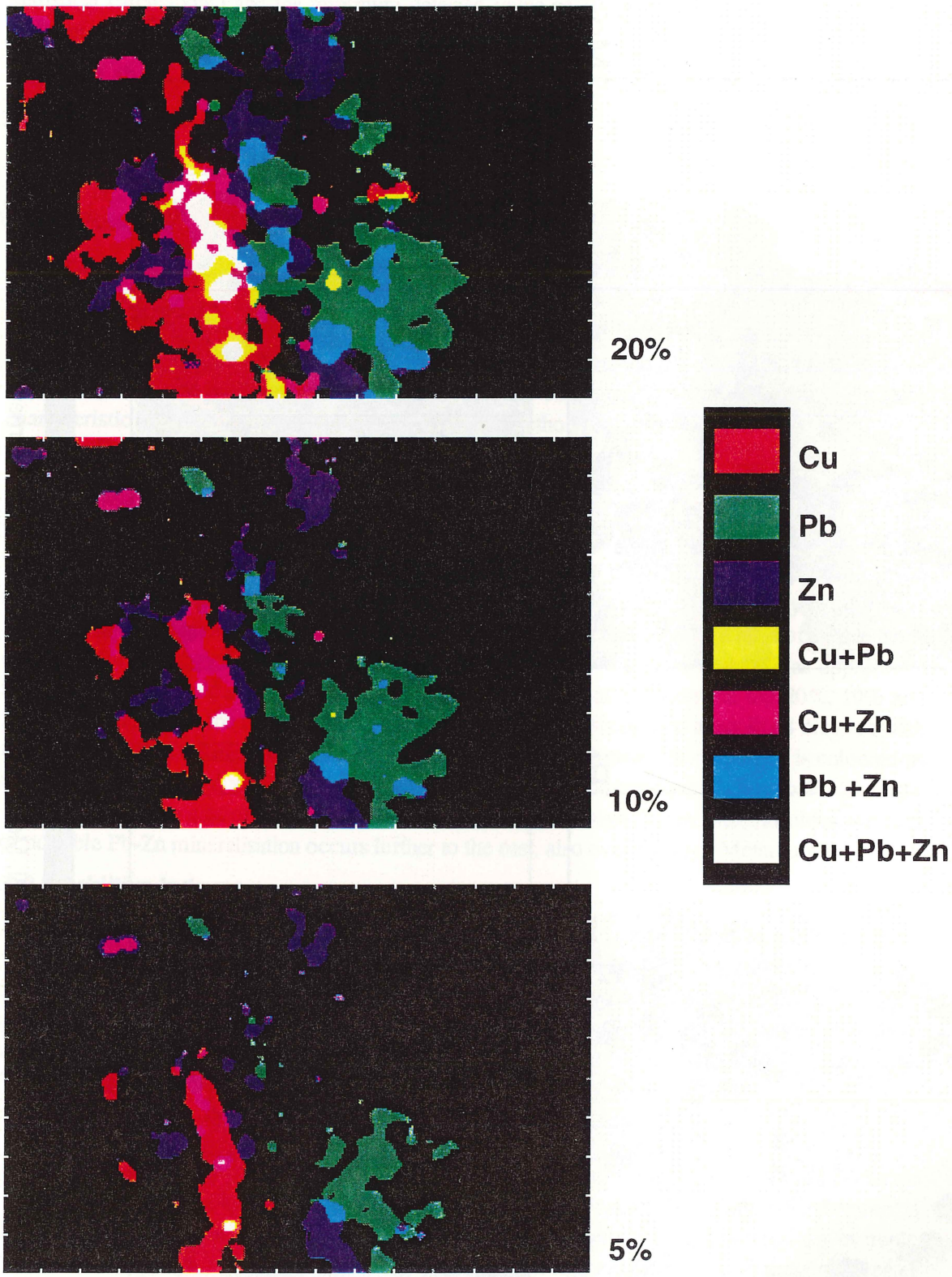

Figure 36 RGB images of the areas covered by the upper 20%, 10% and 5% of grid values for residuals of Cu (RED), Pb (GREEN) and Zn (BLUE). Coincidence of 2 or more of the elements produces the colours shown.

Residual values for U, Cu, Zn and Pb have been used in place of the total or as measured values. Index values for a number of mineralisation types were calculated for each sample, gridded and are presented as images. The choice of elements to be included in an index is essentially arbitrary but should be based on common element/mineralisation associations and any available knowledge of mineralisation in the general area. The mineralisation types and the elements used to calculate the indexes are:

Gold Index (AuI) – Ag* + As + Au# + Sb*

Gold taken from the Hamilton Goldfield contained a high proportion of Ag and veins contained 'masses of pyrites and galena' (Ball, 1901). The 'pyrites' included arsenopyrite, galena and stibnite (Whitaker & Gibson, 1977), although Pb has not been included in the index because its other more obvious (base metal) associations may overprint an Au pattern.

Figure 37 shows the image of AuI with the Hamilton Goldfield high-lighted because of high Au values (See Figure 31) and Spion Kop because of a single very high As value (see Figure 17). Two large areas over the Holroyd Metamorphics (mostly Strathburn Formation in the north, and Strathburn, Strathmay and Newirie Formations in the south) are also high-lighted due to the combined effects of As, Au and Sb and may be prospective. Several others areas are annotated with the elements responsible.

Base Metal Index (BMI) – Ba + Cu(res) + Pb(res) + Zn(res)

The BMI represents simple Cu-Pb-Zn or Pb-Zn mineralisation. The element association is from Levinson (1974). Figure 38 shows an image of the BMI, with two areas showing promise. In the west the area over Holroyd Metamorphics (mostly Newirie and Astrea Formations and Carew Greenstone) is due mainly to residual Cu but also shows two high (black) points corresponding to the white high points in Figure 36, probably due to Cu-Pb-Zn coincidences. The other area is over Kintore Granite (Pb and Ba) in the north-east, Ebagoola Granite (Pb) in the centre and Holroyd Metamorphics (mostly Strathburn Formation and Gorge Quartzite – Zn) in the south. This corresponds, in part, to the Pb-Zn coincidence in Figure 36. These areas may be prospective.

Heavy Mineral Index (HMI) – Ce + La + Nd + P* + Th + Y

The heavy mineral index, HMI, is for the Rare Earth-bearing phosphate minerals *Monazite* and *Xenotime* and is shown in Figure 39. The areas over the Coen and Newberry Metamorphics in the north are *Monazite*-rich (section 5.1) with highs in the Rare-Earth elements Ce, La and Nd, plus Th, whereas in the south, over the Ebagoola and Kintore Granites, *Xenotime* appears to dominate with a large Y high (see Figure 10(a-c)). The northern area has been explored for heavy minerals but without economic success.

Porphyry Copper Index (PCI) – Cu(res) + Mo* + Rb

Porphyry copper deposits at Moonmera in central coastal Queensland (Dummett, 1978), and at Coalstoun in southeast Queensland (Ashley & others, 1978) also contain Mo. Rb enrichment in the mineralised zone was also noted at Moonmera so Rb was included in PCI. The PCI is shown in Figure 40 with an area of highs corresponding to the high residual Cu (see Figure 21), modified by Mo, but with little contribution from Rb (see Figure 23). The area to the east is due to Mo plus Rb with little or no contribution from residual Cu. Potential for porphyry Cu mineralisation is not considered to be high.

Platinum Index (PTI) – Cr + Ni + (Pd# + Pt#) + V

PTI defines areas likely to contain mafic/ultramafic rocks which may have potential for platinum group elements. The probity of the Platinum Group Elements Pd# and Pt# is questionable because only two values were reported for each element, namely ND ('Not Detected' or ppt) and 10ppt.

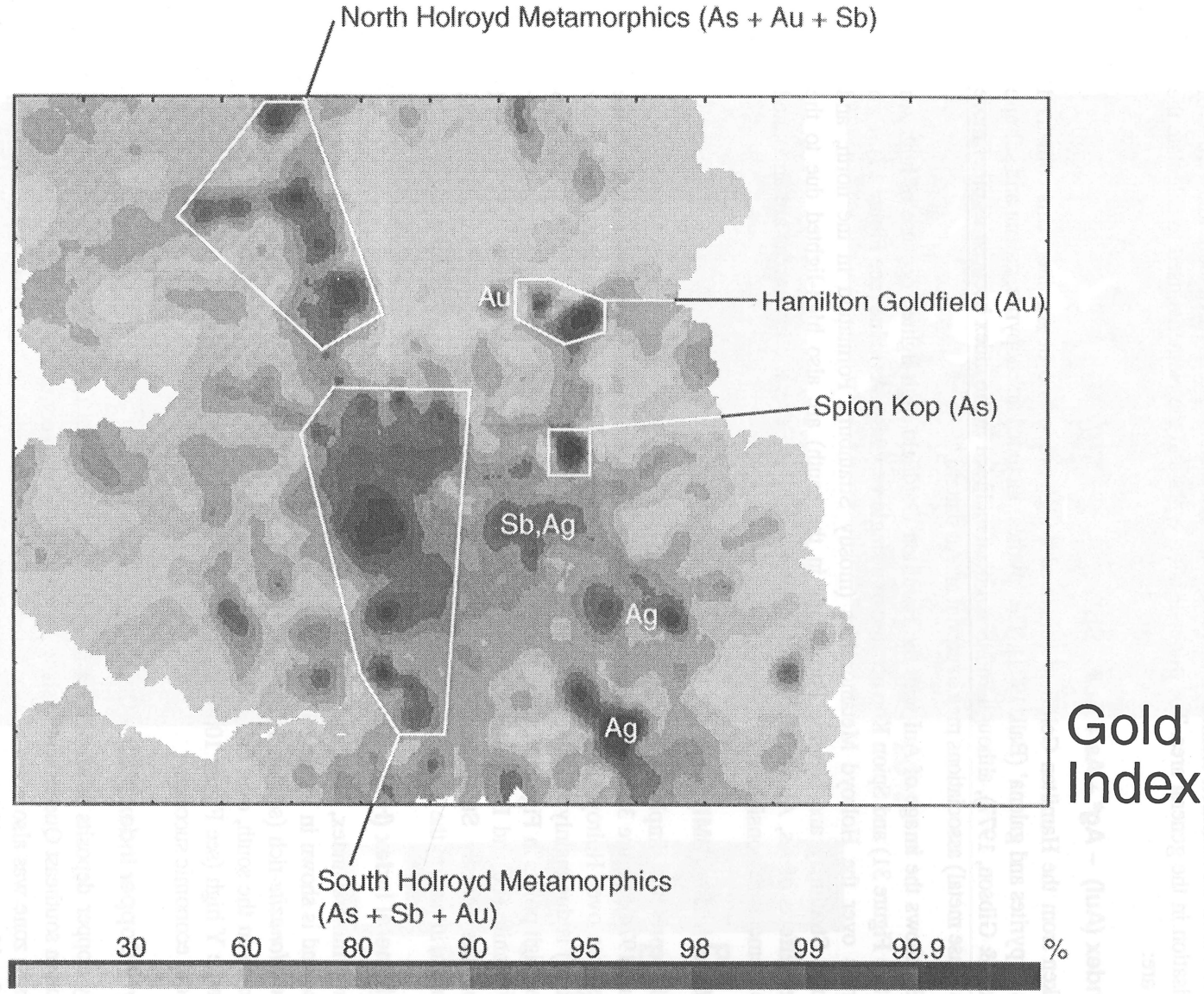

Figure 37 Image map of additive index for Gold (Ag*+As+Au#+Sb*).

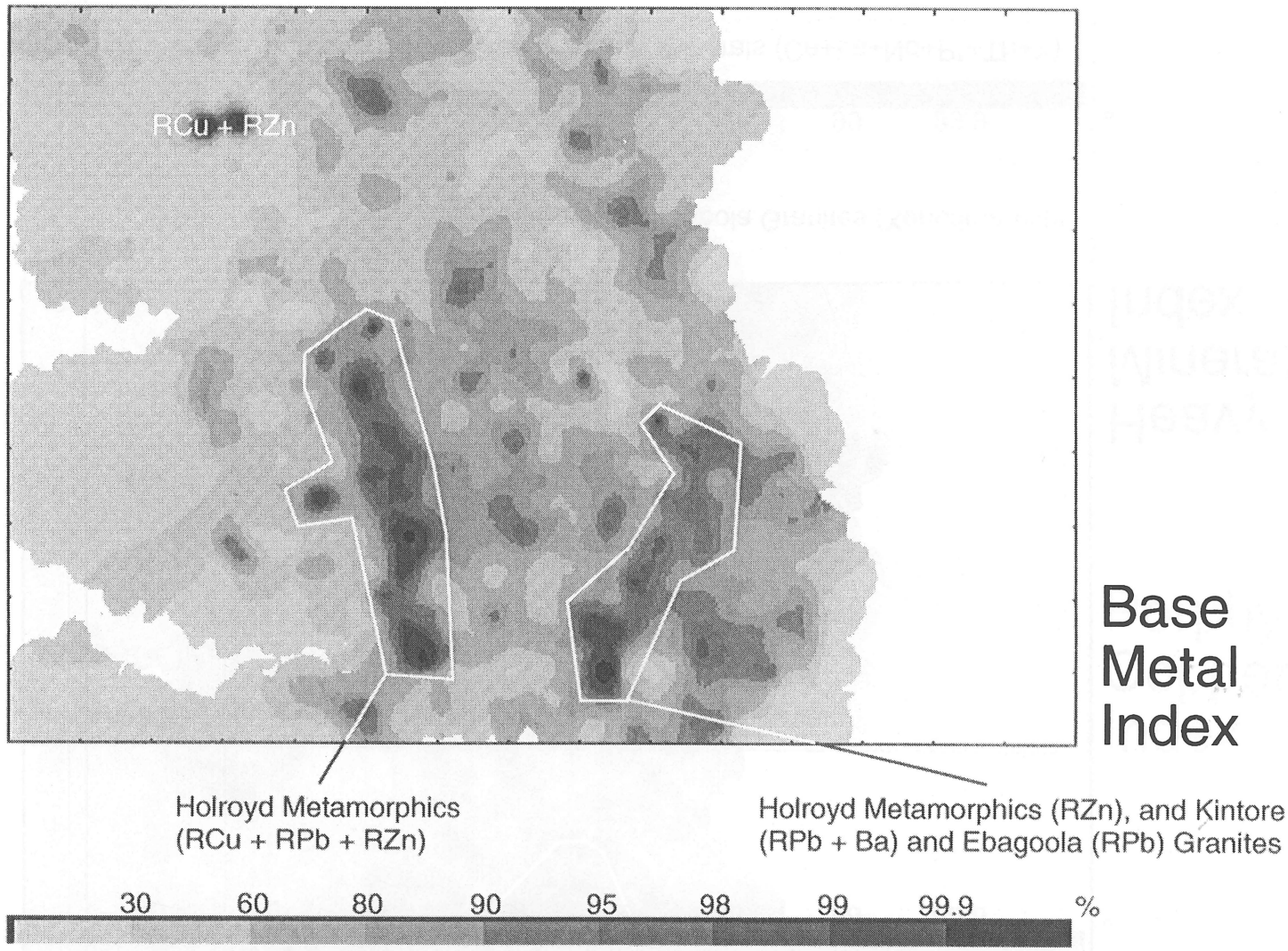

Figure 38 Image map of additive index for base metals (Ba+Cu(res)+Pb(res)+Zn(res)).

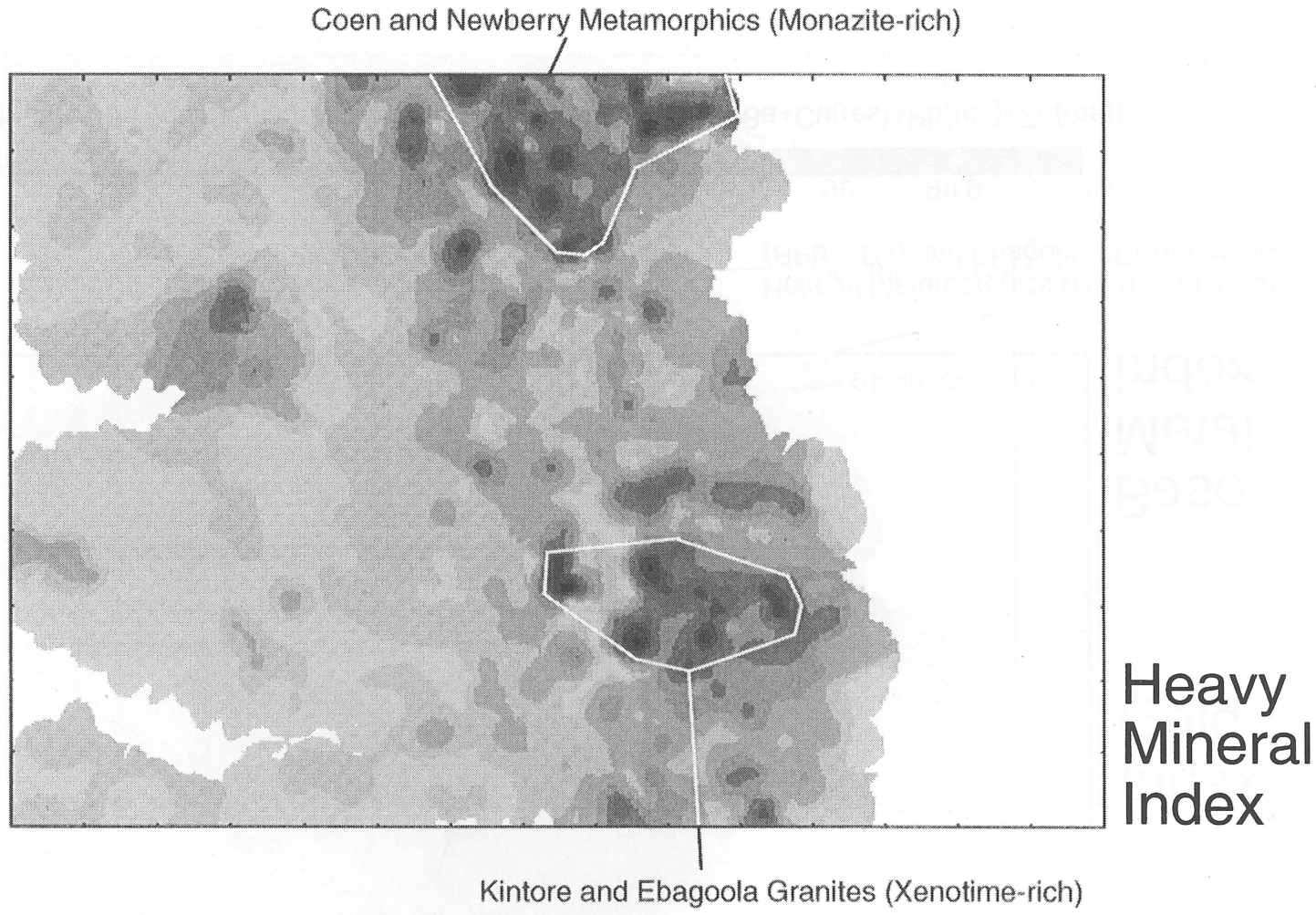

Figure 39 Image map of additive index for heavy minerals (Ce+La+Nd+P*+Th+Y).

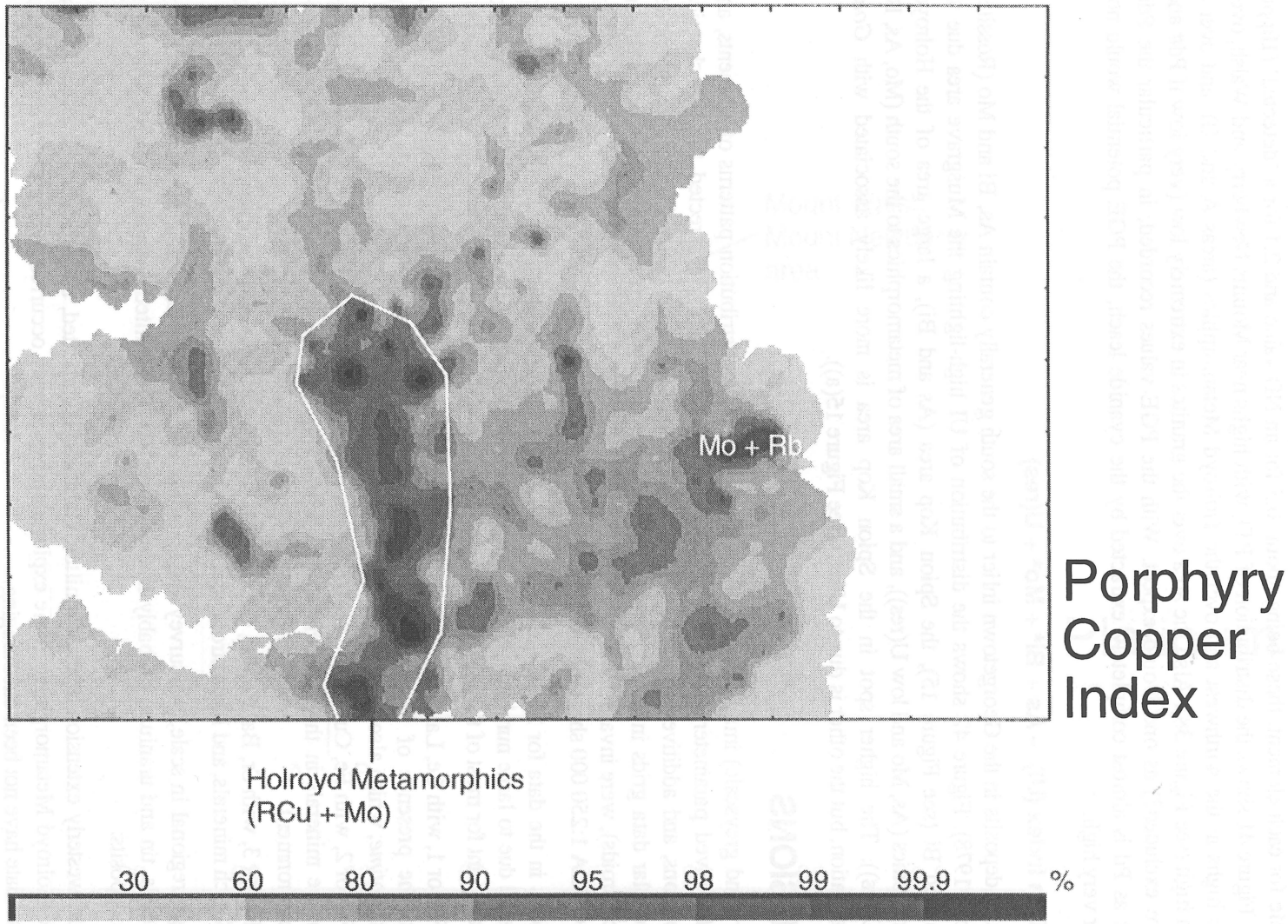

Figure 40 Image map of additive index for porphyry copper (Cu(res)+Mo*+Rb).

With a value of half the detection limit substituted for any ND value, only two index values were possible for each element, these being about -0.5 for an ND value and 2.1 for a 'detected' (10ppt) value. Figure 41 shows the distribution of PTI, with highs near Mounts Newberry and Walsh, over the Fe highs in the northwest and over the Holroyd Metamorphics (areas A and B), and over a Cu-Zn high (see Figure 38). Also the area over the granites in extremely low (very low if Pd# and Pt# are excluded?) as one would expect. With the PGE values recorded, in particular the Pd# values as Pd is almost completely extracted by the cyanide leach, the PGE potential would not appear very high.

Uranium Index (UI) – As + Bi* + Mo* + U(res)

Uranium deposits in the Georgetown inlier to the south generally contain As, Bi and Mo (Rossiter & Scott, 1978). Figure 42 shows the distribution of UI high-lighting the Musgrave area due to U(res) and Bi (see Figure 15), the Spion Kop area (As and Bi), a large area of the Holroyd Metamorphics (As, Mo and low U(res)), and a small area of metamorphics to the south (Mo, As, Bi and U(res)). The higher spot in the Spion Kop area is more likely associated with *Gold* mineralisation, but the other is due to U(res) (see Figure 15(a)).

CONCLUSIONS

Colour (and greyscale) image maps effectively represent the distribution patterns of elements, and also of derived parameters such as factor scores, element residuals corrected for lithochemical contributions, and additive indices based on possible mineralisation types. The images, generated from regular data grids interpolated from random sample data points (sample sites or catchment basin centroids), were invaluable in interpretating the regional stream sediment geochemistry of the EBAGOOLA 1:250 000 sheet area.

Variations in the data for 37 of the 43 sets of element values (with Bi, Mo, Pd#, Pt#, Se and Ta eliminated due to large numbers of ND values) can be explained by the extraction of 7 factors, 3 of which account for most of the variation. These are:

- Factor 1, with Ce, La, Nd, Th, U, Y, P*, W and Nb as major contributors, is believed to be due to the presence of the resistant Rare Earth Element/ Phosphate minerals *Monazite* and *Xenotime*, which also contain Th and U.
- Factor 2, with Fe, Cu, Ni, V, Sc, Cr, Zn, Ti and As, is believed to be due to the geochemistry of Fe minerals in the bedrock, and/or scavenging by hydrated Fe-oxides in the secondary environment.
- Factor 3, with Sr, Ba, Rb, Pb, Ga, Be*, Tl* and Mn, is believed to be due to the weathering of K-rich minerals, and has a strong association with Factor 1.

Although regional in scale, the survey suggests that the area's greatest mineral potential is in gold, base metals, tin and uranium, probably in that order, but with limited potential for large scale, near surface deposits.

A minor, westerly extension of the Hamilton Goldfield is indicated, as are several interesting areas over the Holroyd Metamorphics. Some exploration has already occurred over parts of the latter but results to date have not been encouraging.

Two areas of possible Pb/Zn and Cu/Pb/Zn mineralisation occur over the southern areas of the Holroyd Metamorphics are highlighted by RGB overlays of residuals and by a base metal additive index. The former is in the area of the Bustard Pb/Zn lease.

A number of tin anomalies occur, not over or near granites as might be expected, but to the west of the inlier over sedimentary rocks. The source of the anomalies is not obvious but paleodrainage channels have been observed near or leading into several.

An area west of Musgrave homestead may have potential for U, as shown by U residuals. Sediments from the area contain *Xenotime* but also drain a relatively 'hot' granite, the Ebagoola Granite.

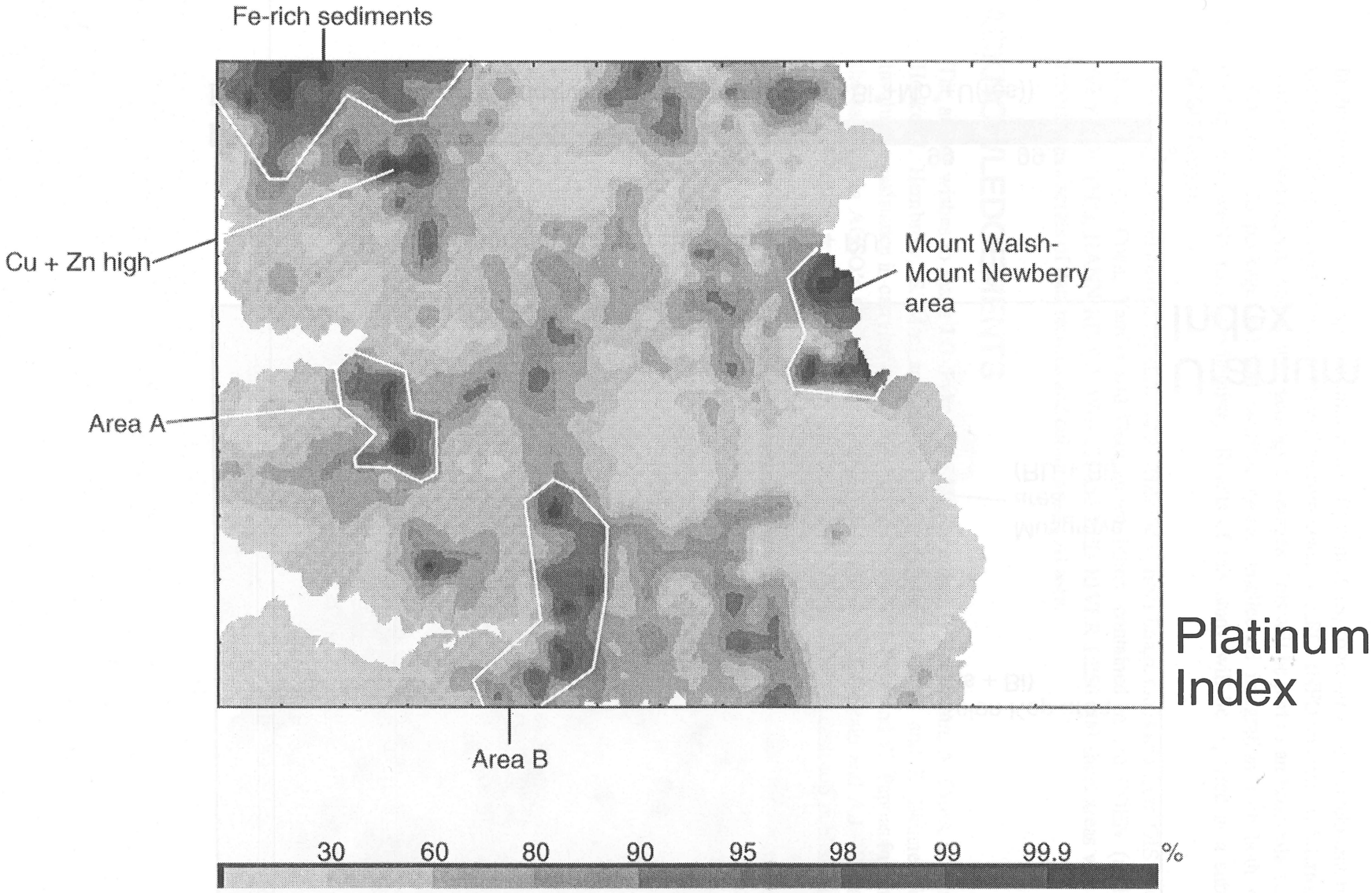

Figure 41 Image map of additive index for platinum (Cr+Ni+(Pd#+Pt#)+v).

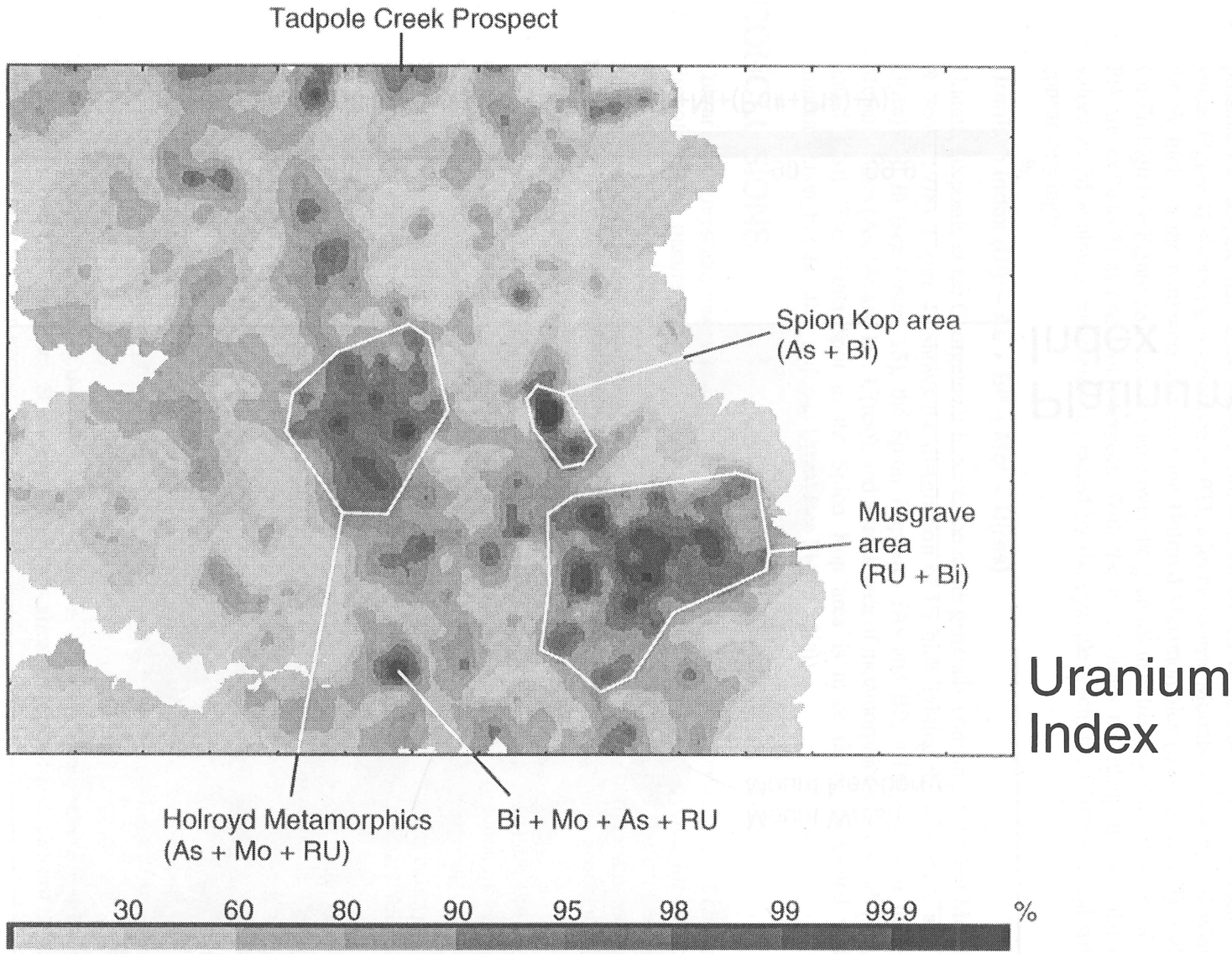

Figure 42 Image map of additive index for uranium (As+Bi*+Mo*+U(res)).

FUTURE WORK

In the near future a Geographical Information System (GIS) coverage of the catchment basins of the EBAGOOLA sheet area samples will be completed on ARC- INFO and will be interrogated in relation to the regolith and general geology coverages. This will be part of an Ebagoola 1:250 000 sheet area GIS package and will facilitate greater intellectual integration with both regolith, geology and whole rock geochemistry. Results of this study will be reported in a subsequent AGSO Record.

Ultimately interpretation of the surficial geochemistry, from image maps and from GIS coverages, of areas of the Coen, Yambo and Georgetown Inliers contained in the COEN (and CAPE WEYMOUTH?), HANN RIVER, WALSH and RED RIVER 1:250 000 sheet areas will also be reported in a series of data records and colour image Atlases.

ACKNOWLEDGEMENTS

The author wishes to thank J.G. Pyke and F.M. Kane, and F. Beckmann, A. Cross, G. Gagler, J. Hedke, J. Hembrow, S. MacLaughlin, J. Pye, L. Roberts, J. Ryall and R. Skinner for their invaluable assistance in carrying out the sampling program, J.G. Pyke and W. Pappas for analysing the samples in AGSO's Geochemical Laboratory, J.H.C. Bain, C.F. Pain and A.J. Whitaker for their their critical review of the manuscript, and Julie Haldane for the desk-top publishing of the manuscript.

REFERENCES

ASHLEY, P.M., BILLINGTON, W.G., GRAHAM, R.L., & NEALE, R.C., 1978. Geology of the Coalstoun porphyry copper prospect, southeast Queensland, Australia. *Economic Geology*, v73,p945-965.

BALL, L.C., 1901. Hamilton and Coen goldfields. *Queensland Government Mining Journal*, v2, p358-64, p415-20 and p472-477.

BLEWETT, R.S., & von GNIELINSKI, F.E., 1991. Geology of the Coen Metamorphics with special reference to the Coen andEbagoola Shear Zones. *Australian Geological Survey Organisation, Canberra, Record* 1991/14 (unpublished).

BLEWETT, R.S., MACKENZIE, D.E., TRAIL, D.S., WELLMAN, P., KNUTSON, J., von GNIELINSKI, F.E., & BAIN, J.H.C., 1992a. Ebagoola - basement geology (1:250 000 scale map),(preliminary edition), *Australian Geological Survey Organisation*, Canberra.

BLEWETT, R.S., TRAIL, D.S., & von GNIELINSKI, F.E., 1992b. The stratigraphy of metamorphic rocks of the Ebagoola 1:250 000 sheet area in Cape York Peninsula, north Queensland. *Australian Geological Survey Organisation, Canberra, Record* 1992/74 (unpublished).

BLEWETT, R.S., TRAIL, D.S., & von GNIELNSKI, F.E., 1992c. Proterozoic. In EWERS, G.R., and BAIN, J.H.C., (Editors), Preliminary map commentary - Australia 1:250 000 basement geology and regolith landforms: Ebagoola (SD54-12), Queensland. *Australian Geological Survey Organisation, Canberra, Record* 1992/71 (unpublished).

BONHAM-CARTER, G.F., ROGERS, P.J., & ELLWOOD, D.J., 1987. Catchment basin analysis applied to surficial geochemical data, Cobequid Highlands, Nova Scotia. *Journal of Geochemical Exploration*, v29, p259-278.

BUREAU of METEOROLOGY, 1971. Bureau of Meteorology (1971) climatic survey - region 16. *Bureau of Meteorology, Australia.*

BURTON, J.D., & CULKIN, F., 1972. Gallium. In K.H. Wedepohl (Editor), *Handbook of Geochemistry*, vII-3, Springer-Verlag, Berlin.

CAMERON, W.E., 1906. Some goldfields of Cape York Peninsula. The Starke, Alice River (Philp), Hamilton and Coen. *Queensland Government Mining Journal*, v7, p643-7.

CHAFFEE, M.A., 1983. SCORESUM - a technique for displaying and evaluating multi-element geochemical information, with examples of its use in regional mineral assessment programs. In: PARSLOW, G.R., (Editor), Geochemical Exploration, 1982. *Journal of Geochemical Exploration*, v19, pp361-381.

CONNELL WAGNER, 1989. *Cape York Peninsula Resource Analysis.* Connell Wagner (Qld) Pty Ltd, Cairns, Australia

CRUIKSHANK, B., 1990. Stream-sediment geochemistry of the original Kakadu Conservation Zone, *BMR Research Newsletter*, No. 12 (April, 1990), Bureau of Mineral Resources, Canberra.

CRUIKSHANK, B.I., & BUTROVSKI, D., 1993. Ebagoola stream sediment geochemical atlas, *Australian Geological Survey Organisation, Canberra.*

CRUIKSHANK, B.I., HOATSON, D.M., & PYKE, J.G., 1993. A stream- sediment geochemical orientation survey of the Davenport Province, Northern Territory. *AGSO Journal of Australian Geology and Geophysics*, v15, p77-95.

CRUIKSHANK, B.I., & PYKE, J.G., 1993. Analytical methods used in Minerals and Land Use Program's geochemical laboratory. *Australian Geological Survey Organisation, Canberra, Record* 1993/26 (unpublished).

CULPEPER, L.G., 1993. Mineral Occurrences - Carpentaria and Karumba Basins, Cape York Peninsula, Queensland. *Queensland Resource Industries, Australia, Record* 1993/19 (unpublished).

CULPEPER, L.G., DENARO, T.J., WILLMOTT, W.F., WHITAKER, W.G., BRUVEL, F.J., MORWOOD, D.A., & SHIELD, C.J., 1992a. A

review of mineral exploration, Cape York Peninsula, 1969 to 1990. *Queensland Resource Industries, Australia, Record* 1992/10 (unpublished).

CULPEPER, L.G., GARRAD, P.D., & BURROWS, P.E., 1992b. Mineral occurrences Ebagoola 1:250 000 sheet area, Cape York Peninsula, Queensland. *Queensland Resource Industries, Australia, Record* 1992/14 (unpublished).

DARNLEY, A.G., 1991. International geochemical mapping and the environment. *Journal of Geochemical Exploration*, v41, p81- 83.

de ALBUQUERQUE, C.A.R., & SHAW, D.M., 1972. Thallium. In K.H. Wedepohl (Editor), Handbook of Geochemistry, vII-5, Springer-Verlag, Berlin. de KEYSER, F., & LUCAS, K.G., 1968. Geology of the Hodgkinson and Laura Basins, north Queensland. *Bureau of Mineral Resources, Canberra, Bulletin* 84.

DILLON, W.R., & GOLDSTEIN, M., 1984. *Multivariate analysis, methods and applications.* John Wiley and sons, New York.

DUMMETT, H.T., 1978. Geology of the Moonmera porphyry deposit, Queensland, Australia. *Economic Geology* v73,p922- 944.

EGGO, A.J., HARDING, A.E., & BAIN, J.H.C., in prep. Georgetown region stream sediment geochemistry. *Australian Geological Survey Organisation, Canberra, Record* (in preparation).

ELLIOTT, S.M., & TOWSEY, C.A., 1989. *Regional drainage geochemical gold exploration techniques used in Queensland, Australia.* NQ Gold '89 Conference, Townsville.

ELLIS, P.J., & STEELE, T.W., 1982. Five robust indicators of central value. *Geostandards Newsletter,* v6(2), p207-216.

EWERS, G.R., & BAIN, J.H.C., 1992. (Editors) Preliminary map commentary - Australia 1:250 000 basement geology and regolith landforms: Ebagoola (SD54-12), Queensland. *Australian Geological Survey Organisation, Canberra, Record* 1992/71 (unpublished).

FAURE, G., 1978. Strontium. In K.H. Wedepohl (Editor), *Handbook of Geochemistry,* vII-4, Springer-Verlag, Berlin.

FELDMAN, D.S., GAGNON, J., HOFMANN, R., & SIMPSON, J., 1990. *Statview II, the solutions for data analysis and presentation graphics* (manual for computer program). Abacus Concepts, Berkeley.

FLETCHER, W.K., 1990. Dispersion and behaviour of gold in stream sediments. Ministry of Energy, Mines and Petroleum Resources, Province of British Columbia, Geological Survey Branch, Open File 1990-28 (unpublished).

FOY, M.F., & GINGRICH, J.E., 1977. A stream-sediment orientationprogramme for uranium in the Alligator River Province, Northern Territory, Australia. *Journal of Geochemical Exploration,* v8, p357-364.

HAWKES, H.E., & WEBB, J.S., 1962. *Geochemistry in mineral exploration.* Harper and Row, New York.

HEIER, K.S., & BILLINGS, G.K., 1970. Rubidium. In K.H. Wedepohl (Editor), *Handbook of Geochemistry*, vII-4, Springer-Verlag, Berlin.

HEINRICH, E.W., 1978. Niobium. In K.H. Wedepohl (Editor), *Handbook of Geochemistry,* vII-4, Springer-Verlag, Berlin.

HORMANN, P.K., 1969. Beryllium. In K.H. Wedepohl (Editor), *Handbook of Geochemistry,* vII-1, Springer-Verlag, Berlin.

KOCH, G.S., HOWARTH, R.J., CARPENTER, R.H., & SCHUENEMEYER, J.H., 1979. Development of data enhancement and display techniques for stream-sediment data collected in the NURE program of the USDOE. DOE-GJO Document No. GJBX-28(80).

KOCH, G.S., & LINK, R., 1970. *Statistical analysis of geological data.* John Wiley and sons, New York.

KOCH, G.S., & LINK, R., 1971. *Statistical analysis of geological data,* volume II. John Wiley and sons, New York.

LABUSCHAGNE, L.S., HOLDSWORTH, R., & STONE, T.P., 1993.Regional stream sediment geochemical survey of South Africa. *Journal of Geochemical Exploration*, v47, p283-296.

LEVINSON, A.A., 1974. *Introduction to exploration geochemistry.* Applied Publishing Ltd., Calgary.

LINDQVIST, Lennart, LUNDHOLM, Ingvar, NISCA, Dan, ESBENSEN, Kim, & WOLD, Svante, 1987. Multivariate geochemical modelling and integration with petrophysical data. *Journal of Geochemical Exploration*, v29, p279-294.

MACKENZIE, D.E., & KNUTSON, J., 1992. Igneous rocks of the Ebagoola 1:250 000 sheet area, Cape York Peninsula, north Queensland: field, petrographic, and geochemical data. *Australian Geological Survey Organisation, Canberra, Record* 1992/75 (unpublished).

MACKENZIE, D.E., KNUTSON, J., BLACK, L.P., & SUN, S-S., 1992. Palaeozoic. In EWERS, G.R., and BAIN, J.H.C., (Editors), Preliminary map commentary - Australia 1:250 000 basement geology and regolith landforms: Ebagoola (SD54-12), Queensland. *Australian Geological Survey Organisation, Canberra, Record* 1992/71 (unpublished).

MACKENZIE, D.E., & WILFORD, J.R., 1992. Gamma ray spectrometric data. In EWERS, G.R., and BAIN J.H.C., (Editors), Preliminary map commentary - Australia 1:250 000 basement geology and regolith landforms: Ebagoola (SD54-12), Queensland. *Australian Geological Survey Organisation, Canberra, Record* 1992/71 (unpublished).

NORRISH, K., & CHAPPELL, B.W., 1977. X-ray fluorescence spectrometry. In ZUSSMAN, J., (Editor), *Physical methods in determinative Mineralogy,* 2nd Edition. Academic Press, London. p201-272.

PAIN, C.F., & WILFORD, J.R., 1992. Ebagoola regolith-landforms (1:250 000 scale map). *Australian Geological Survey Organisation, Canberra.*

PAIN, C.F., WILFORD, John, & DOHRENWEND, John, 1994. Regolith-landforms of the Ebagoola 1:250 000 sheet area (SD54-12) north Queensland, *Australian Geological Survey Organisation, Canberra Record* 1994/7 (unpublished).

PRICE, V., & FERGUSON, R.B., 1980. Stream sediment surveys for uranium. *Journal of Geochemical Exploration*, v13,p285-304.

PUCHELT, H., 1972. Barium. In K.H. Wedepohl (Editor), *Handbook of Geochemistry,* vII-4, Springer-Verlag, Berlin.

ROSSITER, A.G., 1975. An orientation geochemical survey in the Westmoreland area, Northern Territory. *Bureau of Mineral Resources, Canberra, Record* 1975/172 (unpublished).

ROSSITER, A.G., & SCOTT, P.A., 1978. Stream-sediment geochemistry of the Forsayth 1:100 000 sheet area, north Queensland. *Bureau of Mineral Resources, Canberra, Record* 1978/17 (unpublished).

SINCLAIR, A.J., 1974. Selection of threshold values in geochemical data using probability graphs. *Journal of Geochemical Exploration*, v3, p129-149.

SINCLAIR, A.J., 1991. A fundamental approach to threshold estimation in exploration geochemistry; probability plots revisited. *Journal of Geochemical Exploration*, v41, p1-22.

SMART, J., GRIMES, K.G., DOUTCH, H.F., & PINCHIN, J., 1980. The Carpentaria and Karumba Basins, north Queensland. *Bureau of Mineral Resources, Canberra, Bulletin* 202.

STEENFELT, A., 1990. Geochemical patterns related to major tectono-stratigraphic units in the Precambrian of northern Scandinavia and Greenland. *Journal of Geochemical Exploration*, v39, p35-48.

TRAIL, D.S., PONTIFEX, I.R., PALFREYMAN, W.D., WILLMOTT, W.F., & WHITAKER, W.G., 1968. The igneous and metamorphic rocks of the southern part of Cape York Peninsula, Queensland. *Bureau of Mineral Resources, Canberra, Record* 1968/26 (unpublished).

WEDEPOHL, K.H., 1972. Zinc. In K.H. Wedepohl (Editor), *Handbook of Geochemistry,* vII-3, Springer-Verlag, Berlin.

WEDEPOHL, K.H., 1974a. Copper. In K.H. Wedepohl (Editor), *Handbook of Geochemistry,* vII-3, Springer-Verlag, Berlin.

WEDEPOHL, K.H., 1974b. Lead. In K.H. Wedepohl (Editor), *Handbook of Geochemistry*, vII-5, Springer-Verlag, Berlin.

WELLMAN, Peter, 1992a. Interpretation of Ebagoola aeromagnetic and gravity data. *Australian Geological Survey Organisation, Canberra, Record* 1992/76 (unpublished).

WELLMAN, Peter, 1992b. A geological interpretation of the regional gravity and magnetic features of north Queensland. *Australian Geological Survey Organisation, Canberra, Record* 1992/77 (unpublished).

WHITAKER, W.G., & GIBSON, D.L., 1977. Ebagoola 1:250 000 geological series - explanatory notes. *Bureau of Mineral Resources, Canberra.*

WILFORD. J., 1992. Regolith mapping using integrated Landsat TM imagery and high-resolution gamma-ray spectrometric imagery Cape York Peninsula. *Australian Geological Survey Organisation, Canberra, Record* 1992/78 (unpublished).

WILLMOTT, W.F., WHITAKER, W.G., PALFREYMAN, W.D. & TRAIL, D.S., 1973. Igneous and metamorphic rocks of Cape York Peninsula and Torres Strait. *Bureau of Mineral Resources Bulletin* 135, Canberra.

APPENDIX A

X_1 : Ag*ppm

Mean:	Std. Dev.:	Std. Error:	Variance:	Coef. Var.:	Count:
.399	.47	.017	.221	117.625	744
Minimum:	**Maximum:**	**Range:**	**Sum:**	**Sum of Sqr.:**	**# Missing:**
.05	5.71	5.66	297.02	282.414	0
t 95%:	**95% Lower:**	**95% Upper:**	**# < 10th %:**	**10th %:**	**25th %:**
.034	.365	.433	0	.05	.18
50th %:	**75th %:**	**90th %:**	**# > 90th %:**	**Mode:**	**Geo. Mean:**
.31	.47	.7	72	.05	.28
Har. Mean:	**Kurtosis:**	**Skewness:**			
.189	56.474	6.336			

Detection limit is 0.10 ppm - a value of 0.05 ppm has been used in calculations and table.

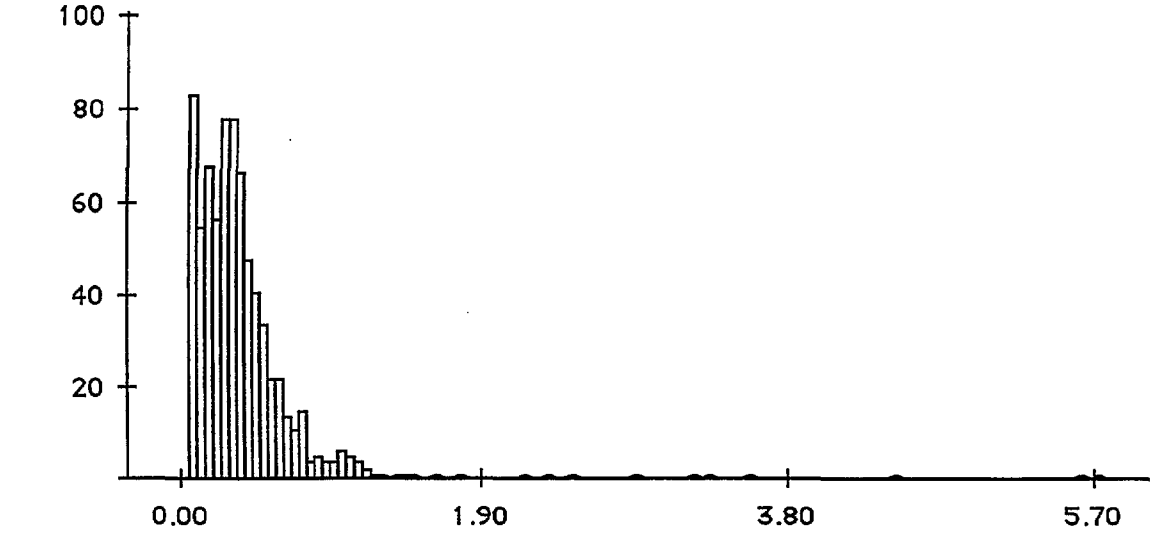

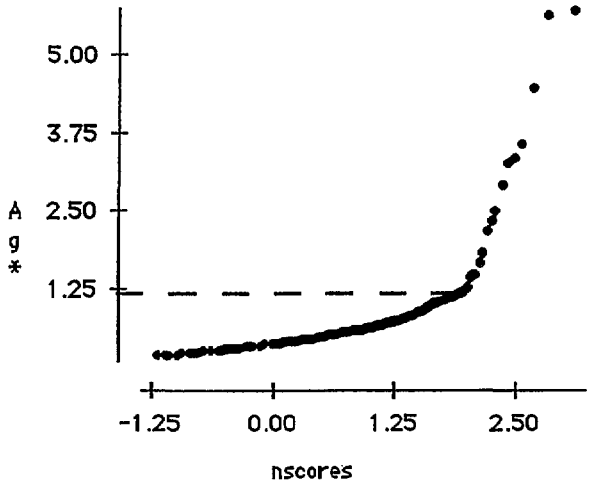

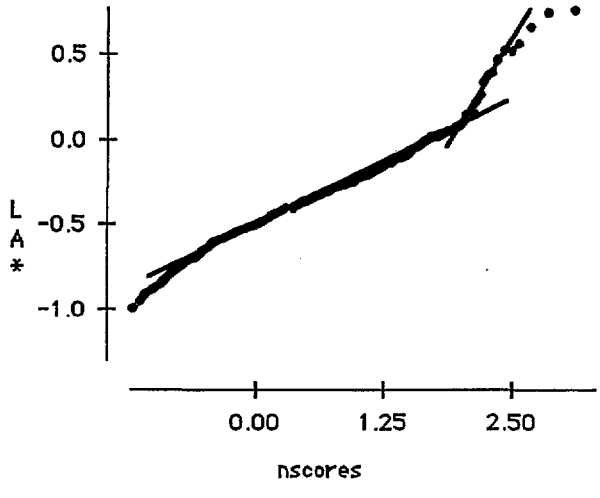

X_1 : As ppm

Mean:	Std. Dev.:	Std. Error:	Variance:	Coef. Var.:	Count:
2.816	3.776	.138	14.259	134.104	744
Minimum:	**Maximum:**	**Range:**	**Sum:**	**Sum of Sqr.:**	**# Missing:**
.25	77.5	77.25	2095	16494	0
t 95%:	**95% Lower:**	**95% Upper:**	**# < 10th %:**	**10th %:**	**25th %:**
.272	2.544	3.088	72	1	1
50th %:	**75th %:**	**90th %:**	**# > 90th %:**	**Mode:**	**Geo. Mean:**
2	3.5	6	71	1	1.927
Har. Mean:	**Kurtosis:**	**Skewness:**			
1.319	206.072	11.251			

Detection limit is 0.5 ppm - a value of 0.25 ppm has been used in calculations and table.

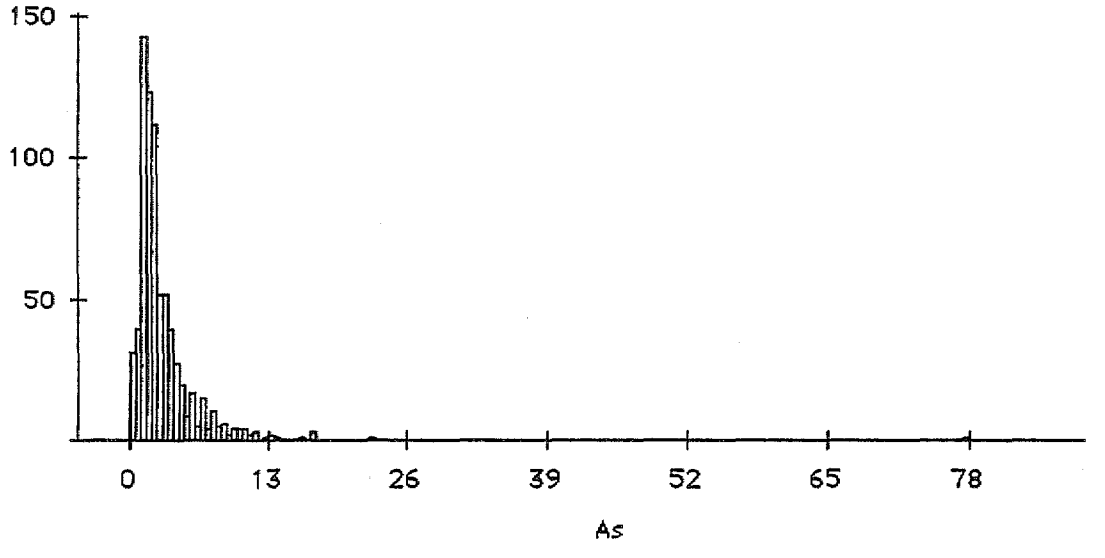

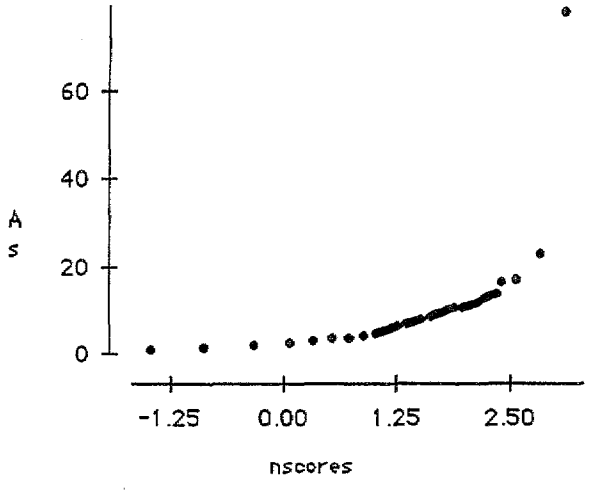

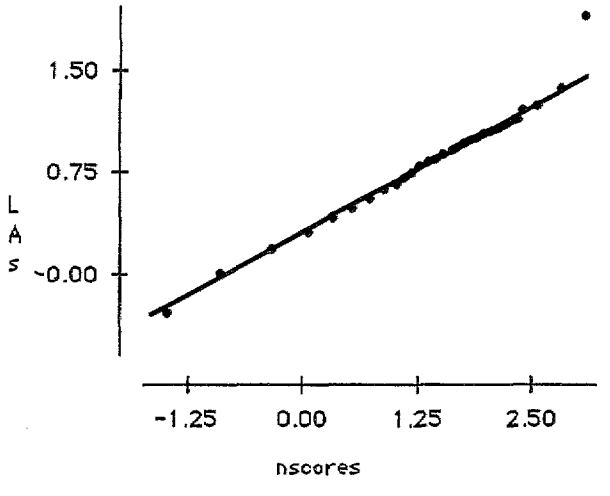

X_1 : Au*ppt

Mean:	Std. Dev.:	Std. Error:	Variance:	Coef. Var.:	Count:
158.374	584.877	21.443	342080.932	369.302	744
Minimum:	**Maximum:**	**Range:**	**Sum:**	**Sum of Sqr.:**	**# Missing:**
5	11200	11195	117830	272827300	0
t 95%:	**95% Lower:**	**95% Upper:**	**# < 10th %:**	**10th %:**	**25th %:**
42.099	116.274	200.473	0	5	5
50th %:	**75th %:**	**90th %:**	**# > 90th %:**	**Mode:**	**Geo. Mean:**
50	140	280	73	5	39.155
Har. Mean:	**Kurtosis:**	**Skewness:**			
13.362	197.545	12.532			

Detection limit is 10 ppt - a value of 5 ppt has been used in calculations and table.

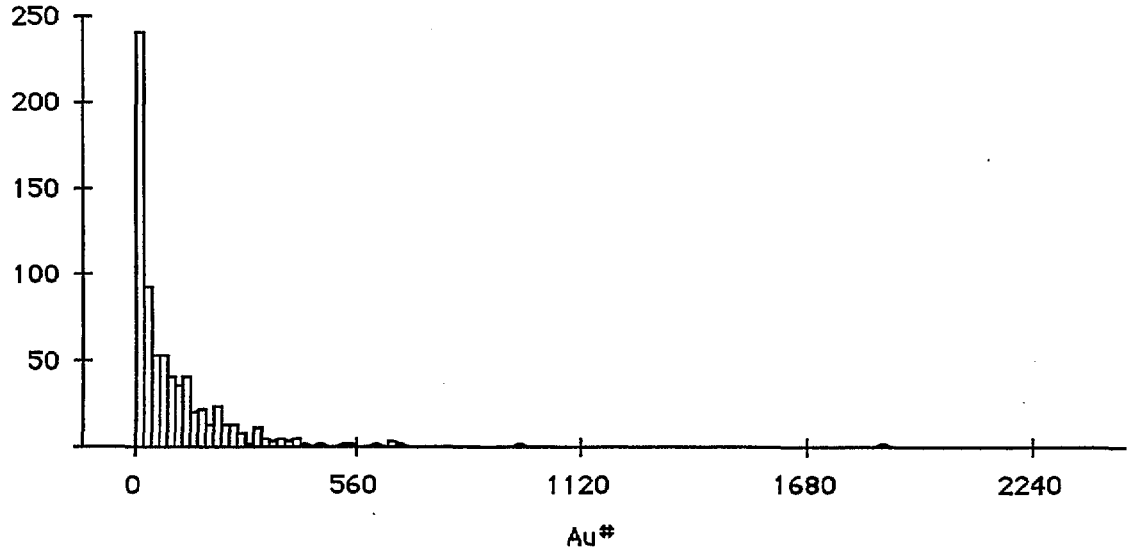

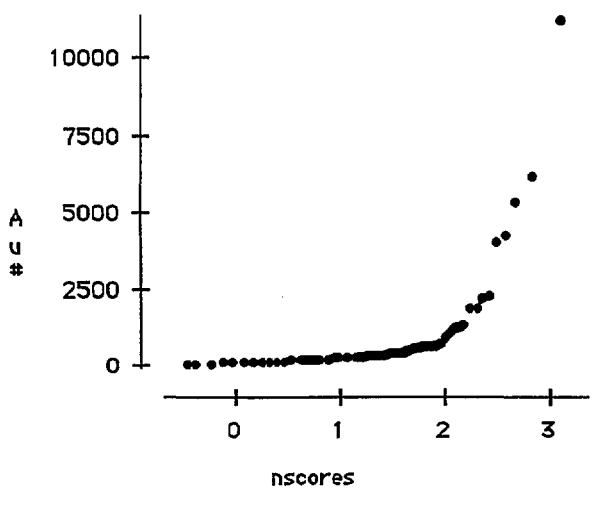

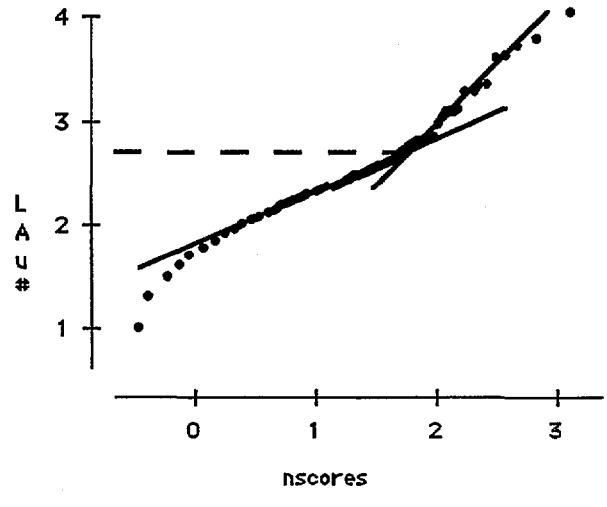

X_1 : Ba ppm

Mean:	Std. Dev.:	Std. Error:	Variance:	Coef. Var.:	Count:
501.579	344.9	12.645	118956.01	68.763	744
Minimum:	**Maximum:**	**Range:**	**Sum:**	**Sum of Sqr.:**	**# Missing:**
23	1694	1671	373175	275561171	0
t 95%:	**95% Lower:**	**95% Upper:**	**# < 10th %:**	**10th %:**	**25th %:**
24.826	476.753	526.405	73	105	201.5
50th %:	**75th %:**	**90th %:**	**# > 90th %:**	**Mode:**	**Geo. Mean:**
422.5	764.5	993.2	74	•	369.436
Har. Mean:	**Kurtosis:**	**Skewness:**			
244.83	-.666	.574			

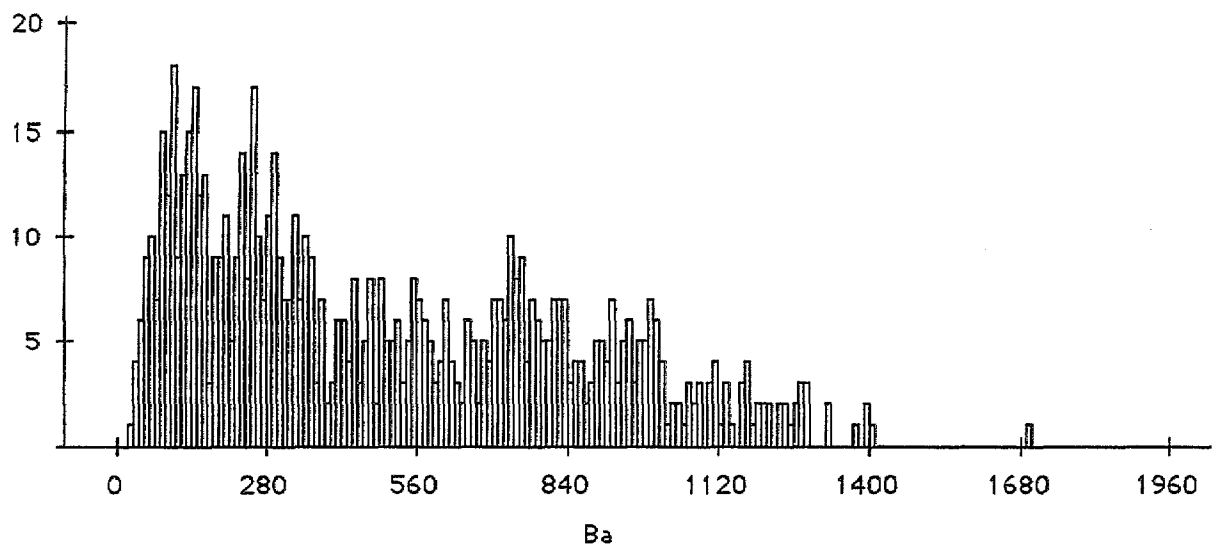

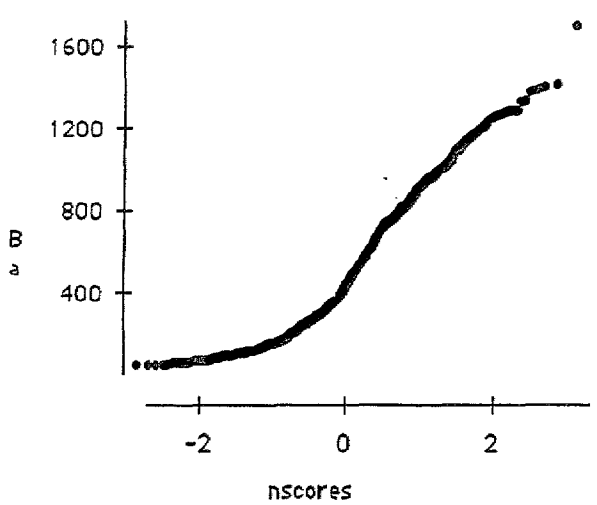

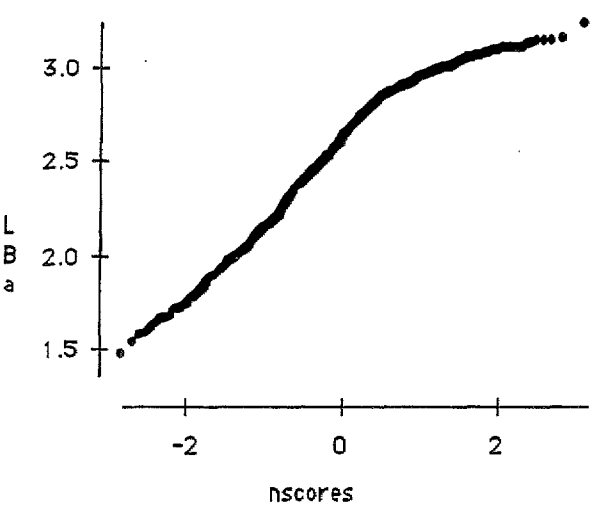

X_1 : Be*ppm

Mean:	Std. Dev.:	Std. Error:	Variance:	Coef. Var.:	Count:
1.423	.777	.029	.604	54.635	744
Minimum:	**Maximum:**	**Range:**	**Sum:**	**Sum of Sqr.:**	**# Missing:**
.14	5.56	5.42	1058.7	1955.593	0
t 95%:	**95% Lower:**	**95% Upper:**	**# < 10th %:**	**10th %:**	**25th %:**
.056	1.367	1.479	72	.56	.89
50th %:	**75th %:**	**90th %:**	**# > 90th %:**	**Mode:**	**Geo. Mean:**
1.29	1.815	2.361	74	1.09	1.224
Har. Mean:	**Kurtosis:**	**Skewness:**			
1.022	2.869	1.292			

Detection limit is 0.10 ppm - a value of 0.05 ppm has been used in calculations and table.

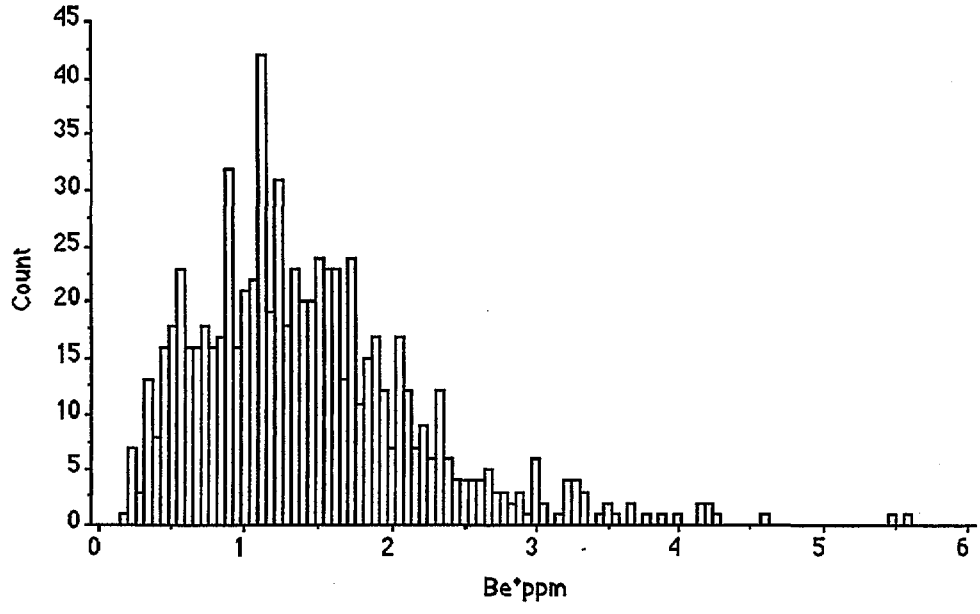

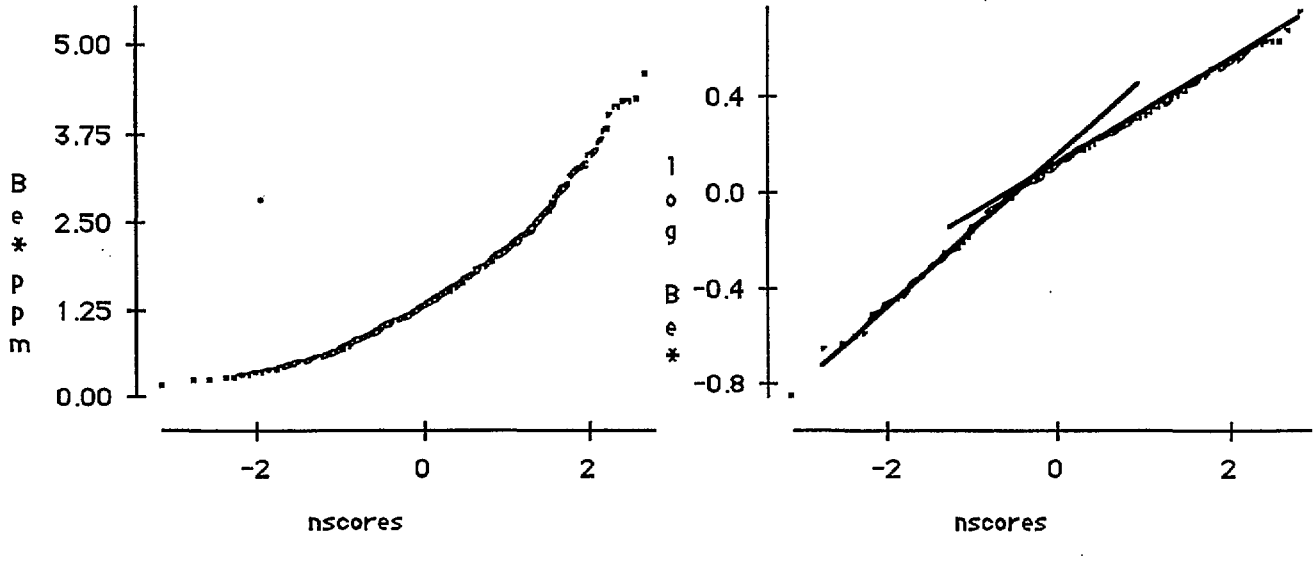

X_1 : Bi*ppm

Mean:	Std. Dev.:	Std. Error:	Variance:	Coef. Var.:	Count:
.271	.212	.008	.045	78.43	744
Minimum:	Maximum:	Range:	Sum:	Sum of Sqr.:	# Missing:
.05	1.59	1.54	201.35	87.966	0
t 95%:	95% Lower:	95% Upper:	# < 10th %:	10th %:	25th %:
.015	.255	.286	0	.05	.14
50th %:	75th %:	90th %:	# > 90th %:	Mode:	Geo. Mean:
.22	.34	.501	74	.05	.209
Har. Mean:	Kurtosis:	Skewness:			
.158	7.462	2.274			

Detection limit is 0.10 ppm - a value of 0.05 ppm has been used in calculations and table.

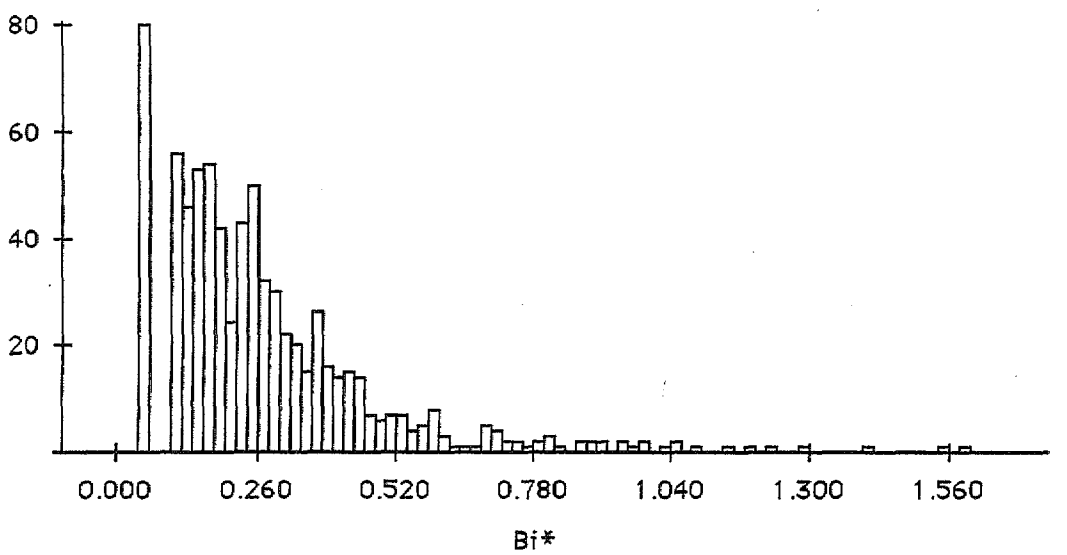

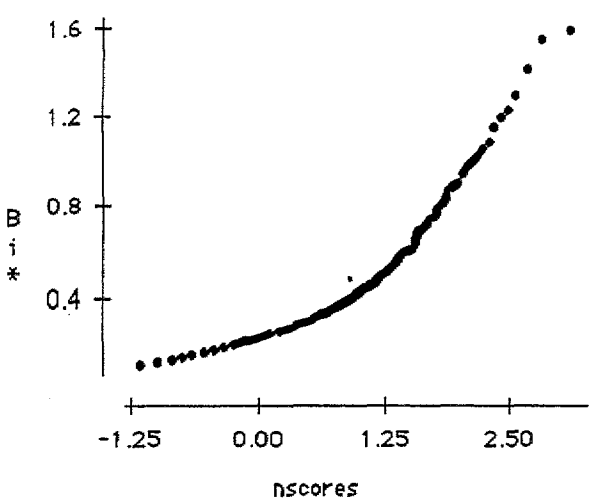

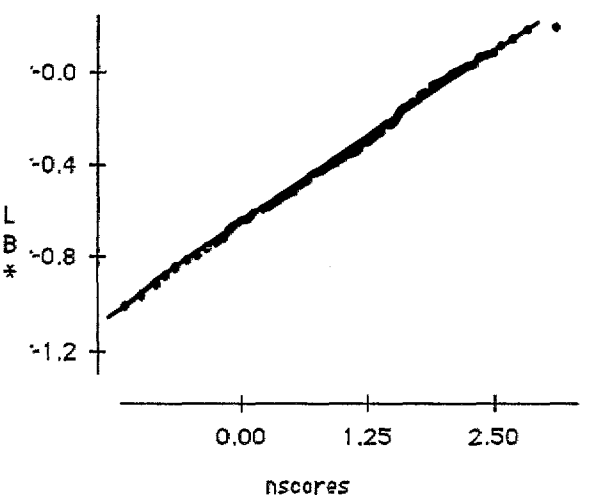

X_1 : Cd*ppm

Mean:	Std. Dev.:	Std. Error:	Variance:	Coef. Var.:	Count:
.162	.109	.004	.012	67.371	744
Minimum:	**Maximum:**	**Range:**	**Sum:**	**Sum of Sqr.:**	**# Missing:**
.05	1.76	1.71	120.36	28.297	0
t 95%:	**95% Lower:**	**95% Upper:**	**# < 10th %:**	**10th %:**	**25th %:**
.008	.154	.17	0	.05	.12
50th %:	**75th %:**	**90th %:**	**# > 90th %:**	**Mode:**	**Geo. Mean:**
.15	.19	.241	74	.05	.141
Har. Mean:	**Kurtosis:**	**Skewness:**			
.123	98.565	7.578			

Detection limit is 0.10 ppm - a value of 0.05 ppm has been used in calculations and table.

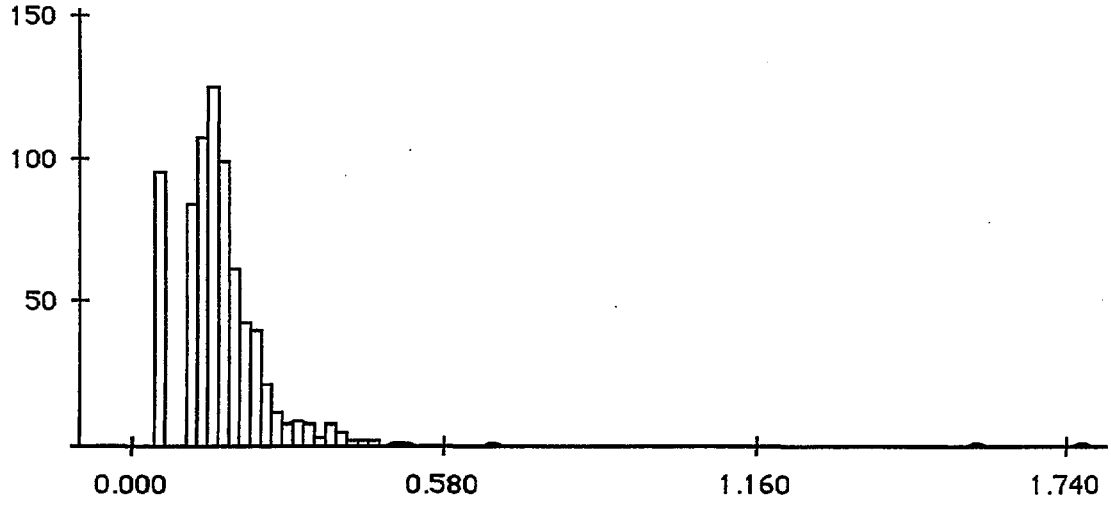

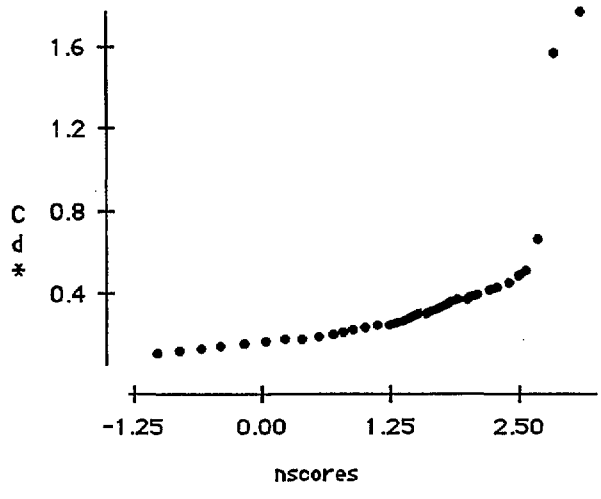

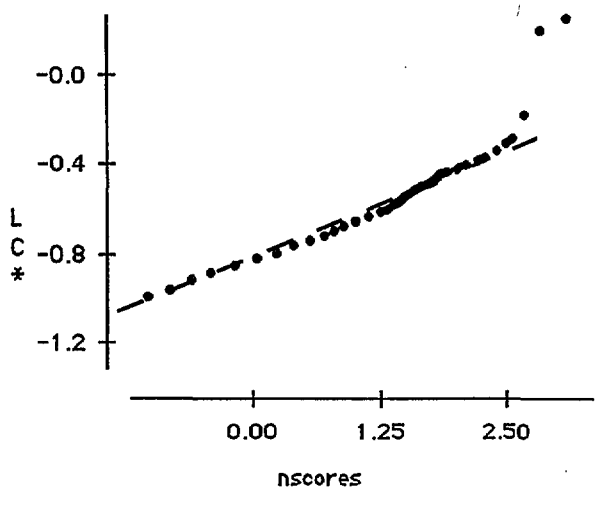

X_1 : Ce ppm

Mean:	Std. Dev.:	Std. Error:	Variance:	Coef. Var.:	Count:
153.035	225.323	8.261	50770.252	147.236	744
Minimum:	**Maximum:**	**Range:**	**Sum:**	**Sum of Sqr.:**	**# Missing:**
10	1946	1936	113858	55146550	0
t 95%:	**95% Lower:**	**95% Upper:**	**# < 10th %:**	**10th %:**	**25th %:**
16.219	136.816	169.254	74	35.9	50
50th %:	**75th %:**	**90th %:**	**# > 90th %:**	**Mode:**	**Geo. Mean:**
78.5	146.5	327.1	74	44	92.343
Har. Mean:	**Kurtosis:**	**Skewness:**			
66.984	20.047	4.037			

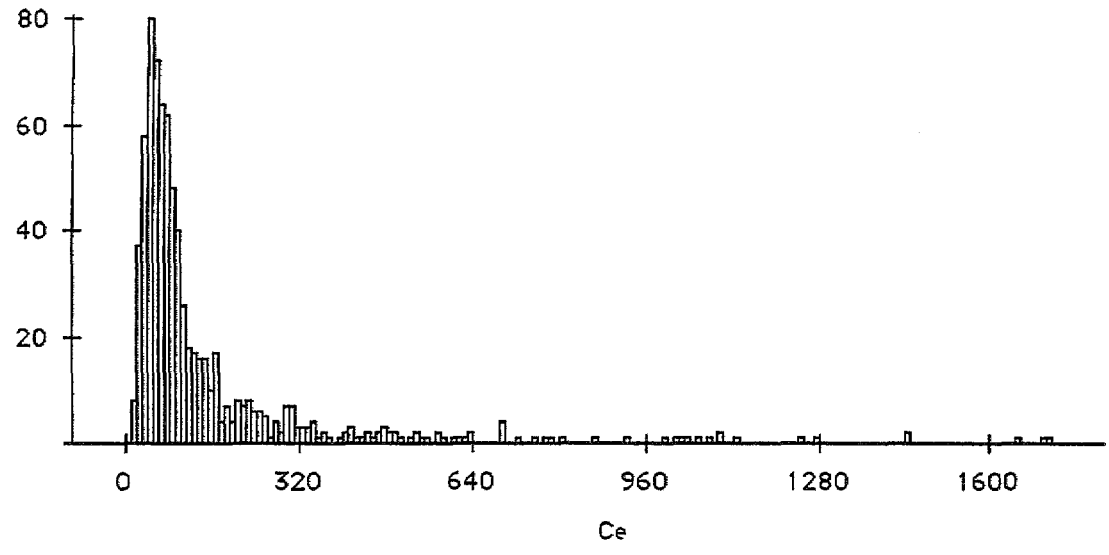

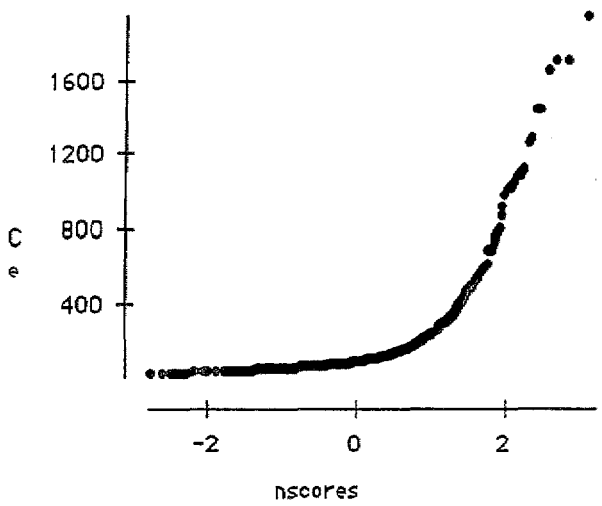

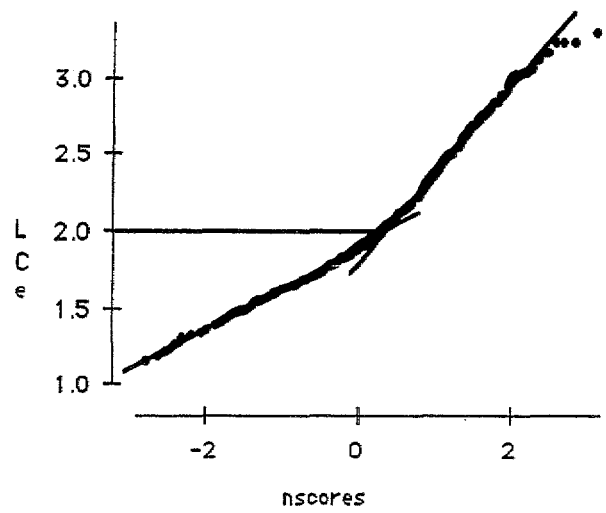

X_1 : Cr ppm

Mean:	Std. Dev.:	Std. Error:	Variance:	Coef. Var.:	Count:
27.247	28.056	1.029	787.148	102.969	744
Minimum:	**Maximum:**	**Range:**	**Sum:**	**Sum of Sqr.:**	**# Missing:**
.5	332	331.5	20272	1137208.5	0
t 95%:	**95% Lower:**	**95% Upper:**	**# < 10th %:**	**10th %:**	**25th %:**
2.019	25.228	29.267	54	3	7
50th %:	**75th %:**	**90th %:**	**# > 90th %:**	**Mode:**	**Geo. Mean:**
21	39	57	72	4	15.904
Har. Mean:	**Kurtosis:**	**Skewness:**			
6.723	23.718	3.369			

Detection limit is 1 ppm - a value of 0.5 ppm has been used in calculations and table.

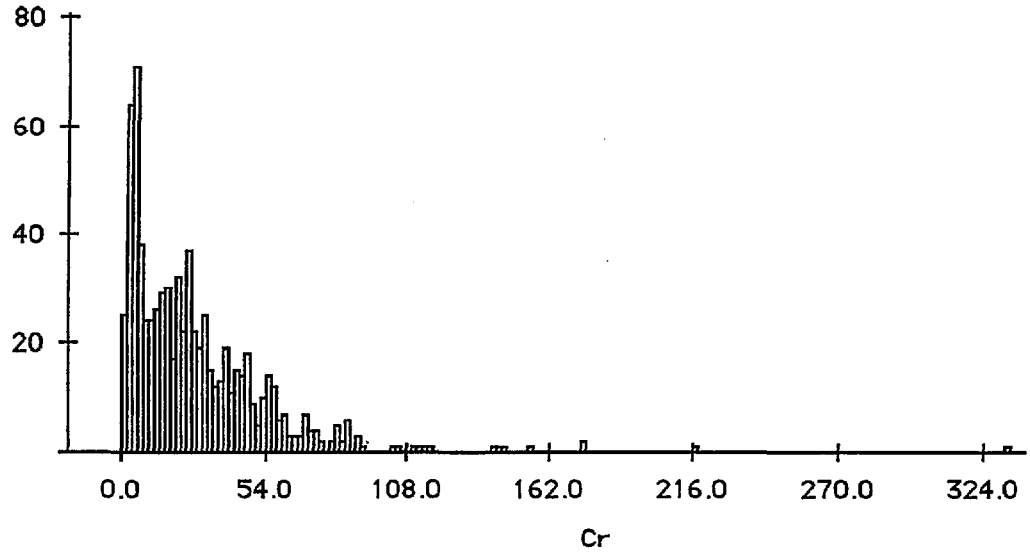

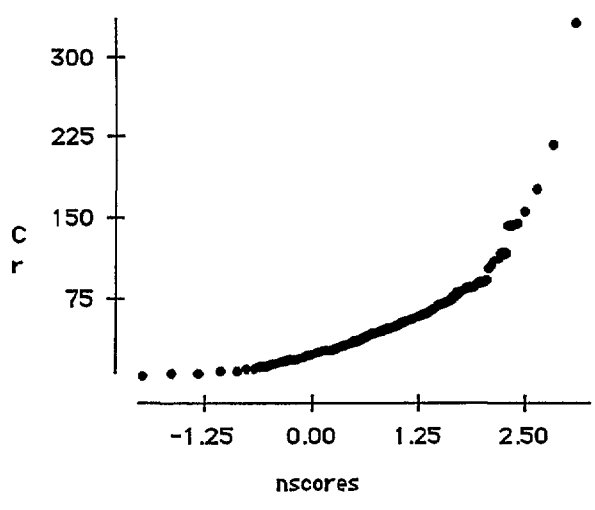

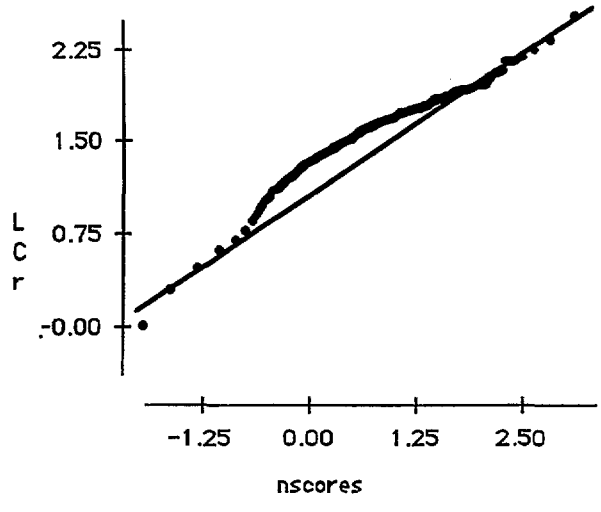

X_1 : Cu ppm

Mean:	Std. Dev.:	Std. Error:	Variance:	Coef. Var.:	Count:
4.124	5.649	.207	31.914	136.996	744
Minimum:	**Maximum:**	**Range:**	**Sum:**	**Sum of Sqr.:**	**# Missing:**
.5	37	36.5	3068	36363.5	0
t 95%:	**95% Lower:**	**95% Upper:**	**# < 10th %:**	**10th %:**	**25th %:**
.407	3.717	4.53	0	.5	.5
50th %:	**75th %:**	**90th %:**	**# > 90th %:**	**Mode:**	**Geo. Mean:**
2	5	10	69	.5	1.97
Har. Mean:	**Kurtosis:**	**Skewness:**			
1.084	10.065	2.839			

Detection limit is 1 ppm - a value of 0.5 ppm has been used in calculations and table.

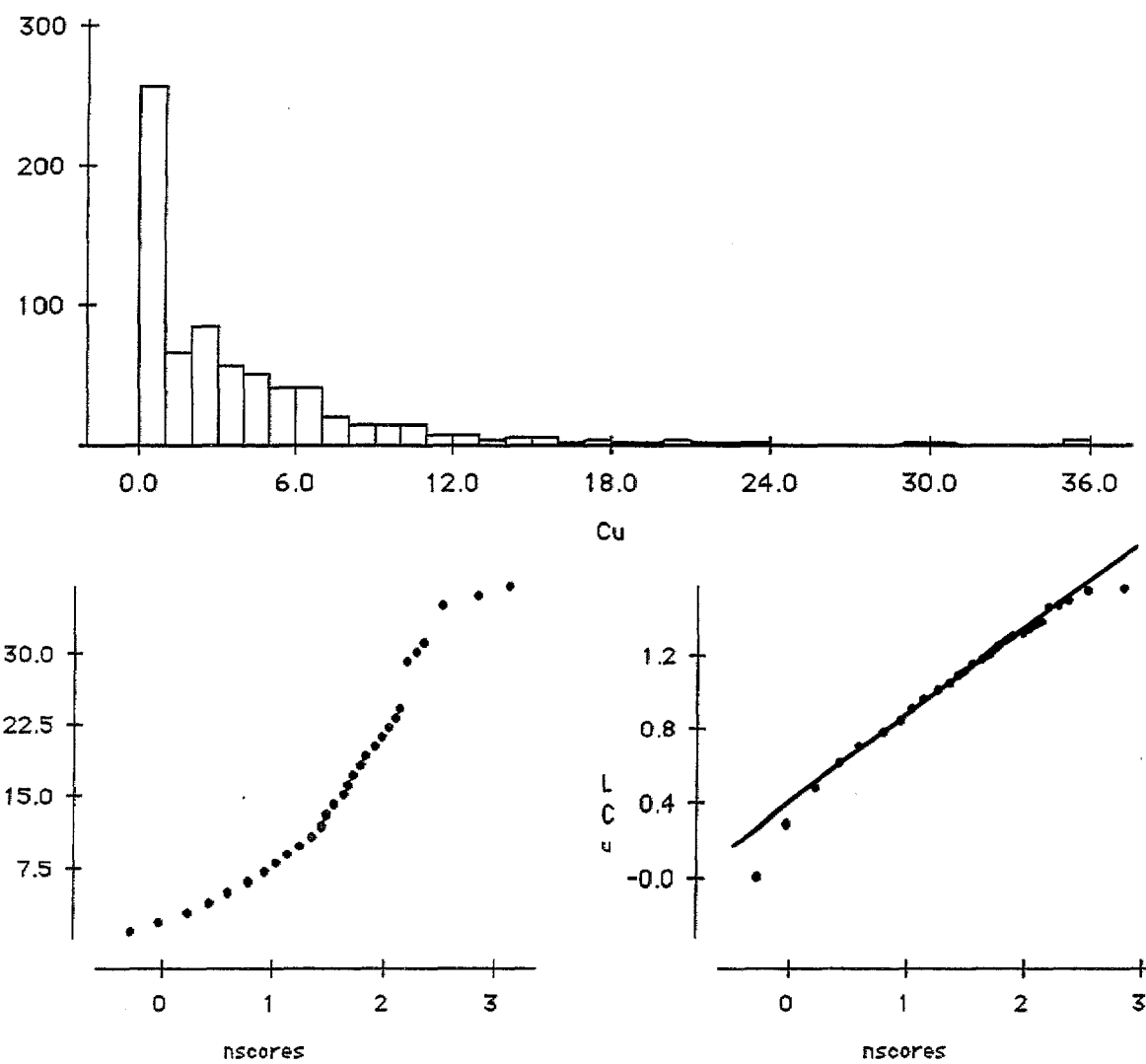

X_1 : Fe ppm

Mean:	Std. Dev.:	Std. Error:	Variance:	Coef. Var.:	Count:
12975.806	10002.662	366.715	1.001E8	77.087	744
Minimum:	**Maximum:**	**Range:**	**Sum:**	**Sum of Sqr.:**	**# Missing:**
2000	75000	73000	9654000	1.996E11	0
t 95%:	**95% Lower:**	**95% Upper:**	**# < 10th %:**	**10th %:**	**25th %:**
719.992	12255.814	13695.798	68	4000	6000
50th %:	**75th %:**	**90th %:**	**# > 90th %:**	**Mode:**	**Geo. Mean:**
10000	17000	27000	68	4000	9897.171
Har. Mean:	**Kurtosis:**	**Skewness:**			
7507.786	4.152	1.722			

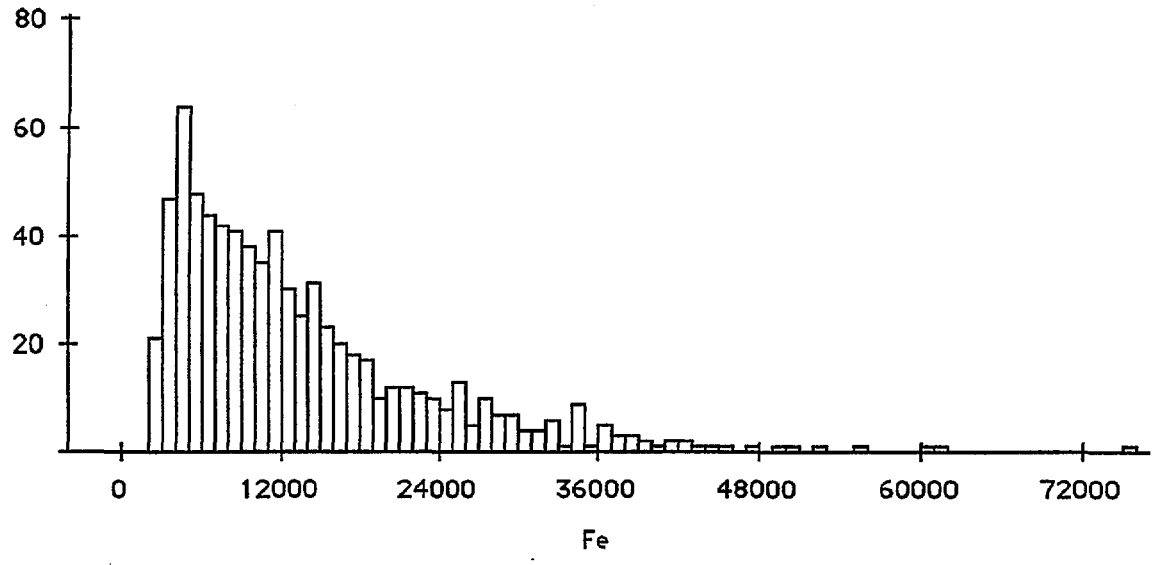

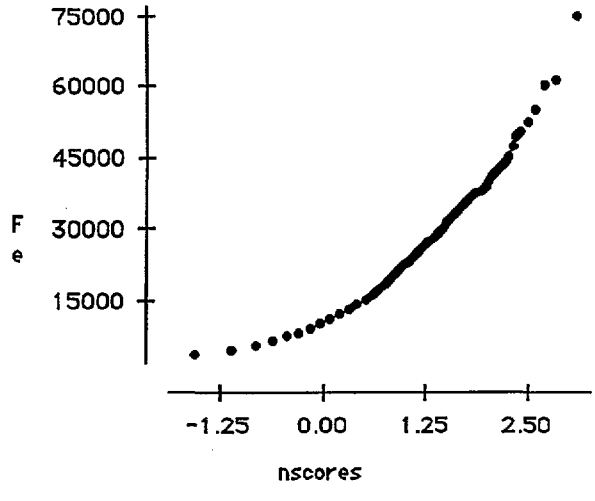

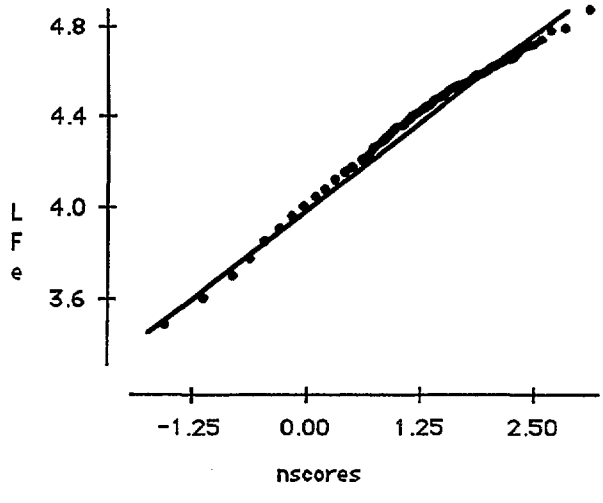

X_1 : Ga ppm

Mean:	Std. Dev.:	Std. Error:	Variance:	Coef. Var.:	Count:
6.977	3.259	.119	10.623	46.714	744
Minimum:	Maximum:	Range:	Sum:	Sum of Sqr.:	# Missing:
.5	19	18.5	5191	44111.5	0
t 95%:	95% Lower:	95% Upper:	# < 10th %:	10th %:	25th %:
.235	6.743	7.212	64	3	5
50th %:	75th %:	90th %:	# > 90th %:	Mode:	Geo. Mean:
7	9	11	67	6	6.084
Har. Mean:	Kurtosis:	Skewness:			
4.88	.183	.467			

Detection limit is 1 ppm - a value of 0.5 ppm has been used in calculations and table.

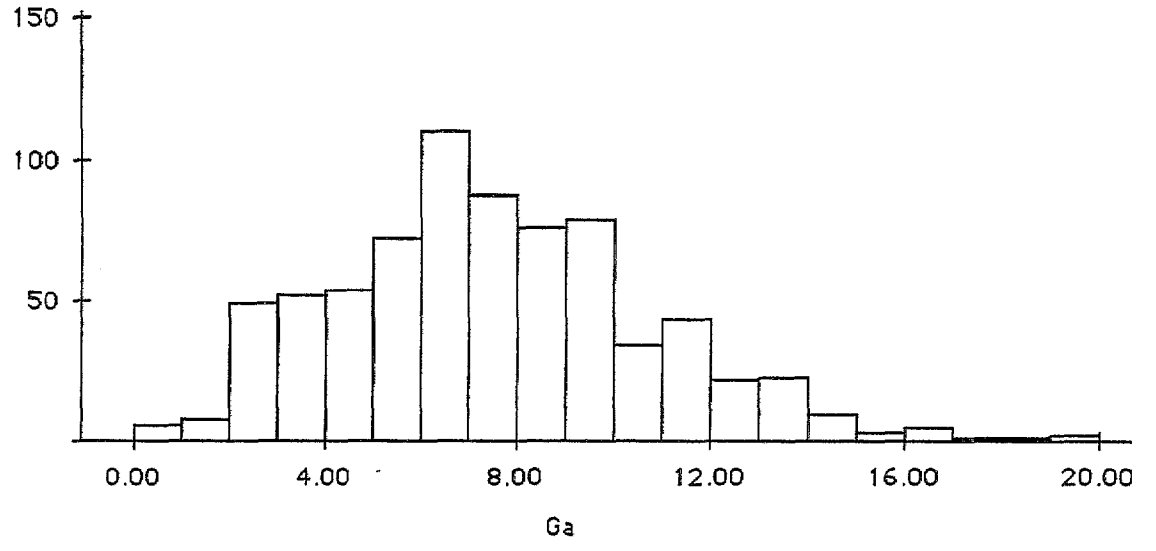

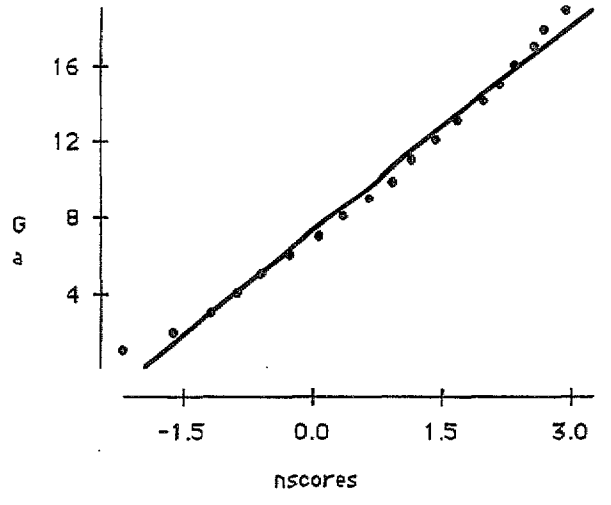

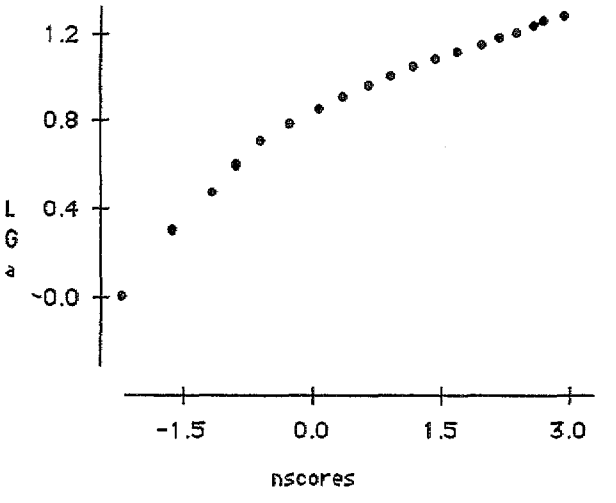

X_1 : Ge ppm

Mean:	Std. Dev.:	Std. Error:	Variance:	Coef. Var.:	Count:
1.561	.295	.011	.087	18.886	744
Minimum:	**Maximum:**	**Range:**	**Sum:**	**Sum of Sqr.:**	**# Missing:**
.25	3	2.75	1161.25	1877.062	0
t 95%:	**95% Lower:**	**95% Upper:**	**# < 10th %:**	**10th %:**	**25th %:**
.021	1.54	1.582	1	1	1.5
50th %:	**75th %:**	**90th %:**	**# > 90th %:**	**Mode:**	**Geo. Mean:**
1.5	1.5	2	6	1.5	1.531
Har. Mean:	**Kurtosis:**	**Skewness:**			
1.496	1.391	.235			

Detection limit is 0.5 ppm - a value of 0.25 ppm has been used in calculations and table.

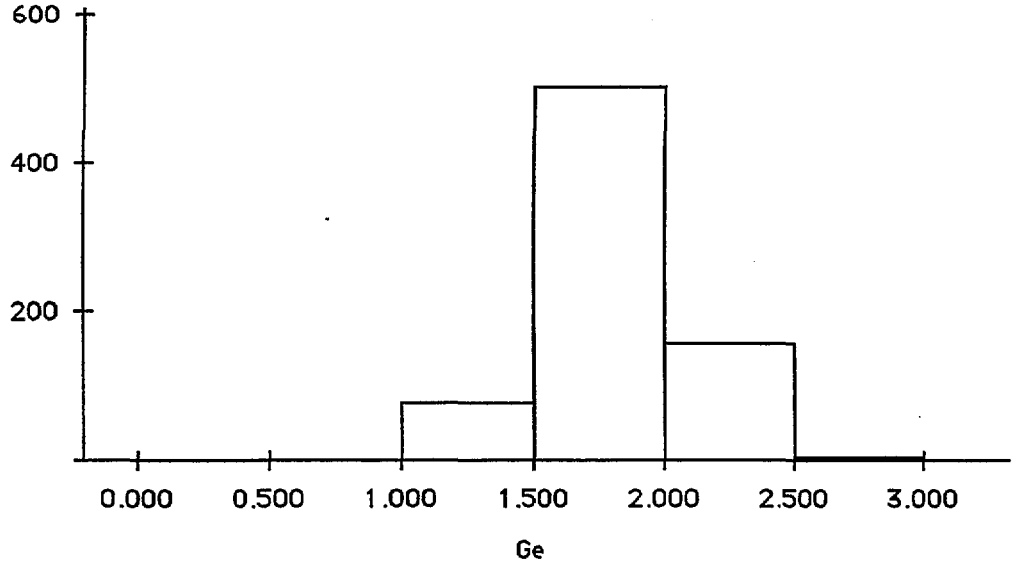

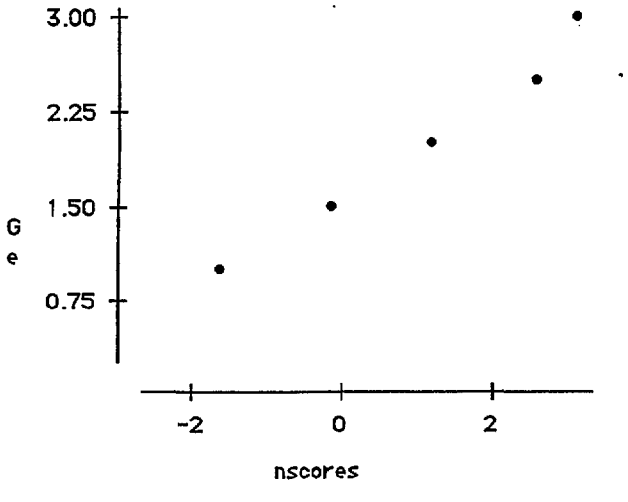

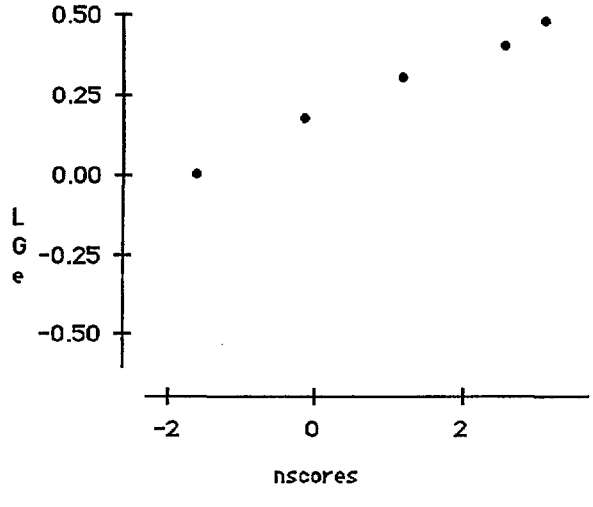

X_1 : Hf ppm

Mean:	Std. Dev.:	Std. Error:	Variance:	Coef. Var.:	Count:
14.273	15.109	.554	228.293	105.861	744
Minimum:	**Maximum:**	**Range:**	**Sum:**	**Sum of Sqr.:**	**# Missing:**
1	251	250	10619	321185	0
t 95%:	**95% Lower:**	**95% Upper:**	**# < 10th %:**	**10th %:**	**25th %:**
1.088	13.185	15.36	46	5	7
50th %:	**75th %:**	**90th %:**	**# > 90th %:**	**Mode:**	**Geo. Mean:**
10	16	26	73	6	10.842
Har. Mean:	**Kurtosis:**	**Skewness:**			
8.602	84.753	6.773			

Detection limit is 2 ppm - a value of 1 ppm has been used in calculations and table.

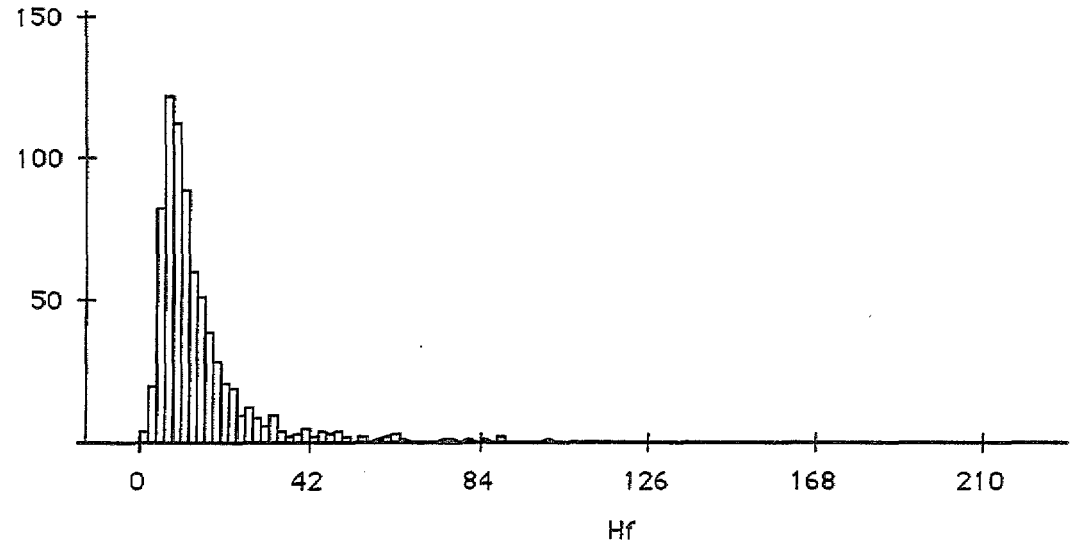

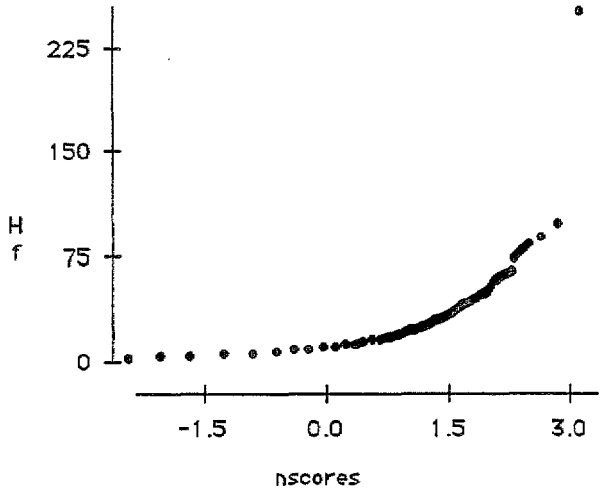

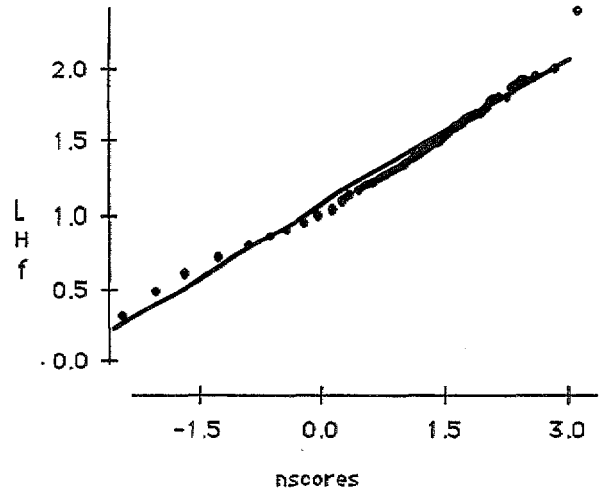

X_1 : La ppm

Mean:	Std. Dev.:	Std. Error:	Variance:	Coef. Var.:	Count:
77.702	116.056	4.255	13468.944	149.361	744
Minimum:	**Maximum:**	**Range:**	**Sum:**	**Sum of Sqr.:**	**# Missing:**
4	1028	1024	57810	14499356	0
t 95%:	**95% Lower:**	**95% Upper:**	**# < 10th %:**	**10th %:**	**25th %:**
8.354	69.348	86.055	65	17	25
50th %:	**75th %:**	**90th %:**	**# > 90th %:**	**Mode:**	**Geo. Mean:**
39.5	75	166	73	24	46.313
Har. Mean:	**Kurtosis:**	**Skewness:**			
32.897	21.156	4.128			

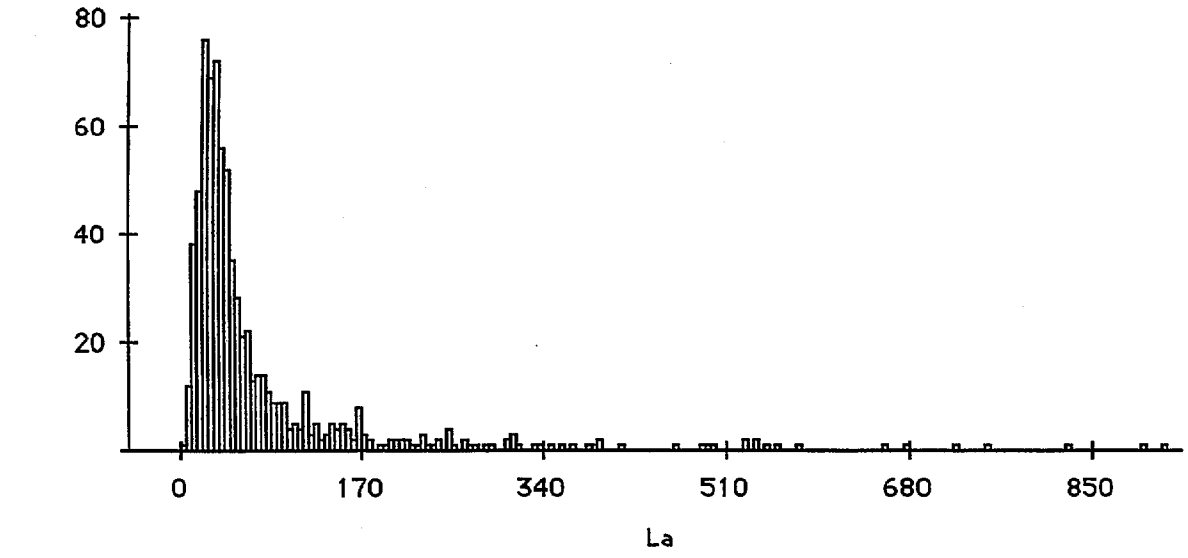

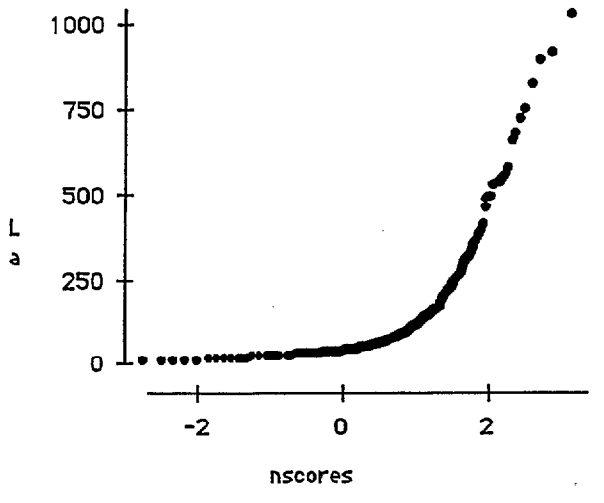

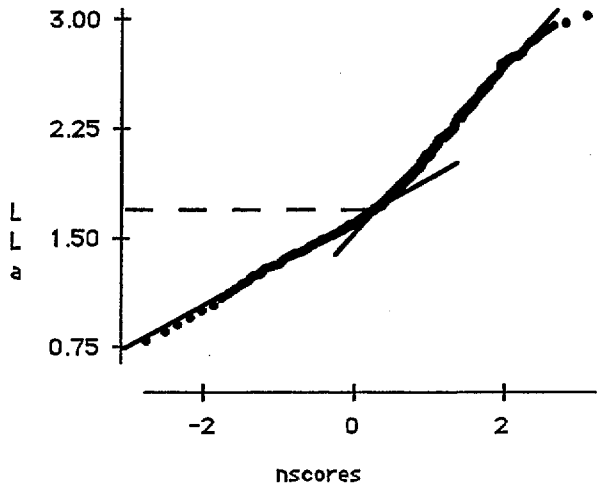

X_1 : Mn ppm

Mean:	Std. Dev.:	Std. Error:	Variance:	Coef. Var.:	Count:
354.163	373.435	13.691	139453.916	105.442	744
Minimum:	**Maximum:**	**Range:**	**Sum:**	**Sum of Sqr.:**	**# Missing:**
9	3064	3055	263497	196935051	0
t 95%:	**95% Lower:**	**95% Upper:**	**# < 10th %:**	**10th %:**	**25th %:**
26.88	327.283	381.043	73	53	136
50th %:	**75th %:**	**90th %:**	**# > 90th %:**	**Mode:**	**Geo. Mean:**
253	435	749.1	74	25	225.191
Har. Mean:	**Kurtosis:**	**Skewness:**			
119.918	12.507	2.983			

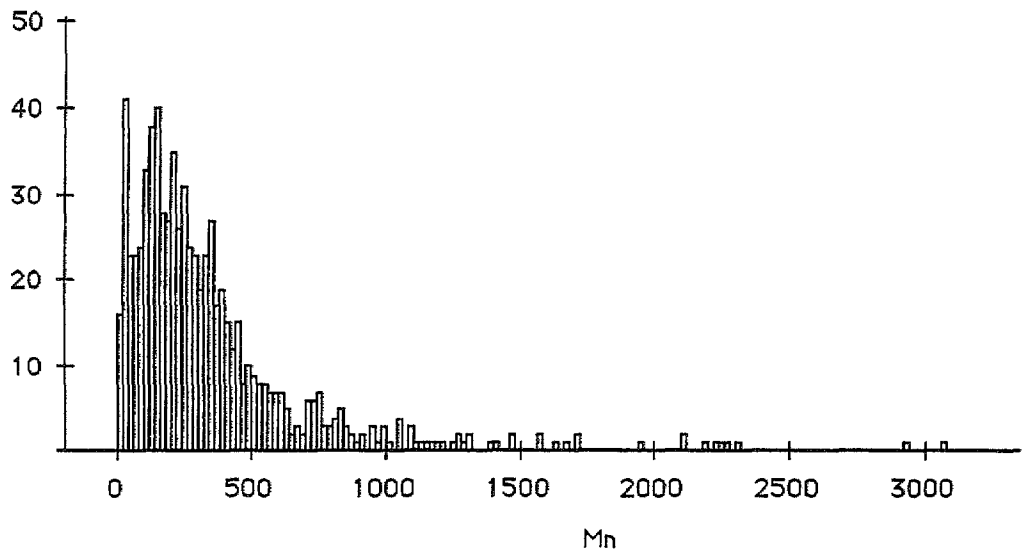

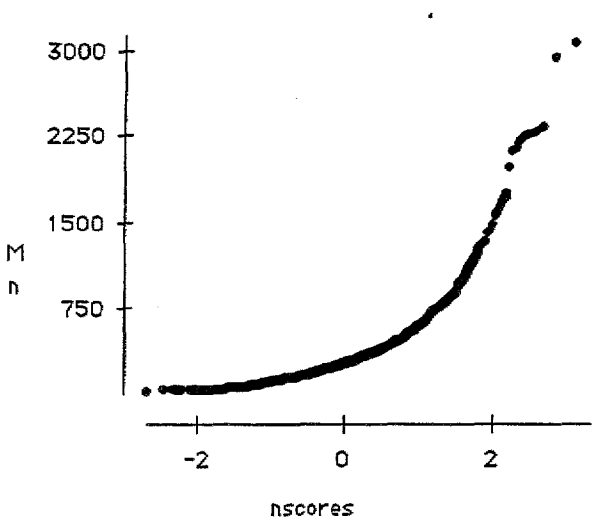

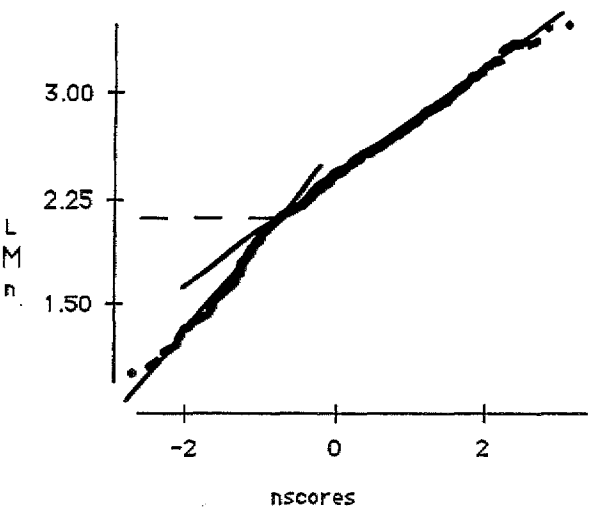

X_1 : Mo*ppm

Mean:	Std. Dev.:	Std. Error:	Variance:	Coef. Var.:	Count:
.557	.397	.015	.158	71.283	744
Minimum:	**Maximum:**	**Range:**	**Sum:**	**Sum of Sqr.:**	**# Missing:**
.05	3.18	3.13	414.59	348.262	0
t 95%:	**95% Lower:**	**95% Upper:**	**# < 10th %:**	**10th %:**	**25th %:**
.029	.529	.586	68	.11	.26
50th %:	**75th %:**	**90th %:**	**# > 90th %:**	**Mode:**	**Geo. Mean:**
.49	.8	1.02	73	.05	.407
Har. Mean:	**Kurtosis:**	**Skewness:**			
.249	3.832	1.365			

Detection limit is 0.10 ppm - a value of 0.05 ppm has been used in calculations and table.

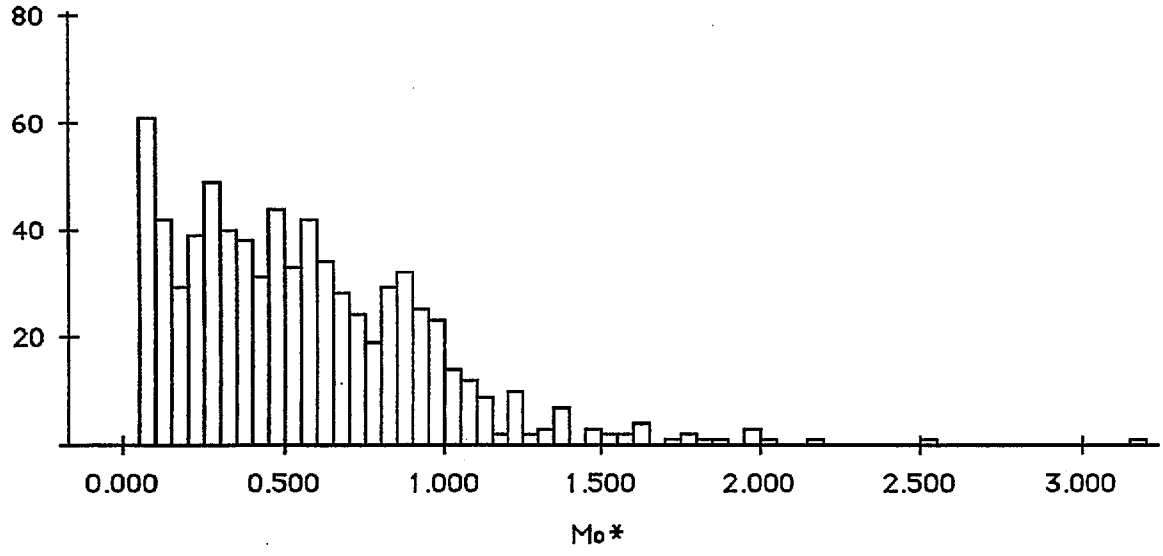

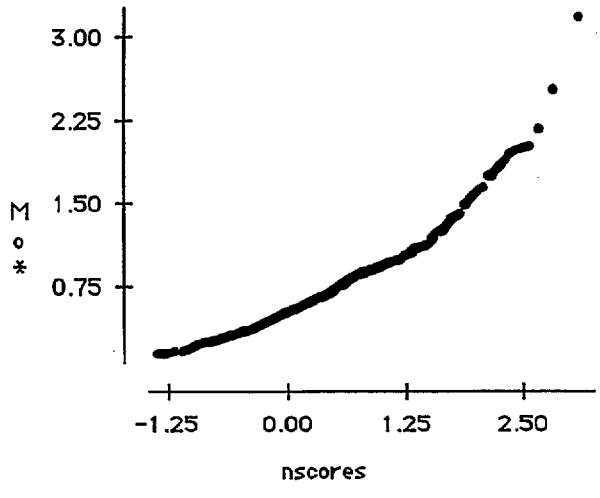

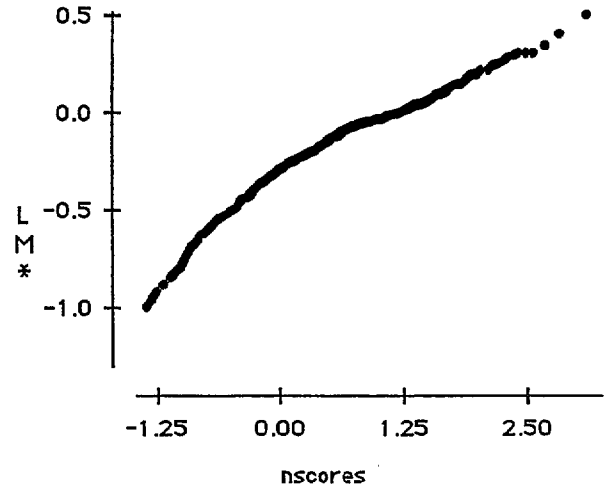

X_1 : Nb ppm

Mean:	Std. Dev.:	Std. Error:	Variance:	Coef. Var.:	Count:
15.567	10.749	.394	115.532	69.046	744
Minimum:	**Maximum:**	**Range:**	**Sum:**	**Sum of Sqr.:**	**# Missing:**
3	127	124	11582	266140	0
t 95%:	**95% Lower:**	**95% Upper:**	**# < 10th %:**	**10th %:**	**25th %:**
.774	14.794	16.341	54	7	9
50th %:	**75th %:**	**90th %:**	**# > 90th %:**	**Mode:**	**Geo. Mean:**
13	18	27	69	10	13.288
Har. Mean:	**Kurtosis:**	**Skewness:**			
11.661	20.832	3.386			

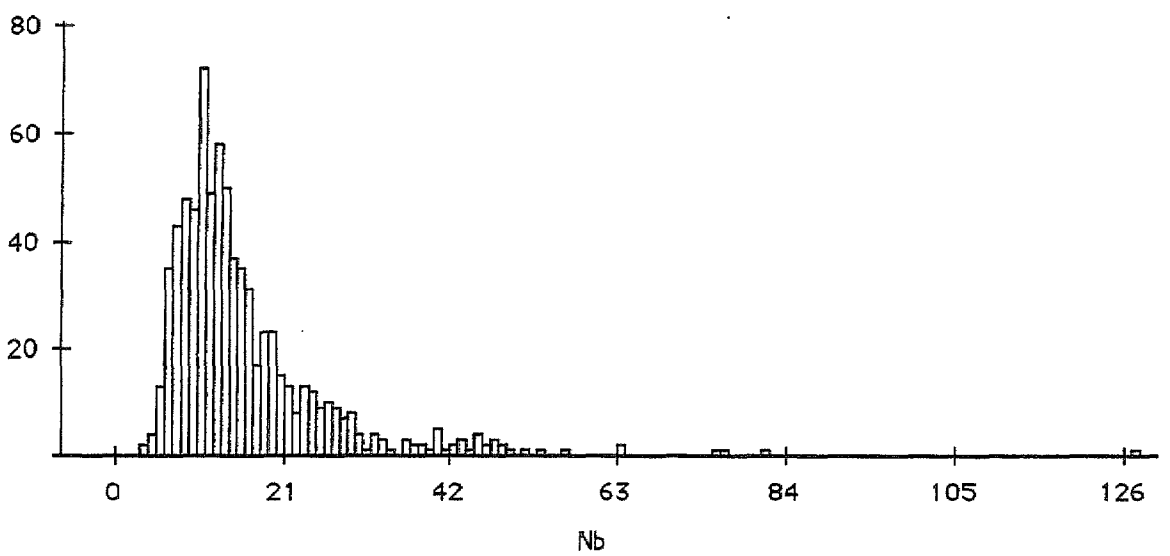

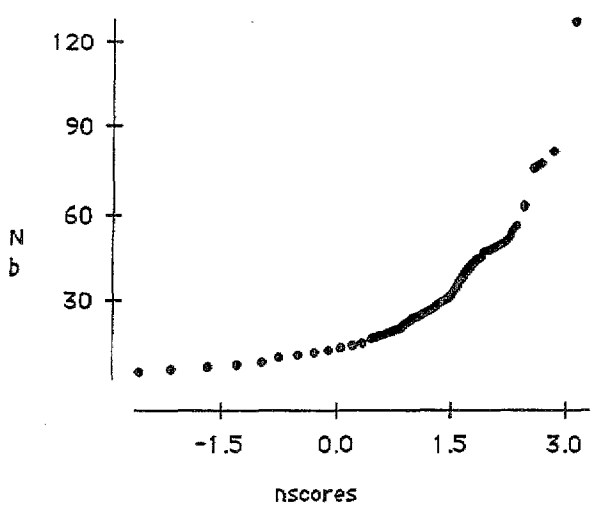

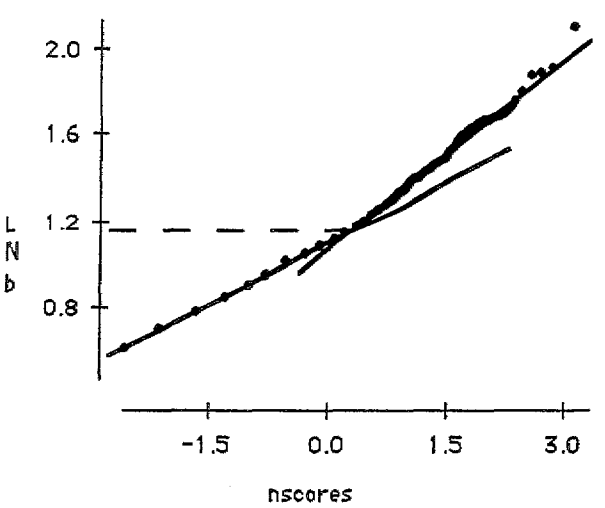

X_1 : Nd ppm

Mean:	Std. Dev.:	Std. Error:	Variance:	Coef. Var.:	Count:
64.206	95.961	3.518	9208.592	149.459	744
Minimum:	**Maximum:**	**Range:**	**Sum:**	**Sum of Sqr.:**	**# Missing:**
4	840	836	47769	9909023	0
t 95%:	**95% Lower:**	**95% Upper:**	**# < 10th %:**	**10th %:**	**25th %:**
6.907	57.298	71.113	72	14	20
50th %:	**75th %:**	**90th %:**	**# > 90th %:**	**Mode:**	**Geo. Mean:**
32	62.5	138.1	74	20	37.795
Har. Mean:	**Kurtosis:**	**Skewness:**			
26.561	20.027	4.028			

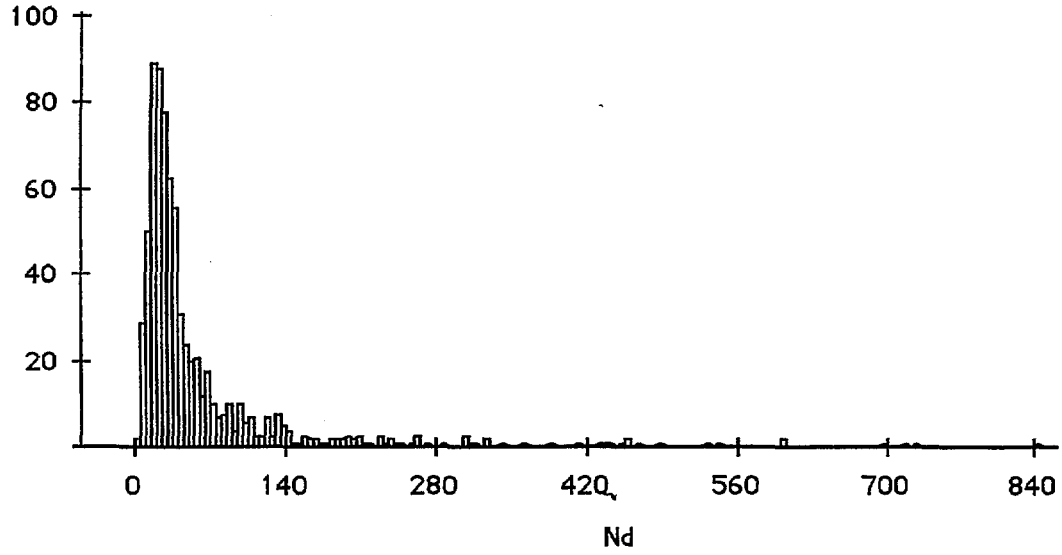

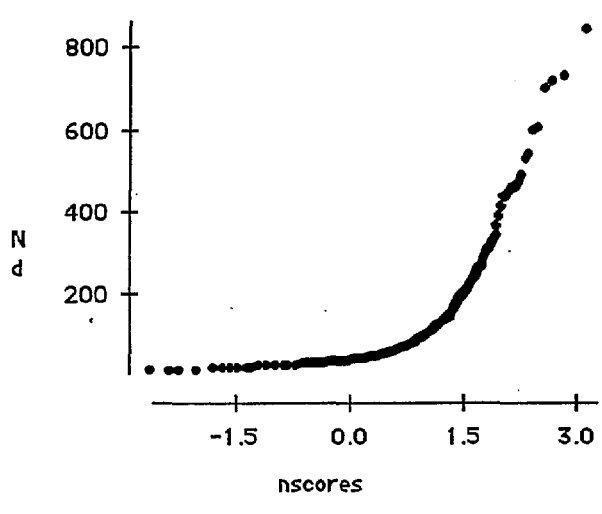

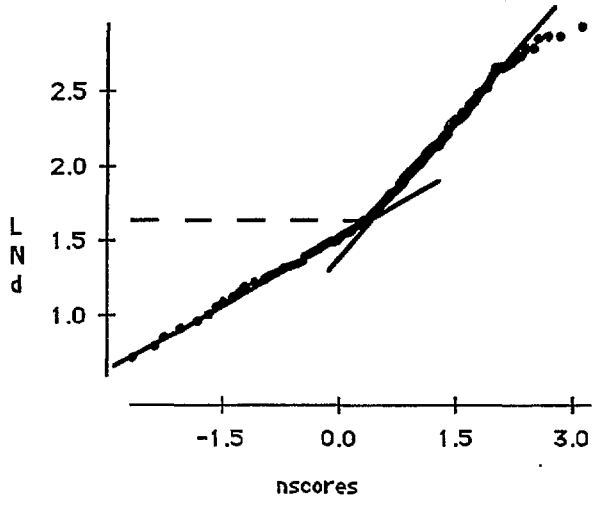

X_1 : Ni ppm

Mean:	Std. Dev.:	Std. Error:	Variance:	Coef. Var.:	Count:
5.295	7.327	.269	53.679	138.367	744
Minimum:	**Maximum:**	**Range:**	**Sum:**	**Sum of Sqr.:**	**# Missing:**
.5	73	72.5	3939.5	60743.25	0
t 95%:	**95% Lower:**	**95% Upper:**	**# < 10th %:**	**10th %:**	**25th %:**
.527	4.768	5.822	0	.5	1
50th %:	**75th %:**	**90th %:**	**# > 90th %:**	**Mode:**	**Geo. Mean:**
3	6	14	70	.5	2.71
Har. Mean:	**Kurtosis:**	**Skewness:**			
1.483	20.813	3.661			

Detection limit is 1 ppm - a value of 0.5 ppm has been used in calculations and table.

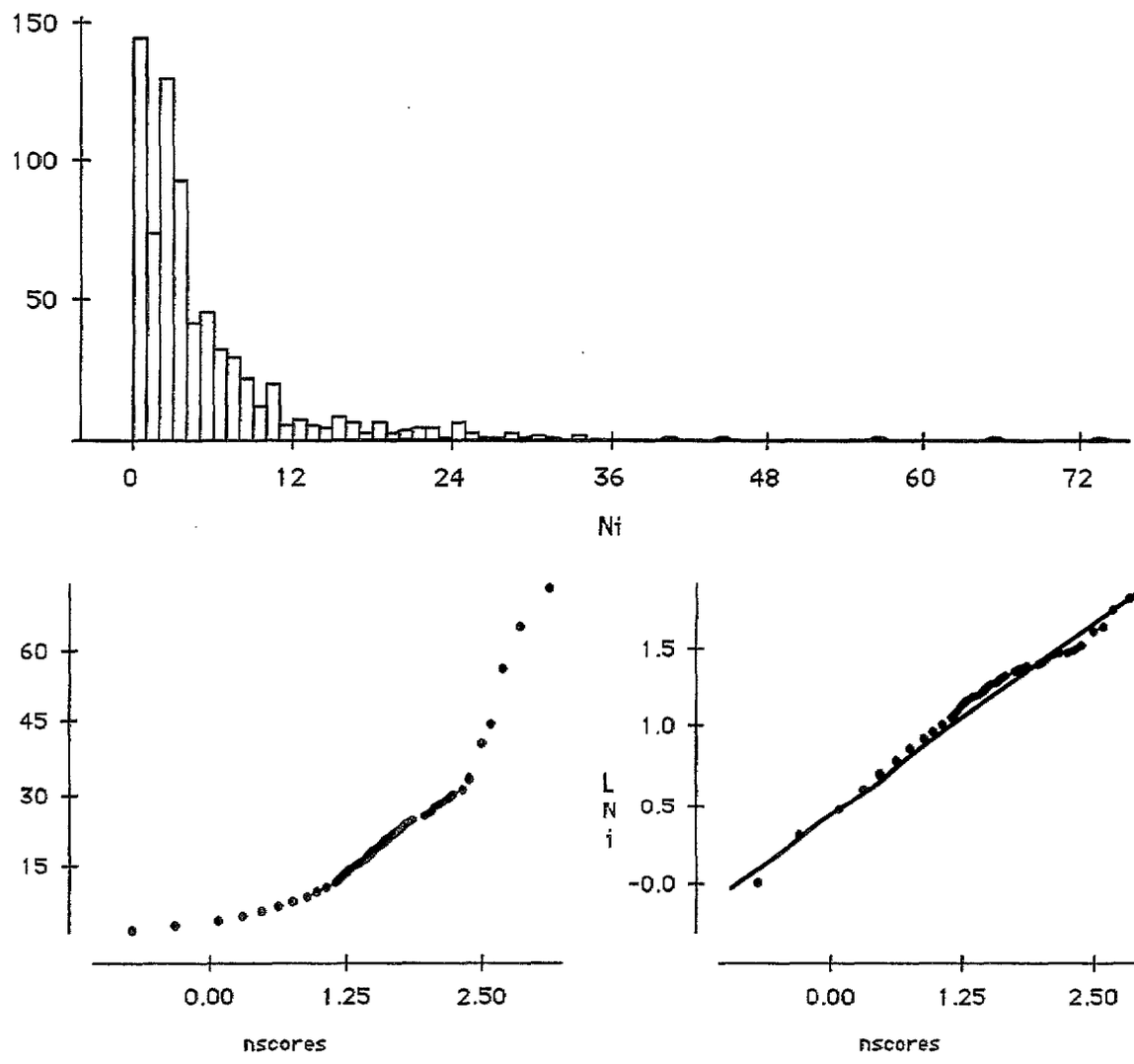

X_1 : P* ppm

Mean:	Std. Dev.:	Std. Error:	Variance:	Coef. Var.:	Count:
292.206	361.172	13.241	130445.569	123.602	744
Minimum:	**Maximum:**	**Range:**	**Sum:**	**Sum of Sqr.:**	**# Missing:**
10	2710	2700	217401	160446857	0
t 95%:	**95% Lower:**	**95% Upper:**	**# < 10th %:**	**10th %:**	**25th %:**
25.997	266.208	318.203	73	39	90.5
50th %:	**75th %:**	**90th %:**	**# > 90th %:**	**Mode:**	**Geo. Mean:**
181	342	630.4	74	10	164.534
Har. Mean:	**Kurtosis:**	**Skewness:**			
77.719	11.666	3.051			

Detection limit is 20 ppm - a value of 10 ppm has been used in calculations and table.

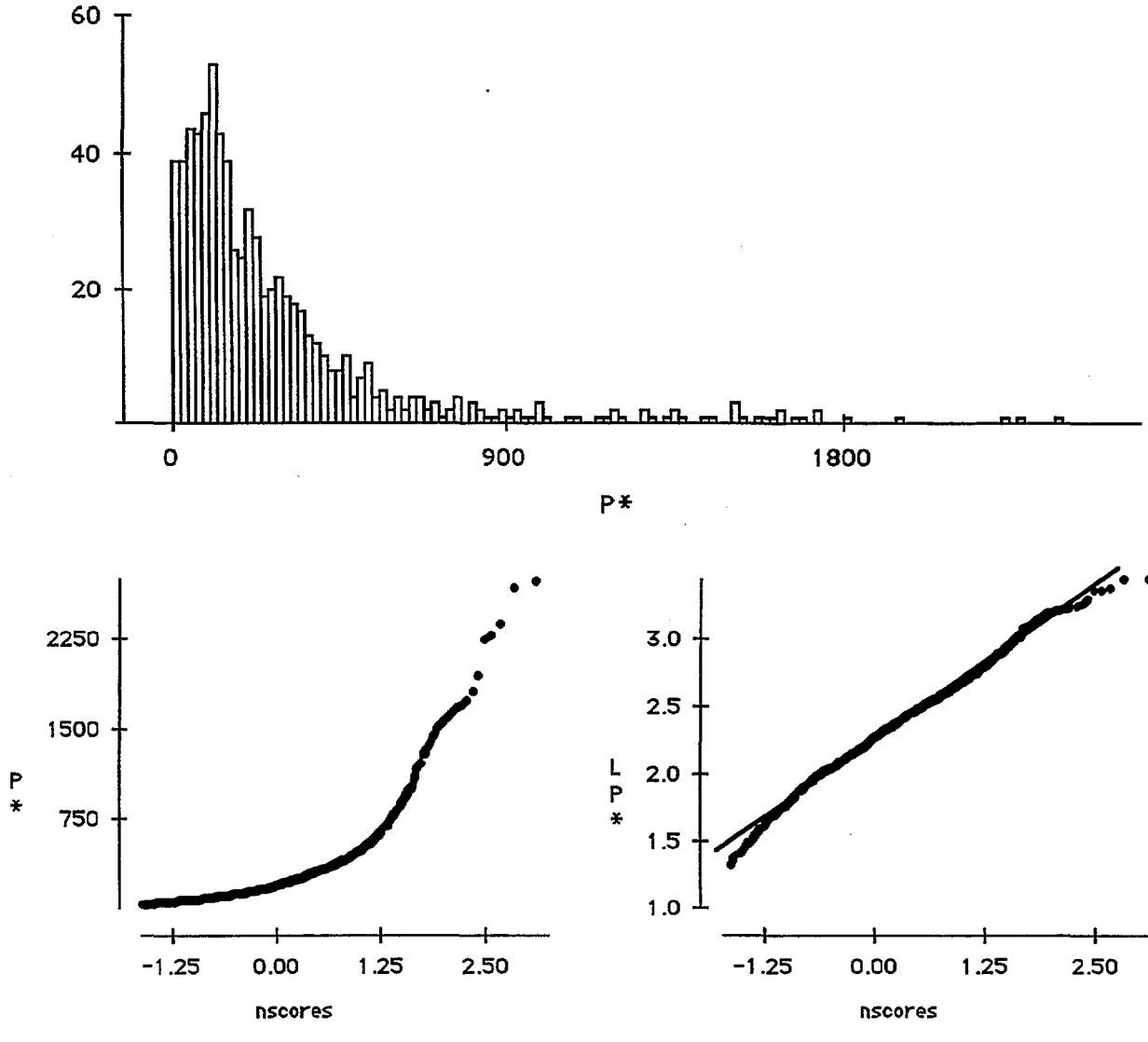

X_1 : Pb ppm

Mean:	Std. Dev.:	Std. Error:	Variance:	Coef. Var.:	Count:
26.531	16.763	.615	280.99	63.182	744
Minimum:	**Maximum:**	**Range:**	**Sum:**	**Sum of Sqr.:**	**# Missing:**
3	75	72	19739	732469	0
t 95%:	**95% Lower:**	**95% Upper:**	**# < 10th %:**	**10th %:**	**25th %:**
1.207	25.324	27.737	68	9	12
50th %:	**75th %:**	**90th %:**	**# > 90th %:**	**Mode:**	**Geo. Mean:**
21	39	53	71	•	21.378
Har. Mean:	**Kurtosis:**	**Skewness:**			
16.911	-.552	.72			

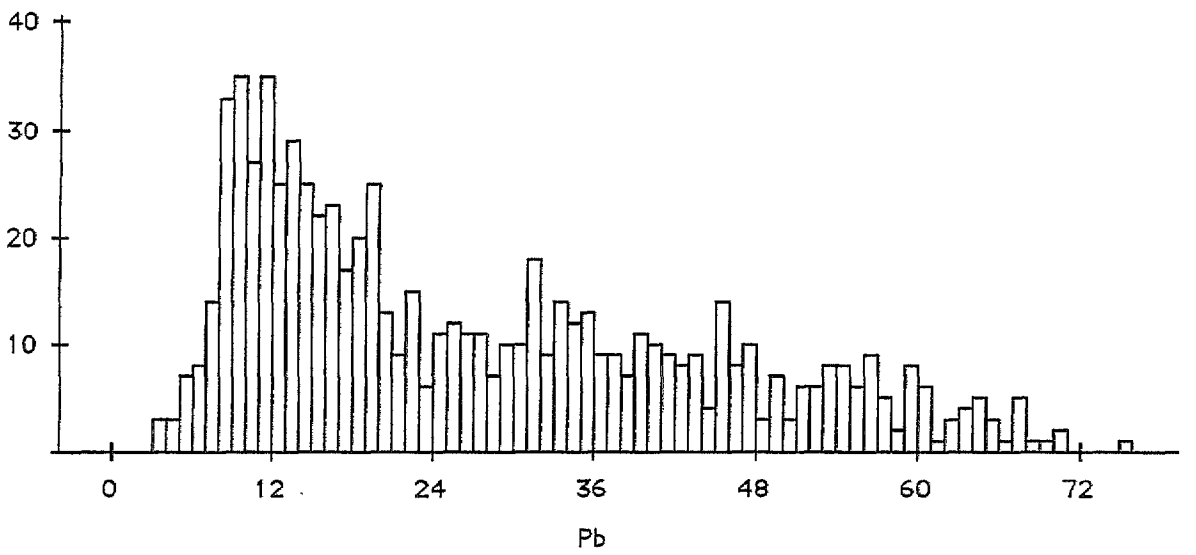

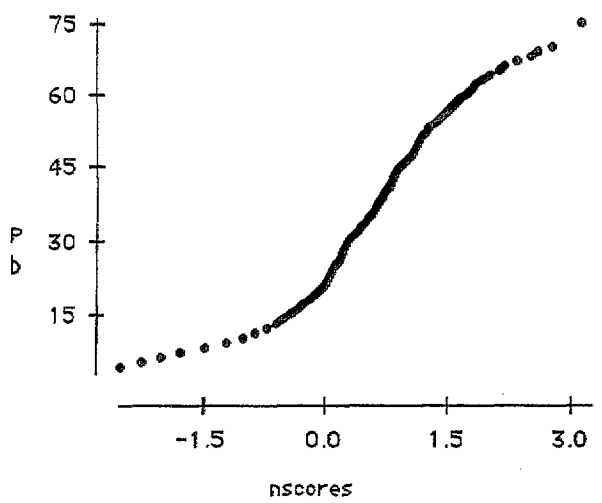

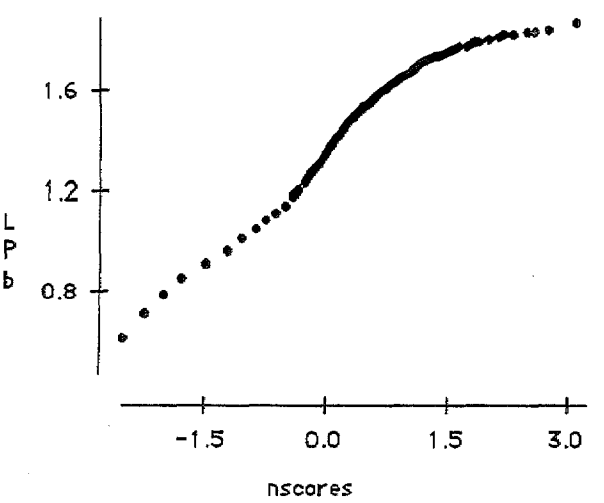

X_1 : Rb ppm

Mean:	Std. Dev.:	Std. Error:	Variance:	Coef. Var.:	Count:
92.98	75.47	2.767	5695.72	81.168	744
Minimum:	**Maximum:**	**Range:**	**Sum:**	**Sum of Sqr.:**	**# Missing:**
.5	287	286.5	69177	10663986	0
t 95%:	**95% Lower:**	**95% Upper:**	**# < 10th %:**	**10th %:**	**25th %:**
5.432	87.548	98.412	74	6.9	27.5
50th %:	**75th %:**	**90th %:**	**# > 90th %:**	**Mode:**	**Geo. Mean:**
71	150.5	207.1	74	3	52.325
Har. Mean:	**Kurtosis:**	**Skewness:**			
14.81	-.787	.592			

Detection limit is 1 ppm - a value of 0.5 ppm has been used in calculations and table.

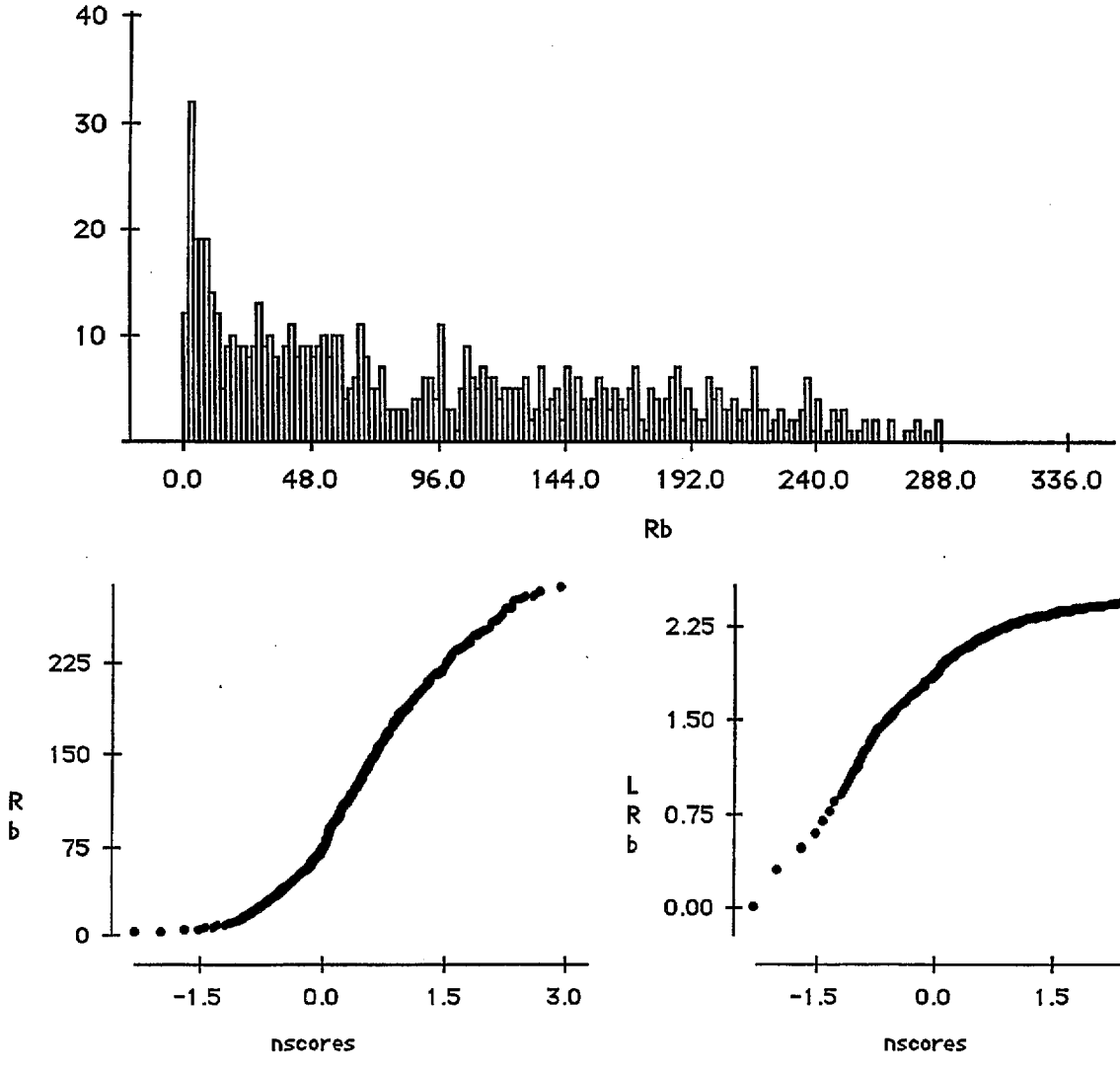

X_1 : Sb*ppm

Mean:	Std. Dev.:	Std. Error:	Variance:	Coef. Var.:	Count:
.525	.417	.015	.174	79.432	744
Minimum:	Maximum:	Range:	Sum:	Sum of Sqr.:	# Missing:
.025	4.32	4.295	390.34	333.832	0
t 95%:	95% Lower:	95% Upper:	# < 10th %:	10th %:	25th %:
.03	.495	.555	72	.13	.255
50th %:	75th %:	90th %:	# > 90th %:	Mode:	Geo. Mean:
.43	.685	.99	72	.025	.385
Har. Mean:	Kurtosis:	Skewness:			
.233	13.438	2.564			

Detection limit is 0.05 ppm - a value of 0.025 ppm has been used in calculations and table.

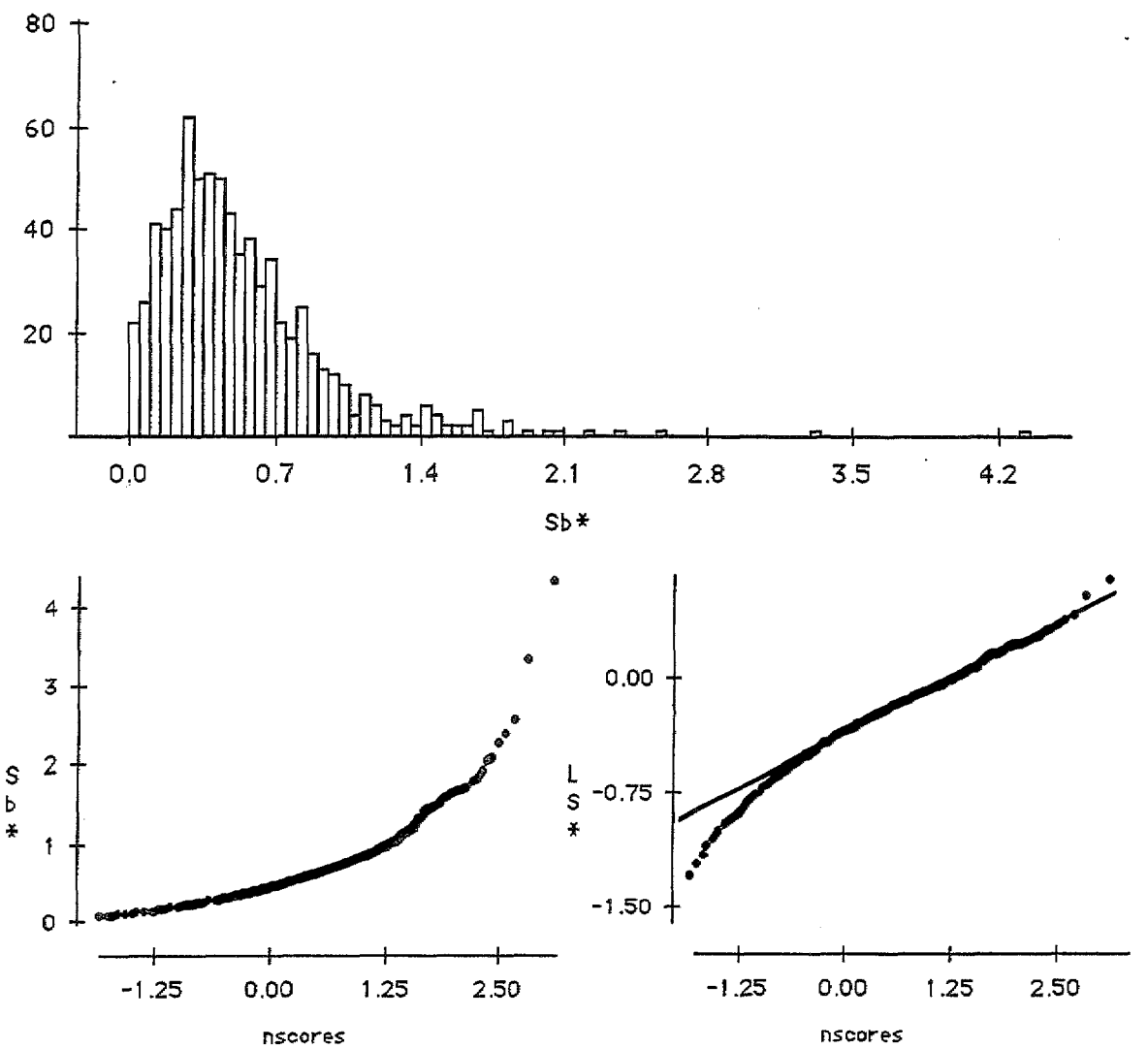

X_1 : Sc ppm

Mean:	Std. Dev.:	Std. Error:	Variance:	Coef. Var.:	Count:
5.077	3.681	.135	13.547	72.502	744
Minimum:	**Maximum:**	**Range:**	**Sum:**	**Sum of Sqr.:**	**# Missing:**
.5	25	24.5	3777	29240	0
t 95%:	**95% Lower:**	**95% Upper:**	**# < 10th %:**	**10th %:**	**25th %:**
.265	4.812	5.342	52	1	2
50th %:	**75th %:**	**90th %:**	**# > 90th %:**	**Mode:**	**Geo. Mean:**
4	7	10	64	•	3.751
Har. Mean:	**Kurtosis:**	**Skewness:**			
2.436	2.205	1.266			

Detection limit is 1 ppm - a value of 0.5 ppm has been used in calculations and table.

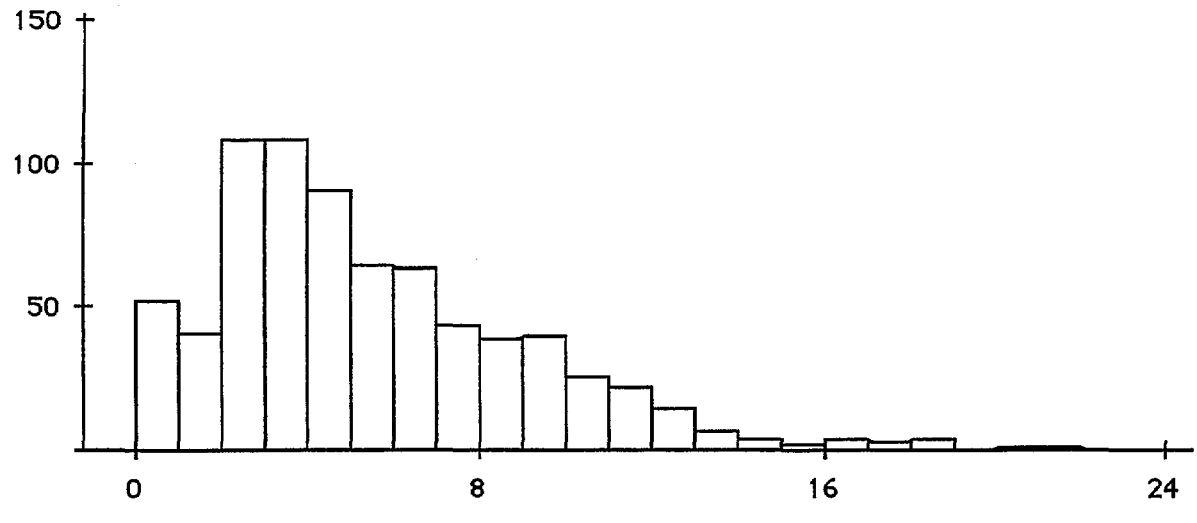

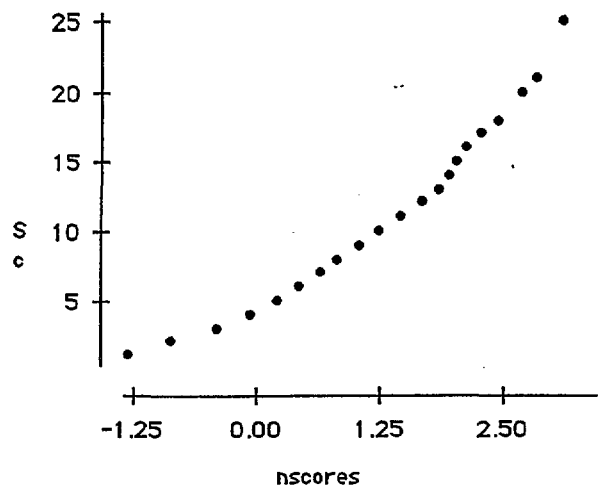

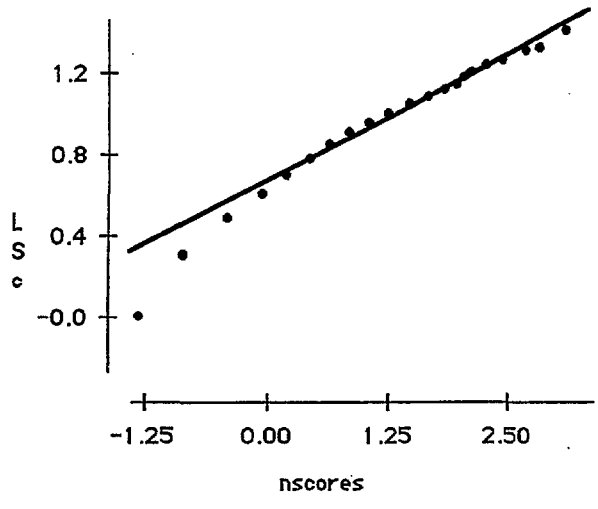

X_1 : Sn ppm

Mean:	Std. Dev.:	Std. Error:	Variance:	Coef. Var.:	Count:
4.946	18.43	.676	339.674	372.612	744
Minimum:	**Maximum:**	**Range:**	**Sum:**	**Sum of Sqr.:**	**# Missing:**
1	348	347	3680	270580	0
t 95%:	**95% Lower:**	**95% Upper:**	**# < 10th %:**	**10th %:**	**25th %:**
1.327	3.62	6.273	0	1	1
50th %:	**75th %:**	**90th %:**	**# > 90th %:**	**Mode:**	**Geo. Mean:**
1	4	9	67	1	2.1
Har. Mean:	**Kurtosis:**	**Skewness:**			
1.515	234.887	14.138			

Detection limit is 2 ppm - a value of 1 ppm has been used in calculations and table.

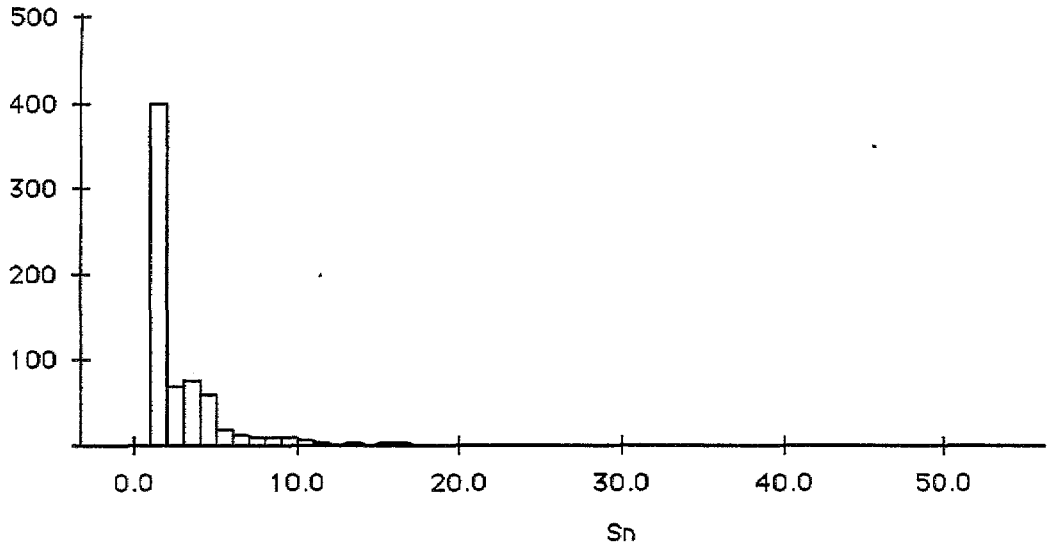

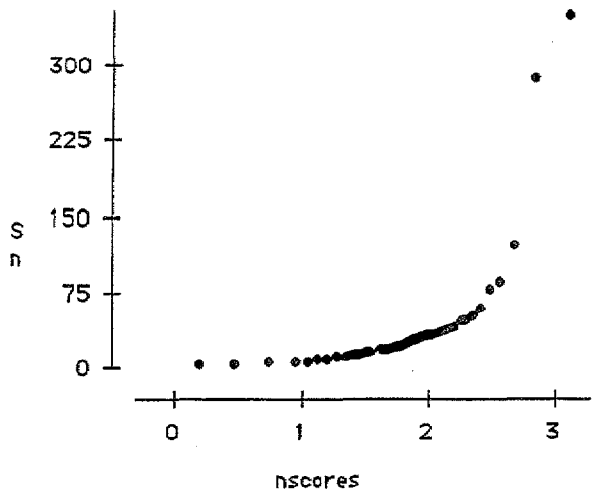

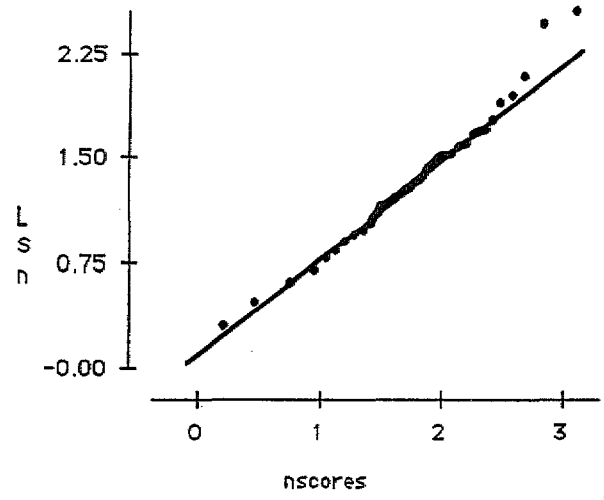

X_1 : Sr ppm

Mean:	Std. Dev.:	Std. Error:	Variance:	Coef. Var.:	Count:
62.61	44.035	1.614	1939.113	70.333	744
Minimum:	**Maximum:**	**Range:**	**Sum:**	**Sum of Sqr.:**	**# Missing:**
3	216	213	46582	4357270	0
t 95%:	**95% Lower:**	**95% Upper:**	**# < 10th %:**	**10th %:**	**25th %:**
3.17	59.441	65.78	74	9.9	26
50th %:	**75th %:**	**90th %:**	**# > 90th %:**	**Mode:**	**Geo. Mean:**
53	98	125	73	5	43.688
Har. Mean:	**Kurtosis:**	**Skewness:**			
24.599	-.659	.53			

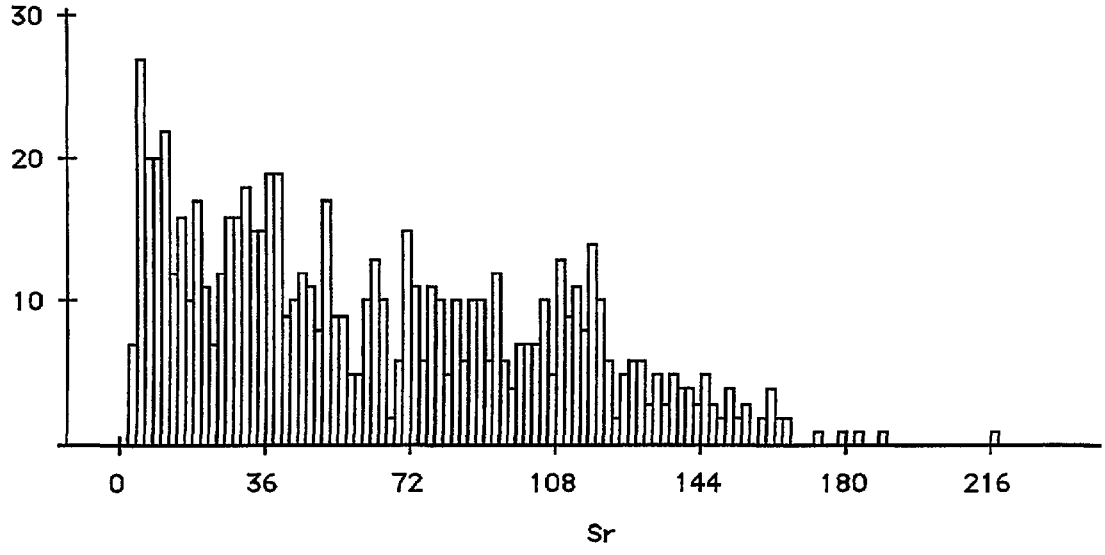

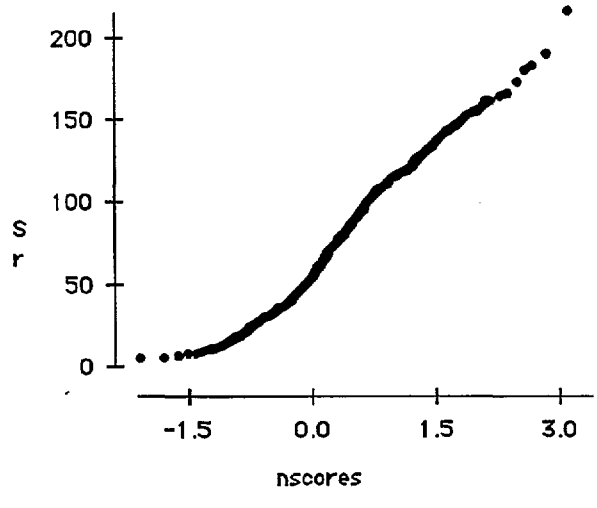

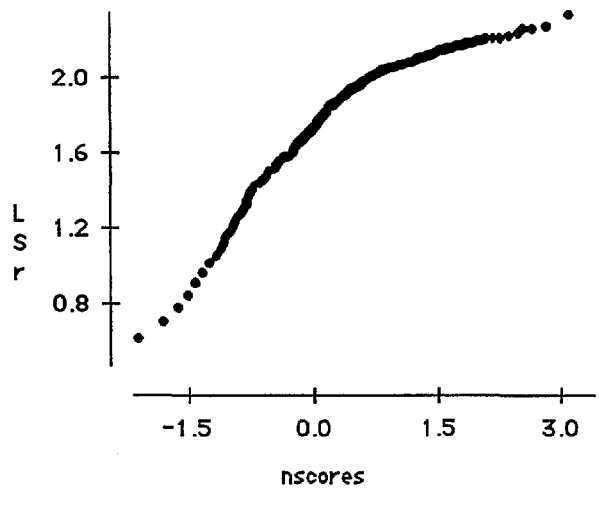

X_1 : Th ppm

Mean:	Std. Dev.:	Std. Error:	Variance:	Coef. Var.:	Count:
41.093	65.489	2.401	4288.776	159.368	744
Minimum:	**Maximum:**	**Range:**	**Sum:**	**Sum of Sqr.:**	**# Missing:**
1	505	504	30573	4442889	0
t 95%:	**95% Lower:**	**95% Upper:**	**# < 10th %:**	**10th %:**	**25th %:**
4.714	36.379	45.807	60	7	10
50th %:	**75th %:**	**90th %:**	**# > 90th %:**	**Mode:**	**Geo. Mean:**
17	39	99.1	74	8	21.528
Har. Mean:	**Kurtosis:**	**Skewness:**			
14.09	15.386	3.635			

Detection limit is 2 ppm - a value of 1 ppm has been used in calculations and table.

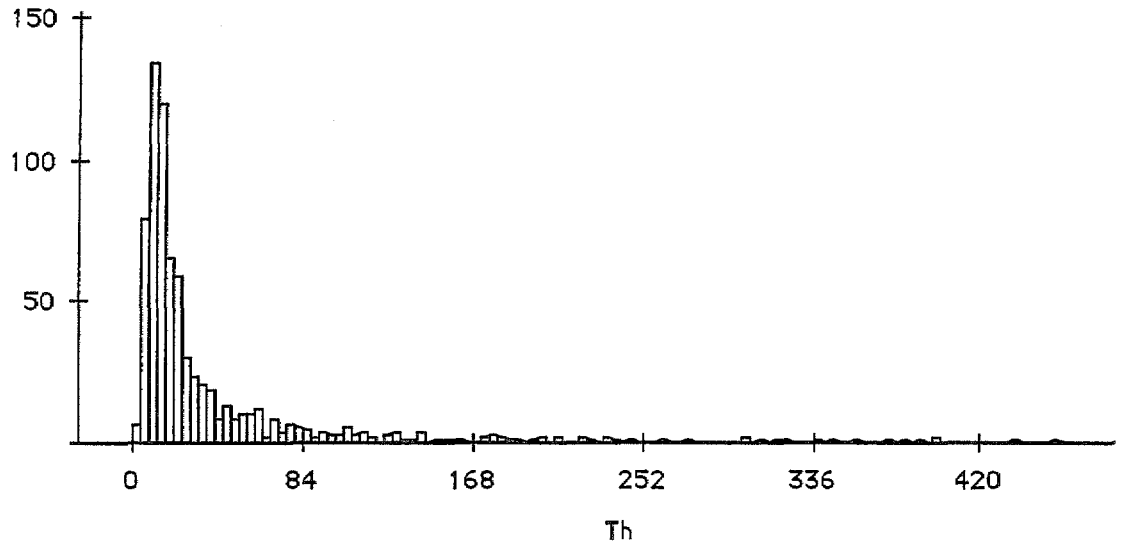

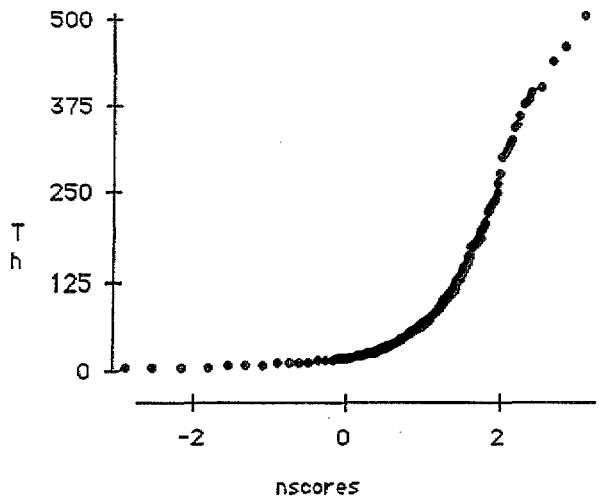

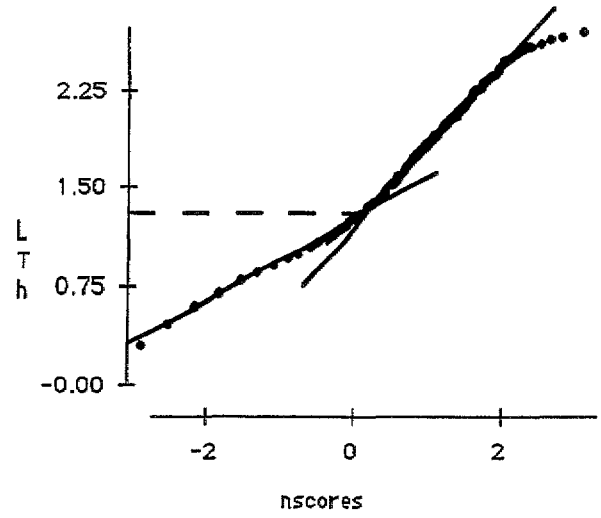

X_1 : Ti ppm

Mean:	Std. Dev.:	Std. Error:	Variance:	Coef. Var.:	Count:
4177.534	4004.009	146.794	1.603E7	95.846	744
Minimum:	**Maximum:**	**Range:**	**Sum:**	**Sum of Sqr.:**	**# Missing:**
314	46779	46465	3108085	2.490E10	0
t 95%:	**95% Lower:**	**95% Upper:**	**# < 10th %:**	**10th %:**	**25th %:**
288.209	3889.325	4465.742	74	1028.8	1920.5
50th %:	**75th %:**	**90th %:**	**# > 90th %:**	**Mode:**	**Geo. Mean:**
3359	5272	7253.5	74	•	3072.257
Har. Mean:	**Kurtosis:**	**Skewness:**			
2171.006	30.681	4.372			

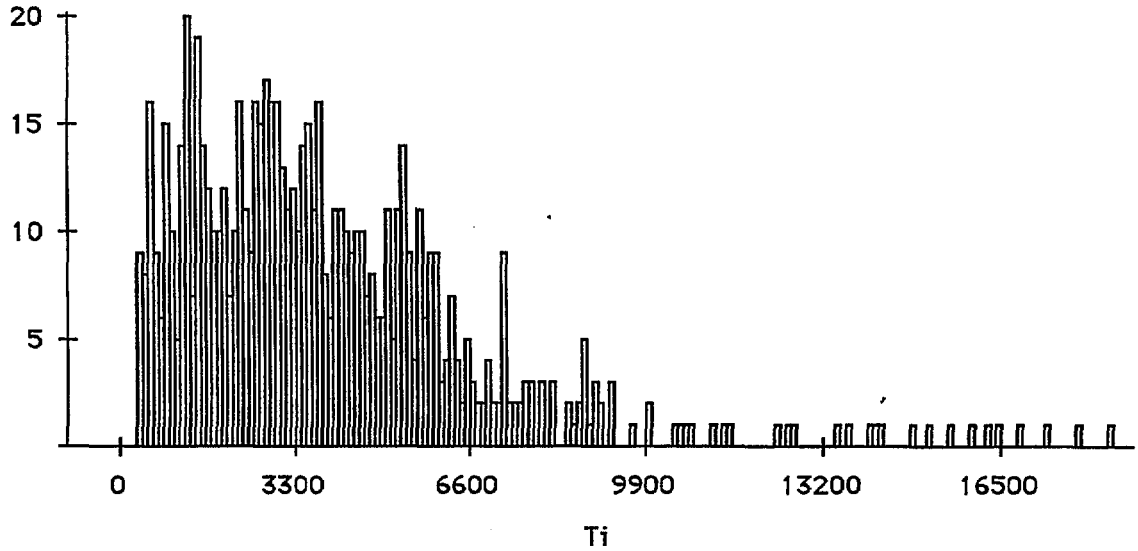

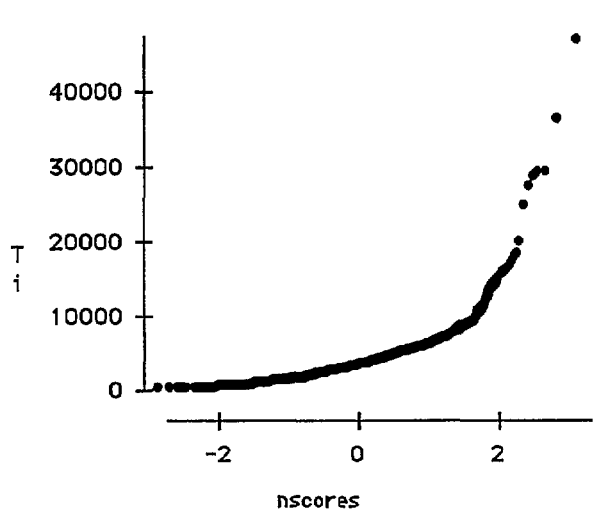

X_1 : Tl*ppm

Mean:	Std. Dev.:	Std. Error:	Variance:	Coef. Var.:	Count:
.761	.51	.019	.26	67.041	744
Minimum:	**Maximum:**	**Range:**	**Sum:**	**Sum of Sqr.:**	**# Missing:**
.25	2.29	2.04	566.26	624.425	0
t 95%:	**95% Lower:**	**95% Upper:**	**# < 10th %:**	**10th %:**	**25th %:**
.037	.724	.798	0	.25	.25
50th %:	**75th %:**	**90th %:**	**# > 90th %:**	**Mode:**	**Geo. Mean:**
.665	1.155	1.5	72	.25	.59
Har. Mean:	**Kurtosis:**	**Skewness:**			
.457	-.656	.623			

Detection limit is 0.5 ppm - a value of 0.25 ppm has been used in calculations and table.

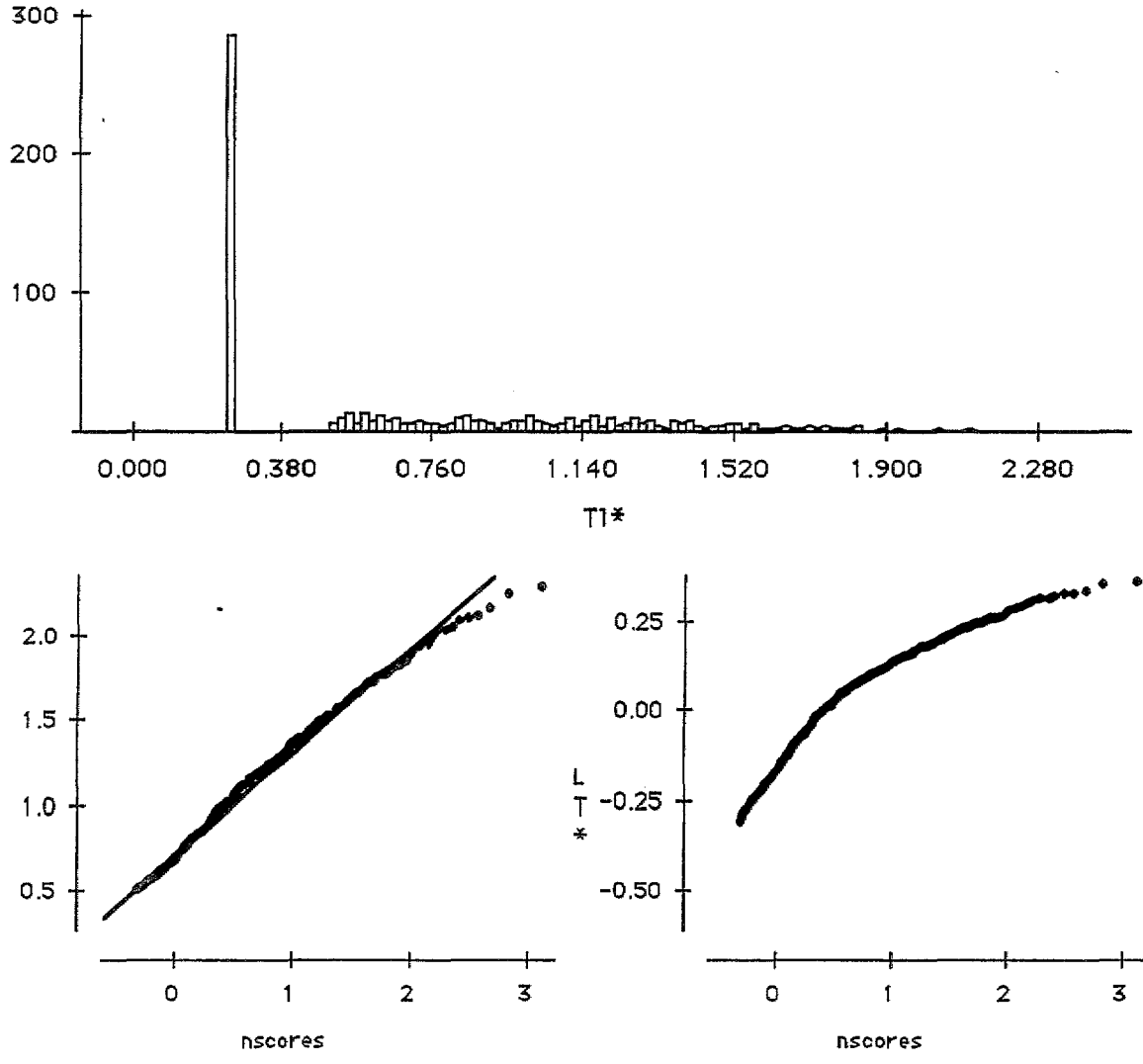

X_1 : U ppm

Mean:	Std. Dev.:	Std. Error:	Variance:	Coef. Var.:	Count:
6.65	9.394	.344	88.251	141.276	744
Minimum:	**Maximum:**	**Range:**	**Sum:**	**Sum of Sqr.:**	**# Missing:**
.25	80.5	80.25	4947.25	98467.312	0
t 95%:	**95% Lower:**	**95% Upper:**	**# < 10th %:**	**10th %:**	**25th %:**
.676	5.973	7.326	47	1.5	2
50th %:	**75th %:**	**90th %:**	**# > 90th %:**	**Mode:**	**Geo. Mean:**
3.5	7	13.55	74	2	3.965
Har. Mean:	**Kurtosis:**	**Skewness:**			
2.666	16.672	3.695			

Detection limit is 0.5 ppm - a value of 0.25 ppm has been used in calculations and table.

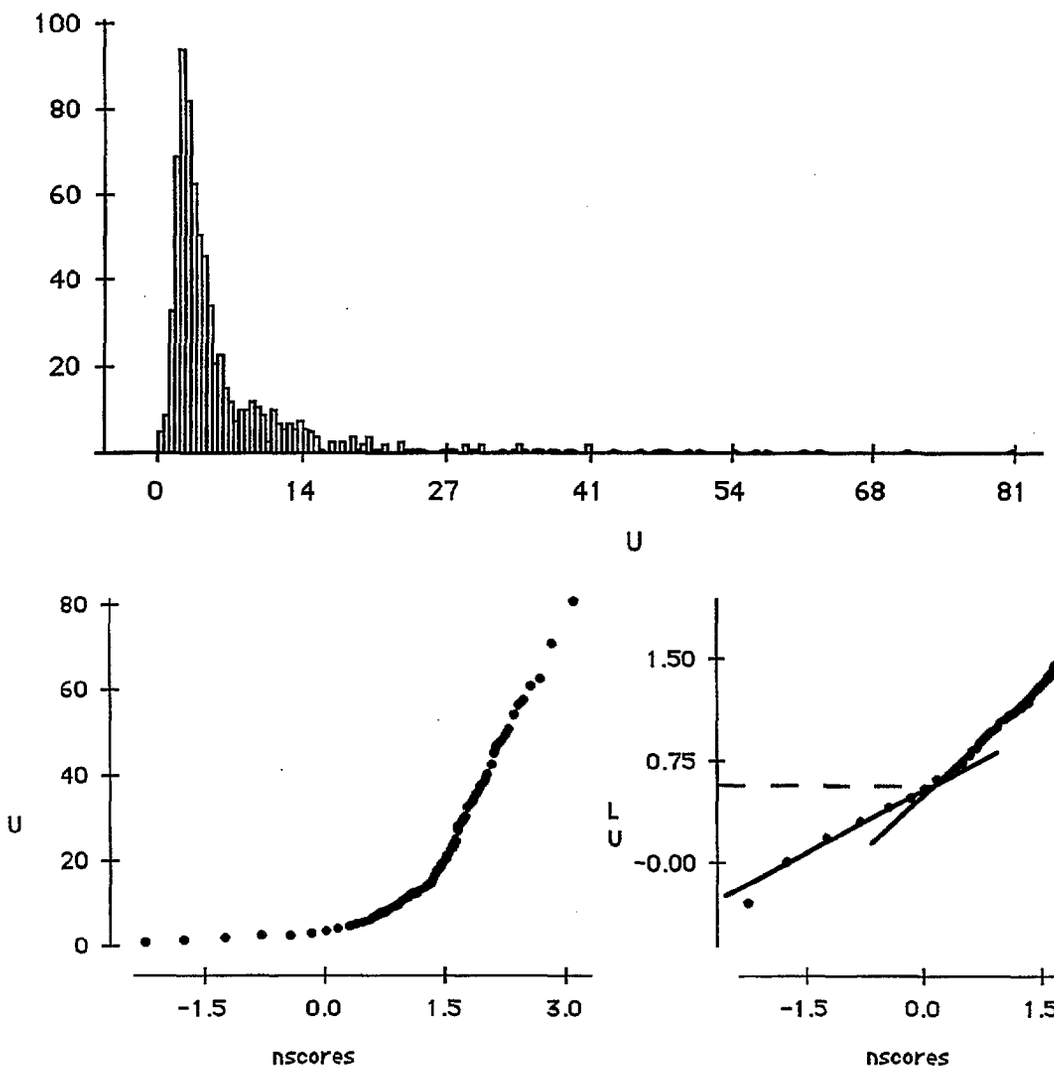

X_1 : V ppm

Mean:	Std. Dev.:	Std. Error:	Variance:	Coef. Var.:	Count:
38.383	35.012	1.284	1225.852	91.218	744
Minimum:	**Maximum:**	**Range:**	**Sum:**	**Sum of Sqr.:**	**# Missing:**
1	262	261	28557	2006913	0
t 95%:	**95% Lower:**	**95% Upper:**	**# < 10th %:**	**10th %:**	**25th %:**
2.52	35.863	40.903	71	6	14
50th %:	**75th %:**	**90th %:**	**# > 90th %:**	**Mode:**	**Geo. Mean:**
29	51	83.1	74	7	24.811
Har. Mean:	**Kurtosis:**	**Skewness:**			
12.678	5.817	1.973			

Detection limit is 2 ppm - a value of 1 ppm has been used in calculations and table.

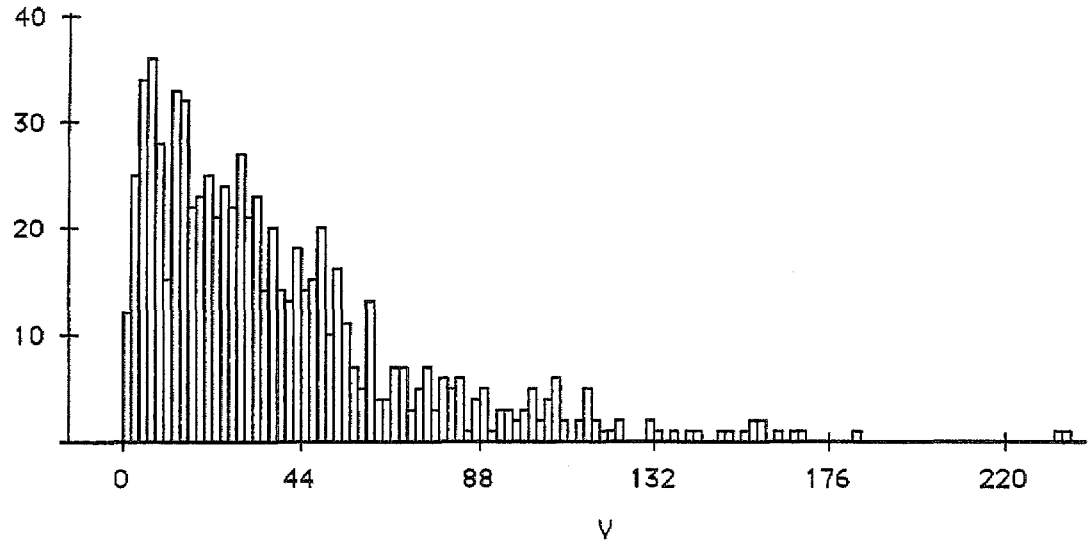

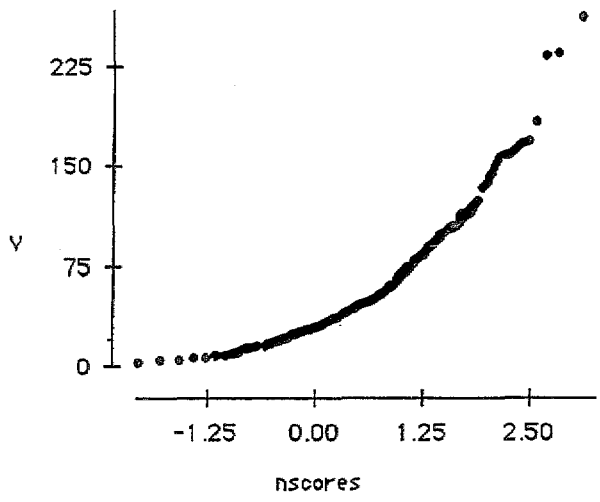

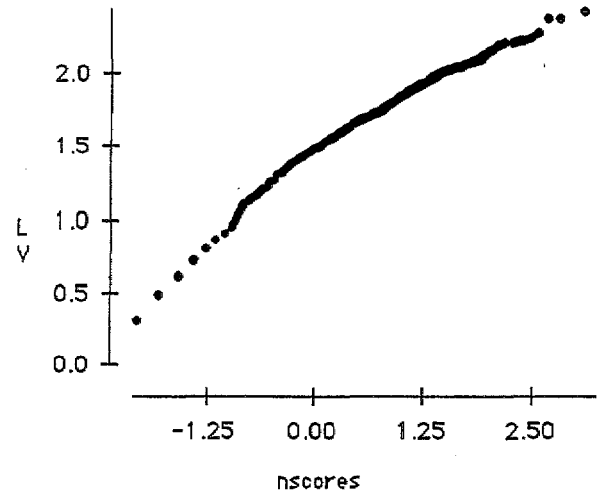

X_1 : W ppm

Mean:	Std. Dev.:	Std. Error:	Variance:	Coef. Var.:	Count:
4.936	4.531	.166	20.529	91.789	744
Minimum:	**Maximum:**	**Range:**	**Sum:**	**Sum of Sqr.:**	**# Missing:**
1.5	50	48.5	3672.5	33380.75	0
t 95%:	**95% Lower:**	**95% Upper:**	**# < 10th %:**	**10th %:**	**25th %:**
.326	4.61	5.262	0	1.5	1.5
50th %:	**75th %:**	**90th %:**	**# > 90th %:**	**Mode:**	**Geo. Mean:**
4	6	8.1	74	1.5	3.773
Har. Mean:	**Kurtosis:**	**Skewness:**			
2.978	26.961	4.118			

Detection limit is 3 ppm - a value of 1.5 ppm has been used in calculations and table.

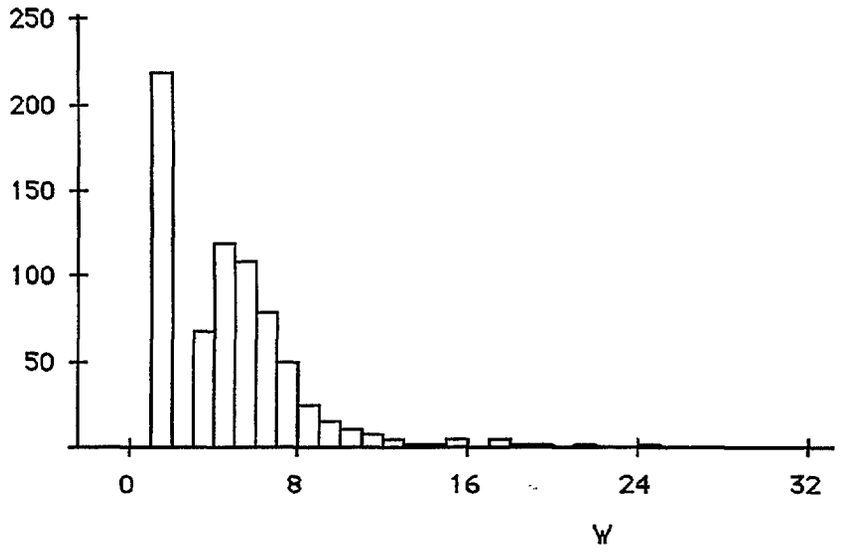

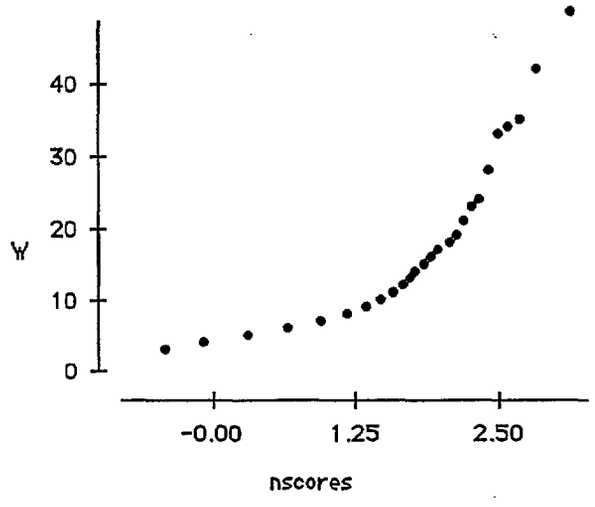

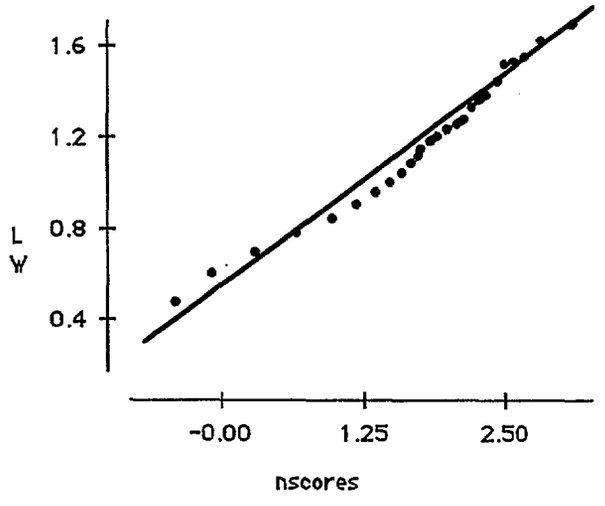

W* ppm

Mean:	Std. Dev.:	Std. Error:	Variance:	Coef. Var.:	Count:
1.85	2.133	.078	4.548	115.281	744
Minimum:	**Maximum:**	**Range:**	**Sum:**	**Sum of Sqr.:**	**# Missing:**
.05	48.2	48.15	1376.3	5924.967	0
t 95%:	**95% Lower:**	**95% Upper:**	**# < 10th %:**	**10th %:**	**25th %:**
.154	1.696	2.003	74	.459	.935
50th %:	**75th %:**	**90th %:**	**# > 90th %:**	**Mode:**	**Geo. Mean:**
1.58	2.41	3.212	74	.05	1.334
Har. Mean:	**Kurtosis:**	**Skewness:**			
.679	299.682	14.311			

Detection limit is 0.10 ppm - a value of 0.05 ppm has been used in calculations and table.

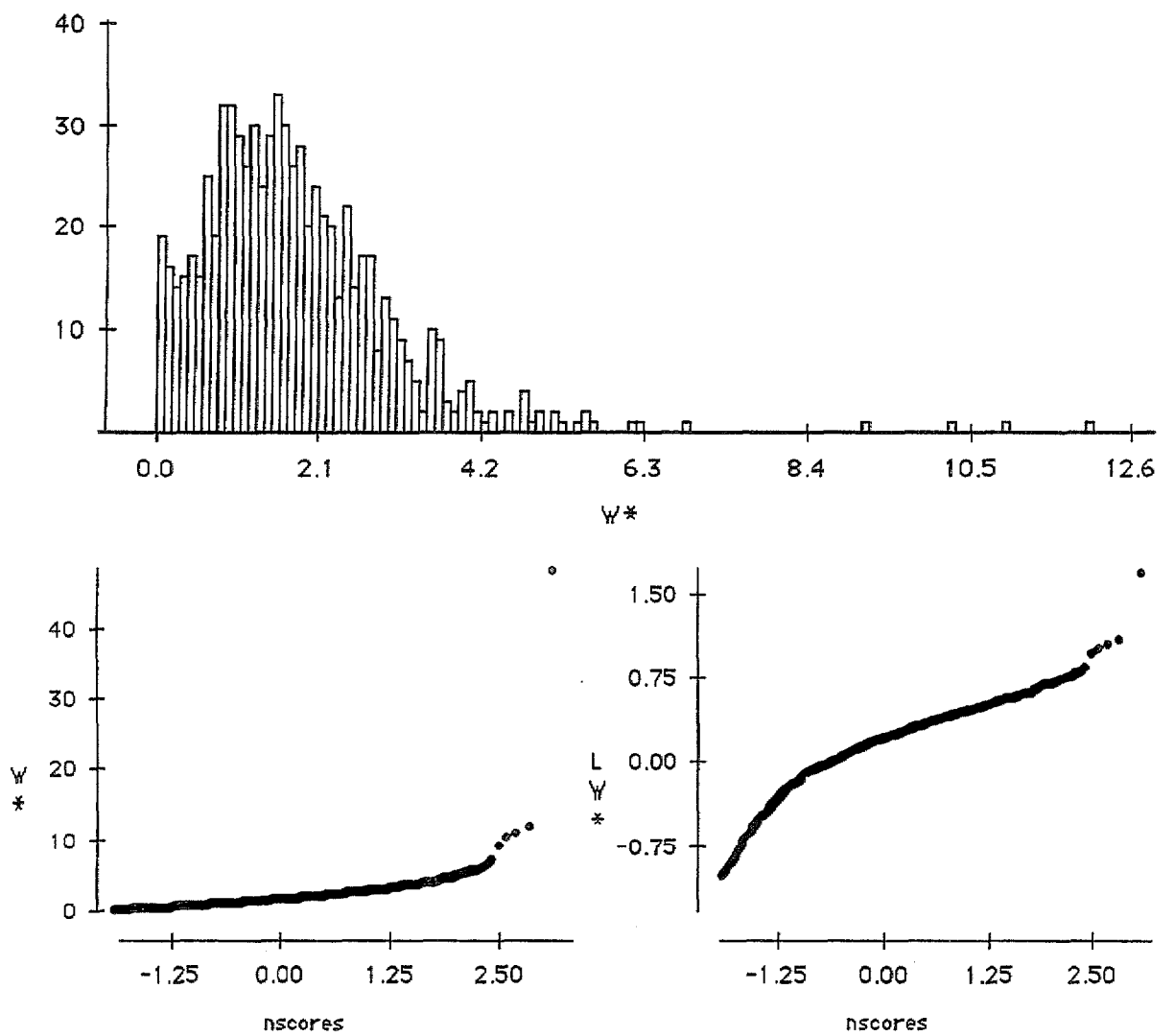

X_1 : Y ppm

Mean:	Std. Dev.:	Std. Error:	Variance:	Coef. Var.:	Count:
61.011	93.774	3.438	8793.647	153.702	744
Minimum:	**Maximum:**	**Range:**	**Sum:**	**Sum of Sqr.:**	**# Missing:**
4	1014	1010	45392	9303080	0
t 95%:	**95% Lower:**	**95% Upper:**	**# < 10th %:**	**10th %:**	**25th %:**
6.75	54.261	67.761	66	16	22
50th %:	**75th %:**	**90th %:**	**# > 90th %:**	**Mode:**	**Geo. Mean:**
31	58	129	73	•	38.355
Har. Mean:	**Kurtosis:**	**Skewness:**			
29.268	33.907	5.066			

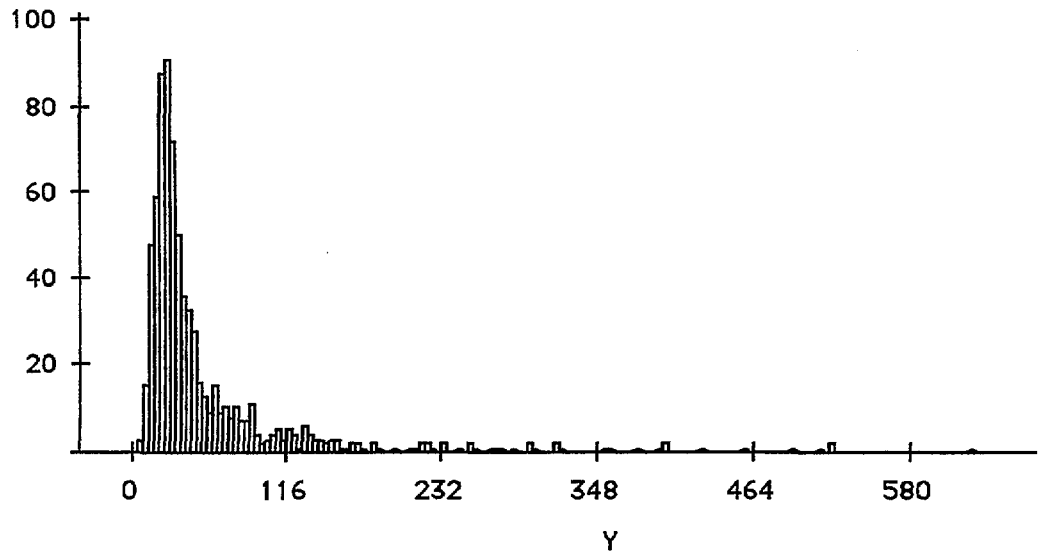

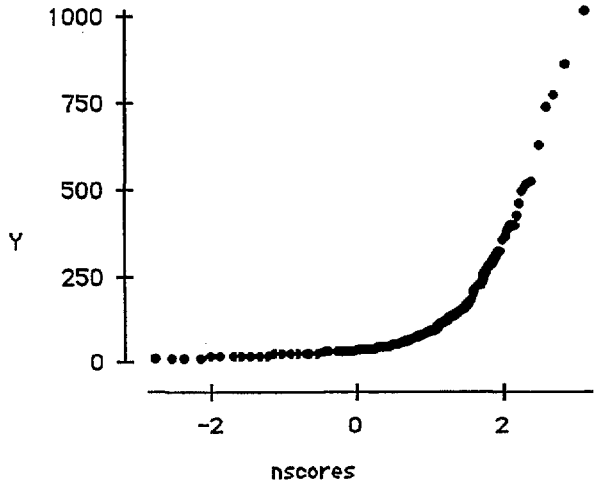

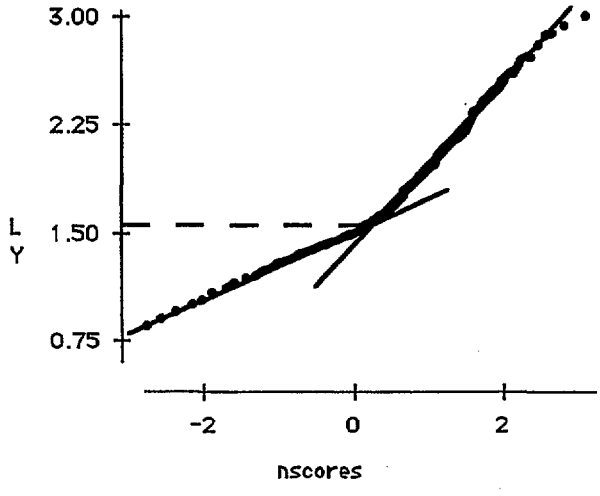

X_1 : Zn ppm

Mean:	Std. Dev.:	Std. Error:	Variance:	Coef. Var.:	Count:
18.079	14.532	.533	211.174	80.378	744
Minimum:	**Maximum:**	**Range:**	**Sum:**	**Sum of Sqr.:**	**# Missing:**
2	201	199	13451	400087	0
t 95%:	**95% Lower:**	**95% Upper:**	**# < 10th %:**	**10th %:**	**25th %:**
1.046	17.033	19.125	47	5	9
50th %:	**75th %:**	**90th %:**	**# > 90th %:**	**Mode:**	**Geo. Mean:**
15	23	34	72	15	14.198
Har. Mean:	**Kurtosis:**	**Skewness:**			
11.047	38.018	4.156			

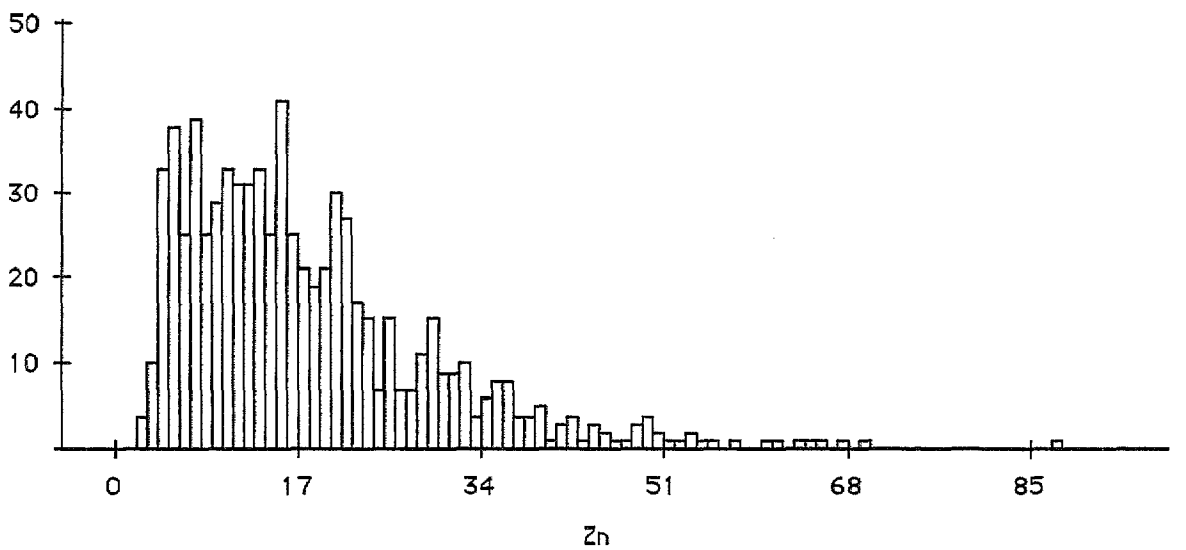

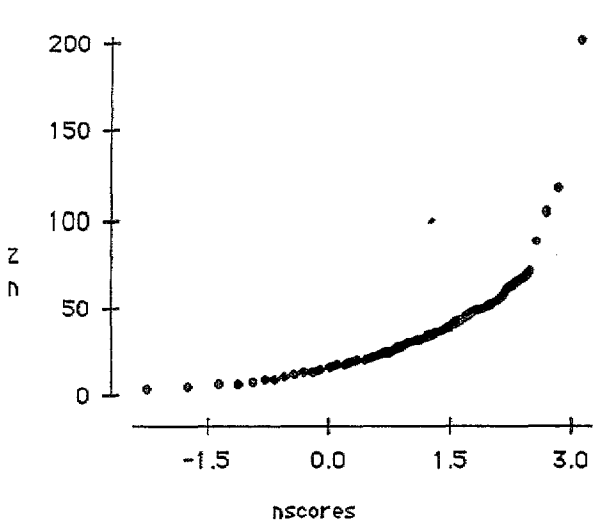

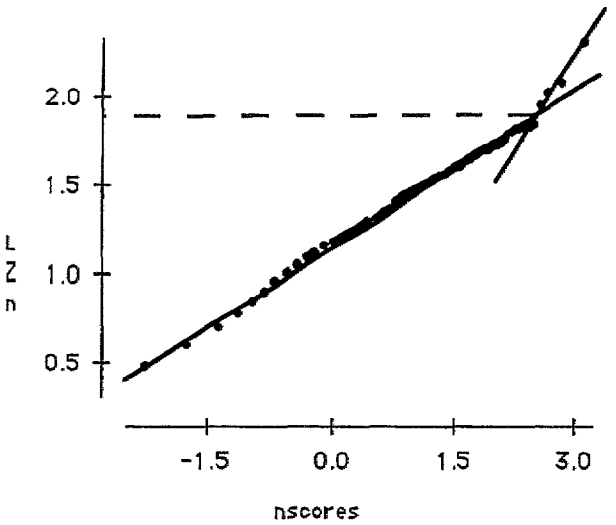

X_1 : Zr ppm

Mean:	Std. Dev.:	Std. Error:	Variance:	Coef. Var.:	Count:
654.301	805.976	29.549	649598.055	123.181	744
Minimum:	**Maximum:**	**Range:**	**Sum:**	**Sum of Sqr.:**	**# Missing:**
54	13944	13890	486800	801165118	0
t 95%:	**95% Lower:**	**95% Upper:**	**# < 10th %:**	**10th %:**	**25th %:**
58.014	596.287	712.315	73	194	282
50th %:	**75th %:**	**90th %:**	**# > 90th %:**	**Mode:**	**Geo. Mean:**
423.5	750	1262.2	74	•	466.188
Har. Mean:	**Kurtosis:**	**Skewness:**			
360.358	103.081	7.587